

On local and long-range transported air pollution in Svalbard

From a single station to international measurement network

—
Alena Dekhtyareva

A dissertation for the degree of Philosophiae Doctor – June 2019



On local and long-range transported air pollution in Svalbard

From a single station to international measurement network

By
Alena Dekhtyareva

*Thesis submitted in fulfilment of the requirements for the
degree of Philosophiae Doctor (PhD)*

UiT –The Arctic University of Norway

Faculty of Science and Technology
Department of Engineering and Safety IVT

June 2019

Dedicated to my beloved husband Vitaly and my kind and loving mother Irina.

*“...I have got the Arctic illness,
And it means I have no choice,
As She took my heart and called me
By Her cool and windy voice.*

*So no matter where I travel,
On the threshold of any spring,
I still rave of the polar trails,
And I see the snowy dreams...”*

(From the poem of

Robert Rozhdestvensky “Arctic Illness”/

Роберт Рождественский “Арктическая болезнь”

translated from the Russian by Alena Dekhtyareva)

Abstract

Climate change, health of the residents and ecosystems in the Arctic region are impacted by local and long-range transported air pollution. Local emissions in the Arctic are important, but overlooked issue. Despite there have been extensive modelling and measurement studies of long-range transport of short-lived climate forcers (SLCFs) to Svalbard, the effect of local emissions from diesel and coal power plants and ship traffic on the concentrations of these compounds in major settlements has not been investigated thoroughly.

The scope of this work is to study temporal and spatial evolution of air pollutant concentrations in Svalbard using the historical chemical and meteorological data collected in Ny-Ålesund and newly obtained observations from three sites: Ny-Ålesund, Longyearbyen and Barentsburg. Remote and local emission sources, concentrations of anthropogenic SLCFs and environmental factors that promote long-range transportation and accumulation of local air pollution in the Svalbard settlements have been investigated.

A strong seasonality in the concentrations of sulphur dioxide (SO₂), nitrogen oxides (NO_x), tropospheric ozone (O₃) and black carbon (BC) in Svalbard has been observed. Measurements in Ny-Ålesund revealed that in autumn, winter and spring the concentrations of SO₂, sulphate and particles of accumulation mode are dominated by the long-range transport of air pollution from remote and regional sources. In summer, the long-range transport of air pollution is limited, and local sources become more important. Indeed, ship traffic emissions in Longyearbyen and Ny-Ålesund promoted significant increase in SO₂ and NO_x concentrations and slight decrease of the O₃ values. Measurements in Barentsburg revealed strong temporarily deterioration of local air quality because of adverse weather conditions promoting transport of polluted air from the local coal power plant to the town. The cases of enhanced accumulation of local ground-level pollution have been revealed in Longyearbyen as well. They have often coincided with long-range transport events when the advection of warm air from mid-latitudes to Svalbard promoted creation of strong temperature inversions and led to increased concentrations of BC detected by the ground-based instrument and in the vertical profiles below 1000 m.

Svalbard archipelago is an area with complex topography. This creates a pronounced spatial and vertical variation in the concentrations of SLCFs. Thus, the springtime NO_x observations demonstrated that there is little correspondence between the data from the three stations. The concentrations of these compounds are controlled by local sources and mostly dependent on prevailing wind direction in each of the settlements. Comparison of the daily SO₂ and sulphate concentrations accumulated in filter samples collected at the low-altitude station in Ny-Ålesund and at the Zeppelin mountain observatory revealed a significant difference in the data obtained at different heights. The correspondence between the observations varies seasonally. It is the best in winter due to stronger winds, more efficient mixing and absence of additional local sources of pollution. In contrast, the correspondence between the two datasets is lowest in summer when insufficient ventilation of atmospheric boundary layer combined with increased emissions from local ship traffic promote accumulation of pollution in the settlement, while the station at the mountain top is often located above the cloud base level and is unaffected by the local emissions.

Acknowledgements

First of all I would like to thank my beloved husband Vitaly for his patience and support. He has always been willing to stay with me till late evening at the University when needed, discuss my work on the way home, and help me with the practicalities at home. Besides, he has been a skilful and smart field assistant and helped me a lot with electronic equipment and data processing during my fieldwork in Longyearbyen in 2018.

I would like to thank my supervisors Associate Professor Kåre Edvardsen and Professor Rune Graversen for all the support which I received during the work on the articles included in current thesis and for giving me the opportunity to develop my own research ideas. I also appreciate your invaluable advice on scientific content and language corrections. In addition, Rune, I am very grateful for your patience, since the last year of the PhD work has been very busy for me and I have been responsible for the external research project while writing my last papers and the thesis at the same time.

I am very thankful to my supervisor Dr. Kim Holmén for fruitful discussions, critical reviews of my articles and logistical support during the fieldwork. Without his guidance in designing of the fields campaigns and help with the access to the data and research infrastructure in Svalbard none of the papers included in the current thesis would have seen the light.

Part of my PhD work has been done in Longyearbyen. There I have always felt myself welcomed at the University Centre in Svalbard (UNIS) where the UNIS staff and employees of the Norwegian Polar Institute provided me with all the practical support needed for my field studies. I am also very grateful for all the knowledge which I have obtained at the two PhD courses taken at UNIS. Although studies there have been challenging, the learning environment has been perfect and I still keep in touch with my fellow students.

I appreciate a lot the openness and engagement of the researchers from the Ny-Ålesund Atmosphere Flagship and Italian Aerosol Society who supported and encouraged my research initiatives. This allowed me to apply for an external grant from the Research Council of Norway and successfully manage my first extensive international scientific project.

Very special gratitude goes to Taimur Rashid, Helene Xue, Johana Evelyn M. Castilla and Albara Mustafa for sharing the office with me and creating a great and friendly working environment. It has been always nice to talk to you during the coffee breaks and discuss some serious and funny things.

A final gratitude goes to all my colleagues at the UiT The Arctic University of Norway for an excellent and friendly working atmosphere. It has also been a pleasure to get to know all the other colleagues during the common social gatherings at the Technology building and trips to Harstad, London, Sommarøy and Helsinki. I would also like to thank the Head of my department Tor Schive, senior advisers Arne Ketil Eidsvik and Helge Lagaard for all the administrative support that I have got for the external research and education projects, which I have managed.

Table of Contents

Abstract.....	vii
Acknowledgements.....	ix
List of Tables.....	xiii
List of Figures.....	xiii
Abbreviations.....	xv
List of appended papers.....	xvii
Part I Thesis summary.....	1
1. Introduction and background.....	3
1.1 Research motivation and problem statement.....	8
1.2 Research questions.....	9
1.3 Research objectives.....	9
2. Methodology.....	11
2.1 Chemistry of SO ₂ , NO _x , O ₃ and BC.....	11
2.2 Meteorological processes affecting air pollution transport and in-situ pollution dispersion.....	13
2.3 Observations.....	15
2.3.1 Measurement sites.....	15
2.3.2 Stationary and portable measurement equipment.....	16
2.4 Reanalysis and trajectory model data.....	17
2.5 Statistical approach.....	17
2.5.1 Kolmogorov-Smirnov test for normality.....	17
2.5.2 Wilcoxon rank sum test.....	18
2.5.3 Pearson and Spearman correlation.....	19
2.5.4 Monte Carlo method.....	19
3. Discussion of the results.....	21
3.1 Paper I.....	21
3.2 Paper II.....	22
3.3 Paper III.....	24
3.4 Paper IV.....	28
3.5 Summary of the appended papers.....	33
4. Research contributions and suggestions for future work.....	35
4.1 Research contributions.....	35
4.1.1 Causes of the pollutant concentrations variation on a different temporal scale.....	35
4.1.2 Spatial variation of the pollutant concentrations between the three main Svalbard settlements.....	36
4.1.3 Influence of ship traffic on air quality in Svalbard settlements.....	37

4.1.4 Meteorological phenomena affecting the ground level concentration of measured compounds and their vertical distribution in the ABL.....	38
4.1.5 Advantages and disadvantages of usage of different measurement techniques for air pollution monitoring in the Arctic	39
4.2 Suggestions for future work	40
References.....	43
Part II Appended papers	49
Paper I	51
Paper II.....	63
Paper III	81
Paper IV	125

List of Tables

Table 1 Accuracy and measurement range for the stationary Onset sensors installed at the UNIS roof and Kestrel 5500 sensors.....	17
Table 2 Authors contributions in Paper I.....	21
Table 3 Authors contributions in Paper II	22
Table 4 Authors contributions in Paper III.....	25
Table 5 Authors contributions in Paper IV.....	28
Table 6 Appended papers addressing the research questions	33

List of Figures

Figure 1 Definitions of the Arctic region (Fig. 1.1 in AMAP 2009).....	3
Figure 2 Map of Svalbard.....	6
Figure 3 Radiative forcing bar chart for the period 1750–2011 based on emitted compounds (gases, aerosols or aerosol precursors) or other changes (Fig. 8.17 in IPCC, 2013)	7
Figure 4 Atmospheric nitrogen cycle (Fig. 3.2 in AMAP, 2006).....	11
Figure 5 Tropospheric O ₃ chemistry where HO _x and RO ₂ are peroxy radicals, R is alkyl radical, H ₂ O ₂ and ROOH are hydrogen and organic hydroperoxides, respectively.....	12
Figure 6 Atmospheric sulphur cycle (Fig. 3.1 in AMAP, 2006).....	13
Figure 7 Mean winter and summer position of the arctic front defining the percentage frequency of major south-to-north transport routes into the Arctic in summer (July) and winter (January) (Fig. 4.1 in AMAP, 2006).....	14
Figure 8 Diagram of the statistically significant factors of influence based on the results of the WRS-test (p < 0.05)	24
Figure 9 Snowmobile route produced using GPS log. The locations of Kestrel stations (001-003) and UNIS automatic weather station (AWS) are shown by the red circles	25
Figure 10 a) Kestrel station installed in Mohnbukta; b) project manager Alena Dekhtyareva with Cairpol NO ₂ sensor attached to the arm to measure NO ₂ concentration during the field trip	26
Figure 11 Comparison of Kestrel and AWS data and correlation coefficients for the: a) wind speed; b) air temperature	30
Figure 12 a) Summer wind roses for 2009, 2010 and 2018; b) NO _x concentration averaged over wind directions for 2009, 2010 and 2018.....	32
Figure 13 NO _x (a) and SO ₂ (b) concentrations (µg·m ⁻³) averaged over wind directions in presence and absence of ships in July and August 2009, 2010 and 2018	33

Abbreviations

Chemical compounds and abbreviations	
AOD	Aerosol optical depth
BC	Black Carbon
CO	Carbon monoxide
NO	Nitrogen monoxide
NO ₂	Nitrogen dioxide
NO _x	Nitrogen oxides
OH	Hydroxyl radical
O ₃	Ozone
PAH	Polycyclic aromatic hydrocarbon
PAN	Peroxy acetyl nitrate
PM	Particulate matter
SO ₂	Sulphur dioxide
VOC	Volatile organic compound
XSO ₄ ²⁻	Non-sea salt sulphate

General abbreviations	
AARI	Russian Arctic and Antarctic Institute
ABL	Atmospheric boundary layer
AWS	Automatic weather station
GT	Gross tonnage
LD	Limit of detection
RF	Radiative forcing
SLCF	Short-lived climate forcer
UNIS	University Centre in Svalbard
WRS-test	Wilcoxon rank sum test

List of appended papers

Paper 1 Dekhtyareva A., Edvardsen K., Holmén K., Hermansen O., & Hansson H.-C., 2016. Influence of local and regional air pollution on atmospheric measurements in Ny-Ålesund. *International Journal of Sustainable Development and Planning*, 11 (4), 578–587. DOI: 10.2495/SDP-V11-N4-578-587

Paper 2 Dekhtyareva A., Holmén K., Maturilli M., Hermansen O., & Graversen R., 2018. Effect of seasonal mesoscale and microscale meteorological conditions in Ny-Ålesund on results of monitoring of long-range transported pollution. *Polar Research*, 37 (1), 1508196. DOI: 10.1080/17518369.2018.1508196

Paper 3 Dekhtyareva A., Hermansen M., Nikulina A., Hermansen O., Svendby T., Graversen R., & Holmén K., 2019. Springtime nitrogen oxides and tropospheric ozone in Svalbard: results from the measurement station network. *Manuscript ready for submission*

Paper 4 Dekhtyareva A., Drotikova T., Nikulina A., Hermansen O., Chernov D.G., Mateos D., Herreras M., Petroselli C., Ferrero L., Gregorič A., 2019. Summer air pollution in Svalbard: emission sources, meteorology and air quality. *Manuscript ready for submission*

Part I Thesis summary

1. Introduction and background

The Arctic region may be defined geographically by the Arctic Circle, climate, vegetation and marine boundaries (Figure 1). In the area north of the Arctic Circle, midnight sun and polar night last at least 24 hours continuously each year. The mean air temperature in July in the region set by the climatic boundaries is below 10 °C. Vegetation boundaries are stated by the treeline, a transition zone between the boreal forest and tundra vegetation. The Arctic ecosystems are often interdependent and consist primarily of cold-adapted biota vulnerable to climate change that alters physical, biogeochemical, and ecological processes (Vincent *et al.*, 2011). On the marine boundaries of the Arctic, warmer and saltier waters from oceans to the south interact with surface waters from the Arctic Ocean, which have lower temperature and salinity. The area, limited by the red line in the Figure 1, is defined as the Arctic by the Arctic Monitoring and Assessment Programme from the perspective of monitoring and assessing the status of and threats to the environment and health of residents in the region (AMAP, 1998).

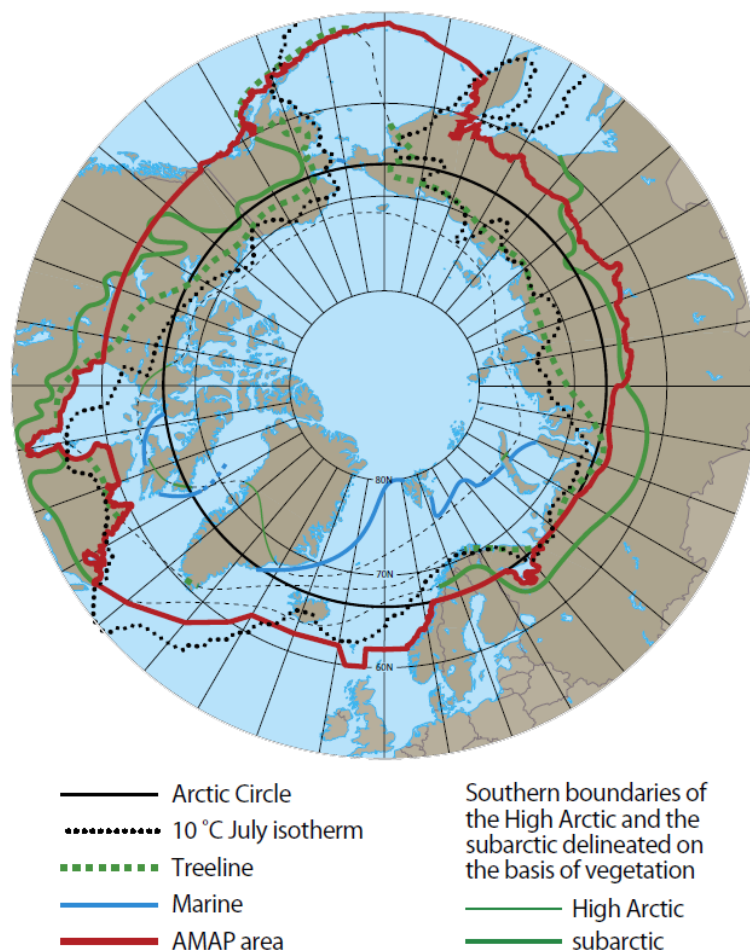


Figure 1 Definitions of the Arctic region (Fig. 1.1 in AMAP 2009)

The population density and urbanization rate varies significantly within the Arctic region (Nuttall, 2012). Lack of infrastructure poses limitations on the development of industrial activities in the Arctic, such as natural resource extraction, shipping and tourism. However, the climate change stimulates the melting of the sea ice, thus creating new opportunities for

improvement of physical connection within the Arctic (Christopher and Fast, 2008). Indeed, the area covered by the annual summer sea ice declines steadily, and ice-free summers are predicted to occur in the perspective of several decades. The oil and gas, shipping and fishing activities in the Arctic have increased to a notably large extent over the last years, and further development of these industrial sectors in the region is likely to happen (Dalsøren *et al.*, 2007).

As a consequence, emissions of such pollutants as nitrogen monoxide (NO), nitrogen dioxide (NO₂), nitrogen oxides (NO+NO₂=NO_x), sulphur dioxide (SO₂), carbon monoxide (CO), volatile organic compounds (VOCs) and BC (Black Carbon) are expected to rise (Dalsøren *et al.*, 2009; Peters *et al.*, 2011). Increased emissions from shipping activities lead to elevated concentrations of NO_x, SO₂, O₃ and BC and rise the number of fine particles with diameter less than 2.5 µm (PM_{2.5}). These substances also have negative effect on human health and are included in the standard air quality observations in urban areas. Long-term exposure to elevated concentrations of PM_{2.5} can cause chronic cardiovascular diseases. Daily variations in BC concentrations are associated with short-term health changes. In addition to this, BC, as a component of PM, may carry toxic chemicals such as polycyclic aromatic hydrocarbons (PAHs) to the lungs and possibly introduce them to the systemic blood circulation (Janssen *et al.*, 2012).

Besides, SO₂ and NO_x emissions may have negative impact on the ecosystems due to acidification of fresh-water, marine and terrestrial environments. The Arctic vegetation is especially sensitive to air pollution due to multiple factors of influence such as climate change and long exposure to sunlight in summertime (Eriksen *et al.*, 2012; Futsaether *et al.*, 2015). At the same time, nitrates produced from NO_x can act as fertilizers to local ecosystems, especially if deposited in nutrients limited Arctic areas (AMAP, 2006).

Increasing anthropogenic activity in the region is one of the reasons to study the local emissions in order to investigate their influence on the near pristine Arctic environment.

In addition to local atmospheric emissions from the above mentioned activities, there is a seasonal long-range transport of air pollution to the region known as Arctic haze (Quinn *et al.*, 2007). SO₂ and non-sea salt sulphate (XSO₄²⁻), along with BC, are the most studied compounds present in the Arctic haze. The air transport efficiency from mid-latitudes towards the North pole depends on the location of the Arctic front and varies seasonally (AMAP, 2006). This transport pattern is most pronounced in winter and spring when specific conditions affecting environmental fate of the atmospheric pollutants are present. For example, lack of sunlight during polar night restricts photochemical reactions, while low air temperatures slow down certain chemical reactions such as thermal decomposition of peroxy acetyl nitrate (PAN). At the same time, low atmospheric humidity decreases the hygroscopic growth of aerosol particles and hampers dry deposition since the efficiency of that process depends on the particle mass. The precipitation is rare, and wet deposition is scarce. These factors lead to prolonged lifetime of the particles in the air masses (Seinfeld and Pandis, 2006).

As the Arctic is warming faster than the rest of the world, especially in winter (Richter-Menge and Mathis, 2017), the conditions preventing removal of pollutants from the air masses during transportation are changing. Increased air temperature, humidity and

precipitation rate may intensify wet deposition of pollutants (Qi *et al.*, 2017). In addition to this, the concentrations of tropospheric ozone (O₃) have increased over last 100 years. Along with several competing climate-dependent factors such as amount of biogenic emissions, water vapour abundance and change of convection and lightning, O₃ may increase the atmospheric abundance of hydroxyl radical (OH), and consequently, the oxidative capacity of the atmosphere, causing reduction in the lifetime of air pollutants (Alexander and Mickley, 2015). Besides, the SO₂ emissions in European countries have declined over the last twenty-five years (Vestreng *et al.*, 2007), while emissions from Asian sources slightly increased (Lu *et al.*, 2010). Thus, it may have affected the concentrations of long-range transported pollutants measured in the Arctic.

The current work focuses on Svalbard, since the archipelago has unique characteristics, which allow us to study ongoing alteration in atmospheric composition and physical processes due to the change in anthropogenic activities and environmental response to the climate change.

Firstly, Svalbard is warming faster than the most of the Arctic territories (Isaksen *et al.*, 2016). Since the region is located on the marine Arctic boundary (Figure 1), several factors contribute to this accelerated warming rate observed there: change in the inflow and temperature of North-Atlantic water on the west coast of Spitzbergen island, sea ice decline, change in atmospheric circulation patterns and properties of air masses (Piechura and Walczowski, 2009; Maturilli, Herber and König-Langlo, 2013; Onarheim *et al.*, 2014; Isaksen *et al.*, 2016; Dahlke and Maturilli, 2017; Maturilli and Kayser, 2017).

Secondly, there are few regional and local sources of air pollution at Spitzbergen, the archipelagos biggest island, thus it is easier to estimate the change in amount of long-range transported and local air pollution, and study the effects of these factors on atmospheric physical and chemical processes.

Long-term observations of atmospheric compounds performed at the Zeppelin station in Ny-Ålesund, a research settlement in the north-western part of the island (Figure 2), allow us to investigate the change in efficiency of long-range transport of air pollutants from mid-latitudes to this region. Hirdman *et al.*, 2010 attributed the significant negative long-term trend in concentrations of elemental BC and sulphate aerosol observed at the Zeppelin station to the reduction in European emissions. However, change in environmental conditions may affect the lifetime of aerosols as well. For example, the aerosol scavenging efficiency varies for different cloud types: it is lowest for ice-phase clouds and increases for warmer mixed-phase clouds (Eckhardt *et al.*, 2015). The sea ice melting facilitates the vertical transfer of moisture which contributes to the liquid cloud phase and may result to the increase of mixed-phase clouds occurrence over the Arctic (Mioche *et al.*, 2015). Long-term radiosonde and ground-based observations in Ny-Ålesund revealed a strong increase in atmospheric temperature and humidity (Maturilli, Herber and König-Langlo, 2013; Maturilli and Kayser, 2017), and the long-term projections for precipitation and temperature in Svalbard indicate further increase (Førland *et al.*, 2011). Moreover, the precipitation over the Arctic is predicted to monotonically increase towards the end of the century (Kusunoki, Mizuta and Hosaka, 2015). Thus, because of changes in the properties of air masses arriving to Svalbard and reduction of European emissions, the concentrations of long-range

transported SO_2 and XSO_4^{2-} have been decreasing and may further decrease in future. In contrast, local sources of emissions may play increasingly important role and deserve special attention.



Figure 2 Map of Svalbard

At the same time, not only long-range transport of air pollutants is affected by the climate change. Local meteorological processes are altered as well. For example, the frequency of decoupling of atmospheric boundary layer (ABL) from free troposphere has increased and the wind speed in the lowest 500m has reduced in all seasons in the period from 1993 to 2014 (Maturilli and Kayser, 2017). This may negatively affect the ventilation within ABL and lead to the accumulation of locally produced primary and secondary atmospheric aerosols of natural and anthropogenic origin. They play an important role in the cloud formation processes (Possner, Ekman and Lohmann, 2017; Jung *et al.*, 2018; Mahmood *et al.*, 2019) which, in turn, are altered by the observed change in air temperature and humidity (Maturilli and Kayser, 2017).

Current study focuses on short-lived climate forcers (SLCFs) which concentrations are increasing because of fossil fuel combustion: SO_2 , NO_x , O_3 and BC. The change in energy flux at the tropopause or at the top of the atmosphere caused by a specific climate driver is called the radiative forcing (RF) (IPCC, 2013). When the increased concentration of the forcer increases the difference between the energy absorbed by the Earth and radiated back to space, the RF is positive and leads to atmospheric warming. In contrast, the driver has

negative RF, when its increased concentration leads to cooling of the atmosphere. Thus, SO₂ and NO_x have negative RF due to formation of light scattering aerosols containing sulphates and nitrates (Figure 3).

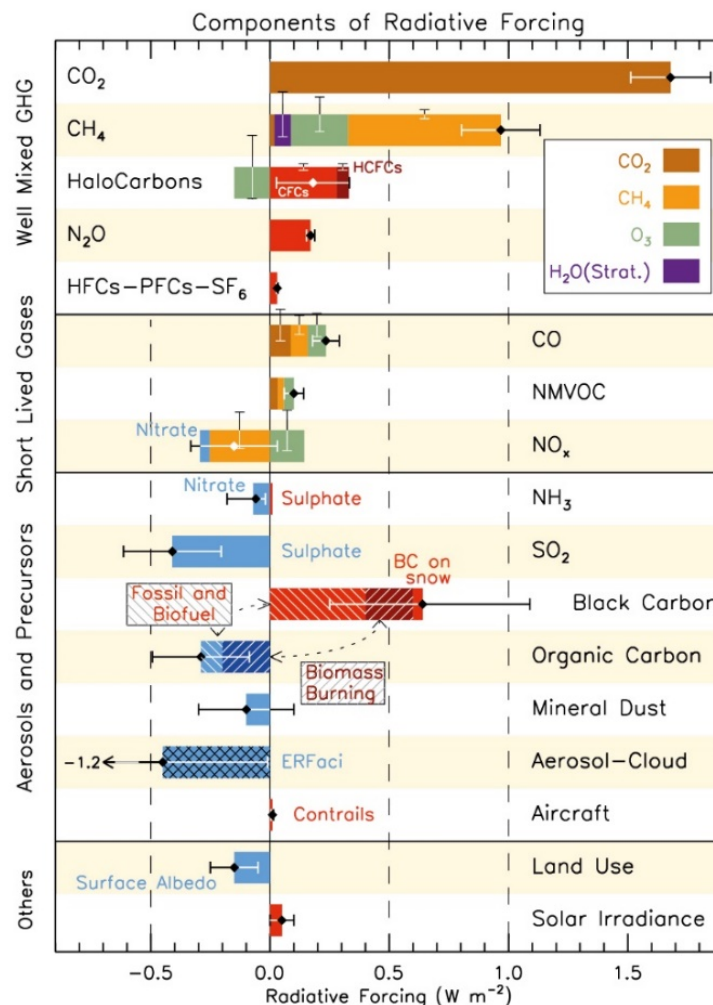


Figure 3 Radiative forcing bar chart for the period 1750–2011 based on emitted compounds (gases, aerosols or aerosol precursors) or other changes (Fig. 8.17 in IPCC, 2013)

Although the total aerosol-cloud interaction has negative radiative forcing of climate (IPCC, 2013), thin Arctic clouds in winter and early spring have positive radiative forcing due to increased downward long-wave radiation, and this effect is enhanced when the anthropogenic aerosols are present (Garrett and Zhao, 2006). In turn, the light absorbing aerosols have significant positive radiative forcing through aerosol-radiation interactions and when deposited on snow and ice because of reduction of surface albedo (IPCC, 2013). However, NO_x also have a positive RF due to formation of tropospheric O₃, a potent greenhouse gas, in presence of CO and VOCs. BC is a component of light-absorbing aerosols, and thus has strongly positive RF. In the real atmosphere the RF of aerosols depends on the ambient relative humidity, which varies strongly horizontally and vertically, aerosol size distribution and refractive index that depends on aerosol composition (Myhre *et al.*, 2004).

A recent modelling study of Sand et al. 2015 stated that the major contribution to the Arctic warming comes due to Asian emissions of the SLCFs, which increase the heating rate in the source region, and therefore affect the equator-pole temperature gradient. However, the regional sensitivity to local emissions within the Arctic is very high due to enhanced warming impact from BC deposited on snow and ice covered surfaces. Indeed, the simulations with additional ship emissions in the Arctic showed significant local increase in RF due to BC deposition over the central Arctic Ocean, but the net cooling effect from the aerosols and their precursors is expected (Gilgen *et al.*, 2018). Similarly, Ødemark *et al.*, 2012 have estimated positive RF from increased BC and O₃ concentrations, but the total negative RF due to formation of sulphate and nitrate containing aerosols from emissions of SO₂ and NO_x because of shipping activity.

1.1 Research motivation and problem statement

There are two factors that make it challenging to assess the current environmental impact of local Arctic emissions and make prognoses for the future. First one is the uncertainty in emission inventories, since, in addition to existing stationary emission sources, there is an ongoing increase of local emissions from shipping. Second factor is the uncertainty in environmental fate of air pollutants due to the lack of meteorological and air pollution observations in the region. Previous studies state that air pollution from local emission sources is an important, but an underestimated issue, and that pollution levels within the region may exceed air quality standards, pose a negative impact on the health of residents and environment (Schmale et al., 2018).

Similarly, the long-range transport of NO_x, SO₂, O₃ and BC to Svalbard has been studied extensively, while little attention has been given to the local sources of these compounds and meteorological conditions promoting in-situ pollution accumulation. For example, last and the only study about influence of shipping emissions on air quality in Svalbard has been based on ten years old data from Ny-Ålesund, while no extensive air quality studies have been performed previously in other Svalbard communities.

Ny-Ålesund is located more than 100km away from the biggest Svalbard settlements. The remoteness and measures, which are applied to reduce anthropogenic impact on the research activity, offer unique opportunities for monitoring of background air composition (The Research Council of Norway, 2019).

However, in contrast to the near pristine Ny-Ålesund environment, there are also places in Svalbard where the anthropogenic activity may significantly affect local air quality. The two mining towns, Longyearbyen and Barentsburg, are located to the south-east from the research settlement. Although the installation of exhaust treatment system on the coal power plant in Longyearbyen led to dramatic reduction of emissions there (Miljødirektoratet, 2019), the Barentsburg coal power plant is still the biggest point source of SO₂ in Norway (Miljødirektoratet, 2018). However, no air quality measurements have been available to assess the magnitude of pollutant concentrations accumulating under different meteorological conditions in these towns.

The current work allows us to combine the air quality studies with monitoring of SLCFs in Svalbard and assess the current concentrations of anthropogenic SLCFs and environmental factors that promote long-range transportation and accumulation of local air pollution in the Svalbard settlements. This study attempts to create a network from existing and temporarily pilot stations and assess the measurement results obtained using the conventional and portable low-cost sensors in Svalbard.

1.2 Research questions

Based on the proposed problem statement, five research questions have been produced:

1. What causes variation in the pollutant concentrations on a different temporal scale (seasonally, daily and diurnally)?
2. How do the pollutant concentrations vary spatially between the three main Svalbard settlements?
3. What is the current influence of ship traffic on air quality in Svalbard settlements?
4. What meteorological phenomena affect the ground level concentration of measured compounds and their vertical distribution in the ABL?
5. What are the advantages and disadvantages of usage of different measurement techniques for air pollution monitoring in the Arctic?

1.3 Research objectives

The following objectives have been performed to answer to the research questions stated above:

- Investigate the long-range transport of air pollution to Svalbard and explore the existing techniques to study it.
- Analyse data series to identify factors affecting long-term observations of long-range transported pollution.
- Perform ground-based SO₂, NO_x, O₃ and BC measurements in Longyearbyen and analyse the acquired data along with the measurement results from Ny-Ålesund and Barentsburg.
- Identify major emission sources in all three settlements and their influence on local air quality.
- Test portable sensors to measure air quality and meteorological parameters and assess performance of these sensors.
- Perform vertical meteorological and air quality measurements in Longyearbyen and identify what affects the vertical distribution of air pollutants.

2. Methodology

The current study focuses on measurements of four SLCFs in Svalbard: SO_2 , NO_x , O_3 and BC. Paper I and II discuss SO_2 and NO_x sources, chemical transformations and factors affecting their ambient concentration in Ny-Ålesund. Paper III considers springtime NO_x and O_3 concentrations measured in Longyearbyen, Ny-Ålesund and Barentsburg in 2017 and atmospheric chemistry of these compounds. Paper IV presents extensive summer measurements of all four compounds performed in the three major Svalbard settlements in 2018 and determines contribution of various local and long-range sources to air quality in Spitzbergen.

2.1 Chemistry of SO_2 , NO_x , O_3 and BC

SO_2 , NO_x and BC are emitted directly in the process of fossil fuel combustion, while O_3 may be produced in the presence of NO_x , VOCs and CO. The atmospheric cycles of nitrogen compounds, O_3 and sulphur compounds are illustrated in Figure 4, Figure 5 and Figure 6, respectively. This work focuses on the small part of the reactions from combustion to NO and NO_2 formation and reactions which may lead to increasing and decreasing of O_3 concentrations in the troposphere (Figure 4).

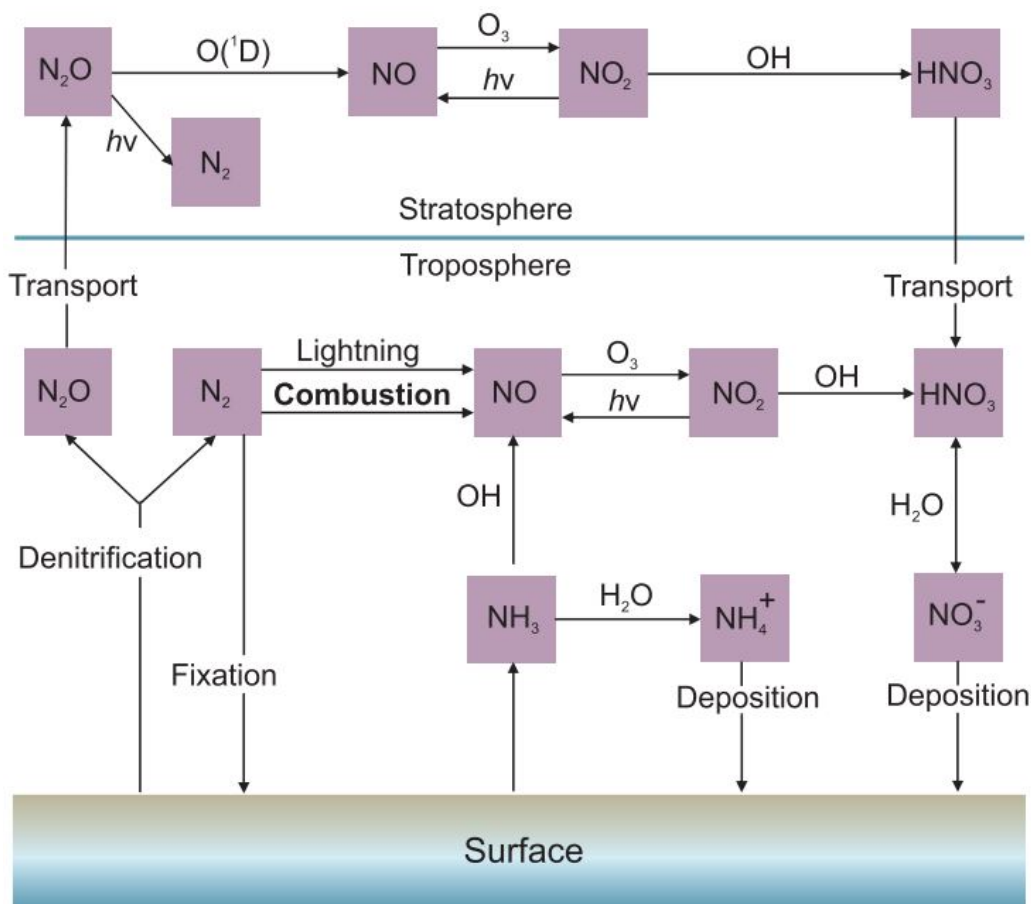


Figure 4 Atmospheric nitrogen cycle (Fig. 3.2 in AMAP, 2006)

The formation of tropospheric O₃ is a non-linear process depending on the ratio between NO_x and VOCs (hydrocarbons (RH) in Figure 5 (Fan and Jacob, 1992; Jacob, 2000; Monks, 2005)). The reactions between O₃ precursors (NO_x, CO and RH), which may lead to O₃ production in the presence of sunlight, are depicted by the two cycles on the right side of the Figure 5. In the VOCs-limited regime, O₃ concentration may decrease due to titration with excess of NO. The production of O₃ in the NO_x-limited regime is independent on VOCs amounts and increases with rising of NO_x concentration. Despite the fact that the concentrations of non-methane hydrocarbons increases with latitude due to long-range transport of pollution (Helmig *et al.*, 2016), the average values in the pristine Arctic environment are lower than in industrial areas, and therefore VOCs-limited regime is expected close to big sources of NO_x such as ships and fossil-fuelled power plants. Further downwind from the source, NO_x are removed from the plume faster and NO_x/VOCs ratio sufficient for O₃ production may be obtained. Similarly, the O₃ production is more efficient in the Arctic, downwind from boreal fires, than in the vicinity of the biomass burning areas (Monks *et al.*, 2015). In the left side of the Figure 5, the heterogeneous photochemical reactions with bromine species on snow or sea-ice surfaces, which may result to springtime tropospheric O₃ depletion in the Arctic, are illustrated (Fan and Jacob, 1992; Monks, 2005).

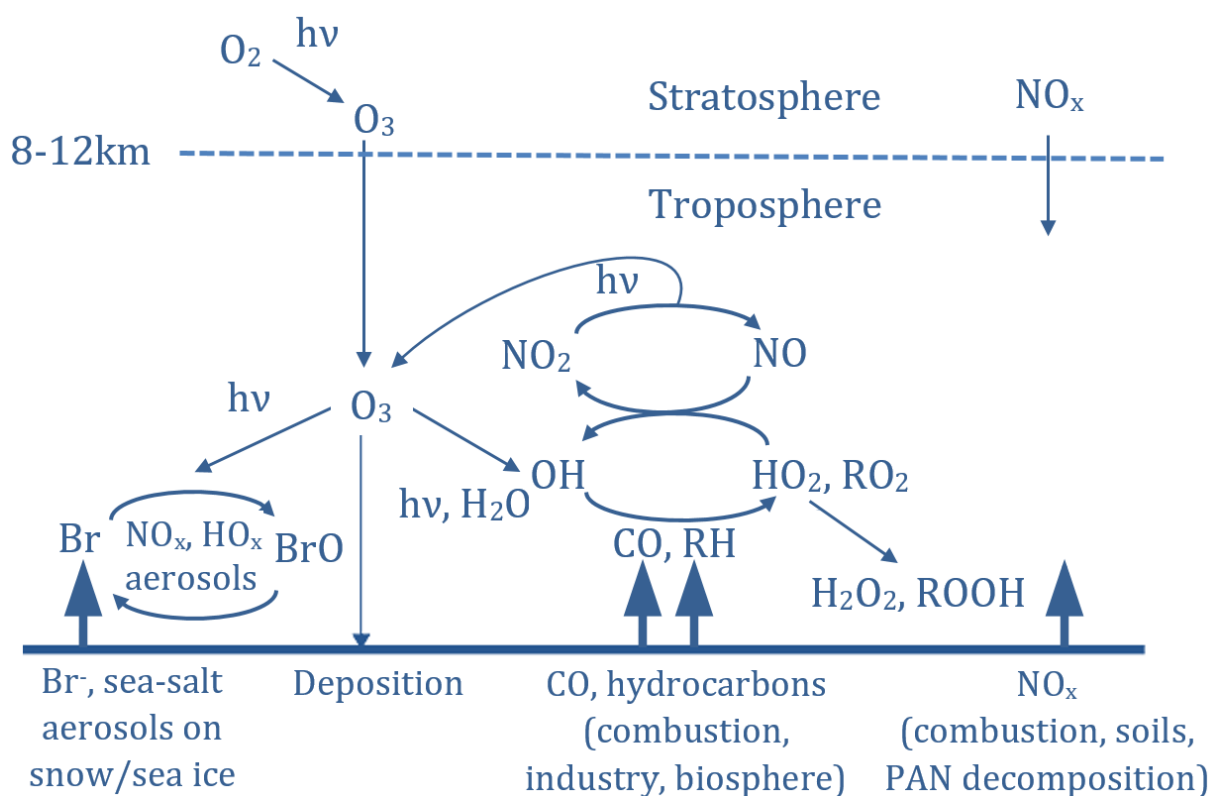


Figure 5 Tropospheric O₃ chemistry where HO_x and RO₂ are peroxy radicals, R is alkyl radical, H₂O₂ and ROOH are hydrogen and organic hydroperoxides, respectively.

The part of the atmospheric sulphur cycle shown in Figure 6, which describes emissions of SO₂ and its precursors and formation of sulphate aerosols, in the troposphere is studied in the current work.

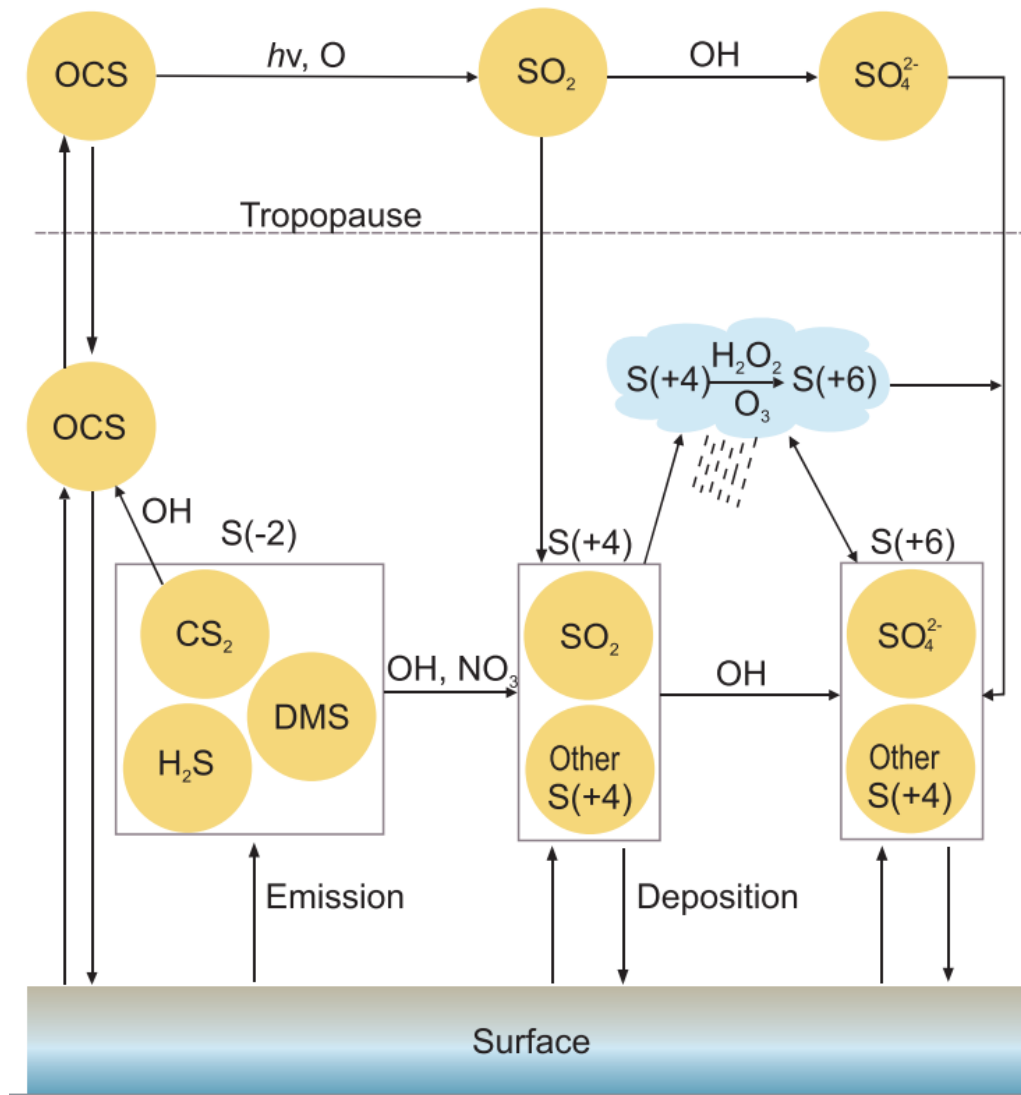
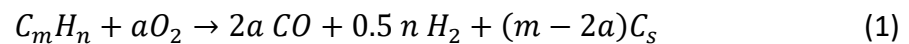


Figure 6 Atmospheric sulphur cycle (Fig. 3.1 in AMAP, 2006)

Another compound, which has been studied in the present work, is BC. It is a main component in soot. The soot is formed in a process of incomplete combustion, and the formation efficiency depends on the ratio of carbon to oxygen (C/O) in the mixture of hydrocarbons and air. For example, if $C/O = m/2a$, following combustion stoichiometry is obtained (Seinfeld and Pandis, 2006):



where C_s is the soot formed.

2.2 Meteorological processes affecting air pollution transport and in-situ pollution dispersion

As Arctic front extends southerly during winter and spring (Figure 7), the long-range transport of pollutants intensifies (Stohl, 2006).

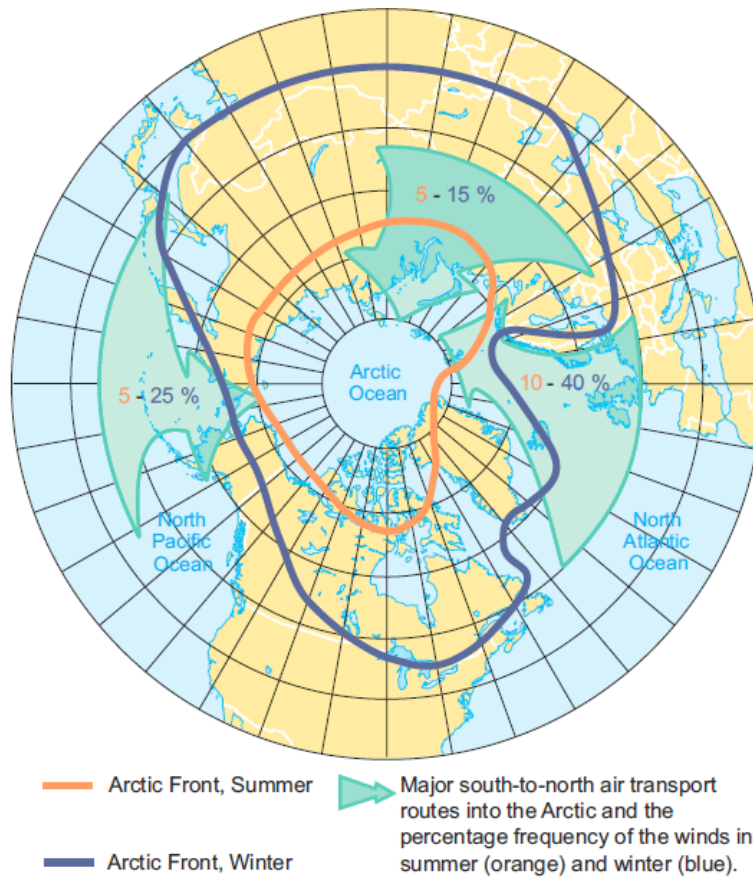


Figure 7 Mean winter and summer position of the arctic front defining the percentage frequency of major south-to-north transport routes into the Arctic in summer (July) and winter (January) (Fig. 4.1 in AMAP, 2006)

In these seasons, the Arctic haze, an anthropogenic aerosol consisting primarily of sulphate containing particles in accumulation mode, has been repeatedly observed in Svalbard and other Arctic regions (Heintzenberg, Hansson and Lannefors, 1981; AMAP, 2006; Quinn *et al.*, 2007). Low air temperature and humidity and lack of sunlight during the polar night extend the lifetime of SLCFs due to reduction of wet scavenging and limited photochemical oxidation (Seinfeld and Pandis, 2006).

At the same time, there are local year-round air pollution sources in Svalbard, which may increase the concentrations of SLCFs in the ABL such as coal power plants in Barentsburg and Longyearbyen and diesel generator in Ny-Ålesund, and seasonally important sources, namely, the ship traffic and biogenic emissions of SO₂ precursors. Calm winds and temperature inversions reduce the efficiency of air pollution dispersion (Arya, 1999). Although the median wind speed is lowest in summer and increases in winter in Svalbard (Maturilli, Herber and König-Langlo, 2013), the frequency of occurrence of temperature inversions is higher in winter as well, because the air is more often stably stratified due to radiative cooling of snow and ice-covered surfaces (Vihma *et al.*, 2011). However, it has been shown that the reduction of the sea ice extent around Svalbard increases the sea-atmosphere energy transfer and decreases the efficiency of inversion formation under the

same high-pressure situations with calm winds, which favour this process over the sea ice (Isaksen *et al.*, 2016).

Using the methodology proposed by Vihma *et al.*, 2011, the temperature inversions have been identified in the radiosonde and tethered balloon profiles as layers thicker than 10 m where the air temperature increases with height on more than 0.3 °C. Additional method to determine the stability in the ABL, suitable for the sites where the airborne measurements have not been performed, but the meteorological observations at two different heights have been available, is to calculate the Richardson number as the ratio between the buoyancy and wind shear terms.

The gradient Richardson number (Arya, 1999) has been calculated for the case study in Barentsburg described in the Paper IV:

$$Ri_m = \frac{g}{T_0} \frac{\overline{\Delta\theta} z_m}{\overline{\Delta u}^2} \ln\left(\frac{z_2}{z_1}\right) \quad (2)$$

where T_0 is the mean temperature for two heights ($z_1=70$ m and $z_2=255$ m), $z_m = (z_1 \cdot z_2)^{1/2}$ is the geometric mean height, $\overline{\Delta\theta}$ - potential temperature difference between z_1 and z_2 , $\overline{\Delta u}$ is wind speed difference between z_1 and z_2 .

The potential temperature, in turn, has been calculated as (Arya, 1999)

$$\theta = T \left(\frac{1000}{p}\right)^k \quad (3)$$

where T is the measured temperature in K, p is atmospheric pressure in millibars, $k \approx 0.286$ is the ratio between the specific gas constant $R=287.04$ J K⁻¹ kg⁻¹ and the specific heat capacity for dry air at constant pressure $C_p \approx 1005$ J K⁻¹ kg⁻¹.

2.3 Observations

2.3.1 Measurement sites

Three different measurement sites have been chosen in this work: Ny-Ålesund, Barentsburg and Longyearbyen (Figure 2). There is an established research infrastructure within the field of the monitoring of atmospheric composition in the first two settlements. High-quality long-term measurements of background air composition, including O₃ and BC concentration, are performed by the Norwegian Institute of Air Research at the Zeppelin station located at the mountaintop (474 m a.s.l.) two kilometres to the south-east from Ny-Ålesund, while SO₂ and NO_x monitors have been installed in the middle of the village to study the local air quality since 2008. In Barentsburg, SO₂, O₃, NO_x and meteorological measurements are performed continuously by the Russian Arctic and Antarctic Institute (AARI) since 2017. Aerosol observations such as BC and aerosol optical depth data are collected by the AARI specialists for the V.E. Zuev Institute of Atmospheric Optics of Siberian Branch of the Russian Academy of Science. Although there are several automatic meteorological stations around Longyearbyen operated by the University Centre in Svalbard (UNIS), there is no continuous measurements of atmospheric composition in the town. Short-term observations of NO_x and

NO_x, SO₂, O₃ and BC were performed by Alena Dekhtyareva in Longyearbyen in spring 2017 and summer 2018, respectively.

2.3.2 Stationary and portable measurement equipment

Hourly data from stationary chemiluminescence NO_x, UV fluorescence SO₂ and UV photometric O₃ analysers and aethalometers have been studied in the current work. The data from different instrument models with the same measurement principle have been available from Ny-Ålesund, Longyearbyen and Barentsburg. This adds some uncertainty to the comparison of measurement results from the three settlements in addition to the different calibration procedure employed there. Beside the hourly data, daily SO₂ and XSO₄²⁻ concentrations accumulated in filter samples collected in Ny-Ålesund have been analysed (NILU, 1996). The data from the condensation particle counters and sun photometers have been studied in addition to the main measurements stated above.

Several portable environmental sensors have been used during the fieldwork in Longyearbyen in spring 2017 and summer 2018.

A broad variety of low-cost sensors is available in the market, however, the performance of the sensors varies significantly (Jiao et al., 2016; Castell et al., 2017). During the fieldwork in Svalbard, three types of sensors for gaseous and particle measurements (Cairpol NO₂ electrochemical sensor, MiniDISC particle counter and microaethalometer AE51 for BC measurements) and the portable weather trackers Kestrel 5500 have been used.

The low-cost mobile gas sensors is a new technological solution for environmental monitoring (Jiao et al., 2016). Advantages of these devices is that they are portable and relatively inexpensive, while disadvantages are decrease in sensitivity with time and measurement interference with other gases. Therefore, the sensors cannot be used alone to measure ambient air concentration without a reference monitor. Thus, combined usage of stationary reference device and mobile sensors may cover broader spectrum of detectable concentrations and may be used for the observations close to the pollution source.

Cairpol is a portable NO₂ sensor for air pollution studies. The sensor may give reliable NO₂ measurement results when higher concentrations than those that are typical for ambient air on rural site are sampled. Therefore, this sensor may be suitable for evaluation of emissions from snowmobiles in the immediate vicinity of the source of pollution.

Main disadvantage of portable gas and particle sensors is their high limit of detection (LD). According to the instruments manufacturers, LD of Cairpol NO₂ sensors is 20ppb, LD of AE51=50-100 ng·m⁻³ (5 minute resolution), while measurement range of the MiniDISC particle counter is 10³-10⁶ particles per cm³ (Fierz *et al.*, 2011). Although high reproducibility have been obtained for microaethalometers in previous studies (Cai *et al.*, 2014), the performance depends on the concentrations (Ferrero *et al.*, 2016), and measurements obtained in the environment with lowest concentrations have the highest noise ratio, and further data post-processing may be needed (Hagler *et al.*, 2011).

The portable meteorological sensors are more suitable for operations in the Arctic conditions. For example, according to the manufacturers' specifications, the range and accuracy of wind speed and air temperature measurements by Kestrel 5500 Weather Meter and Onset stationary sensors are shown in Table 1.

Table 1 Accuracy and measurement range for the stationary Onset sensors installed at the UNIS roof and Kestrel 5500 sensors

Parameter	Accuracy	Measurement range
Air temperature, Kestrel 5500	$\pm 0.5^{\circ}\text{C}$	-29.0°C to 70.0°C
Air temperature, Onset S-THB-M002	$\pm 0.21^{\circ}\text{C}$ (0°C to 50°C)	-40°C to 75°C
Wind speed, Kestrel 5500	$\pm 0.1 \text{ m}\cdot\text{s}^{-1}$	$0.6 \text{ m}\cdot\text{s}^{-1}$ - $40 \text{ m}\cdot\text{s}^{-1}$
Wind speed, Onset S-WCA-M003	$\pm 0.5 \text{ m}\cdot\text{s}^{-1}$ ($u < 17 \text{ m / s}$)	0 to $44 \text{ m}\cdot\text{s}^{-1}$

The comparison of the Kestrel measurements with the data from the Onset sensors is presented further in the current thesis (part 3.4).

2.4 Reanalysis and trajectory model data

ERA-Interim and ERA5 data have been used to assess the synoptic-scale meteorological conditions over Svalbard for the periods of interest. ERA-Interim has a six hours temporal and coarse spatial resolution. In contrast, in ERA5, a new version of the global reanalysis dataset with hourly output frequency, the horizontal and vertical resolutions have increased from 79 km to 31 km and from 60 to 137 levels, respectively. (Dee et al., 2011; Hersbach and Dee, 2016).

Despite the main focus of the current work is local pollution in Svalbard, the backward trajectory modelling has been used to study long-range transport of SLCFs to the measurement sites. FLEXTRA and HYSPLIT are 3-dimensional trajectory models driven with the meteorological data with a spatial resolution of 1.25 degree from the European Centre for Medium-Range Weather Forecasts and 2.5 degrees from global NCEP/NCAR Reanalysis, respectively (Stohl, 1998; Stein et al., 2015). The temporal resolution of the input meteorological data in both models is six hours.

2.5 Statistical approach

2.5.1 Kolmogorov-Smirnov test for normality

The Kolmogorov-Smirnov test for normality has been used to check if the data in x population are normally distributed (Lilliefors, 1967). The test result is the maximum absolute difference between the empirical cumulative distribution function $S_N(X)$ calculated from x and the cumulative distribution function $F^*(X)$ for a standard normal distribution:

$$D = \max_x |F^*(X) - S_N(X)| \quad (4)$$

The D is calculated and the p-value, the probability of observing a test result as extreme as the observed value under the hypothesis that the data in vector x comes from a standard normal distribution, is obtained. If the p-value is less than 0.05, the hypothesis is rejected.

The function *kstest* in the MATLAB software has been applied to perform the calculations (MathWorks, 2019b).

2.5.2 Wilcoxon rank sum test

To compare the two samples from the observational dataset grouped according to some principle, for example, presence or absence of some environmental factor, the two-sided hypotheses that the two populations are equal may be tested using t-test or Wilcoxon rank sum test (WRS-test). The WRS-test has been used in Paper II, III and IV instead of t-test because the former performs better for the discrete samples and the data, which are not normally distributed (Krzywinski and Altman, 2014).

The ranks in the two independent samples of sizes n_X and n_Y , which have been taken from populations X and Y and ordered in the combined sample with size $N = n_X + n_Y$ from smallest to largest, may be used to define, which of the populations has the highest median value. If the sum of ranks in the sample from X population are higher than from the second sample, then the median of the X population is generally higher than the median of the Y population (Gibbons and Chakraborti, 2003).

The WRS-test is equivalent to the Mann-Whitney U-test. We find the Mann-Whitney U-test statistic from the sum of the ranks for the observations, which came from the sample X:

$$U_X = R_X - \frac{n_X(n_X+1)}{2} \quad (5)$$

where R_X is the sum of the ranks in sample X.

Similarly, we find the U-value for the sample Y:

$$U_Y = R_Y - \frac{n_Y(n_Y+1)}{2} \quad (6)$$

Since there is a connection between the ranks of the two samples such that $R_X+R_Y=N(N+1)/2$ and $U_X + U_Y = n_X n_Y$, the MATLAB function calculates only the rank sum of the first sample.

The WRS-test is related to the U-test as:

$$W = U + \frac{n_X(n_X+1)}{2} \quad (7)$$

The smallest value of U is used to define the significance of the result using the significance tables for small samples or z-statistic in case of large samples.

The full description of the MATLAB function *ranksum* is given in the MathWorks web-page (MathWorks, 2019d).

2.5.3 Pearson and Spearman correlation

The MATLAB function *corr* (MathWorks, 2019a) has been used to calculate the Pearson correlation coefficient to check if there is any statistical significant linear relationship between the same parameters measured at different stations such as the correlation between NO_x in Longyearbyen and Ny-Ålesund or by different equipment, for example, correlation between BC values obtained by the AE33 and AE51 aethalometers.

The Pearson correlation coefficient for the two variables x and y is following:

$$r_{yx} = \frac{\sum_{i=1}^n (x_i - \bar{x})(y_i - \bar{y})}{\sqrt{\sum_{i=1}^n (x_i - \bar{x})^2 \sum_{i=1}^n (y_i - \bar{y})^2}} \quad (8)$$

In contrast, the Spearman correlation is used to test for monotonic relationship between the two variables (Chalmer, 1986). The partial Spearman (rank) correlation coefficients have been calculated to test if the concentrations of atmospheric compounds are related to the meteorological parameters in Paper III.

For example, the Spearman partial correlation for the two variables x and y controlling for the variable z is calculated as:

$$\rho_{yx.z} = \frac{\rho_{yx} - \rho_{yz} \cdot \rho_{xz}}{\sqrt{1 - \rho_{yz}^2} \cdot \sqrt{1 - \rho_{yx}^2}} \quad (9)$$

where $\rho_{yx} = 1 - \frac{6 \sum d_{yx}^2}{n(n^2 - 1)}$, $\rho_{yz} = 1 - \frac{6 \sum d_{yz}^2}{n(n^2 - 1)}$ and $\rho_{xz} = 1 - \frac{6 \sum d_{xz}^2}{n(n^2 - 1)}$ are the Spearman correlation coefficients for variables x and y, y and z and x and z, respectively, calculated for d_{yx} , d_{yz} , d_{xz} , the difference between the ranks of the two variables x and y, y and z and x and z, accordingly, and n is the length of each variable.

The partial correlation has been calculated using the MATLAB function *partialcorr* (MathWorks, 2019c).

2.5.4 Monte Carlo method

Monte Carlo method has been used to test the significance of the relationships between the two variables when the correlation coefficient between them has been low ($r < 0.2$) (Graversen, 2006). A new artificial variable with the same power spectra as one of the two variables of interests, but with the shifted phase has been created, and the correlation coefficient has been calculated. The procedure has been repeated 5000 times and the percentage of the correlation coefficients, which are higher than or equal to the original one calculated for the two variables of interest, has been found. The percentage indicates significance of the correlation.

3. Discussion of the results

3.1 Paper I

Dekhtyareva A., Edvardsen K., Holmén K., Hermansen O., & Hansson H.-C., 2016. Influence of local and regional air pollution on atmospheric measurements in Ny-Ålesund. *International Journal of Sustainable Development and Planning*, 11 (4), 578–587. DOI: 10.2495/SDP-V11-N4-578-587

The main author has been responsible for the work on the article. The contribution of each of the authors listed above is stated in the *Table 1*Table 2. In the Table 2,Table 3,Table 4 and Table 5 the conception is an idea for the research; design is the study planning; supervision is taking the responsibility for the work on the article; funding and materials include personnel, logistical and technical support needed for the study; critical review is the reviewing of the article for its intellectual content.

Table 2 Authors contributions in Paper I

The authors contributions	D.A.	E.K.	H.K.	H.O.	H. H.-C.
Conception	+		+		
Design	+		+		
Literature review	+				
Supervision	+				
Funding / materials				+	+
Data collection				+	+
Data processing	+			+	+
Analysis and results interpretation	+	+	+		
Writing	+	+	+		
Critical review		+	+		

The paper discussed lifetimes of NO_x, SO₂ and aerosol particles of different size and seasonal variation of their concentration in Ny-Ålesund from 2008 to 2010. The importance of the Zeppelin Observatory as an international research station for monitoring of background air composition is also stated in the paper. Diesel power plant and ships in Ny-Ålesund and coal power plants in Longyearbyen and Barentsburg are defined as local and regional emission sources, respectively, which may affect the concentration of compounds measured at the Zeppelin station. FLEXTRA air mass trajectory have been used to identify cases when the air masses arriving at the Zeppelin station may have been impacted by the long-range, regional and local emission sources.

It has been observed that the summer wind conditions measured in Ny-Ålesund and at the Zeppelin station as well as at the Svalbard airport in Longyearbyen differ significantly from other seasons: the mean wind speed is lower and onshore wind is observed more often. The westerly wind prevails in summer in Longyearbyen, thus the influence of towns pollution on the measurements at the Zeppelin station is unlikely. In contrast, south-easterly and south-westerly wind may bring regional pollution to Ny-Ålesund. The lack of meteorological observations in Barentsburg restricted analysis of seasonal wind patterns in this settlement.

The seasonality in SO₂, NO_x, XSO₄²⁻ concentrations and particle size distribution have been explained by the influence of different emission sources and change in environmental conditions in Svalbard. Higher concentrations of smaller particles have been observed in summer at the Zeppelin station, while accumulation mode particles has prevailed in spring. Local NO_x sources have been important in summer and winter, while long-range transported pollution has dominated in autumn and spring. SO₂ concentrations have been the highest in winter and spring due to long-range transport of pollution from regional and remote sources.

To clarify the influence of regional pollution sources on air quality in Svalbard and measurements at the Zeppelin station, local air quality monitoring campaigns and sampling of the plume from the coal power plants in Barentsburg and Longyearbyen have been recommended. It has been stated that the results of these measurements may be further used for the plume modelling to study the environmental fate of air pollutants emitted from the largest sources in Svalbard.

In addition to this, the uncertainty in future emission scenarios from ships and power plants in Svalbard and the need for follow-up measurements in all three settlements have been stated in the paper.

3.2 Paper II

Dekhtyareva A., Holmén K., Maturilli M., Hermansen O., & Graversen R., 2018. Effect of seasonal mesoscale and microscale meteorological conditions in Ny-Ålesund on results of monitoring of long-range transported pollution. *Polar Research*, 37 (1), 1508196. DOI: 10.1080/17518369.2018.1508196

The work on the article has been managed by the main author. Table 3 indicates the contribution of each of the authors listed above *Table 1*.

Table 3 Authors contributions in Paper II

The authors contributions	D.A.	H.K.	M.M.	H.O.	G.R.
Conception	+	+			
Design	+	+			
Literature review	+	+			
Supervision	+				+
Funding / materials		+	+	+	
Data collection			+	+	
Data processing	+		+	+	
Analysis and results interpretation	+				
Writing	+	+			+
Critical review		+	+		+

The seasonality in concentrations of particles and gases in Ny-Ålesund has been described in Paper I. However, the vertical distribution of measurement compounds has not been discussed. The settlement is located in the area with complex topography, and local meteorological processes differ at the various measurement altitudes. The vertical

distribution of local and long-range transported aerosols is dependent on the ABL dynamics and is controlled by the mesoscale and microscale meteorological phenomena.

Paper II investigates correspondence between the daily SO_2 and XSO_4^{2-} concentrations detected in the filter samples in Ny-Ålesund (8 m a.s.l.) and at the Zeppelin station (474 m a.s.l.) and analyses the seasonality in the influence of the different environmental factors on the concentrations measured on the two sites. The microscale and mesoscale meteorological conditions have been studied using observations at the two stations and ERA-Interim reanalysis dataset, respectively. In addition to this, the daily radiosonde soundings have been used to investigate the atmospheric stability and wind conditions in the first 500 m of the ABL.

The correlation between the daily SO_2 and XSO_4^{2-} data sets from the Ny-Ålesund and the Zeppelin stations has been calculated for different seasons. There is no significant correlation between the SO_2 data sets from the two stations in summer, while it is very strong in winter. The values of Pearson correlation coefficient in autumn and spring are intermediate to moderate. The correlation between the XSO_4^{2-} data sets is significant for all seasons, but it is the lowest for the summer data.

The seasonal influence of four major factors on the observations on both sites have been investigated. Three of them may introduce disturbance in the correlation between the data at the two stations, increasing ground-level concentration of pollutants in Ny-Ålesund, while having no effect on the measurements at the Zeppelin station: temperature and humidity inversions, directional wind shear and local summertime emissions from ship traffic. In contrast, the wind speed shear is the factor that may reduce the difference between the two datasets due to enhanced mixing and more effective dispersion of local pollutants. The significance of impact of different factors has been verified by applying of the WRS-test on the two groups of measurements from each of the stations for the days when the specific factor of influence has been present and absent, respectively.

The diagram of the statistically significant factors of influence based on the results of the WRS-test is shown in Figure 8. One can see that all the factors except the directional wind shear are affecting the concentration in Ny-Ålesund in different seasons. Lowest correlation between the datasets at the two stations in summer may be explained by the fact that the Ny-Ålesund data is influenced by several different factors: emissions from ship traffic and insufficient dispersion of local pollution when there is no vertical wind speed shear and strong humidity inversion is present. However, they do not have any significant effect on the median concentrations at the Zeppelin station. In contrast, the significant influence on the concentrations both at the Zeppelin station and in Ny-Ålesund has been observed only for the temperature inversions in spring. The temperature inversions in spring have been formed due to radiative cooling when cold air masses have been transported to Svalbard from east-north-east, and higher concentrations of SO_2 and XSO_4^{2-} have been observed in these days.

The correlation between the datasets at the two stations varies due to the influence of different micrometeorological phenomena and local pollution. Modelling of these environmental factors is still challenging, and it needs to be considered when one compares

modelling results with measurements taken at different heights in the area with complex topography.

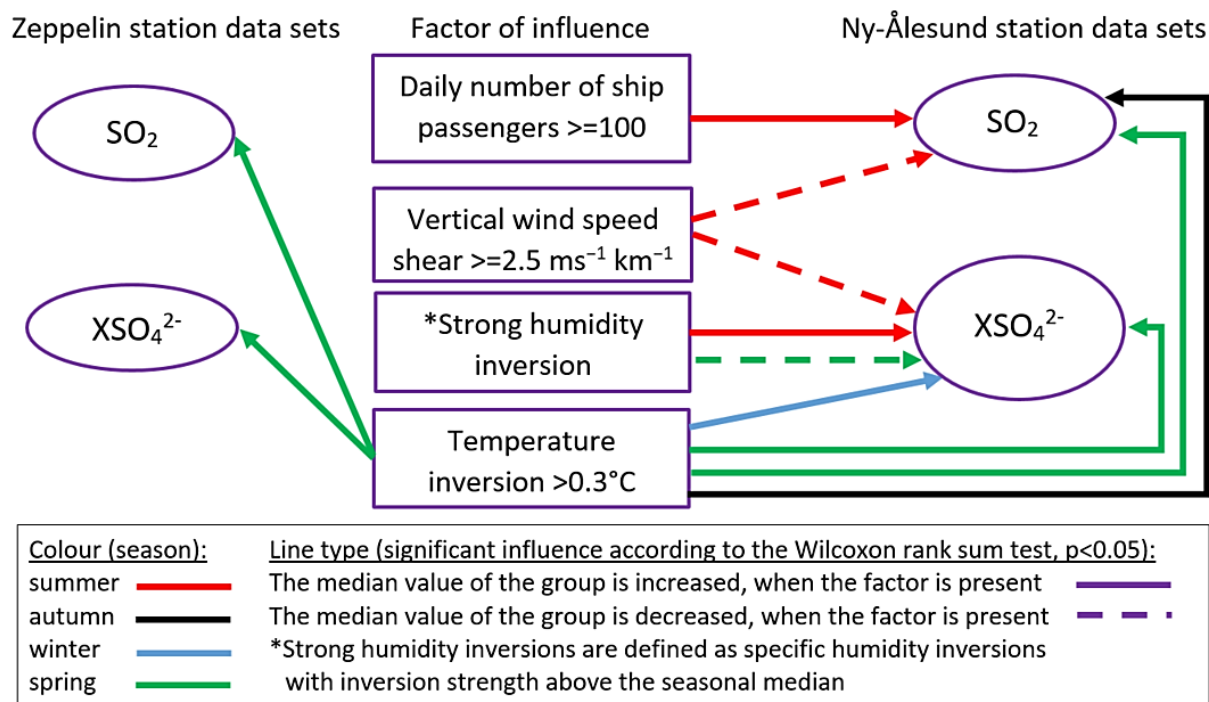


Figure 8 Diagram of the statistically significant factors of influence based on the results of the WRS-test ($p < 0.05$)

3.3 Paper III

Dekhtyareva A., Hermanson M., Nikulina A., Hermansen O., Svendby T., Graversen R., & Holmén K., 2019. Springtime nitrogen oxides and tropospheric ozone in Svalbard: results from the measurement station network. *Manuscript ready*

The work on Paper III has been managed by the main author. The contribution of each of the authors listed above is stated in the Table 4Table 1.

The importance of long-range transported NO_x for springtime O_3 chemistry in the Arctic has been stated in several papers (Beine, Jaffe, Herring, *et al.*, 1997; Beine, Jaffe, Stordal, *et al.*, 1997; Custard *et al.*, 2015). However, only few studies investigate the relationship between NO_x and O_3 near the pollution sources within the Arctic (Beine *et al.*, 1996; Custard *et al.*, 2015). Furthermore, the emissions from snowmobile traffic in Svalbard have not been studied until present time. Paper I underlined the necessity of local measurements in Longyearbyen and Barentsburg. In Paper II, the role of complex topography and local micrometeorological processes in creating the difference in concentrations of measured compounds at the two stations located at the distance of two kilometres from each other and at different altitudes have been discussed.

Table 4 Authors contributions in Paper III

The authors contributions	D.A.	H.M.	N.A.	H.O.	S.T.	G.R.	H.K.
Conception	+						+
Design	+						+
Literature review	+						
Supervision	+						
Funding / materials	+	+	+	+	+		+
Data collection	+	+	+	+	+		
Data processing	+		+	+	+		
Analysis and results interpretation	+		+		+	+	
Writing	+	+				+	+
Critical review		+				+	+

The measurements in Longyearbyen were financed via the Arctic field grant for which Alena Dekhtyareva had applied in October 2016. The project “Monitoring of nitrogen oxides from stationary and mobile sources at Svalbard” had been funded in January 2017. The proposal incorporated testing of portable NO₂ sensors to monitor the emissions from snowmobiles and comparison of the results with the standard stationary NO_x monitor.

The mobile NO₂ Cairpol sensor and Kestrel 5500 Pocket Weather Tracker were used during the fieldwork trip on snowmobiles to Mohnbukta organized by the UNIS course AT-831 “Arctic Environmental Pollution: Atmospheric Distribution and Processes” on the 05th of May 2017 (Figure 9). Kestrel weather station has been temporarily installed in Sassendalen (001), Mohnbukta (002) and Koningsbergbreen (003).



Figure 9 Snowmobile route produced using GPS log. The locations of Kestrel stations (001-003) and UNIS automatic weather station (AWS) are shown by the red circles

The Kestrel tracker has been installed on a tripod for short-term stationary measurements during the stops (Figure 10a). The Cairpol NO₂ sensor has been attached to arm of the author during the snowmobile trip (Figure 10b).

The surface wind speed and direction depended strongly on local topographical features, and channelling along the glaciers and valleys has been observed. Most of elevated NO₂ values have been detected when the snowmobiles stopped at the measurement stations (up to 24 ppb), while concentrations of the measured compound have been low during the ride (0 ppb).

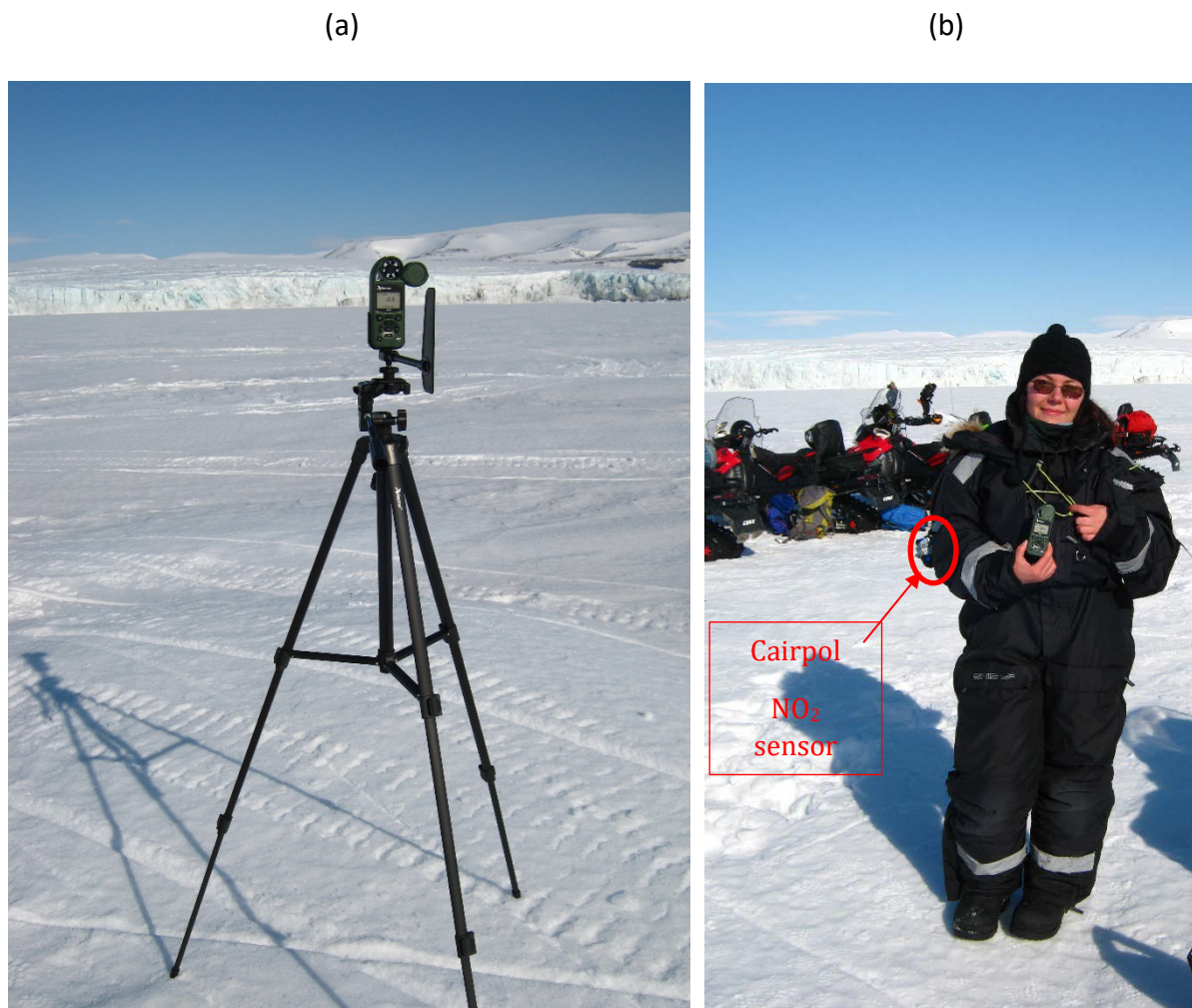


Figure 10 a) Kestrel station installed in Mohnbukta; b) project manager Alena Dekhtyareva with Cairpol NO₂ sensor attached to the arm to measure NO₂ concentration during the field trip

Negligible concentrations of NO₂ have been observed during the ride most probably because NO is formed first in the process of fuel combustion, and then it is further converted to NO₂ (Seinfeld and Pandis, 2006). The conversion rate depends on the concentration of NO, therefore, when several snowmobiles stop simultaneously, NO accumulates and we can see the production of NO₂. The snowmobile with the sensor has been the second from the end in the motorcade of 13 snowmobiles, therefore the air polluted by the emissions from the 11 snowmobiles, which arrived first, has been sampled.

The measurement results obtained from the portable sensors have not been included in the Paper III, since the *in-situ* calibration with the stationary NO_x monitor showed very low correlation between the two instruments ($r=0.22$, $p=0.003$). The Cairpol NO₂ sensor

underestimated the concentrations measured at UNIS during the case study when the ships have been near the port of Longyearbyen. The 1-minute NO₂ concentrations detected by the stationary NO_x monitor have been up to 26.7 ppb, while Cairpol sensor showed 0 ppb during the whole time of calibration with only three 1-minute values of 1 ppb.

While the portable sensor data are not valid for publication, the measurement results obtained from the stationary NO_x monitor are included in Paper III where they are combined with the data from Ny-Ålesund and Barentsburg.

The main aim of Paper III is to analyse NO_x and O₃ observations from the three Svalbard settlements, Ny-Ålesund, Longyearbyen and Barentsburg, in order to study the spatial variability in the concentrations of measured compounds and the effect of emissions from various local sources on the measurement results. Synoptic and micrometeorological conditions affecting the values of observed compounds have been studied using the ERA5 reanalysis dataset, ground-based observations and radiosonde soundings from Ny-Ålesund.

The NO_x concentrations in the three settlements are mostly influenced by the local atmospheric circulation controlling the frequency of transport of polluted air masses from the local sources to the measurement stations. However, the synoptic-scale situations, which promote light winds conditions and formation of temperature inversions, decrease the efficiency of dispersion of local pollutants in the ABL and increase the concentration of NO_x at all stations. In addition to influence from the snowmobile and power plant emissions in Longyearbyen, elevated concentrations of NO_x have been detected when ships have been near the harbour and further investigation of the effect of ship emissions on the air quality in town has been recommended.

In contrast to NO_x, the local emission sources in Barentsburg and Ny-Ålesund affect the O₃ values insignificantly, and the concentrations are controlled by the prevailing synoptic-scale situation and long-range transport of air masses. Several cases of transport of O₃ depleted and enriched air masses have been described and studied with the help of HYSPLIT air mass trajectories.

The main weakness of the study has been the absence of measurements of halogenic species and VOCs playing important role in both O₃ and NO_x chemistry in the Arctic. For example, Custard *et al.*, 2015 performed comparison of measurements and modelling of O₃ depletion events in low and high NO_x environments and revealed decreased O₃ net loss rate in high NO_x environments due to reactions with BrO. However, no such effect has been noticed on the O₃ concentrations measured during the O₃ depletion events in Ny-Ålesund and Barentsburg studied in Paper III, where only titration of O₃ with NO has been pronounced. The modelling of O₃/NO_x species could have been done in Paper III as well.

The paper uses outdated emission data from Vestreng, Kallenborn and Økstad, 2009. The only newer data available is yearly reported emissions from the coal power plants in Longyearbyen and Barentsburg published at the <https://www.norskeutslipp.no/>. However, there is no newer data about local emissions from ships, snowmobiles and generators in all three settlements. If these data would have been available, the local flux of NO_x in Svalbard could have been compared to the horizontal flux of long-range transported NO_x coming to

Svalbard. Then the performed NO_x measurements could have been used to correct the emissions estimates.

In addition to this, the precise estimations of the variability in local emissions in Longyearbyen and Barentsburg are needed. For example, it is unclear if the diesel generator has been working 16.05.2018 during the case study in Longyearbyen, but there is no publicly available information on it.

There have been particular observational challenges in this study, which add some uncertainty to the interpretations of the measurement results: NO_x and O₃ monitors have been located at different places in Ny-Ålesund, NO_x monitor in Barentsburg has not been calibrated in the same manner as in Ny-Ålesund and Longyearbyen, and there have been no O₃ measurements in Longyearbyen. These issues have been taken into consideration in the process of preparing of the fieldwork to collect summer data in 2018 utilized in Paper IV.

3.4 Paper IV

Dekhtyareva A., Drotikova T., Nikulina A., Hermansen O., Chernov D.G., Mateos D., Herreras M., Petroselli C., Ferrero L., Gregorič A., 2019. Summer air pollution in Svalbard: emission sources, meteorology and air quality. *Manuscript ready*

The work on Paper IV has been supervised by the main author. The contribution of each of the authors listed above is stated in the *Table 1*Table 5.

Table 5 Authors contributions in Paper IV

The authors contributions	D.A.	D.T.	N.A.	H.O.	C.D.G.	M.D.	H.M.	P.C.	F.L.	G.A.
Conception	+									
Design	+									
Literature review	+									
Supervision	+									
Funding / materials	+	+	+	+	+	+	+	+	+	+
Data collection	+	+	+	+	+	+		+		+
Data processing	+	+	+	+	+	+	+	+		+
Analysis and results interpretation	+	+	+			+	+	+	+	+
Writing	+	+				+				
Critical review		+				+		+	+	+

The importance of summertime NO_x observations in Longyearbyen to quantify the influence of ships emissions on the local air quality has been defined in Paper III. Thus, to perform the measurement campaign there and compare the data with measurements in Ny-Ålesund and Barentsburg, application for the project “Strengthening cooperation on air pollution research in Svalbard” had been sent by the author of the current work to the Research

Council of Norway in November 2017. The pilot study in Longyearbyen was incorporated in the project proposal for the Svalbard Strategic Grant and was funded in January 2018.

As a result, a ground-based measurements have been performed at UNIS and tethered balloon meteorological and BC soundings in Adventdalen valley in the period from June to August 2018. The BC, SO₂, NO_x, O₃ and atmospheric optical depth (AOD) observations from Longyearbyen have been compared with the data from Barentsburg and Ny-Ålesund. The data from airborne measurements from Adventdalen have been compared with the radiosonde soundings from Ny-Ålesund.

Significant increase of SO₂ and NO_x concentrations and decrease of tropospheric O₃ values have been observed due to ship traffic emissions in Longyearbyen and Ny-Ålesund. In Barentsburg, the coal power plant has the most significant impact on the air quality, and at times, the pollution level exceeds Norwegian and Russian air quality standards. Long-range transport events have been identified using CO and O₃ data from the Zeppelin station and AOD values from Ny-Ålesund. It has been observed that warm air advection from mid-latitudes to Svalbard brings air enriched in O₃ and CO in summer, but it also creates strong temperature inversions, beneath which air pollution from the local sources may be trapped and higher concentrations of BC may accumulate.

In addition to the hourly SO₂, NO_x, BC and O₃ observations in Longyearbyen, daily filter samples for PAH analysis have been collected there. The selection of the samples for analysis based on the daily BC concentration has been determined by the fact that PAHs are both precursors for soot formation in the fossil fuel burning process and may be further absorbed by the combustion particles. Firstly, the fuel is pyrolyzed and/or oxidized into hydrocarbon molecules with lower number of carbon atoms such as acetylene and PAHs. Secondly, these gas molecules are polymerized to produce larger PAHs molecules, and when the concentration of these reaches its peak values, soot nuclei may form as a result of reactive collisions between these molecules. Thirdly, the growth of soot nuclei continues until they exceed 10 nm in diameter and start to coagulate and form chain-like structures. When the combustion products cool down, the PAHs are effectively absorbed by the soot particles and may accumulate in high quantities (Seinfeld and Pandis, 2006).

The dominating PAH compound measured in the filters in Longyearbyen in summer has been naphthalene. This result may be partly influenced by the selection of samples collected in the days with highest BC concentrations. Fuels with high naphthalene content have higher sooting tendency (Seinfeld and Pandis, 2006), and therefore there is a natural prerequisite to occurrence of higher naphthalene content in the samples when the concentration of BC, a main component of soot, has been higher. At the same time, naphthalene accumulating on the soot particles may be both from surviving combustion and formed pyrosynthetically (Rhead and Pemberton, 1996).

The PAHs and BC measurements from Ny-Ålesund have not been available at the time of working on Paper IV, therefore concentrations of these compounds have not be compared with the data from Longyearbyen.

Airborne observations performed during the fieldwork in 2018 allowed identifying how different weather regimes affected the stratification of the ABL in Adventdalen and Ny-

Ålesund and BC concentration in the profiles. However, more detailed analysis of the BC profiles and classification on different profile types could have been done as in the work of Ferrero *et al.*, 2016.

Several portable sensors have been used during the field campaign in Longyearbyen: MiniDISC particle counter, Kestrel 5500 weather tracker and AE51 microaethalometer.

The performance of the Kestrel 5500 weather tracker has been assessed *in-situ* using the data from the Onset AWS installed at the UNIS roof. 1-minute Kestrel data have been averaged to the 12-minute sampling interval of the UNIS AWS. The two meteorological parameters, which have been used the most in Paper IV, are wind speed and temperature. The comparison of the data from two portable sensors (serial numbers: 17 and 15) with the data from the AWS is shown in Figure 11a) and Figure 11b), respectively.

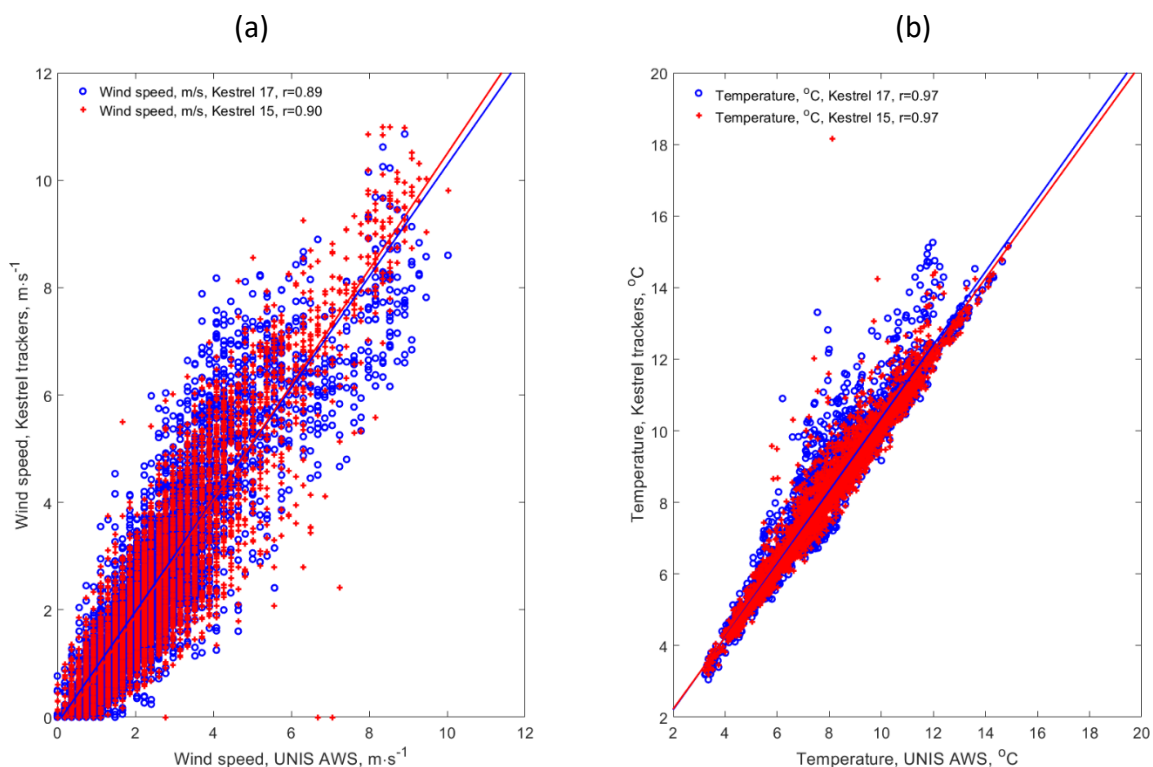


Figure 11 Comparison of Kestrel and AWS data and correlation coefficients for the: a) wind speed; b) air temperature

One can see that the correlation between the data from the Kestrel trackers and AWS is very strong. While the measurement accuracy varies from $-3.1 \text{ m}\cdot\text{s}^{-1}$ to $4.2 \text{ m}\cdot\text{s}^{-1}$ and from $-7 \text{ m}\cdot\text{s}^{-1}$ to $3.8 \text{ m}\cdot\text{s}^{-1}$ for Kestrel 17 and Kestrel 15 trackers, respectively, the median difference in wind speed between the data from the portable sensors and AWS has been $-0.12 \text{ m}\cdot\text{s}^{-1}$ and on $-0.16 \text{ m}\cdot\text{s}^{-1}$ for Kestrel 17 and Kestrel 15 trackers, respectively. This result is close to the instruments accuracy of $0.1 \text{ m}\cdot\text{s}^{-1}$. However, it worth to note that the median underestimation of the wind speed by both portable sensors is $\sim 0.2 \text{ m}\cdot\text{s}^{-1}$ under low wind speed conditions ($< 2 \text{ m}\cdot\text{s}^{-1}$), and sensors performance improves when the wind speed is above $2 \text{ m}\cdot\text{s}^{-1}$. The precision of the measurements in terms of standard deviation is $1.9 \text{ m}\cdot\text{s}^{-1}$ for the Kestrel sensors and $1.6 \text{ m}\cdot\text{s}^{-1}$ for the AWS. The measured accuracy of the

temperature sensors varied in the range of $-1.0\text{ }^{\circ}\text{C}$ - $5.8\text{ }^{\circ}\text{C}$ and $-0.79\text{ }^{\circ}\text{C}$ - $16.2\text{ }^{\circ}\text{C}$ for Kestrel 17 and Kestrel 15, respectively, with median values of $0.18\text{ }^{\circ}\text{C}$ for both Kestrel sensors, which is within the accuracy range stated in the Table 1. The observed warm bias may be reduced by the shielding of the portable sensors from the sun, however, then it may be challenging to keep the wind measurements unobstructed in this case. The precision of temperature measurements is $\pm 2.0\text{ }^{\circ}\text{C}$, $\pm 1.9\text{ }^{\circ}\text{C}$ and $\pm 1.9\text{ }^{\circ}\text{C}$ for Kestrel 17, Kestrel 15 and AWS, respectively.

Unfortunately, no stationary particle counter has been installed in Longyearbyen to compare its data with MiniDISC measurements, since the MiniDISC sensor has been not planned to be used in the campaign. The sensor has been offered for the tethered balloon measurements in addition to AE51 by the project partners during the fieldwork.

The performance of the microaethalometer AE51 is discussed in the Discussion part of Paper IV.

Different types of the ship traffic data have been available for Paper I, II and IV. In the first two papers, the port calls in Ny-Ålesund have been registered manually by the harbour authorities in Ny-Ålesund and the number of passengers has been indicated. In the last paper, the ship traffic log has been based on the automatic identification system data reported to the marinetraffic.com where the gross tonnage (GT) for most of the ships may be found as well. However, the number of passengers has not been available in 2018. The difference between the approaches to the ship traffic analysis makes it challenging to compare the absolute influence of the ship traffic on the concentrations of SO_2 and NO_x in 2009, 2010 and 2018. In addition to this, in Paper I only passenger ships are taken into account, while in Paper IV all ships with the $\text{GT}>100$ are considered. Another difference is that only ships registered in the Ny-Ålesund port log obtained from marinetraffic.com have been considered in 2018, while ships anchored in the fjord have not been taken into account.

Furthermore, in Paper I only values of SO_2 and NO_x above $\text{LD}=0.4\text{ ppb}$ are considered. If we use all the summer data from 2008, 2009 and 2010 including those below LD as it is done in Paper IV, we will see much stronger influence of ships emissions: increase of mean SO_2 values on 59% and increase of mean NO_x values on 28%, and the result will be comparable with the data presented in Paper IV.

The comparison of summer concentrations (July and August) in 2009, 2010 studied in Paper I and 2018 using the WRS-test reveals significant reduction in concentrations of SO_2 and NO_x in Ny-Ålesund in 2018. However, the median wind speed has been slightly higher in 2018 ($2.1\text{ m}\cdot\text{s}^{-1}$) than in 2009 ($1.7\text{ m}\cdot\text{s}^{-1}$) and 2010 ($1.9\text{ m}\cdot\text{s}^{-1}$), thus the dispersion of local pollution might have been more efficient in 2018.

The highest median NO_x concentrations were observed in 2010, when north-westerly wind has been detected more often than in other two years (Figure 12a), while the highest mean concentrations were observed in summer 2018. This may indicate, that the emissions from sources located to the north from the station increased although they do not affect the median summer concentrations strongly due to prevailing south-easterly wind (Figure 12a).

Indeed, the mean concentration of NO_x coming from northerly direction increased from 32.0 µg·m⁻³ in 2009 to 54.4 µg·m⁻³ in 2018 (Figure 12b).

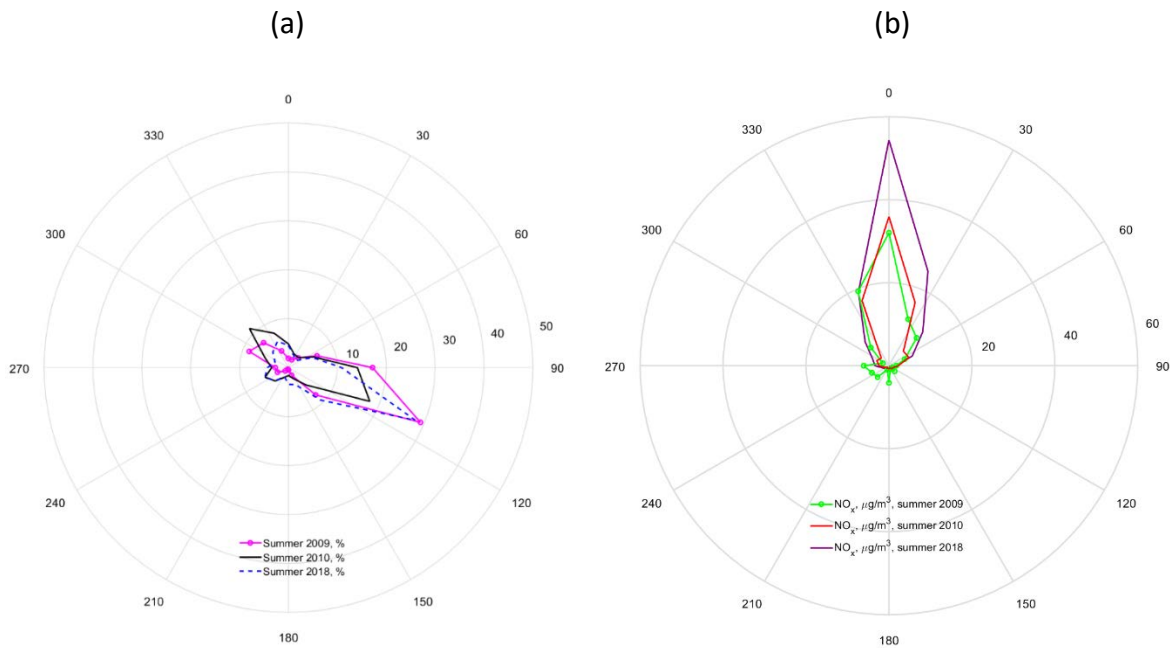


Figure 12 a) Summer wind roses for 2009, 2010 and 2018; b) NO_x concentration averaged over wind directions for 2009, 2010 and 2018

Although, in Paper IV we assume that the emissions from the diesel generator in Ny-Ålesund have not changed significantly since 2013, one can see that the concentrations of NO_x observed when the wind was coming from the north were higher in summer 2018 than in summer 2010 and 2009 even in absence of ships (Figure 13a). This means that updated information about emissions from the power plant is needed, and the reduction of emissions may be recommended to decrease the disturbance of atmospheric measurements in the settlement as it has been stated in previous reports (Shears *et al.*, 1998; Sander, Holst and Shears, 2006; Sander, 2014). The mean concentrations of SO₂ for the hours when the ships were present in Ny-Ålesund reduced from 0.38 µg·m⁻³ and 0.28 µg·m⁻³ in 2009 and 2010, respectively, to 0.16 µg·m⁻³ in 2018 probably due to the restrictions on use of heavy fuel oil in Ny-Ålesund since 2015. However, the change in distribution of average SO₂ concentrations over wind directions may be noticed in 2018 indicating a possible new source of SO₂ located to the south-west from the measurement station (Figure 13b). This needs to be investigated further.

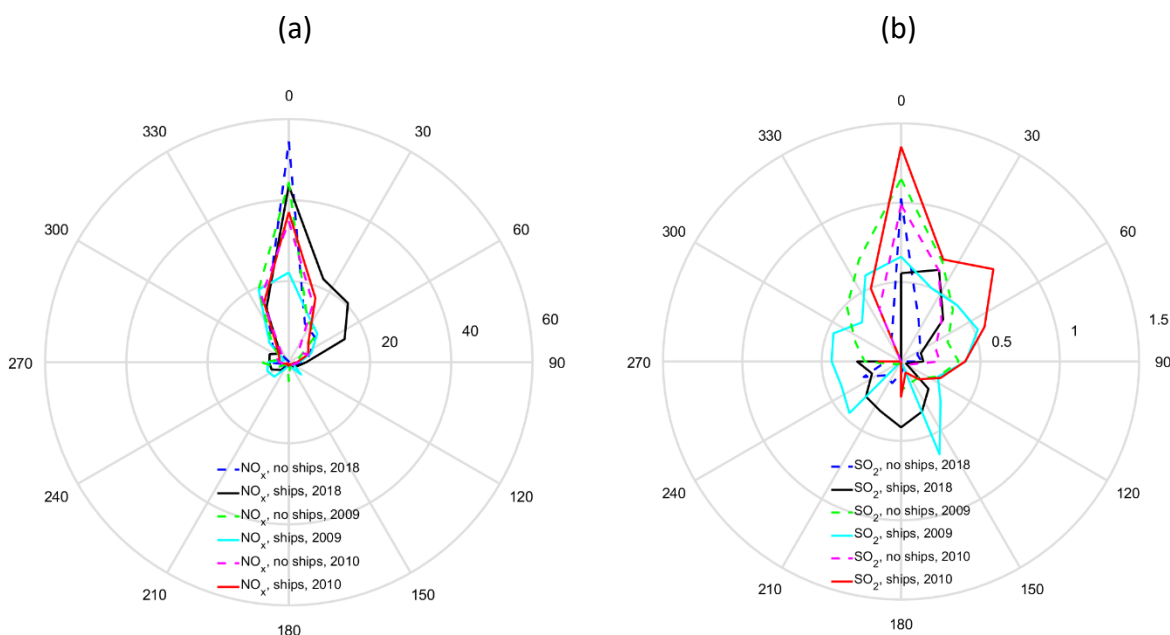


Figure 13 NO_x (a) and SO₂ (b) concentrations ($\mu\text{g}\cdot\text{m}^{-3}$) averaged over wind directions in presence and absence of ships in July and August 2009, 2010 and 2018

3.5 Summary of the appended papers

Table 6 describes how the appended papers address the research questions stated in the current study with weakest relationship denoted by “+” sign and strongest by the “+++” sign, respectively. Although the thesis focuses on four different SLCFs measured in the three Svalbard settlements, only Paper IV intends to cover the whole range of compounds on all measurement sites. This is because the studies in Longyearbyen have been done with an external financial support that has been received in the third year of the current PhD project.

Table 6 Appended papers addressing the research questions

Paper	Measurement sites	Compounds	Research questions				
			1	2	3	4	5
I	Ny-Ålesund	SO ₂ , SO ₄ ²⁻ , NO _x	+++		++	+	+
II	Ny-Ålesund	SO ₂ , SO ₄ ²⁻	+++		+	+++	++
III	Ny-Ålesund, Longyearbyen, Barentsburg	NO _x , O ₃	++	+++	+	++	++
IV	Ny-Ålesund, Longyearbyen, Barentsburg	SO ₂ , NO _x , O ₃ , BC	++	+++	+++	+++	+++

Paper I studies the seasonal evolution of SO₂, NO_x and particle concentrations and indicates different remote and local sources, which may affect the concentrations, measured in the settlement. Paper II compares the filter data obtained at two different elevations and studies the processes which may cause discrepancies between the two datasets in different seasons. The long-term measurements have been analysed in both papers, and thus, they can answer to the research question 1 about the seasonal and daily variation in the pollutant concentrations.

However, Paper I and II are based on the data from one measurement site, Ny-Ålesund; thus, they cannot answer to the research question 2 and describe how the pollutant concentrations vary spatially between the three main Svalbard settlements. Paper III and IV are based on short-term measurement campaigns, which capture particular atmospheric composition and meteorological events present during the measurement periods in spring 2017 and summer 2018. The advantage of the field observations has been that higher spatial data coverage has been obtained with three stations around Svalbard. Thus, the research question 2 could be answered only in Paper III and IV. On the other side, the total duration of the measurements has been short, around two months for the data presented in each of the papers. Therefore, the last two papers are to a lesser extent related to the research question 1 since only daily and diurnal variation in the pollutant concentrations have been studied due to the short fieldwork period.

Research question 3 about the current influence of ship traffic on air quality in Svalbard settlements is touched in all papers, however, only Paper IV focuses on the impact on all SLCFs concentrations in both Ny-Ålesund and Longyearbyen.

All papers study the effect of different meteorological phenomena on the ground-level concentration of measured compounds, but only Paper II and IV additionally analyse the impact of microscale and synoptic scale meteorology on the vertical distribution of air pollutants in the ABL and addressed the research question 4 to a higher extent.

Data obtained using different measurement techniques is analysed in the papers, and all of them to some extent describe the advantages and disadvantages of different methods, however, broader variety of methods has been assessed in Paper IV, thus the relationship of this paper to the research question 5 is stronger.

4. Research contributions and suggestions for future work

4.1 Research contributions

Svalbard is a unique laboratory for environmental studies. Despite its remote location, the consequences of the changes in mid-latitude emissions and global climate are dramatic there. In addition to this, its near-pristine environment is affected by increasing amount of anthropogenic activities in the Arctic region. Studies of changes in both local and long-range transported air pollution performed in Svalbard are of high importance since it is a harbinger of the changing Arctic.

The current work focuses on measurements in Svalbard in all seasons, and hereby provides the opportunity to study the seasonality of air pollution varying due to long-range transport patterns, atmospheric chemistry and intensity of local emissions in the major settlements. The main emission sources in Svalbard are local power plants, however, substantial additional deterioration of the air quality by ship emissions has been revealed in Ny-Ålesund and Longyearbyen. The data from chemical observations performed in the current study under different meteorological conditions can be used to understand the environmental fate of air pollutants better and can be applied to model their future concentrations due to alterations in long-range transport patterns, local emissions, synoptic-scale conditions and micrometeorology.

As it is illustrated in the Table 6, the four appended papers address the five research questions stated in the chapter 1 of the current thesis in a specific way. The main findings from the papers giving summarized answers to the research questions are presented in the current chapter. The following subchapters are dedicated to each of the research questions.

4.1.1 Causes of the pollutant concentrations variation on a different temporal scale

The seasonality of sulphur species and NO_x concentrations in Ny-Ålesund is investigated in Paper I and Paper II. The findings confirm the results from previous studies (e.g. Heintzenberg and Leck, 1994) showing that the highest concentrations of SO₂ and XSO₄²⁻ are observed in winter and spring when the long-range transport of air pollution to Svalbard prevails, however, in Paper I, specific attention is given to possible pollution transport from regional sources in Longyearbyen in these seasons. This is due to the prevailing SE-wind direction observed there in this time of year. In addition to this, high NO_x concentrations were observed in Ny-Ålesund in winter even in absence of long-range transported pollution indicating importance of local emissions.

The two papers also show that there is a seasonal variation in local wind speed and direction. In summer, in contrast to other seasons, the onshore wind direction in Ny-Ålesund and Longyearbyen is more frequently observed. This creates conditions favourable for transport of the air masses influenced by the marine traffic and biogenic emissions to the measurement stations. At the same time, low wind speed conditions reduce the efficiency of mechanical mixing of the ABL and promote accumulation of local pollution in the settlements. Indeed, the comparison of NO and NO₂ observations from Ny-Ålesund studied in Paper III and Paper IV revealed that the summer median levels of these compounds are

more than two times higher than the spring ones. However, as it is shown in Paper II, mixing height obtained from the radiosonde soundings in Ny-Ålesund has often been lower than the altitude of Zeppelin observatory. This indicates that the chemical measurements performed there are less influenced by the local summer emissions than the sea-level station in the settlement.

The daily variations in SO₂ and XSO₄²⁻ concentrations at both stations depend on the source region of the air masses arriving to Svalbard. The most polluted air masses have been brought from the east and south-east in winter and spring. According to the spring and summer tethered balloon measurements performed by Ferrero *et al.*, 2016, the aerosols are often inhomogeneously distributed in the ABL in Ny-Ålesund. The soundings represent the aerosol profile structure at the time of observations; however, diurnal evolution of the ABL structure is unknown. In contrast, the high-volume air sampling comprises continuous accumulation of particles and gases in the filter. The comparison of the filter data in Ny-Ålesund performed in Paper II indicates that the layering effect is persistent on a daily scale, and there is a difference in the concentration of daily samples collected at different elevations in the settlement. For example, in days with strong humidity inversion in spring when the moist marine air has arrived to Ny-Ålesund, the concentrations of non-sea salt sulphate have been lower at the sea-level station than at the Zeppelin mountain observatory. In summer, there is also day-to-day variation in the intensity of local shipping emissions in Longyearbyen and Ny-Ålesund and in the efficiency of pollution dispersion. In the days with strong temperature inversions such that occurred in summer 2018 due to transport of extremely warm air masses from Scandinavia to Svalbard, the highest concentrations of BC and NO₂ have been observed in Longyearbyen.

The diurnal variation of concentrations in Ny-Ålesund, Longyearbyen and Barentsburg is studied in Paper III and Paper IV. The concentrations of NO_x and SO₂ have increased in the daytime and decreased in the nighttime following the diurnal variations of the anthropogenic activities in the three Svalbard settlements, while the concentrations of O₃ have shown significant daytime O₃ titration with NO_x only in Longyearbyen indicating that the emission quantities of nitrogen oxides are higher there.

In summary: There is a strong seasonality in long-range transport of air pollution to Svalbard with peak concentrations of sulphur compounds observed in winter and spring. However, it has also been shown that the local emissions have a pronounced seasonal and diurnal pattern as well. In summer, the ship traffic emissions have significant influence on the air quality in Longyearbyen and Ny-Ålesund. Moreover, median wind speed is lowest in summer, which reduces the ABL mixing, promotes accumulation of locally emitted pollution, and creates discrepancies in the filter measurements obtained at two heights in Ny-Ålesund, at the sea-level station and at the Zeppelin mountain observatory.

4.1.2 Spatial variation of the pollutant concentrations between the three main Svalbard settlements

The springtime and summertime spatial variation of the pollutant concentrations between Ny-Ålesund, Longyearbyen and Barentsburg is studied in Paper III and Paper IV, respectively. The concentrations of SLCFs in Svalbard settlements depend on the long-range transport of

air pollution, intensity of emissions from local stationary and mobile sources and local meteorological conditions. The main challenge for the comparison of the data from the three settlements is the usage of different instrumentation and calibration routine. Similar equipment has been used in Longyearbyen and Ny-Ålesund. The instruments have been calibrated at the same laboratory at the Norwegian Institute for Air Research before transportation to Svalbard, and the same sampling and zero and span calibration procedure has been followed during the observations at the both sites. In contrast, different monitors are deployed in Barentsburg and the in-situ calibration routines and calibration frequency are different. The transportation of calibration SO₂ and NO gases by boat from Longyearbyen to Barentsburg presents a logistical difficulty. Thus, in this settlement, the in-situ span calibration with the standard gases used in Longyearbyen has been done by the UiT personnel only once in the summer field campaign 2018. During that calibration procedure an overestimation of the SO₂ and NO concentrations by 22% and 30%, respectively, has been revealed. Normally, if the calibration period is one week as it has been in Ny-Ålesund and Longyearbyen, the data may be scaled linearly according to the values obtained in the span and zero check. This has not been done with the Barentsburg data as only one reference point was obtained. This surely affects the measurement results, thus the direct comparison of the concentration magnitude at the three sites is challenging. However, one can compare the NO_x, SO₂ and O₃ values from Ny-Ålesund and Longyearbyen presented in Paper IV. In Ny-Ålesund, median summertime NO and NO₂ values have been approximately 6 and 9 times lower, accordingly, than in Longyearbyen. In this settlement, the pronounced titration of O₃ with NO_x resulted in reduction of median O₃ concentrations by 12% from the median background value observed at the Zeppelin station. Median and mean SO₂ values in Longyearbyen have been much higher than in Ny-Ålesund, but the air quality standards have not been exceeded in any of the two settlements. In contrast, the highest median SO₂ values were detected in Barentsburg and extremely high concentrations of this compound were observed there on the 10th of July 2018. If we take into account possible overestimation of the concentration by the monitor, the recalculated average SO₂ value for that day would be 119 µg·m⁻³, which is 88 times higher than the maximum daily value detected in Ny-Ålesund. Thus, further follow-up air quality studies with standardized calibration routine are urgently needed in Barentsburg.

In summary: There is a broad span of SLFCs concentrations in the three major settlements in Svalbard. As expected from the emission inventories presented in Paper IV, the lowest median concentrations of SO₂ and NO have been detected in Ny-Ålesund, intermediate in Longyearbyen and highest in Barentsburg. However, the median BC values in Barentsburg are lower because the car traffic is less intensive and the wind flow bringing pollution from the local coal power plant is less frequent there than in Longyearbyen. The highest mean values of SO₂, NO and BC were observed in Barentsburg. However, additional long-term studies with well-established measurement and calibration routines are needed to assess the frequency of occurrence of extremely high SLFCs concentrations there.

4.1.3 Influence of ship traffic on air quality in Svalbard settlements

The analysis of the port call data performed in Paper IV revealed that marine traffic emissions significantly increase concentrations of SO₂ and NO_x in Ny-Ålesund and Longyearbyen. The concentrations of PAH and BC have increased due to ship emissions in

Longyearbyen as well. Moreover, the magnitude of total PAH concentrations has correlated positively with the ship size. A slight O₃ titration with NO_x in Longyearbyen and Ny-Ålesund has been observed in the period of two hours before arrival to two hours after departure of the ships with total gross tonnage exceeding 100. In Paper I and Paper II, significant influence of ships emissions on the concentrations of SO₂ and XSO₄²⁻ in filter samples collected in Ny-Ålesund and XSO₄²⁻ and particles with diameter from 50 to 100nm observed at the Zeppelin station has been revealed.

In summary: The impact of ship emissions on air quality in Svalbard settlements is pronounced in summer. This is revealed for all range of SLCFs studied in the current work as well as for the concentrations of particles and PAH. Since the efficiency of the ABL ventilation is lowest in summer, the influence on air quality is proportional to the ship size and total number of ships. Thus, the ship traffic restrictions limiting the total number of ships of a specific size visiting port simultaneously are efficient measures, which could be applied in future to reduce the SLCFs concentrations in this season.

4.1.4 Meteorological phenomena affecting the ground level concentration of measured compounds and their vertical distribution in the ABL

As it is stated in Paper III and Paper IV, the ground-level concentrations of SO₂, NO_x and BC depend strongly on prevailing wind direction at each of the measurement locations. Due to topographic channelling of the wind along the fjords and valleys, elevated pollution levels may be observed in one of the Svalbard settlements and absent in others under the same synoptic weather conditions. At the same time, low wind speed and temperature inversions are the conditions promoting accumulation of air pollutants in the ABL at all stations.

In Paper III, it is observed that the concentrations of NO_x have been higher in calm and cold days due to radiative temperature inversions and suppressed ABL mixing in spring. In contrast, higher concentrations of O₃ have been observed in Barentsburg and at the Zeppelin station when warmer air masses have been transported from mid-latitudes to Svalbard, meanwhile colder air arriving from the north has been depleted in O₃.

In Paper II, strong seasonality in correspondence between the SO₂ and XSO₄²⁻ data obtained at two heights in Ny-Ålesund is revealed due to influence of local micrometeorological conditions. The lowest correlation between the two datasets is observed in summer due to insufficient mixing of the ABL and additional local ground-level emissions from the ship traffic.

The tethered balloon measurement results presented in Paper IV, revealed cases of insufficient ABL ventilation and pollution accumulation in Longyearbyen in days when the temperature inversions occurred due to advection of warmer air masses from mid-latitudes to the archipelago. During these events, the background concentration of O₃ has increased as well due to long-range transport of air pollution. The frequency of occurrence of such events in summer needs to be investigated and taken into account along with the development of shipping emissions in the Svalbard zone.

In summary: The long-range transport events, topographic wind channelling, temperature inversions due to radiative surface cooling in winter and spring, and advection of warmer air masses from mid-latitudes to Svalbard in summer are the factors affecting the ground level concentrations of SLCFs and their distribution within the ABL.

4.1.5 Advantages and disadvantages of usage of different measurement techniques for air pollution monitoring in the Arctic

Additional practical achievements of this study are testing of portable and conventional sensors for meteorological and chemical observations in the Arctic environment and attempt to create a measurement network in Svalbard by combination of the data from existing research stations, Ny-Ålesund and Barentsburg, and establishing of new temporal station in Longyearbyen for spring and summer measurements in 2017 and 2018, respectively.

Conventional measurement techniques such as high volume filter samplers, gas monitors and aethalometers have been widely used for the air quality studies and monitoring of long-range transported pollution. Thus, the stations where these instruments are deployed may be easier included in an observational network, the information about the instruments' performance under different environmental conditions is available, and there is plenty of reliable reference measurements to compare with.

However, the usage of conventional ground-based and airborne instruments has a number of disadvantages. A common issue for all ground-based gas monitors and aethalometers are restrictions regarding the location of the measurement station. There should be a continuous and reliable power supply and the instruments must be installed in a heated room with inlets placed outside of the window or secured on the roof. Thus, these measurement techniques allow observations of the SLCFs concentration only in one location and at one vertical level. Sun photometer data contain information about aerosol content in the air column above the station, but the frequency of valid observations is low due to cloudy conditions often observed in summer in the Arctic. Tethered balloon observations allow receiving valuable data about vertical variation in particle concentration and meteorological parameters, but the measurements are time-consuming, and, due to weather and aircraft traffic restrictions, there is rarely a possibility to perform more than one up and down sounding per day. The radiosonde and ozone sonde measurements are less time-consuming, but much more costly, thus the frequency of observations is normally daily and weekly, respectively.

High LD is a common issue for both conventional measurement techniques such as stationary SO_2 and NO_x monitors and filter sampling described in Paper I and Paper II, respectively, and portable sensors, NO_2 electrochemical sensor and microaethalometer used in work on Paper III and Paper IV, accordingly. This problem may be solved using zero- and span-calibration for the stationary monitors and setting longer sampling time for filters and aethalometers. However, further development of reliable portable sensors with high temporal resolution of measurements is needed for applications in airborne observations and creating a network of stations equipped with the low-cost instruments. In addition to this, the *in-situ* assessment of the performance of these new monitors is needed in the Arctic.

In summary: There are advantages and disadvantages of various measurement techniques used for air pollution measurements in the Arctic. Thus, to combine different methods and study concentrations of different SLCFs simultaneously at different locations and altitudes, an international cooperation and joint field campaigns, such as the pilot study performed in summer 2018 in Svalbard, are needed. This allows setting the measurement results in a broader perspective and permits investigation of the state of environment on a regional scale. However, such extensive studies with conventional monitors are costly and need external financial support. Therefore, further development of reliable portable low-cost sensors would allow for increasing the number of observations at different locations in the region. In this case, the measurements could be included in various educational and scientific activities routinely performed at UNIS and research stations around Svalbard.

4.2 Suggestions for future work

The meteorological data from daily tethered balloon soundings performed in Longyearbyen in 2018 may be combined with continuous LIDAR observations performed in Ny-Ålesund to study the effect of temporal evolution of the ABL height on the concentration of air pollutants in Longyearbyen and Ny-Ålesund.

There is a great interest in the scientific community in combining the studies of the atmosphere by means of airborne instruments and high-resolution models as they give insight into lower atmosphere layers that are not monitored by the ground-based stations (Kral *et al.*, 2018). The radiosonde measurements are routinely used to supply vertical data for the numerical weather prediction models; however, the temporal and spatial resolution of these measurements is poor. Recently several campaigns have been performed in the polar regions using tethered balloon and Unmanned Aerial Vehicles (UAVs) for meteorological and aerosol measurements (Argentini *et al.*, 2003; Vihma *et al.*, 2011; Jonassen *et al.*, 2015; Moroni *et al.*, 2015; Kral *et al.*, 2018; Leibniz Institute for Tropospheric Research (TROPOS), 2018). The aerosol and turbulence data from the airborne instruments are unique, since they allow to observe local phenomena at high temporal resolution and assess the capability of the large-scale model to reproduce processes important for the environmental fate of air pollutants (Bärfuss *et al.*, 2018; Kral *et al.*, 2018; Leibniz Institute for Tropospheric Research (TROPOS), 2018). However, although some tests on the performance of the portable environmental sensors in Svalbard have been done in the current work, further investigations are needed with more frequent inter-calibration *in-situ* measurements at different concentrations and ambient conditions in order to use the low-cost sensors for airborne measurements described above.

In addition to this, unified approach to the analysis of the ship traffic data is needed to assess the evolution of impact from ship emissions on the concentrations of measured compounds in all three settlements. Besides, the emissions from ship traffic around Svalbard may cause diffuse signal in measurements at the stations due to more diluted concentrations of air pollutants, which may mimic long-range transport events in summer. There have been a number of ship-based campaigns performed at the research vessel Oceania (Ferrero *et al.*, 2019). The data from these campaigns may be compared with the long-term homogeneous ship traffic dataset for the Svalbard zone that may be obtained for research purposes from the Norwegian Coast Guard. Analysis of this dataset together with

the data from research cruises would allow estimating the contribution of marine traffic to the background concentrations of air pollutants in the Arctic.

Long-term measurements in the Arctic emission hot spots such as Barentsburg and plume modelling for different atmospheric conditions are needed to put these observations into a broader perspective. The local emissions of air pollutants in the Arctic are expected to rise with increasing industrial activity, however, the pollutants' lifetime may be decreasing at the same time due to ongoing changes in environmental conditions such as increased air temperature and humidity. High-resolution plume and deposition modelling may be performed to define where the local pollutants from ships and power plants are transported and deposited.

There is an established system for long term monitoring of air quality in Ny-Ålesund, however, no modelling of air quality has been applied (Sander, 2014). According to the strategy proposed by the Research Council of Norway for further development of Ny-Ålesund (The Research Council of Norway, 2019), there is an intent to make it "a world leading observation and research platform for natural sciences". Thus, both the Norwegian and international research projects would benefit from open access high-resolution modelling system for air quality with coupled chemistry and meteorology that would allow to correct the atmospheric measurements performed in the settlement and facilitate scientific activities.

References

- Alexander, B. and Mickley, L. J. (2015) 'Paleo-Perspectives on Potential Future Changes in the Oxidative Capacity of the Atmosphere Due to Climate Change and Anthropogenic Emissions', *Current Pollution Reports*, 15(2), pp. 57–69. doi: 10.1007/s40726-015-0006-0.
- AMAP (1998) *AMAP Assessment Report: Arctic Pollution Issues*. Oslo, Norway.
- AMAP (2006) *AMAP Assessment 2006: Acidifying Pollutants, Arctic Haze, and Acidification in the Arctic*. Oslo, Norway.
- Argentini, S. *et al.* (2003) 'Characteristics of the boundary layer at Ny-Alesund in the Arctic during the ARTIST field experiment', *Annals of Geophysics*, 46(2), pp. 185–196.
- Arya, S. P. (1999) *Air pollution meteorology and dispersion*. New York: Oxford University press.
- Bärfuss, K. *et al.* (2018) 'New Setup of the UAS ALADINA for Measuring Boundary Layer Properties , Atmospheric Particles and Solar Radiation', *Atmosphere*, 9(28). doi: 10.3390/atmos9010028.
- Beine, H. J. *et al.* (1996) 'Measurements of NO_x and aerosol particles at the Ny-Ålesund Zeppelin mountain station on Svalbard: influence of regional and local pollution sources', *Atmospheric Environment*, 30(7), pp. 1067–1079.
- Beine, H. J., Jaffe, D. A., Herring, J. A., *et al.* (1997) 'High-Latitude Springtime Photochemistry . Part I : NO_x , PAN and Ozone Relationships', *Journal of Atmospheric Chemistry*, 27, pp. 127–153.
- Beine, H. J., Jaffe, D. A., Stordal, F., *et al.* (1997) 'NO_x during ozone depletion events in the arctic troposphere at Ny-Ålesund, Svalbard', *Tellus, Series B: Chemical and Physical Meteorology*, 49(5), pp. 556–565. doi: 10.3402/tellusb.v49i5.16008.
- Cai, J. *et al.* (2014) 'Validation of MicroAeth[®] as a Black Carbon Monitor for Fixed-Site Measurement and Optimization for Personal Exposure Characterization', *Aerosol and Air Quality Research*, 14, pp. 1–9. doi: 10.4209/aaqr.2013.03.0088.
- Castell, N. *et al.* (2017) 'Can commercial low-cost sensor platforms contribute to air quality monitoring and exposure estimates?', *Environment International*. The Authors, 99, pp. 293–302. doi: 10.1016/j.envint.2016.12.007.
- Chalmer, B. J. (1986) *Understanding Statistics*. New York, United States of America: Marcel Dekker Inc.
- Christopher, J. and Fast, E. (2008) *The Arctic: Transportation, Infrastructure and Communication, InfoSeries*. Parliament of Canada, Ottawa.
- Custard, K. D. *et al.* (2015) 'The NO_x dependence of bromine chemistry in the Arctic', *Atmospheric Chemistry & Physics*, 15, pp. 10799–10809. doi: 10.5194/acp-15-10799-2015.
- Dahlke, S. and Maturilli, M. (2017) 'Contribution of Atmospheric Advection to the Amplified Winter Warming in the Arctic North Atlantic Region', *Advances in Meteorology*, 2017, p. Article ID 4928620. doi: 10.1155/2017/4928620.
- Dalsøren, S. B. *et al.* (2007) 'Environmental impacts of the expected increase in sea transportation, with a particular focus on oil and gas scenarios for Norway and northwest Russia', *Journal of Geophysical Research*, 112(D2), p. D02310. doi: 10.1029/2005JD006927.

- Dalsøren, S. B. *et al.* (2009) 'Update on emissions and environmental impacts from the international fleet of ships : the contribution from major ship types and ports', *Atmospheric Chemistry and Physics*, 9(6), pp. 2171–2194. doi: 10.5194/acp-9-2171-2009.
- Dee, D. P. *et al.* (2011) 'The ERA-Interim reanalysis : configuration and performance of the data assimilation system', *Quarterly Journal of the Royal Meteorological Society*, 137(April), pp. 553–597. doi: 10.1002/qj.828.
- Eckhardt, S. *et al.* (2015) 'Current model capabilities for simulating black carbon and sulfate concentrations in the Arctic atmosphere: A multi-model evaluation using a comprehensive measurement data set', *Atmospheric Chemistry and Physics*, 15(16), pp. 9413–9433. doi: 10.5194/acp-15-9413-2015.
- Eriksen, A. B. *et al.* (2012) 'Reversible phytochrome regulation influenced the severity of ozone-induced visible foliar injuries in *Trifolium subterraneum* L.', *Plant Growth Regulation*, 68(3), pp. 517–523. doi: 10.1007/s10725-012-9729-8.
- Fan, S.-M. and Jacob, D. J. (1992) 'Surface ozone depletion in Arctic spring sustained by bromine reactions on aerosols', *Nature*, 359, pp. 522–524.
- Ferrero, L. *et al.* (2016) 'Vertical profiles of aerosol and black carbon in the Arctic : a seasonal phenomenology along 2 years (2011 – 2012) of field campaigns', *Atmospheric Chemistry and Physics*, 16, pp. 12601–12629. doi: 10.5194/acp-16-12601-2016.
- Ferrero, L. *et al.* (2019) 'Chemical Composition of Aerosol over the Arctic Ocean from Summer ARctic EXpedition (AREX) 2011 – 2012 Cruises : Ions , Amines , Elemental Carbon , Organic Matter , Polycyclic Aromatic Hydrocarbons , n-Alkanes , Metals , and Rare Earth Elements', *Atmosphere*, 10(54), pp. 1–32. doi: 10.3390/atmos10020054.
- Fierz, M. *et al.* (2011) 'Design , Calibration , and Field Performance of a Miniature Diffusion Size Classifier Design , Calibration , and Field Performance of a Miniature Diffusion Size Classifier', *Aerosol Science and Technology*, 6826(45), pp. 1–10. doi: 10.1080/02786826.2010.516283.
- Førland, E. J. *et al.* (2011) 'Temperature and Precipitation Development at Svalbard 1900 – 2100', *Advances in Meteorology*, 2011, p. Article ID 893790. doi: 10.1155/2011/893790.
- Futsaether, C. M. *et al.* (2015) 'Daylength influences the response of three clover species (*Trifolium* spp.) to short-term ozone stress', *Boreal Environment Research*, 20(1), pp. 90–104.
- Garrett, T. J. and Zhao, C. (2006) 'Increased Arctic cloud longwave emissivity associated with pollution from mid-latitudes', *Nature*, 440(April), pp. 787–789. doi: 10.1038/nature04636.
- Gibbons, J. D. and Chakraborti, S. (2003) *Nonparametric Statistical Inference*. 4th edn. New York, United States of America: MARCEL DEKKER, INC.
- Gilgen, A. *et al.* (2018) 'How important are future marine and shipping aerosol emissions in a warming Arctic summer and autumn?', *Atmospheric Chemistry and Physics*, 18(14), pp. 10521–10555. doi: 10.5194/acp-18-10521-2018.
- Graversen, R. G. (2006) 'Do Changes in the Midlatitude Circulation Have Any Impact on the Arctic Surface Air Temperature Trend?', *Journal of Climate*, 19, pp. 5422–5438.
- Hagler, G. S. W. *et al.* (2011) 'Post-processing method to reduce noise while preserving high time resolution in aethalometer real-time black carbon data', *Aerosol and Air Quality Research*, 11(5), pp. 539–546. doi: 10.4209/aaqr.2011.05.0055.

- Heintzenberg, J., Hansson, H.-C. and Lannefors, H. (1981) 'The chemical composition of arctic haze at Ny-Ålesund, Spitsbergen', *Tellus*, 33(2), pp. 162–171. doi: 10.3402/tellusa.v33i2.10705.
- Heintzenberg, J. and Leck, C. (1994) 'Seasonal variation of the atmospheric aerosol near the top of the marine boundary layer over Spitsbergen related to the Arctic sulphur cycle', *Tellus B*, 46, pp. 52–67. doi: 10.1034/j.1600-0889.1994.00005.x.
- Helmig, D. *et al.* (2016) 'Reversal of global atmospheric ethane and propane trends largely due to US oil and natural gas production', *Nature Geoscience*, 9(June), pp. 490–498. doi: 10.1038/NGEO2721.
- Hersbach, H. and Dee, D. (2016) 'ERA5 reanalysis is in production', *ECMWF newsletter*, (number 147), p. 7.
- IPCC (2013) *IPCC, 2013: Climate Change 2013: The Physical Science Basis. Contribution of Working Group I to the Fifth Assessment Report of the Intergovernmental Panel on Climate Change*. Edited by T. F. Stocker *et al.* Cambridge, United Kingdom and New York, NY, USA: Cambridge University Press. Available at: http://www.ipcc.ch/pdf/assessment-report/ar5/wg1/WG1AR5_ALL_FINAL.pdf.
- Isaksen, K. *et al.* (2016) 'Recent warming on Spitsbergen—Influence of atmospheric circulation and sea ice cover', *Journal of Geophysical Research: Atmospheres*, 121(11), pp. 913–931. doi: 10.1002/2016JD025606. Received.
- Jacob, D. J. (2000) 'Heterogeneous chemistry and tropospheric ozone', *Atmospheric Environment*, 34(12–14), pp. 2131–2159. doi: 10.1016/S1352-2310(99)00462-8.
- Janssen, N. A. *et al.* (2012) *Health effects of black carbon*. Copenhagen, Denmark.
- Jiao, W. *et al.* (2016) 'Community Air Sensor Network (CAIRSENSE) project : evaluation of low-cost sensor performance in a suburban environment in the southeastern United States', *Atmospheric Measurement Techniques*, 9, pp. 5281–5292. doi: 10.5194/amt-9-5281-2016.
- Jonassen, M. O. *et al.* (2015) 'Application of remotely piloted aircraft systems in observing the atmospheric boundary layer over Antarctic sea ice in winter', *Polar Research*, 34(1), p. 25651. doi: 10.3402/polar.v34.25651.
- Jung, C. H. *et al.* (2018) 'The seasonal characteristics of cloud condensation nuclei (CCN) in the arctic lower troposphere', *Tellus B: Chemical and Physical Meteorology*. Taylor & Francis, 70(1), pp. 1–13. doi: 10.1080/16000889.2018.1513291.
- Kral, S. T. *et al.* (2018) 'Innovative Strategies for Observations in the Arctic Atmospheric Boundary Layer (ISOBAR)-the Hailuoto 2017 campaign', *Atmosphere*, 9(7). doi: 10.3390/atmos9070268.
- Krzywinski, M. and Altman, N. (2014) 'Points of significance: Nonparametric tests', *Nature Methods*, 11(5), pp. 467–469. doi: 10.1038/nmeth.2937.
- Kusunoki, S., Mizuta, R. and Hosaka, M. (2015) 'Future changes in precipitation intensity over the Arctic projected by a global atmospheric model with a 60-km grid size', *Polar Science*. Elsevier B.V. and NIPR, 9(3), pp. 277–292. doi: 10.1016/j.polar.2015.08.001.
- Leibniz Institute for Tropospheric Research (TROPOS) (2018) *UAV aircraft provide new insights into the formation of the smallest particles in Arctic*. Available at: <https://phys.org/news/2018-06-uav-aircrafts-insights-formation-smallest.html> (Accessed: 12 December 2018).

- Lilliefors, H. W. (1967) 'On the Kolmogorov-Smirnov Test for Normality with Mean and Variance Unknown', *Journal of the American Statistical Association*, 62(318), pp. 399–402.
- Lu, Z. *et al.* (2010) 'Sulfur dioxide emissions in China and sulfur trends in East Asia since 2000', *Atmospheric Chemistry & Physics*, 10, pp. 6311–6331. doi: 10.5194/acp-10-6311-2010.
- Mahmood, R. *et al.* (2019) 'Sensitivity of Arctic sulfate aerosol and clouds to changes in future surface seawater dimethylsulfide concentrations', *Atmospheric Chemistry & Physics*, 19, pp. 6419–6435. doi: 10.5194/acp-19-6419-2019.
- MathWorks (2019a) *corr*, *Linear or rank correlation*. Available at: <https://se.mathworks.com/help/stats/corr.html> (Accessed: 21 June 2019).
- MathWorks (2019b) *kstest*, *One-sample Kolmogorov-Smirnov test*. Available at: https://se.mathworks.com/help/stats/kstest.html?searchHighlight=kstest&s_tid=doc_srchtit le#btn37p4 (Accessed: 21 June 2019).
- MathWorks (2019c) *partialcorr*, *Linear or rank partial correlation coefficients*. Available at: <https://se.mathworks.com/help/stats/partialcorr.html?searchHighlight=partialcorr#btw0d3 1-1> (Accessed: 21 June 2019).
- MathWorks (2019d) *ranksum*, *Wilcoxon rank sum test*. Available at: <https://se.mathworks.com/help/stats/ranksum.html> (Accessed: 21 June 2019).
- Maturilli, M., Herber, A. and König-Langlo, G. (2013) 'Climatology and time series of surface meteorology in Ny-Ålesund, Svalbard', *Earth System Science Data*, 5(1), pp. 155–163. doi: 10.5194/essd-5-155-2013.
- Maturilli, M. and Kayser, M. (2017) 'Arctic warming, moisture increase and circulation changes observed in the Ny-Ålesund homogenized radiosonde record', *Theoretical and Applied Climatology*. *Theoretical and Applied Climatology*, 130, pp. 1–17. doi: 10.1007/s00704-016-1864-0.
- Miljødirektoratet (2018) *Trust Arcticugol Barentsburg, kraftverk og gruvevirksomhet*. Available at: <https://www.norskeutslipp.no/no/Diverse/Virksomhet/?CompanyID=23694> (Accessed: 3 April 2019).
- Miljødirektoratet (2019) *Longyearbyen lokalstyre, Longyear Energiverk*. Available at: <https://www.norskeutslipp.no/no/Diverse/Virksomhet/?CompanyID=5115#> (Accessed: 3 April 2019).
- Mioche, G. *et al.* (2015) 'Variability of the mixed-phase clouds in the Arctic with a focus on the Svalbard region: a study based on spaceborne active remote sensing', *Atmospheric Chemistry & Physics*, 15, pp. 2445–2461. doi: 10.5194/acp-15-2445-2015.
- Monks, P. S. (2005) 'Gas-phase radical chemistry in the troposphere', *Chemical Society reviews*, 34, pp. 376–395. doi: 10.1039/b307982c.
- Monks, P. S. *et al.* (2015) 'Tropospheric ozone and its precursors from the urban to the global scale from air quality to short-lived climate forcer', *Atmospheric Chemistry & Physics*, 15, pp. 8889–8973. doi: 10.5194/acp-15-8889-2015.
- Moroni, B. *et al.* (2015) 'Vertical Profiles and Chemical Properties of Aerosol Particles upon Ny-Ålesund (Svalbard Islands)', *Advances in Meteorology*, 2015, pp. 1–11. Available at: <http://dx.doi.org/10.1155/2015/292081>.

- Myhre, G. *et al.* (2004) 'Uncertainties in the Radiative Forcing Due to Sulfate Aerosols', *Journal of Atmospheric Sciences*, 61(5), pp. 485–498.
- NILU (1996) *EMEP manual for sampling and chemical analysis*.
- Nuttall, M. (2012) 'Urbanization', in *Encyclopedia of the Arctic*. Hoboken, New Jersey, pp. 2087–2115.
- Ødemark, K. *et al.* (2012) 'Short-lived climate forcers from current shipping and petroleum activities in the Arctic', *Atmospheric Chemistry and Physics*, 12(4), pp. 1979–1993. doi: 10.5194/acp-12-1979-2012.
- Onarheim, I. H. *et al.* (2014) 'Loss of sea ice during winter north of Svalbard', *Tellus, Series A: Dynamic Meteorology and Oceanography*, 66, p. 23933. doi: 10.3402/tellusa.v66.23933.
- Peters, G. P. *et al.* (2011) 'Future emissions from shipping and petroleum activities in the Arctic', *Atmospheric Chemistry and Physics*, 11, pp. 5305–5320. doi: 10.5194/acp-11-5305-2011.
- Piechura, J. and Walczowski, W. (2009) 'Warming of the West Spitsbergen Current and sea ice north of Svalbard', *Oceanologia*, 51(2), pp. 147–164. doi: 10.5697/oc.51-2.147.
- Possner, A., Ekman, A. M. L. and Lohmann, U. (2017) 'Cloud response and feedback processes in stratiform mixed-phase clouds perturbed by ship exhaust', *Geophysical Research Letters*, 44, pp. 1964–1972. doi: 10.1002/2016GL071358.
- Qi, L. *et al.* (2017) 'Factors controlling black carbon distribution in the Arctic', *Atmospheric Chemistry & Physics*, 17, pp. 1037–1059. doi: 10.5194/acp-17-1037-2017.
- Quinn, P. K. *et al.* (2007) 'Arctic haze: current trends and knowledge gaps', *Tellus B*, 59(1), pp. 99–114. doi: 10.1111/j.1600-0889.2006.00238.x.
- Rhead, M. M. and Pemberton, R. D. (1996) 'Sources of Naphthalene in Diesel Exhaust Emissions', *Energy & Fuels*, 10, pp. 837–843. doi: 10.1021/ef9502261.
- Richter-Menge, J. and Mathis, J. T. (2017) 'THE ARCTIC', in Blunden, J. and Arndt, D. S. (eds) *STATE OF THE CLIMATE IN 2016*. Bulletin of the American Meteorological Society, pp. 129–130. doi: 10.1175/2017BAMSStateoftheClimate.1.
- Sander, G. (2014) *Limits of acceptable change caused by local activities in Ny-Ålesund. Report from a pre-project, containing a proposal for a main project*. Tromsø.
- Sander, G., Holst, A. and Shears, J. (2006) *Environmental impact assessment of the research activities in Ny-Ålesund 2006*.
- Schmale, J. *et al.* (2018) 'Local Arctic Air Pollution : A Neglected but Serious Problem', *Earth's Future*, 6, pp. 1385–1412. doi: 10.1029/2018EF000952.
- Seinfeld, J. H. and Pandis, S. N. (2006) *Atmospheric Chemistry and Physics: From Air Pollution to Climate Change*. 2nd edn. New York, U.S.: John Wiley & Sons, Inc.
- Shears, J. *et al.* (1998) *Environmental impact assessment. Ny-Ålesund international scientific research and monitoring station, Svalbard*. Tromsø.
- Stein, A. F. *et al.* (2015) 'NOAA's HYSPLIT atmospheric transport and dispersion modeling system', *Bulletin of the American Meteorological Society*, (February), pp. 2059–2077. doi: 10.1175/BAMS-D-14-00110.1.
- Stohl, A. (1998) 'Computation, accuracy and applications of trajectories—A review and

- bibliography', *Atmospheric Environment*, 32(6), pp. 947–966. doi: 10.1016/S1352-2310(97)00457-3.
- Stohl, A. (2006) 'Characteristics of atmospheric transport into the Arctic troposphere', *Journal of Geophysical Research*, 111(D11), p. D11306. doi: 10.1029/2005JD006888.
- The Research Council of Norway (2019) *Ny-Ålesund Research Station. Research Strategy Applicable from 2019*. Lysaker, Norway.
- Vestreng, V. *et al.* (2007) 'Twenty-five years of continuous sulphur dioxide emission reduction in Europe', *Atmospheric Chemistry and Physics*, 7(13), pp. 3663–3681. doi: 10.5194/acp-7-3663-2007.
- Vestreng, V., Kallenborn, R. and Økstad, E. (2009) *Climate influencing emissions, scenarios and mitigation options at Svalbard*. Klima- og forurensningsdirektoratet, Oslo, Norway.
- Vihma, T. *et al.* (2011) 'Characteristics of Temperature and Humidity Inversions and Low-Level Jets over Svalbard Fjords in Spring', *Advances in Meteorology*, 2011(c), p. 14. doi: 10.1155/2011/486807.
- Vincent, W. F. *et al.* (2011) 'Ecological Implications of Changes in the Arctic Cryosphere', *Ambio*, 40, pp. 87–99. doi: 10.1007/s13280-011-0218-5.

Part II Appended papers

INFLUENCE OF LOCAL AND REGIONAL AIR POLLUTION ON ATMOSPHERIC MEASUREMENTS IN NY-ÅLESUND

A. DEKHTYAREVA¹, K. EDVARDSEN^{1,3}, K. HOLMÉN², O. HERMANSEN³ & H.-C. HANSSON⁴

¹UiT The Arctic University of Norway, Norway.

²Norwegian Polar Institute, Norway.

³NILU – Norwegian Institute for Air Research, Norway.

⁴Stockholm University, Sweden.

ABSTRACT

The Zeppelin observatory is a research station near the village Ny-Ålesund in Svalbard. The facility delivers data to international projects devoted to high data quality monitoring of the background air pollution in the Arctic. An approach for quantifying the influence of local and regional pollution on measurements that may be misinterpreted as long-range transported one, is presented here.

The hourly gas and aerosol data measured in Ny-Ålesund and at the Zeppelin station, respectively, have been analysed along with the meteorological data from Ny-Ålesund, Zeppelin station and Long-yearbyen (south-east of Ny-Ålesund).

Seasonal fluctuation of the average measured values of SO₂ and NO_x has been observed. Three main wind directions coincided with the peak concentration of SO₂ and NO_x. The NW-N flow may bring local pollution from ship traffic and diesel power plant as well as biogenic SO₂ from the oxidation of DMS. The monthly average number of particles with diameter characteristic for ship plume (50–100 nm), was elevated for the hours when ships have been registered in the local call list. The number concentration of particles with diameter 200 nm, typical for Arctic haze events, and concentration of non-sea salt sulphate rise during springtime. The FLEXTRA-trajectory analysis indicated that most pollution brought by E-SE and SW flows may be of long-range and/or regional origin. Events with these flow directions need to be interpreted with caution.

Keywords: aerosol, Arctic, local pollution, long-range transport, trajectory.

1 INTRODUCTION

Nitrogen oxides NO_x, (NO+NO₂), and sulphur dioxide SO₂ are emitted in large amounts from combustion of various fossil fuels worldwide. Monks [1] among others stated that NO_x, in the presence of volatile organic compounds (VOC) and/or carbon monoxide CO, are responsible for the production of tropospheric ozone, O₃, through the photochemical reactions in urban smog. In turn, as was reported by the Intergovernmental Panel on Climate Change (IPCC) [2], tropospheric O₃ is an important greenhouse gas, and being a strong oxidant, it effects the concentration of other greenhouse gases. Moreover, both NO_x and SO₂ are acidifying agents, and, according to the Arctic Monitoring and Assessment Programme (AMAP) reports [3, 4], their deposition may have a strong negative effect on many terrestrial ecosystems, specifically vulnerable in the Arctic under rapidly changing climatic conditions, while the impact of emissions of acidifying agents from increasing shipping traffic in the Arctic on marine coastal ecosystems needs to be investigated.

Jacob [5] stated that the lifetime of NO_x is on the order of one day in the lower troposphere at mid-latitudes, and Lelieveld *et al.* [6] reported the lifetime of SO₂ and non-sea salt sulphate

to be approximately 2 days and 5 days, respectively. Therefore, according to the “classic” air pollution literature, the sources of NO_x and SO_2 are mostly regional or local. Furthermore, in mid-latitudes, the local air pollution is mainly characterized by higher concentrations, while long-range transported pollution is considered to be more dispersed. However, physical conditions, such as low air temperatures and low humidity, limited turbulent mixing and the absence of sunlight during the polar night, as well as atmospheric dynamics, namely the position of the Arctic front, increase lifetime of pollutants during winter- and springtime Stohl [7]. Due to this, the lifetimes of NO_x and SO_2 were estimated by Beine *et al.* [8] and Lee *et al.* [9] as 10 days and 4 days north of the Arctic front, respectively.

During winter the Arctic front barrier, formed by the surfaces of constant potential temperature increasing with height, extends further south (up to 50°N). Consequently, according to Quinn *et al.* [10], in the winter and spring the Arctic haze, polluted air masses transported mainly from Europe and Asia, may be observed in polar regions. On the other hand, during summer the Arctic front is located further north and air may remain continuously north of 80°N in the lower troposphere up to 14 days. Results from several studies, [7,11,12], show that this prevents the transport of pollutants from Eurasia during this season, and local aerosol sources on Svalbard are considered to be more important during this time of the year.

Svalbard’s archipelago is nearly a pristine Arctic environment with only a few local and regional anthropogenic pollution sources. Therefore, much of the atmospheric research activities there are devoted to the monitoring of long-range transported pollution in the Arctic.

The Zeppelin Observatory is the Norwegian atmospheric monitoring station situated on a mountain ridge 2 km away from a small research settlement Ny-Ålesund. The station is of high importance for the Global Atmosphere Watch, The European Monitoring and Evaluation Programme (EMEP), AMAP and many other research projects due to unique opportunities for monitoring of background air composition, meteorological and climatological studies.

The main purpose of this article is to discuss ambiguities related to the process of identification of possible sources of air pollution on Svalbard and present an approach for quantifying the influence of local and regional pollution on measurements in Ny-Ålesund.

2 AIR POLLUTION SOURCES ON SVALBARD

Coal-fired power plants are operated in the two settlements of Longyearbyen and Barentsburg located to the south-east of Ny-Ålesund. According to Vestreng *et al.* [13], these are the largest year-round anthropogenic point sources of SO_2 in Svalbard. Both have seasonally variable emission rates, Fig. 1a.

According to the environmental impact assessment of Ny-Ålesund as an international scientific research and monitoring station (Shears *et al.* [14]), the power plant fuelled by low sulphur diesel, is the largest local year-round point source of NO_x in Ny-Ålesund. It too has seasonally variable emission rates. The monitoring station is installed south of the power plant, Fig. 1b.

In addition to this, combustion engines on tourist ships produce fumes that contain NO_x , SO_2 and particulate matter. Shears *et al.* [14] and Eckhardt *et al.* [15] noted that these summertime local sources of emissions have significant impact on atmospheric measurements in Ny-Ålesund. The impact rate depends on emission rates (ship’s size and number of ships present in the fjord simultaneously) and atmospheric conditions.

The overview of the emissions from the main sources is given in Table 1. The emission rates for the first three sources and for the last two sources in the table are calculated from hourly and annual values defined in Shears *et al.* [14] and Miljødirektoratet [16], respectively.

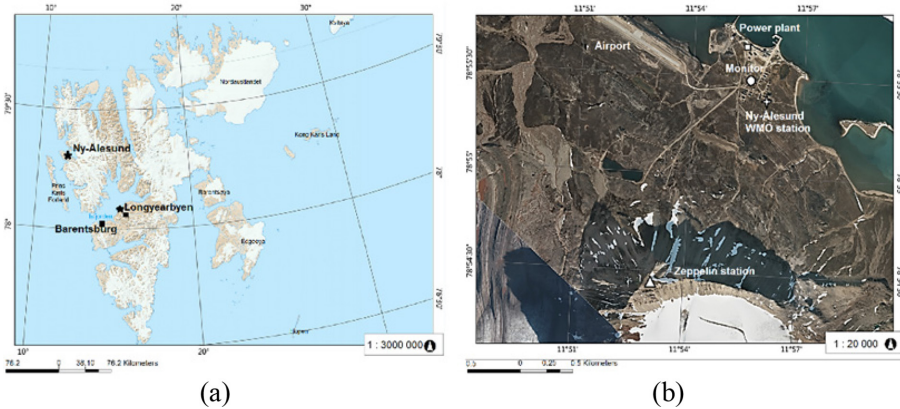


Figure 1: Study area: (a) map of Svalbard showing Barentsburg and Longyearbyen and meteorological stations as squares and stars, respectively, and (b) local map of Ny-Ålesund showing power plant, monitor, Ny-Ålesund WMO station and Zeppelin station as square, circle, star and triangle, respectively.

Table 1: Main sources of emissions in Ny-Ålesund and on Svalbard.

Source	$\text{SO}_2, \cdot 10^{-5} \text{ kgs}^{-1}$	$\text{NO}_x, \cdot 10^{-5} \text{ kgs}^{-1}$
1 Diesel generators and central heating in Ny-Ålesund	32	117
2 Small ships in Ny-Ålesund	14	83
3 Cruise ships in Ny-Ålesund	1444	3889
4 Barentsburg power plant (average 2010–2013)	7191	447
5 Longyearbyen power plant (average 2009–2014)	1368	490

3 MATERIALS AND METHODS

The ground-based SO_2 and NO_x observations have been sorted according to the prevailing wind direction and compared with ship traffic statistics. When concentrations of SO_2 and NO_x were above a lower detectable limit (LDL), the FLEXTRA-trajectory model output was examined for distinguishing between local and long-range transport of pollutants. By analogy with Stohl [7], if air resided exclusively north of 70°N during the previous 7 days for trajectory arriving at altitude 500 m to the Zeppelin station, it was considered to be no long-range transport of pollutants (NLRT case). If the trajectory data were missing, or there were values of latitude $<70^\circ\text{N}$, it was assigned as a possible long-range transport (LRT) case. According to Brock *et al.* [17], the sub- $0.1\text{-}\mu\text{m}$ particles often prevail in the particle number population of aged coal power plant plumes several hours after the emission. In addition, experimental studies of Petzold *et al.* [18] show that the combustion particles have modal diameters centred at 50 nm and 100 nm for raw emissions and for a plume age of 1 hour, respectively. Therefore, the particle mode with $d = 50\text{--}100$ nm has been chosen to check the

possible year-round influence of coal power plant and summertime ship emissions on Zeppelin measurements.

3.1 Measurements description

The SO₂ and NO_x data were collected by Norwegian Institute for Air Research (NILU) during the project Local Air Quality Monitoring 2008–2010 in Ny-Ålesund [19] from 14.07.2008 to 24.08.2010. Both analysers used in the project, had LDL = 0.4 ppb. Most of the data have been below this value, which is too high for the near pristine environment of Ny-Ålesund. Therefore, the data equal to or higher than LDL have been considered as peaks in this work. The aerosol measurements presented here have been performed by Stockholm University at the Zeppelin station. The daily filter samples data collected by NILU at the Zeppelin station are part of the “Cooperative programme for monitoring and evaluation of long-range transmission of air pollutants in Europe” (EMEP). The non-sea salt sulphate has been defined according to the non-sea salt sulphate correction algorithm presented in the WMO report [20]. An overview of the chemical and aerosol data is shown in Table 2.

Combined analysis of ground-based hourly meteorological data from the monitor with gas analysers and Ny-Ålesund WMO station (78.9230 N, 11.9333 E), operated by NILU and Norwegian Meteorological Institute, respectively, provides coverage for the whole period of air quality measurements. In addition, data from the Zeppelin station and from the Svalbard lufthavn (Svalbard airport) (28 m a.s.l., 78.2453 N, 15.5015 E) have been used, Fig. 1a and b.

3.2 Model data description

The FLEXTRA 3D backward trajectories (www.nilu.no/trajectories) used in this study are provided by NILU. They run 7 days backward in time and are based on ECMWF (European Centre for Medium Range Weather Forecasts) meteorological data with spatial resolution of 1.25° and temporal resolution of 6 hours. The nearest trajectory to the time of the peak has been chosen, and when the peak value falls in between two trajectories both have been assessed. If at least one of them passed south of 70°N, then it was considered to be an LRT-case. The modelled data are available for the whole period of interest. Four percent of data is missing (most of the dates in December 2008 and several other discrete days in 2008). As reported by Stohl [26], the position errors in FLEXTRA are in the order of 20% of the travelled distance

Table 2: Data analysed in the paper.

Equipment and reference	Measured component and units	Location
Chemiluminescence NO _x analyser (model 200E) [21]	NO, NO ₂ , NO _x , µg/m ³	Monitor, 78.9247N, 11.9262E
UV Fluorescence SO ₂ analyser (model 100E) [22]	SO ₂ , µg/m ³	
Condensation particle counters (TSI CPC 3025 and TSI CPC 3010) [23, 24]	Integral aerosol number density and size distribution, cm ⁻³	Zeppelin station, 78.9073N, 11.8859 E
Aerosol filter [25]	SO ₄ ²⁻ (p), µg S/m ³	

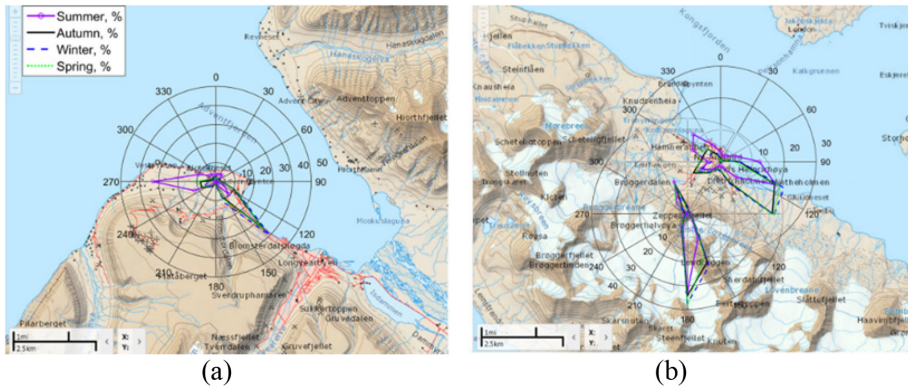


Figure 2: Seasonal wind roses: (a) Svalbard lufthavn station north-west of Longyearbyen and (b) Ny-Ålesund WMO (upper wind rose) and Zeppelin (lower wind rose) stations.

and the performance varies with the meteorological conditions, but the approximate pathway of the air mass may be estimated.

4 RESULTS AND DISCUSSION

The seasonal wind roses for the period of measurements are plotted (Fig. 2) for 16 wind directions (22.5° for each sector).

One can see that the prevailing wind direction differs significantly for summer at all stations comparing to other seasons. Most likely, the reason for this is that increasing temperature differences between the land and water facilitate the formation of on shore circulation. The lowest mean seasonal wind speed is observed in summer also. The seasonal wind speed rises gradually and is highest in winter likely due to enhancing influence of mesoscale cyclonic activity, as discussed in Maturilli *et al.* [27]. Additionally, the topographical wind channelling plays important role year-round at all three stations.

The change of wind direction and speed may influence the dispersion of pollutants. The plume from the power plant located to the south-east of the Svalbard lufthavn station in the Longyearbyen town may be trapped in the valleys nearby, Longyeardalen and Adventdalen, due to the prevailing westerly wind direction in summer (Fig. 2a). Therefore, this pollution source is unlikely to influence the measurement results in Ny-Ålesund during this season.

The Zeppelin station is located at the height of 474 m above sea level. The most frequently observed wind direction at the Zeppelin observatory is south and south-south-east due to shadowing effect of nearby mountains, Fig. 2b. From the wind roses for Ny-Ålesund and Zeppelin stations, one can see that the wind direction varies significantly, even within distance of 2 km, due to complex topography.

Analogously, although Longyearbyen and Barentsburg are located in the inner part of the same fjord, Isfjorden, the data from Svalbard lufthavn station most probably can't be utilized for assessment of spreading of pollution from Barentsburg power plant, and separate dataset for Barentsburg is needed (see Fig. 1a).

However, the on shore circulation may bring the pollution from the ships cruising in the Kongsfjorden or attached to pier in Ny-Ålesund in summer, Fig. 2b.

Indeed, despite only 31% and 8% of all NO_x and SO_2 hourly data being defined as peak, seasonal fluctuation of the average measured values of SO_2 and NO_x has been observed with increasing concentration of gases every summer and winter, Fig. 3. Mean SO_2 and NO_x concentrations and number of particles with $d = 50\text{--}100\text{ nm}$ values were higher on 21%, 16% and 55%, respectively, for time interval of 2 hours before arrival to 2 hours after departure registered in the cruise call list comparing to hours without ships. Elevated values of SO_2 in presence of ships mainly coincide with NNW-N wind, which is natural, because the harbour is located north of the monitor (Fig. 1b). However, one peculiar feature of local pollution dispersion pattern has been revealed. Although there are glaciers 3 km south-west from monitor and, according to meteorological studies [27], wind from this direction is of katabatic origin, SW-WSW wind brings at times SO_2 , NO_x and particles emitted by big anchored ships according to the cruise calls list. These cases are rare but they affect the mean summer concentration of SO_2 for this wind direction significantly. Mean NO_x concentrations were approximately five times higher year-round when NW-NNW wind had been observed due to emissions from diesel power plant north of the monitor in Ny-Ålesund.

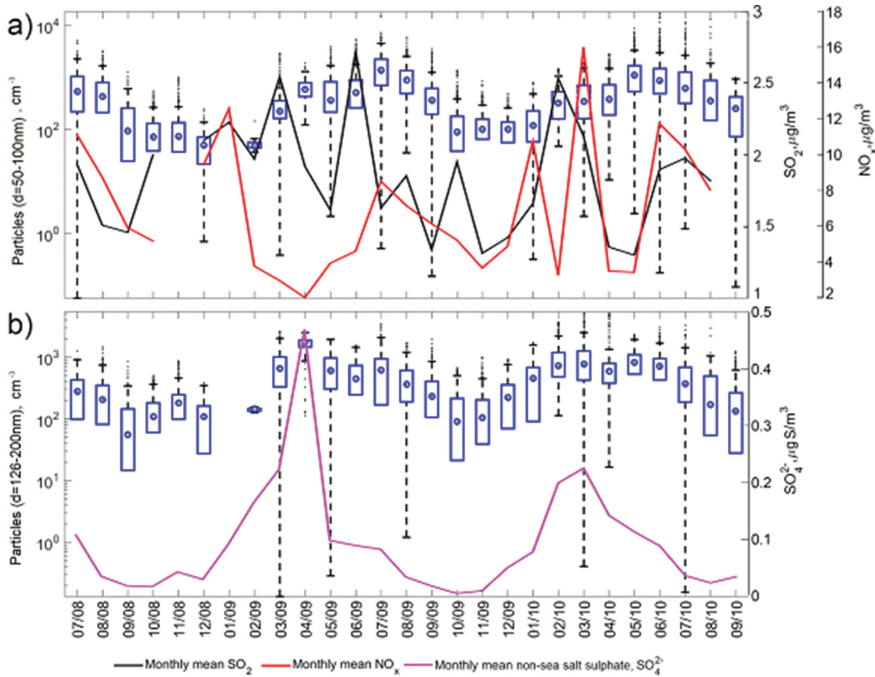


Figure 3: Monthly statistics of integral aerosol number density (box and whiskers plots) and gas analysers and filter samples data (lines): a) integral aerosol number density for particles with $d = 50\text{--}100\text{ nm}$, cm^{-3} , and monthly mean SO_2 and NO_x from gas analysers, $\mu\text{g}/\text{m}^3$; b) integral aerosol number density for particles with $d = 126\text{--}200\text{ nm}$, cm^{-3} , and monthly mean non-sea salt sulphate from filter samples, $\mu\text{g S}/\text{m}^3$. The logarithmic scale has been used for aerosol data (left y-axis on both figures). The central mark is the median, the edges of the box are the 25th and 75th percentiles, the whiskers extend to the most extreme data points not considered outliers, and statistical outliers are plotted individually on each box.

The integral aerosol number density of particles with size 10–40 nm increases every summer significantly, which indicates boundary layer nucleation events. High mean number of particles were at times observed for northerly wind direction and coincided with SO₂ peak even in absence of ships. This supports previous studies of fine particle composition performed by Heintzenberg and Leck [28] that revealed the importance of marine biogenic sources of sulphur compounds on Svalbard.

The concentrations of particles with size 50–100 nm decrease in wintertime and start increasing again in spring with the peak in summer, Fig. 3a. One possible reason for this is that there is no influence of coal power plant emissions on measurements in Ny-Ålesund. However, one may notice that the growth in particle number of this mode starts in February, when the polar night season on Svalbard is over, although there is still no direct sunlight. According to Brock *et al.* [17], the particulate sulphate formation in coal power plant plumes takes place mostly through oxidation of SO₂ by OH. The oxidation may occur in aqueous phase as well. However, both processes are restricted due to Arctic environmental conditions in winter, thus the number of particles of this mode is not an applicable parameter for determination of regional pollution on Svalbard in winter. The number of particles with diameter 126–200 nm rises during springtime, and similar pattern is observed for non-sea salt sulphate from filter samples collected at the Zeppelin station, Fig. 3b. This is in good agreement with Seinfeld and Pandis [29] who stated that the Arctic haze phenomena is the long-range transported polar aerosol consisting to a large extent of non-sea salt sulphate of anthropogenic origin.

The trajectory analysis revealed that during summer there is no difference in NO_x mean value whether it was a LRT or a NLRT case, and the concentration depends solely on the wind direction. Concentration decreases during autumn and spring, and mean NO_x value was higher for LRT cases. During winter, values of NO_x for NLRT cases are higher than for LRT ones, probably due to increasing of emissions from the diesel power plant because of enhanced fuel consumption and limited dispersion because of prevailing stable stratification of atmospheric boundary layer. SO₂ values for LRT cases were higher for winter and spring and lower than NLRT cases for autumn and summer. In general, the trajectory analysis indicated that most of pollution brought by E-SE and SW flows, 66% and 60%, respectively, may be of long-range and/or regional origin (possibly from two coal power plants located to SE from Ny-Ålesund). There were some cases in wintertime when trajectory analysis did not show possible long-range transport of pollution, however, elevated concentrations of SO₂ have been measured and SE wind direction has been detected both in Ny-Ålesund and at the Svalbard lufthavn station several hours earlier. Therefore, either there was influence of regional pollution from coal power plants, or modelled trajectory was erroneous. In order to check this, simple backward trajectory FLEXTRA-model results may be replaced in future work by Lagrangian particle dispersion model results, for example, FLEXPART, as it has been suggested by Stohl *et al.* [30] for more accurate interpretation of measured data. Additionally, case study modelling using a plume dispersion model may be done for the dates of interests for power plants in Longyearbyen and Barentsburg.

The changes in the amount of emissions from ships and power plants are expected. A three-stage treatment system of emissions to reduce NO_x, particles and SO₂ is planned to be installed in the Longyearbyen coal power. Barentsburg power plant has been stated as the biggest SO₂ source in Norway, it is currently operated with a permission for emissions of up to 2400 tons SO₂/year as reported by Norwegian Environmental Agency (Miljødirektoratet) [31]. As there is a high rate of uncertainty in the future emission scenarios for the power plants, field campaigns should be performed.

It is restricted to use heavy fuel in Ny-Ålesund since January 1, 2015, and only marine gas oil (MGO) with maximum sulphur content 1.5% is permitted. The emission restrictions will give a steep decline in the number of port calls by cruise ships. However, the NO_x and particle pollution may still be present in summer even if big ships will use MGO instead of heavy fuel. The present study should be continued to quantify the magnitude of improvement in air quality resulting from the emission restriction.

5 CONCLUSIONS

The air quality and meteorological data from Ny-Ålesund have been analysed concurrently. The distinct characteristics for the near pristine coastal Arctic site have been defined, such as seasonal patterns in prevailing wind direction and aerosol integral number density specific for different particle diameters and importance of long-range transported pollution.

FLEXTRA-trajectory analysis revealed that most of the total number of SO_2 peaks from SE and SW flow may be of long-range and/or regional origin with prevailing LRT cases during winter and spring.

During wintertime, there are no ships or biogenic sources in Ny-Ålesund and due to environmental conditions the oxidation of SO_2 to SO_4^{-2} is limited. Because of this, the long-range transport of SO_2 plays major role. However, the same conditions favour regional transport of sulphur dioxide from sources located SE from Ny-Ålesund due to prevailing wind direction. In addition, the fuel consumption at the coal power plants may increase during wintertime. The separation of LRT and regional emissions is therefore ambiguous. Data from Hornsund or Hopen could be very powerful agents to diminish this uncertainty in our ability to quantify the regional influence on the quality of the Ny-Ålesund data.

During summer, long-range transported pollution is less important. Despite decreased fuel consumption at the diesel and coal power plants, local pollution from ships in Ny-Ålesund has been significant during summer. However, analysis of integral aerosol number density of particles with size 10–40 nm and SO_2 data revealed that biogenic sulphur and ultrafine particle sources have to be taken into account also.

The Lagrangian particle dispersion and plume modelling may be done to clarify the pathways and environmental fate of regional pollution from coal power plants on Svalbard. The measurement campaign for sampling of the plume from the coal power plants in Barentsburg and Longyearbyen may be recommended to determine current rate and composition of emissions.

ACKNOWLEDGEMENTS

Norwegian Polar Institute and Norwegian Meteorological Institute are acknowledged for the excellent and freely available online map of Svalbard (<http://svalbardkartet.npolar.no>) and meteorological data from Longyearbyen and Ny-Ålesund (<http://eklima.no>), respectively.

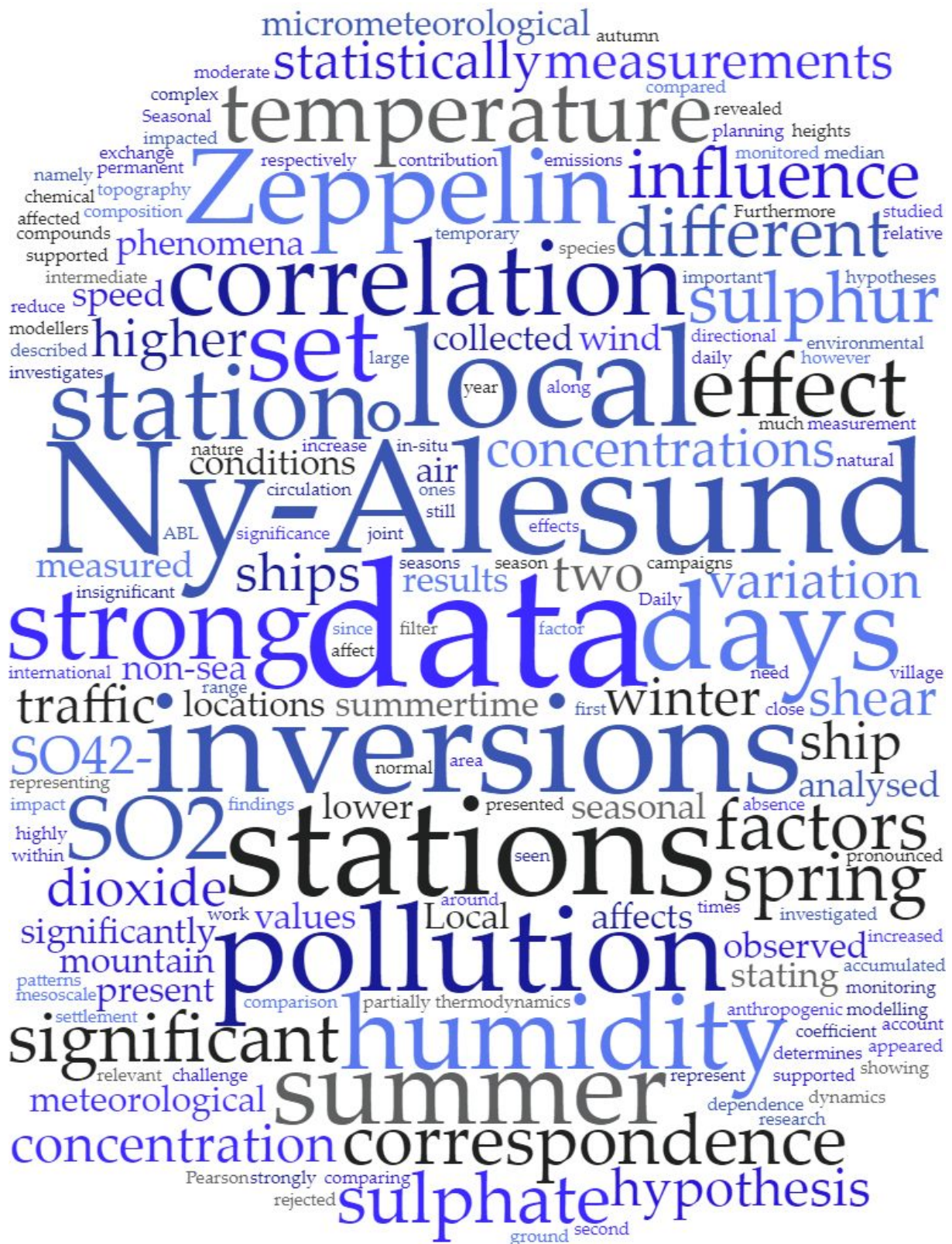
REFERENCES

- [1] Monks, P.S., Gas-phase radical chemistry in the troposphere. *Chemical Society Reviews*, **34**, pp. 376–395, 2005.
<http://dx.doi.org/10.1039/b307982c>
- [2] Hartmann, D.L., et al. Observations: atmosphere and surface (Chapter 2). *IPCC, 2013: Climate Change 2013: The Physical Science Basis. Contribution of Working Group I to the Fifth Assessment Report of the Intergovernmental Panel on Climate Change*, eds., T.F. Stocker, et al, Cambridge University Press: Cambridge, United Kingdom and New York, NY, USA, pp. 159–255, 2013.

- [3] Skjelkvåle, B.L. et al. Effects on freshwater ecosystems (Chapter 6). *AMAP Assessment 2006: Acidifying Pollutants, Arctic Haze, and Acidification in the Arctic*, Oslo, pp. 64–90, 2006.
- [4] Bellerby R. et al. Acidification in the Arctic Ocean Region (Chapter 2). *AMAP Assessment 2013: Arctic Ocean Acidification*, Oslo, pp. 9–36, 2013.
- [5] Jacob, D.J., *Introduction to Atmospheric Chemistry*, Princeton University Press: Princeton, NJ, pp. 211–215, 1999.
- [6] Lelieveld, J., Roelofs, G.-J., Ganzeveld, L., Feichter, J. & Rodhe, H., Terrestrial sources and distribution of atmospheric sulphur. *Philosophical Transactions of the Royal Society B Biological Sciences*, **352**(1350), pp. 149–158, 1997.
<http://dx.doi.org/10.1098/rstb.1997.0010>
- [7] Stohl, A., Characteristics of atmospheric transport into the Arctic troposphere. *Journal of Geophysical Research*, **111**(D11), p. D11306, 2006.
<http://dx.doi.org/10.1029/2005JD006888>
- [8] Beine, H.J., Engard, M., Jaffe, D.A., Hoy, O., Holme, K. & Stordal, F., Measurements of NO_x and aerosol particles at the Ny-Ålesund Zeppelin mountain station on Svalbard: influence of regional and local pollution sources. *Atmospheric Environment*, **30**(7), pp. 1067–1079, 1996.
[http://dx.doi.org/10.1016/1352-2310\(95\)00410-6](http://dx.doi.org/10.1016/1352-2310(95)00410-6)
- [9] Lee, C., Martin, R.V., Donkelaar, A.V., Lee, H., Dickerson, R.R., Hains, J.C., Krotkov, N., Richter, A., Vinnikov, K. & Schwab, J.J., SO₂ emissions and lifetimes: estimates from inverse modeling using in situ and global, space-based (SCIAMACHY and OMI) observations. *Journal of Geophysical Research*, **116**(D6), p. D06304, 2011.
<http://dx.doi.org/10.1029/2010JD014758>
- [10] Quinn, P.K., Shaw, G., Andrews, E., Dutton, E.G., Ruoho-airola, T. & Gong, S.L., Arctic haze: current trends and knowledge gaps. *Tellus B*, **59**(1), pp. 99–114, 2007.
<http://dx.doi.org/10.1111/j.1600-0889.2006.00238.x>
- [11] Zhan, J. & Gao, Y., Impact of summertime anthropogenic emissions on atmospheric black carbon at Ny-Ålesund in the Arctic. *Polar Research*, **33**, p. 21821, 2014.
<http://dx.doi.org/10.3402/polar.v33.21821>
- [12] Weinbruch, S., Wiesemann, D., Ebert, M., Schutze, K., Kallenborn, R. & Strom, J., Chemical composition and sources of aerosol particles at Zeppelin Mountain (Ny Ålesund, Svalbard): an electron microscopy study. *Atmospheric Environment*, **49**, pp. 142–150, 2012.
<http://dx.doi.org/10.1016/j.atmosenv.2011.12.008>
- [13] Vestreng, V., Kallenborn, R. & Økstad, E., Climate influencing emissions, scenarios and mitigation options at Svalbard, p.16, 2009.
- [14] Shears, J., Fredrik, T., Are, B. & Stefan, N., Identification and prediction of environmental impacts (Chapter 8). *Environmental Impact Assessment. Ny-ålesund International Scientific Research and Monitoring station*, Svalbard, Tromsø, pp. 32–40, 1998.
- [15] Eckhardt, S., Hermansen, O., Grythe, H., Fiebig, M., Stebel, K., Cassiani, M., Baecklund, A. & Stohl, A., The influence of cruise ship emissions on air pollution in Svalbard – a harbinger of a more polluted Arctic? *Atmospheric Chemistry and Physics*, **13**(16), pp. 8401–8409, 2013.
<http://dx.doi.org/10.5194/acp-13-8401-2013>
- [16] Miljødirektoratet, Norske utslipp, available at www.norskeutslipp.no/

- [17] Brock, C.A., Washenfelder, R.A., Trainer, M., Ryerson, T.B., Wilson, J.C., Reeves, J.M., Huey, L.G., Holloway, J.S., Parrish, D.D., Hubler, G. & Fehsenfeld, F.C., Particle growth in the plumes of coal-fired power plants. *Journal of Geophysical Research*, **107**(D12), pp. AAC 9–1–AAC 9–14, 2002.
- [18] Petzold, A., Hasselbach, J., Lauer, P., Baumann, R., Franke, K., Gurk, C., Schlager, H. & Weingartner, E., Experimental studies on particle emissions from cruising ship, their characteristic properties, transformation and atmospheric lifetime in the marine boundary layer. *Atmospheric Chemistry and Physics*, **8**(9), pp. 2387–2403, 2008.
<http://dx.doi.org/10.5194/acp-8-2387-2008>
- [19] Hermansen, O., Wasseng, J., Backlund, A., Strom, J., Noon, B., Henning, T., Schulze, D. & Barth, V.L., Air quality Ny-Ålesund. Monitoring of local air quality 2008–2010. Measurement results, Kjeller, pp. 7–13, 2011.
- [20] WMO, Manual for the GAW precipitation chemistry programme. *Guidelines, Data Quality Objectives and Standard Operating Procedures, in WMO Report*, **160**, ed M.A. Allan, pp. 159–160, 2004.
- [21] Teledyne Advanced Pollution Instrumentation, Model 200E Nitrogen Oxide Analyzer, Technical Manual, San Diego, 2010.
- [22] Teledyne Advanced Pollution Instrumentation, Model 100E UV Fluorescence SO₂ Analyzer, Operation Manual, San Diego, 2011.
- [23] TSI, Model 3010 Condensation Particle Counter, Instruction Manual, 2002.
- [24] TSI, Model 3025A Ultrafine Condensation Particle Counter, Instruction Manual, 2002.
- [25] EMEP, Sampling of sulphur dioxide, sulphate, nitric acid, ammonia, nitrate and ammonium using the filter pack method (Chapter 3.2). *EMEP Manual For Sampling and Chemical Analysis. Norwegian Institute for Air Research. EMEP CCC Report 1/95*, Kjeller, pp. 3-13–3-28, 1996.
- [26] Stohl, A., Computation, accuracy and applications of trajectories—a review and bibliography. *Atmospheric Environment*, **32**(6), pp. 947–966, 1998.
[http://dx.doi.org/10.1016/S1352-2310\(97\)00457-3](http://dx.doi.org/10.1016/S1352-2310(97)00457-3)
- [27] Maturilli, M., Herber, A. & König-Langlo, G., Climatology and time series of surface meteorology in Ny-Ålesund, Svalbard. *Earth System Science Data*, **5**(1), pp. 155–163, 2013.
<http://dx.doi.org/10.5194/essd-5-155-2013>
- [28] Heintzenberg, J. & Leck, C., Seasonal variation of the atmospheric aerosol near the top of the marine boundary layer over Spitsbergen related to the Arctic sulphur cycle. *Tellus B*, **46**, pp. 52–67, 1994.
<http://dx.doi.org/10.1034/j.1600-0889.1994.00005.x>
- [29] Seinfeld, J.H. & Pandis, S.N., *Atmospheric Chemistry and Physics: From Air Pollution to Climate Change*, 2nd edn., John Wiley & Sons, Inc, pp. 378–379, 2006.
- [30] Stohl, A., Eckhardt, S., Forster, C., James, P., Spichtinger, N. & Petra, S., A replacement for simple back trajectory calculations in the interpretation of atmospheric trace substance measurements. *Atmospheric Environment*, **36**(29), pp. 4635–4648, 2002.
[http://dx.doi.org/10.1016/S1352-2310\(02\)00416-8](http://dx.doi.org/10.1016/S1352-2310(02)00416-8)
- [31] Sørby, H. & Sørmo, G., Tillatelse til virksomhet etter svalbardmiljøloven for Trust Arcticugol, Barentsburg, Miljødirektoratet, Trondheim, pp. 5–13, 2010.

Paper II





Effect of seasonal mesoscale and microscale meteorological conditions in Ny-Ålesund on results of monitoring of long-range transported pollution

Alena Dekhtyareva, Kim Holmén, Marion Maturilli, Ove Hermansen & Rune Graversen

To cite this article: Alena Dekhtyareva, Kim Holmén, Marion Maturilli, Ove Hermansen & Rune Graversen (2018) Effect of seasonal mesoscale and microscale meteorological conditions in Ny-Ålesund on results of monitoring of long-range transported pollution, *Polar Research*, 37:1, 1508196

To link to this article: <https://doi.org/10.1080/17518369.2018.1508196>



© 2018 The Author(s). Published by Informa UK Limited, trading as Taylor & Francis Group.



Published online: 06 Sep 2018.



Submit your article to this journal [↗](#)



View Crossmark data [↗](#)

RESEARCH ARTICLE



Effect of seasonal mesoscale and microscale meteorological conditions in Ny-Ålesund on results of monitoring of long-range transported pollution

Alena Dekhtyareva ^a, Kim Holmén^b, Marion Maturilli ^c, Ove Hermansen^d & Rune Graversen^e

^aDepartment of Engineering and Safety, Faculty of Engineering and Technology, UiT—The Arctic University of Norway, Tromsø, Norway; ^bNorwegian Polar Institute, Longyearbyen, Norway; ^cClimate Sciences Department, Alfred Wegener Institute Helmholtz Centre for Polar and Marine Research, Potsdam, Germany; ^dDepartment of Monitoring and Information Technology, Norwegian Institute for Air Research, Kjeller, Norway; ^eDepartment of Physics and Technology, Faculty of Science and Technology, UiT—The Arctic University of Norway, Tromsø, Norway

ABSTRACT

Ny-Ålesund is an international research settlement where the thermodynamics and chemical composition of the air are monitored. The present work investigates the effects of micro-meteorological conditions, mesoscale dynamics and local air pollution on the data collected at two different locations around the village. Daily filter measurements of sulphur dioxide and non-sea salt sulphate from the temporary Ny-Ålesund station and permanent Zeppelin mountain station have been analysed along with meteorological data. The influence of different factors representing micrometeorological phenomena and local pollution from ships has been statistically investigated. Seasonal variation of the correlation between the data from Ny-Ålesund and Zeppelin stations is revealed, and the seasonal dependence of the relative contribution of different factors has been analysed. The median concentrations of SO_4^{2-} measured in Ny-Ålesund increased significantly on days with temperature inversions in winter. In spring, concentrations of SO_2 and SO_4^{2-} were higher than normal at both stations on days with temperature inversions, but lower on days with strong humidity inversions. In summer, local ship traffic affects the SO_2 data set from Ny-Ålesund, while no statistically significant influence on the Zeppelin data set has been observed. The pollution from ships has an effect on SO_4^{2-} values at both stations; however, the concentrations in Ny-Ålesund were higher when local pollution accumulated close to the ground in days with strong humidity inversions.

KEYWORDS

Micrometeorology; air pollution; Arctic haze; atmospheric inversion; aerosol; sulphate



ABBREVIATIONS

ABL: atmospheric boundary layer; DMS: dimethyl sulphide; WRS: Wilcoxon rank sum

Introduction

A small community on the north-west Coast of Spitsbergen island, in the Svalbard Archipelago, Ny-Ålesund is a place for fruitful international cooperation in connection with environmental monitoring. Data and knowledge exchange between researchers from 12 different nations leads to joint publications and improves our scientific understanding of various processes in a rapidly changing Arctic (Norwegian Polar Institute 2016). Specific attention is given to the study of the Arctic haze phenomena, aerosol of anthropogenic origin enriched in non-sea salt sulphate (XSO_4^{2-}) and transported over long distances from mid-latitudes to the Arctic during winter and spring (Quinn et al. 2007; Dekhtyareva et al. 2016; Ferrero et al. 2016). Ny-Ålesund is situated far from major industrial areas, and is therefore considered suitable for monitoring of long-range transported pollution. This study considers whether the data collected at different locations around the village show differences due to local environmental peculiarities of this site.

The settlement is in a mountainous coastal area near the narrow fjord Kongsfjorden, which has two glaciers at the one end and the Greenland Sea at the other (Fig. 1a). Thermally driven circulations, such as katabatic winds and sea-land breeze, channelling of mesoscale wind along the fjord and the shielding effect of surrounding mountains, are local topographically induced features (Esau & Repina 2012; Maturilli et al. 2013; Maturilli & Kayser 2016). Wind shear and turbulence, affecting the mixing and dilution of air pollutants, may be induced or suppressed by these features (Fisher 2002). Furthermore, temperature and humidity inversions often occur in the ABL as a result of surface cooling during winter and spring and are frequently observed in Svalbard (Vihma et al. 2011). Mixing processes are limited in the stable ABL. This leads to variation in humidity with altitude, and therefore affects the amount of water, condensation processes and particle growth (Stull 1988; Seinfeld & Pandis 2006). Consequently, different aerosol content appearing at different altitudes have been observed during several

CONTACT Alena Dekhtyareva  alena.dekhtyareva@uit.no  Department of Engineering and Safety, Faculty of Engineering and Technology, UiT—The Arctic University of Norway, P.O. Box 6050 Langnes, NO-9037 Tromsø, Norway

© 2018 The Author(s). Published by Informa UK Limited, trading as Taylor & Francis Group.

This is an Open Access article distributed under the terms of the Creative Commons Attribution-NonCommercial License (<http://creativecommons.org/licenses/by-nc/4.0/>), which permits unrestricted non-commercial use, distribution, and reproduction in any medium, provided the original work is properly cited.

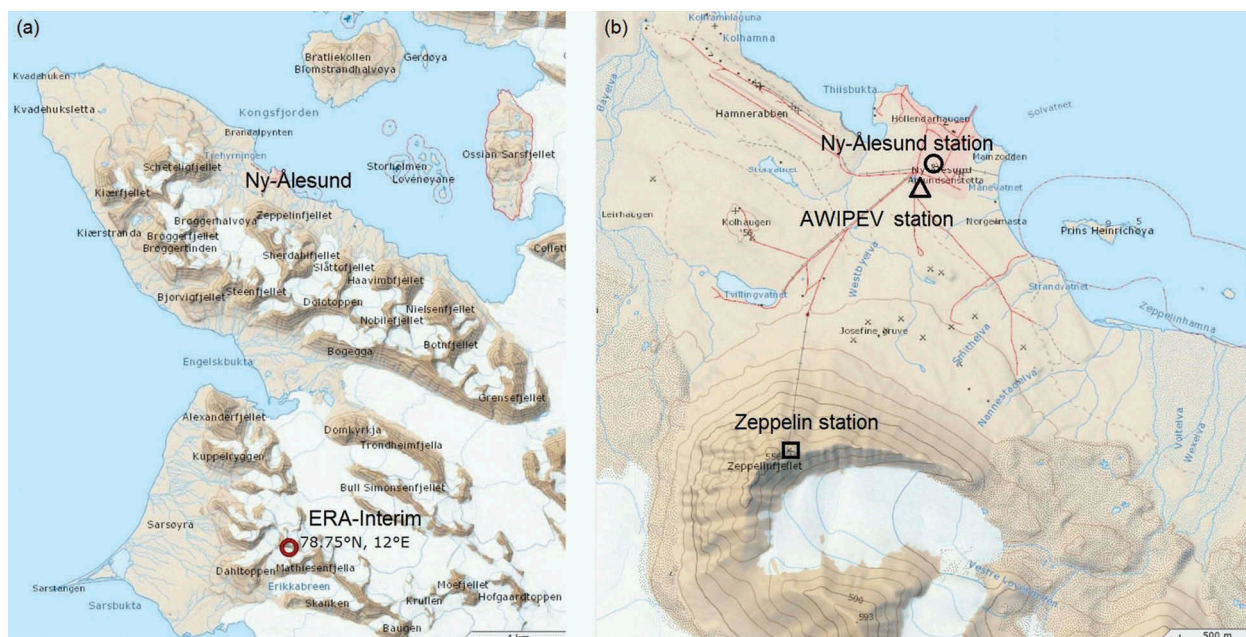


Figure 1. (a) The location of Ny-Ålesund on western Spitsbergen and the ERA-Interim data grid point (circled); (b) map of Ny-Ålesund, indicating the locations of the measurement stations.

field campaigns in Svalbard (Moroni et al. 2015; Ferrero et al. 2016). However, the humidity inversions are not always linked to the temperature inversions and may be associated with the unequal distribution of moisture with height in the air masses advected over the measurement site (Nygård et al. 2014).

Long-range transported pollution is dominant during all seasons of the year except summer, when instead ship traffic has been shown to be a significant local source of pollution (Eckhardt et al. 2013; Dekhtyareva et al. 2016). In summer, the mixing height of the ABL may increase, especially due to radiative heating of the surface leading to convection, and therefore local pollution may be transported aloft (Stull 1988). However, studies of wind climate in Kongsfjorden showed that despite this process, the thickness of local surface winds is lowest in summer, when it is estimated to be around 500 m (Esau & Repina 2012). Therefore, it is questionable to what extent convective mixing promotes the even distribution of pollutants within the local ABL. Pollution may also be trapped beneath an inversion layer and accumulate close to the ground, when the air above the measurement site descends and undergoes adiabatic compression and warming. Subsidence inversions may occur in the Arctic troposphere in summer as a response to diabatic heating and convection over land masses in the sub-Arctic (50°–55°N) after the springtime snowmelt (Matsumura et al. 2014). Another source of local pollution in Ny-Ålesund is the small power plant running on low-sulphur diesel year-round (Dekhtyareva et al. 2016). In order to prevent interference of local pollution in the

monitoring of background air composition, the Zeppelin Observatory was established 2 km away from the settlement, on the top of Mount Zeppelin at 474 m a.s.l. (Fig. 1b; Braathen et al. 1990; Beine et al. 1996).

There is also a local biogenic source of sulphate in Ny-Ålesund. Sulphate is produced from oxidation of DMS, which is emitted by marine plankton (Keller et al. 1989; Seinfeld & Pandis 2006), and SO₂ is an intermediate product of this reaction (Yin et al. 1990). Previous studies have shown that the concentration of chlorophyll *a* increases in April–May, July and September in Kongsfjorden, suggesting multiple blooms of algae in the fjord (Seuthe et al. 2011). The occurrence of the blooms varies from year to year depending on sea-ice cover, dominating water masses in the fjord and the inflow of freshwater from glaciers and land (Hodal et al. 2012). Although there is a significant positive correlation between algal chlorophyll *a* and DMS concentration in seawater, the actual DMS concentration depends on the taxonomic composition of the plankton community and trophic interactions within it (Yoch 2002). Because the combination of sunlight and ice-free conditions favours increased DMS emissions, this marine source of biogenic sulphur may be considered significant only in late spring, summer and early autumn (Shikai et al. 2012; Levasseur 2013).

Taking into account these local micrometeorological features and sources of sulphur agents, we address the correlation of the daily concentrations of anthropogenic sulphur compounds measured on filter samples at the Zeppelin station (474 m a.s.l.) and in Ny-Ålesund

(8 m a.s.l.) and their seasonally dependent variations (Fig. 1b).

Chemical and meteorological data were used to test the following hypotheses. (1) Low-level temperature and humidity inversions during winter and spring prevent even mixing of pollutants with height and disturb correspondence between the Ny-Ålesund and Zeppelin station data sets. (2) If the wind direction is dissimilar at the two stations, we expect differences in the concentrations of pollutants as the air sampled at the two sites may have different origins, affecting the correlation between the measurements at sea level and on the mountain top. (3) Wind shear has a significant effect on the dilution of local pollution in the ABL and reduces differences in the measurements from the two stations. (4) Local summertime ship traffic has a strong impact on the Ny-Ålesund data set and induces deviations from the Zeppelin data set.

Methods

Study area and materials

Measurements of two key long-range transported sulphur compounds have been analysed in this work: sulphate, SO_4^{2-} (particulate), and sulphur dioxide, SO_2 (gaseous). Daily filter samples were collected in Ny-Ålesund during the Monitoring of Local Air Quality in Ny-Ålesund project from 1 July 2008 until 31 December 2009 (Hermansen et al. 2011). A temporary measurement cabin, hereafter called the Ny-Ålesund station, (Fig. 1b), was installed in the middle of the settlement. Measurement results from the Zeppelin station (Fig. 1b) for the same period are available at the website <http://ebas.nilu.no/>. The sampling procedure was identical to the one used in the European Monitoring and Evaluation Programme (NILU 1996). No correction of filter sampling volume for temperature and pressure has been done, as only the inlets were placed outside while the measurement equipment was kept indoors at both sites, so the equipment was not subject to changes in the environmental parameters (NILU 1996). Only SO_2 and XSO_4^{2-} data have been utilized in the present work. The data owner, the Norwegian Institute for Air Research, has performed a correction for sea salt. This institute also provided hourly temperature, pressure, relative humidity, wind speed and wind direction data obtained at the two stations. Previous studies have shown that the local wind measurements at the Zeppelin station are subject to a wind-shielding effect from nearby mountains, so these data cannot be used for comparison with measurement results from Ny-Ålesund (Dekhtyareva et al. 2016). Therefore, atmospheric stratification and local wind flows in the lowest atmosphere (0–500 m height)

were studied using atmospheric radiosoundings performed by the Alfred Wegener Institute in Ny-Ålesund. Wind speed and direction, atmospheric temperature and relative humidity data were retrieved from measurements taken with the Vaisala RS92 radiosonde launched from the French–German AWIPEV station (Fig. 1b; Maturilli & Kayser 2016). The soundings provided by the Alfred Wegener Institute cover the whole measurement period except for one day, 8 December 2008. For days with more than one sounding available, the profile closest to the 12 UTC standard launch time has been chosen to maintain consistency.

Vihma et al. 2011 studied meteorological data at the pressure level of 850 hPa and at the surface to assess the influence of prevailing mesoscale meteorological situation on local wind flows and vertical stratification in the ABL. Similarly, we have analysed air temperature, specific humidity, wind speed and wind direction at these two vertical levels in Svalbard and at the point closest to the Zeppelin station (Fig. 1a). For this purpose, meteorological values for 12 UTC have been chosen from the global ERA-Interim reanalysis data set with a 0.75×0.75 degrees resolution, and no interpolation has been done (Dee et al. 2011).

Data analysis

Vertical wind shear is identified as a change in wind direction and/or speed with altitude (Markowski & Richardson 2006). Directional and speed shears were analysed separately in the study reported here. In order to assess the influence of variation in wind direction with height on correlation between the data sets, the daily measurements for each season were divided into two categories: those with and those without a change in wind direction with height of more than 90 degrees. In each radiosonde profile, all measurement points with wind speed above 2 ms^{-1} were defined to exclude cases with very weak winds, which may introduce ambiguity in the wind direction data (EPA 2000). Then the wind direction at each point was compared with values at points located higher in the profile, and the lowest height, when wind direction changes by more than 90 degrees, was defined. If this change happened in the lowermost 500 m, then the day was classified as a day with directional wind shear. The simulation done by Walcek (2002) with a vertical wind shear of $2.5 \text{ ms}^{-1} \text{ km}^{-1}$ shows the significant influence of higher wind speed above the surface on reducing the maximum concentrations and horizontal spreading of polluted air masses. Similarly, in our study, the effect of vertical speed shear was investigated by identifying two separate groups: one in which the wind speed increased by 1.25 ms^{-1} or more per 500 m height and one where it was not observed.

Table 1. Meteorological phenomena observed in the radiosonde profiles in different seasons.

Phenomena observed in the lowermost 500 m	Parameter	Season			
		summer (n = 154)	autumn (n = 182)	winter (n = 121)	spring (n = 92)
Temperature inversion	Frequency of occurrence (%)	36	51	66	60
	Median inversion strength TIS (°C)	0.80	0.95	0.90	1.10
Humidity inversion	Frequency of occurrence (%)	93	85	77	76
	Median inversion strength QIS (g/kg)	0.22	0.10	0.07	0.09
Both temperature and humidity inversion	Frequency of occurrence (%)	35	44	56	48
Low wind speed conditions	Frequency of occurrence (%)	50	16	13	23
Low-level cloud	Frequency of occurrence (%)	45	24	19	17

To assess whether air in the ABL is well mixed, moisture variation with altitude was estimated using relative humidity, air temperature and pressure retrieved from radiosoundings (Stull 1988). Formulas presented by Bolton (1980) and Wallace & Hobbs (2006) have been applied to calculate saturated vapour pressure and specific humidity, respectively.

In order to investigate the influence of temperature and humidity inversions on the correlation between the two data sets, a methodology for inversion detection identical to the one described by Vihma et al. (2011) was used. The height and temperature of the inversion base zT_b and T_b , respectively, were defined at the point in the radiosonde vertical temperature profile where temperature begins to increase with height. The height and temperature of the level where temperature starts decreasing with height are defined as zT_t and T_t , respectively. Similarly, using specific humidity profiles, height and humidity values at the humidity inversions' top, zQ_t and Q_t , and bottom, zQ_b and Q_b , were found. The temperature and humidity inversion strengths were calculated as the difference of these parameters at the top and bottom levels: TIS and QIS. Following Vihma et al. (2011), temperature and specific humidity changes of more than 0.3°C and $0.02\text{ g}\cdot\text{kg}^{-1}$, respectively, through the levels with depth more than 10 m were defined as inversions.

The seasonal SO_2 and XSO_4^{2-} data sets from the Ny-Ålesund and the Zeppelin stations were divided into groups according to the absence or presence of the factor of interest: directional and wind speed shear, temperature inversion and/or humidity inversion, and local summertime pollution from ships. To assess the influence of these factors on the seasonal concentrations on filter samples from both stations, the WRS test was chosen, because it is more powerful for discrete samples and data from skewed distributions than the t-test (Krzywinski & Altman 2014). The WRS test checks whether two independent samples, grouped according to a specific factor, come from distributions with equal medians. In other words, if the hypothesis in this test is rejected at the 5% confidence level ($p < 0.05$), there is a statistically significant difference between the two

samples, and the factor on the basis of which the data were grouped is recognized as being important.

Another relevant characteristic affecting the possibility of local pollution reaching the Zeppelin station in summer is the height of the mixed layer in the lowest atmosphere. The mixed layer has low variation in specific humidity, wind speed and wind direction (Stull 1988). According to Chernokulsky et al. (2017), mean total cloud cover for Svalbard is highest in summer and constitutes around 80%. To calculate the mixing height, a method combining information about the lapse rate, vertical variation of water content and mixing within clouds, was applied based on a three-step procedure (Wang & Wang 2014). First, mixing height h_0 was defined based on vertical gradients of potential temperature, relative and specific humidity and refractivity. Second, the location of a cloud was identified using relative humidity thresholds specific for altitude range from 0 to 2 km (table 1 in Wang & Wang 2014). Third, if a cloud base was lower than h_0 and there was a stable layer within the cloud, the consistent mixing layer height h_{con} was set to the height of the sharpest inversion within this layer. The detailed procedure of determining h_{con} is described by Wang & Wang (2014).

Results and discussion

The seasonal variation of different meteorological phenomena in the lowermost 500 m is presented in Table 1. Temperature inversions were detected most often in winter, but the highest average temperature inversion strength was observed in spring. The rate of days when both temperature and humidity inversions were present is highest for winter. The strongest specific humidity inversions were detected in summer. In general, similarly to results reported by Nygård et al. (2014), humidity inversions were observed most of days, irrespective of the season. Hence, all days were divided into two groups of similar size within each season: (1) with no humidity inversion and humidity inversion with QIS below or equal to the seasonal median; and (2) with inversions with QIS above the seasonal median. This was done to statistically assess the influence of strong humidity inversions on filter measurements by using these

groups in the WRS test for SO_2 and XSO_4^{2-} data from the Ny-Ålesund and Zeppelin stations. In low wind speed conditions, the dispersion of pollutants is controlled by a meandering horizontal flow and weak sporadic turbulence, and air stagnation may occur (Anfossi et al. 2004). Low wind speed conditions are defined here as when the median wind speed is below 2 ms^{-1} in the lowest 500 m. The seasonal percentage of profiles with low wind speed conditions was highest in summer and reached its minimum in winter. This may indicate that in summer the measurements are potentially more affected by local processes, while the influence of cyclonic activity and advection is stronger in other seasons (Maturilli et al. 2013). Using the procedure described by Wang and Wang (2014), the cloud location in each radiosonde profile was identified. Low-level clouds were observed in nearly half of all summer days, while they were rarely detected in winter and spring. The frequency of occurrence of the phenomena described above indicate that there is a distinct difference between local micrometeorological conditions in summer and other seasons in Ny-Ålesund.

Figure 2 shows the seasonal data sets of SO_2 and XSO_4^{2-} collected at the Ny-Ålesund and Zeppelin stations. Statistically significant positive correlations ($p < 0.05$) of SO_2 and XSO_4^{2-} data sets between the stations are observed for all seasons except for summer SO_2 data, and values of Pearson correlation coefficient r are shown in each plot of the seasonal data. In order to explain dramatic seasonal variation in correspondence between the data sets from the Ny-Ålesund and Zeppelin stations, the WRS test was applied to SO_2 and XSO_4^{2-} data from both stations.

Both SO_2 and XSO_4^{2-} data sets show the weakest correlation in summer. According to the WRS test, several factors led to this: strong humidity inversions, insufficient vertical wind speed shear and local pollution from ships (Table 2).

The test results show that only XSO_4^{2-} data from the Ny-Ålesund station had significantly higher median concentration for the days with strong humidity inversions than for the days with normal and no humidity inversion. The mesoscale meteorological situation for the days from both humidity inversion groups is shown in Fig. 3. The location of the isobars shows the area of local high pressure that may be linked to subsidence inversion (Fig. 3a). The mean sea-level pressure for the point closest to the Zeppelin station (Fig. 1a) was higher for the days with strong humidity inversion (1017 hPa) than for the days when strong humidity inversion was absent (1014 hPa). Indeed, there is a weak ($r = 0.19$), but statistically significant ($p = 0.02$), positive correlation between summer QIS and mean sea-level pressure. The mean wind speed was also lower for the first

group (Fig. 3a) than for the second one (Fig. 3b). Meteorological observations at the Ny-Ålesund station show a similar picture as the reanalysis results: easterly winds with very low wind speed (1 ms^{-1}) prevailed during the days with strong humidity inversion. Taking into account the location of the station (Fig. 1b), these winds may bring local pollution from the ships anchored in the fjord and/or biogenic sulphur from Kongsfjorden. The presence of strong specific humidity inversion illustrates that pollutants were unevenly distributed with altitude. At the same time, light winds inhibited their removal from the ABL. This indicates that the air was more localized, and if any pollutants had been emitted close to the ground level, they might have persisted for a while.

The presence of gases that may become particle precursors, and enhanced photochemical oxidation, may lead to new particle formation (Seinfeld & Pandis 2006). The factor controlling dry deposition of particles is the particle size. Hygroscopic aerosol particles containing XSO_4^{2-} absorb water vapour from the air, dissolve as humidity increases, and saturated droplets form. The diameter of the particles increases abruptly. If humidity increases further, the particle diameter and mass grows, and the particles may eventually be deposited (Orr et al. 1958). Therefore, the strong humidity inversions in summer may have a cleansing effect, decreasing aerosol concentration to the ambient level above the inversion. Indeed, when the strong humidity inversion was located below the level of the Zeppelin station, no effect of the pollution accumulation in the ABL was seen on the Zeppelin sulphate measurements, whereas a statistically significant influence was observed at the Ny-Ålesund station.

According to the test, the directional wind shear is not a statistically significant factor. However, wind speed shear was an important factor decreasing the median concentration of SO_2 and XSO_4^{2-} at the Ny-Ålesund station in summer, while no shift of median in the Zeppelin XSO_4^{2-} data was observed (Table 2). SO_2 is a moderately soluble gas, therefore oxidation to sulphate and dry deposition are the major pathways for SO_2 removal from the troposphere on non-cloudy days (Liang & Jacobson 1999; Seinfeld & Pandis 2006). The dry deposition velocity depends strongly on wind speed and turbulence strength. Indeed, the concentrations of SO_2 and XSO_4^{2-} in Ny-Ålesund were almost two times lower when a vertical wind speed shear was observed. In the absence of wind speed shear, concentrations of both compounds increased dramatically in Ny-Ålesund, while no such effect was observed in the data from the Zeppelin station. Long-term studies based on the Ny-Ålesund radiosonde data record have shown that the ventilation within the ABL above Ny-Ålesund has decreased over the last two decades, as smaller wind

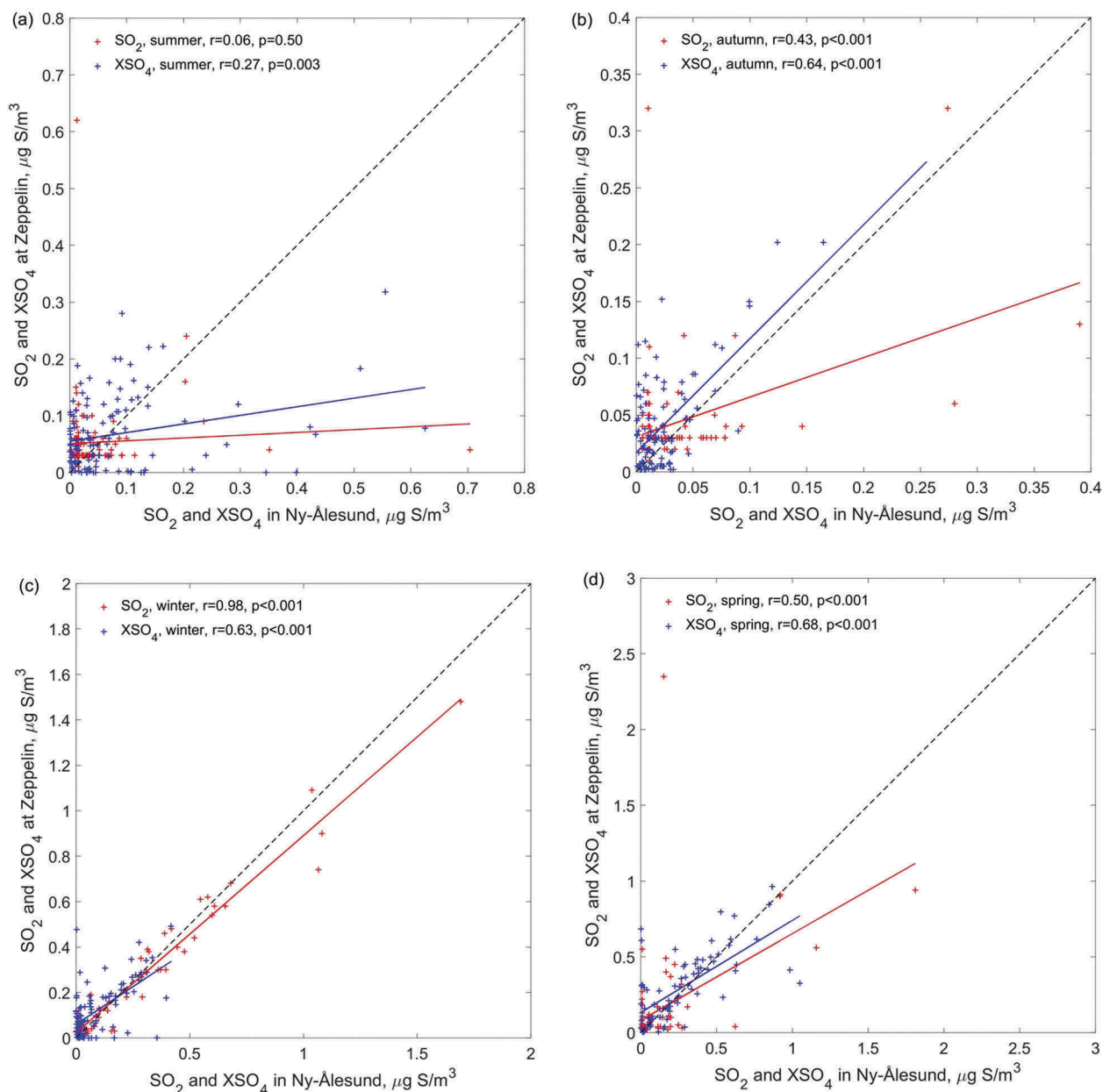


Figure 2. Seasonal SO_2 and XSO_4^{2-} data from Ny-Ålesund (x axes) and Zeppelin station (y axes): (a) summer; (b) autumn; (c) winter; (d) spring.

Table 2. Significant results of WRS-test ($p < 0.05$).

Season	Compound and station	Factor of influence	p value	Median of the group where the factor of influence is absent ($\mu\text{gS}\cdot\text{m}^{-3}$)	Median of the group where the factor of influence is present ($\mu\text{gS}\cdot\text{m}^{-3}$)
Summer	XSO_4^{2-} , Ny-Ålesund	Vertical wind speed shear	< 0.01	0.0510	0.0235
		Strong humidity inversion	< 0.01	0.0296	0.0635
	SO_2 , Ny-Ålesund	Daily number of ship passengers above or equal to 100	0.02	0.0125	0.0220
		Vertical wind speed shear	< 0.01	0.0230	0.0133
Autumn	SO_2 , Ny-Ålesund	Temperature inversion	0.01	0.0115	0.0120
Winter	XSO_4^{2-} , Ny-Ålesund	Temperature inversion	0.01	0.0292	0.0723
Spring	SO_2 , Ny-Ålesund	Temperature inversion	0.03	0.0118	0.0350
		Temperature inversion	0.01	0.1618	0.2675
	SO_2 , Zeppelin		< 0.01	0.0300	0.0400
	XSO_4^{2-} , Zeppelin		< 0.01	0.1390	0.3210
	XSO_4^{2-} , Ny-Ålesund	Strong humidity inversion	< 0.01	0.2865	0.1218

velocities are being observed more frequently in all seasons (Maturilli & Kayser 2016). This implies that

the conditions favourable for the accumulation of pollution in the ABL may occur more often.

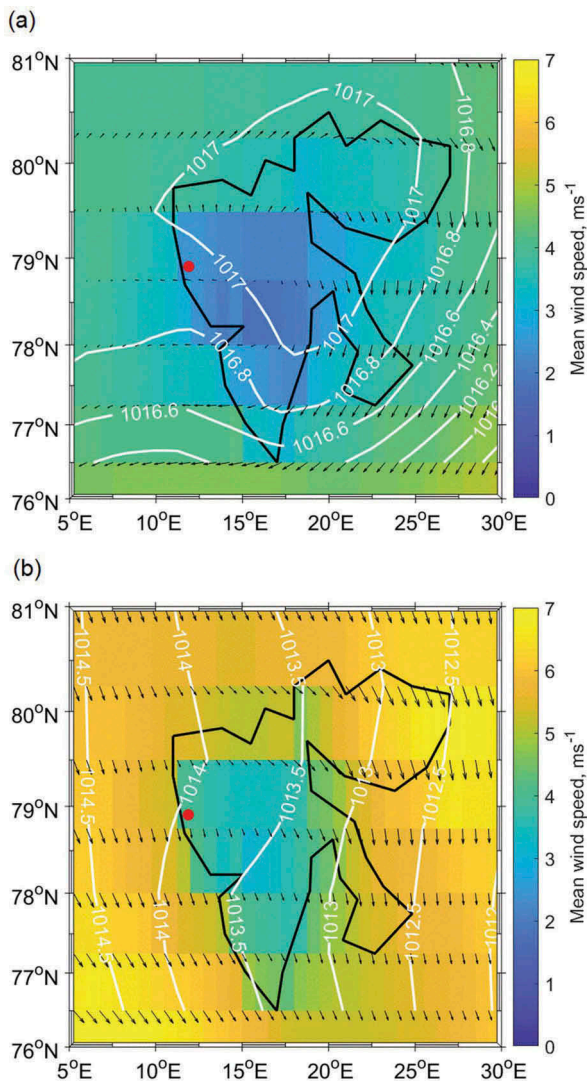


Figure 3. Summer mean wind speed in $\text{m}\cdot\text{s}^{-1}$ (colour scale), wind direction (black arrows with the length relative to the wind speed) and mean sea-level pressure in mbar (white lines) in the Svalbard area (black outline) and Ny-Ålesund (red dot), obtained from surface ERA-Interim data: (a) for days with strong humidity inversion; (b) for days with normal or no humidity inversion.

In order to assess influence of the ship traffic emissions on the measurements at both stations, all summer days were divided into two groups: one group with the daily number of people visiting Ny-Ålesund by ship above or equal to 100; and one group with the number of passengers below 100. The number of people is an indicator of ship size and, hence, the amount of emissions. In total, 66% of the summer data may have been impacted by pollution from the ships, since 101 out of 154 days of summer measurements belong to the first group. However, as Fig. 2 shows, summer SO_2 concentrations measured at both the Zeppelin and Ny-Ålesund stations were usually much lower than in winter and spring. There may be a few reasons for this. Firstly, long-range transported pollution prevailing in the Arctic in winter and spring decreases in summer because of the change in the position of the Arctic

Front, which prevents effective south-to-north long-range air transport (AMAP 2006). Secondly, there are few local anthropogenic sources of air pollution in the Arctic and some of them have intermittent emission rates, e.g., ship traffic (Dekhtyareva et al. 2016). Thirdly, the conversion rate of SO_2 to SO_4^{2-} increases in summer, a process governed by two major mechanisms. The first mechanism is the oxidation of gaseous SO_2 by hydroxyl radical in clear-sky conditions. Studies have shown that the conversion rate increases with increasing temperature and relative humidity and is a function of Julian day (Meagher & Bailey 1983; Eatough et al. 1994). The second mechanism is the conversion of SO_2 to SO_4^{2-} through various chemical reactions in the aqueous solutions in clouds and fog (Eatough et al. 1994; Seinfeld & Pandis 2006). Despite very low average summer concentrations of SO_2 measured at the Ny-Ålesund station, there was a noticeable impact of local pollution from ships on the Ny-Ålesund data set.

Mean SO_2 values measured at the Ny-Ålesund station for the days in the first group were almost three times higher ($0.05 \mu\text{g}\cdot\text{m}^{-3}$) than for days from the second group ($0.02 \mu\text{g}\cdot\text{m}^{-3}$), while the Zeppelin data showed almost no difference for these two groups ($0.05 \mu\text{g}\cdot\text{m}^{-3}$ vs $0.06 \mu\text{g}\cdot\text{m}^{-3}$). This finding is supported by the WRS test that showed that median SO_2 value for the first group of days in Ny-Ålesund measurements was significantly higher than for the second one, while no difference was found for SO_2 measurements at the Zeppelin station (Table 2).

Mean XSO_4^{2-} values at the Ny-Ålesund and Zeppelin stations for the first group of days (≥ 100 passengers) were 50% higher ($0.09 \mu\text{g}\cdot\text{m}^{-3}$) than for the second one (< 100 passengers; $0.06 \mu\text{g}\cdot\text{m}^{-3}$). This finding corresponds well with a previous study showing that at the Zeppelin station there was an 55% increase in the number of particles with diameters characteristic of aged ship plumes, due to local pollution from ships (Dekhtyareva et al. 2016). However, the WRS test did not show a significant difference in medians for the two groups, which indicates that the sulphate measurements were infrequently affected by local pollution, but sufficiently to influence the mean value, which was increased on account of a few high concentration values.

Total daily number of passengers, indicating the size of ships, shows moderate ($r = 0.38$), but significant ($p < 0.001$), positive correlation with SO_2 concentration on filters in Ny-Ålesund, while no significant correlation between these parameters has been found for the Zeppelin data set. In contrast, both the Zeppelin and Ny-Ålesund XSO_4^{2-} data sets show significant ($p = 0.03$), but weak positive correlations ($r = 0.20$) with number of passengers. A possible explanation to this is proximity to the emission source. Whether the ships were docked at the pier or anchored in the fjord, they were closer to the

measurement station in Ny-Ålesund than to the Zeppelin station. The proximity to the source of emission is important because the oxidation from SO_2 to XSO_4^{2-} in aqueous and gas phases are major pathways for SO_2 removal during the summertime (AMAP 2006), and therefore pollution emitted by ships may contribute to the total sulphate concentration but not to the sulphur dioxide measured at the Zeppelin station.

One may conclude that emissions from ships have an impact on both data sets in a different manner. Sulphur agents emitted by ships reach Zeppelin mostly in the oxidized form of XSO_4^{2-} , while the influence on measurements in the village is directly seen on the SO_2 data set.

Median and mean consistent mixing layer heights were 546 m and 657 m, respectively. However, only 47% of all profiles showed a mixing height higher than 474 m. This finding supports the original argument for positioning of the Zeppelin station at the mountain top in order to prevent the influence of local pollution on measurements (Braathen et al. 1990). Furthermore, during days with little vertical mixing and strong humidity inversions below the Zeppelin station the local pollution does not reach the station, while higher concentrations were observed in the filter samples in Ny-Ålesund.

An examination of two small sub-groups of summer days serves as an example. In both groups, the mixing height was lower than 474 m and the daily number of ship passengers exceeded 100. The only parameter that was different is the presence of strong humidity inversions in the first group (28 days) and the absence of them in the second one (21 days). On the days in the first group, a slightly lower average wind speed was observed in Ny-Ålesund than on the days in the second group (1.6 ms^{-1} vs 2.1 ms^{-1}). The percentage of days when no cloud base was detected and when the cloud base was identified above the Zeppelin station was 39% and 18%, respectively, in the first group of days, and 20% and 12% in the second one. Mean XSO_4^{2-} concentrations in the first group were $0.13 \mu\text{gS}\cdot\text{m}^{-3}$ and $0.09 \mu\text{gS}\cdot\text{m}^{-3}$ at the Ny-Ålesund and Zeppelin stations, respectively. Mean XSO_4^{2-} concentrations in the second group were $0.07 \mu\text{gS}\cdot\text{m}^{-3}$ and $0.09 \mu\text{gS}\cdot\text{m}^{-3}$ at the Ny-Ålesund and Zeppelin stations, respectively. In presence of a strong humidity inversion in the lowest 500 m of the ABL, concentrations in Ny-Ålesund increased, while at the Zeppelin station the average concentrations for both groups, with and without strong humidity inversion, were identical.

The processes affecting concentration distribution of aerosols are complex and depend on the particle size and parameters of the atmospheric turbulent boundary layer and the temperature inversion layer if the inversion is present (Elperin et al. 2007). For example, thermal diffusion increases near-surface

concentration of coarse particles (PM_{10}) in inversely stratified flows over elevated terrain, while for gases and fine particles ($\text{PM}_{2.5}$) the effect is small (Sofiev et al. 2009). The shipping emissions increase concentrations of SO_2 , $\text{PM}_{2.5}$ and PM_{10} (Viana et al. 2014). $\text{PM}_{2.5}$ and gases remain in the air for a longer time after emission and may be transported over long distances from the source, while PM_{10} have limited spatial distribution and are often deposited downwind of the pollution sources. At the same time, sulphate may be present in both $\text{PM}_{2.5}$ and PM_{10} (Chan et al. 1997), while SO_2 oxidizes and contributes to the XSO_4^{2-} concentration as well. Moreover, the processes affecting aerosol population cannot be thoroughly investigated without studying the evolution of vertical aerosol profiles (Kupiszewski et al. 2013). However, no particulate matter or vertical aerosol profiles data are available for the current study period, and the time resolution of the filter samples used in this study is too coarse to discuss the aerosol and gas processes in detail.

The WRS test showed that only SO_2 measurements in Ny-Ålesund were influenced by temperature inversions in autumn (Table 2). However, the medians for both groups were very low and quite similar. This is due to the generally very low concentration during autumn. No other statistically significant impact was revealed in autumn.

In winter, according to the WRS test, temperature inversions become an important factor increasing the median concentration in the Ny-Ålesund XSO_4^{2-} data set, but not affecting the Zeppelin station (Table 2). Change of wind direction with height and humidity inversions did not affect either of the data sets. This can be explained by low specific humidity variation with height (average standard deviation of specific humidity is $0.07 \text{ g}\cdot\text{kg}^{-1}$ in the lowest 500 m in winter versus $0.18 \text{ g}\cdot\text{kg}^{-1}$ in summer), low median QIS, low number of days with directional wind shear and high seasonal average median profile wind speed within the lowest 500 m (5.7 ms^{-1}).

In spring, in accordance with the test, temperature inversions affect SO_2 and XSO_4^{2-} data sets from both stations. The samples from the group of days with temperature inversions had significantly higher median values of both compounds than from the group without temperature inversions (Table 2). Average air temperature at 850 hPa was -15°C and -12°C in the first and second groups of days, respectively. The orientation of the wind velocity vectors and the location of the isobars in Fig. 4a show that there was a horizontal advection of colder air masses from the east-north-east in the first group of days, with higher concentrations. The air flow from the Arctic Ocean to the north-west of Svalbard prevailed for

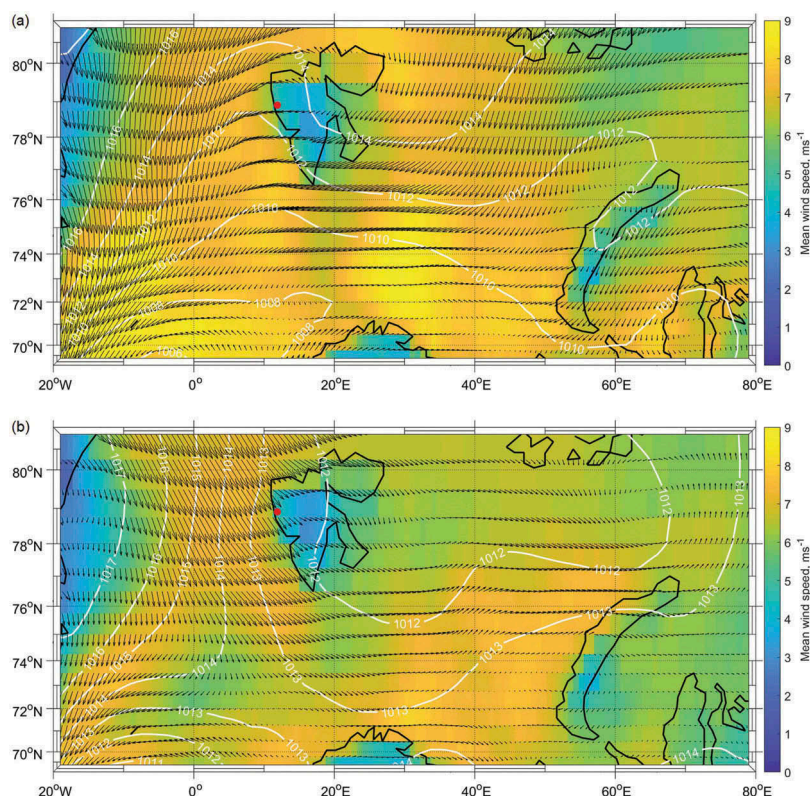


Figure 4. Spring mean wind speed in $\text{m}\cdot\text{s}^{-1}$ (colour scale), wind direction (black arrows with the length relative to the wind speed) and mean sea-level pressure in mbar (white lines) in the Greenland and Barents seas, obtained from surface ERA-Interim data: (a) for days with temperature inversion; (b) for days without temperature inversion.

Table 3. Mean spring concentrations in daily filter samples at the Ny-Ålesund and Zeppelin stations, $\mu\text{g}\cdot\text{m}^{-3}$. The values in boldface correspond to significant results of the WRS test shown in Table 2.

Measured compound and station	Seasonal	Change in wind direction	No change in wind direction	Temperature inversion	No Temperature inversion	Strong humidity inversion	Normal or no humidity inversion
SO_2 , Ny-Ålesund	0.124	0.087	0.141	0.175	0.031	0.042	0.177
XSO_4^{2-} , Ny-Ålesund	0.270	0.334	0.239	0.326	0.169	0.194	0.320
SO_2 , Zeppelin	0.146	0.133	0.152	0.200	0.058	0.082	0.185
XSO_4^{2-} , Zeppelin	0.297	0.356	0.269	0.363	0.195	0.264	0.318

the second group of days, with lower concentrations (Fig. 4b).

The mean spring concentrations on daily filter samples from the Ny-Ålesund and Zeppelin stations are shown in Table 3. The values for the groups for which the WRS test detected significant difference in medians are indicated. The mean spring SO_2 and XSO_4^{2-} values changed dramatically at both the Ny-Ålesund and Zeppelin stations, depending on the presence or absence of strong humidity inversions. Mean spring SO_2 values for days with strong humidity inversions were four times and two times lower at the Ny-Ålesund station and at the Zeppelin station, respectively, than mean SO_2 values for the days when no strong humidity inversions were observed. Mean spring XSO_4^{2-} values for the first group of days were 65% and 17% lower at the Ny-Ålesund and Zeppelin stations, respectively, than the mean value for the days without strong humidity inversions. However, the magnitude of the reduction of the SO_2 and XSO_4^{2-} concentrations suggests that these conditions

affect measurements at the Ny-Ålesund station more than at the Zeppelin station. Indeed, according to the test, the median XSO_4^{2-} values in the Ny-Ålesund station data are significantly lower for the group of days with strong humidity inversions, while no difference was found in the data from the Zeppelin station. Strong humidity inversions have the opposite effect on filter measurement results to the one from temperature inversions. This may be explained by the different origin of air masses. Strong humidity inversions were observed when the wind direction at 850 hPa was from the south and west and the average air temperature at that pressure level was -11.3°C , while for the days with no strong humidity inversions it was -15°C . Figure 5a shows that there was a transport of warmer and more humid air from the Atlantic Ocean south of Svalbard during the days with strong humidity inversions. Prevailing weather conditions at 850 hPa for the days with strong humidity inversions correspond very well with the ones described by Vihma et al. (2011), who characterized the effect of

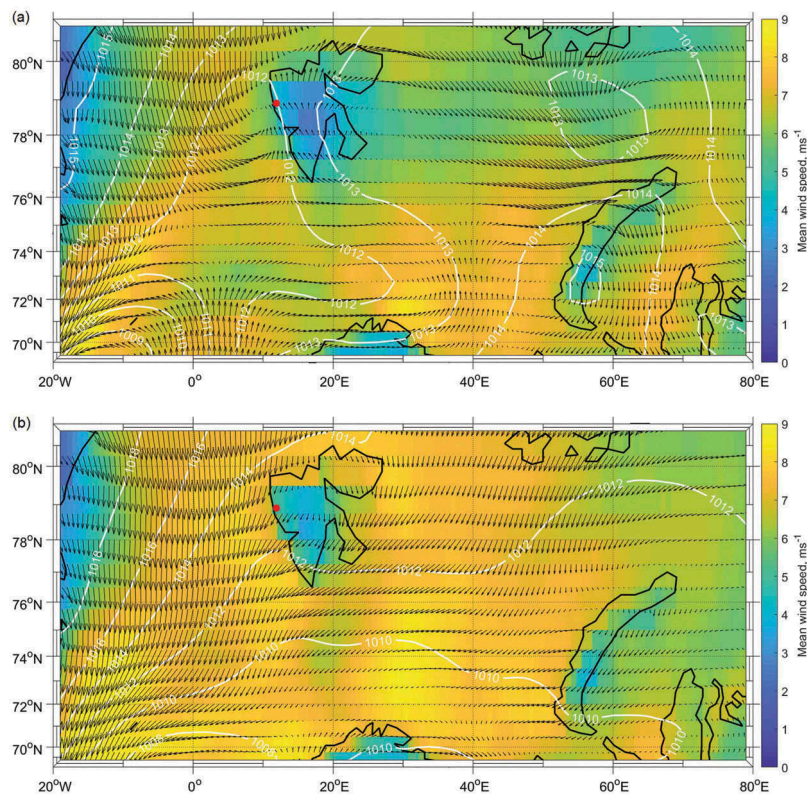


Figure 5. Spring mean wind speed in $\text{m}\cdot\text{s}^{-1}$ (colour scale), wind direction (black arrows with the length relative to the wind speed) and mean sea level pressure in mbar (white lines) in the Greenland and Barents seas, obtained from surface ERA-Interim data: (a) for days with strong humidity inversion; (b) for days without strong humidity inversion.

warm and humid air masses from the marine sector ($200\text{--}290^\circ$) on the formation of humidity inversions. In contrast, the location of isobars in Fig. 5b for the group without strong humidity inversions was similar to the one for the group of days with temperature inversions (Fig. 4a), indicating the transport of colder air masses with higher concentrations of sulphur compounds from the east. Moreover, the temperature at the level of 850 hPa correlates differently with temperature and humidity inversion strengths in spring. There is a statistically significant negative correlation between TIS ($r = -0.30$, $p = 0.004$) and the air temperature at 850 hPa, while the correlation with QIS is positive ($r = 0.26$, $p = 0.01$). This indicates that strong humidity inversions are caused by the horizontal transport of warmer air masses and not by the radiative cooling of the surface layer. Lower concentration of XSO_4^{2-} in Ny-Ålesund than at the Zeppelin station may be explained by the fact that the air masses are of marine nature, and the deposition velocities above the air–water interface may be slightly higher compared with deposition to dry surfaces because of growth of hygroscopic particles in the humid boundary layer (Seinfeld & Pandis 2006).

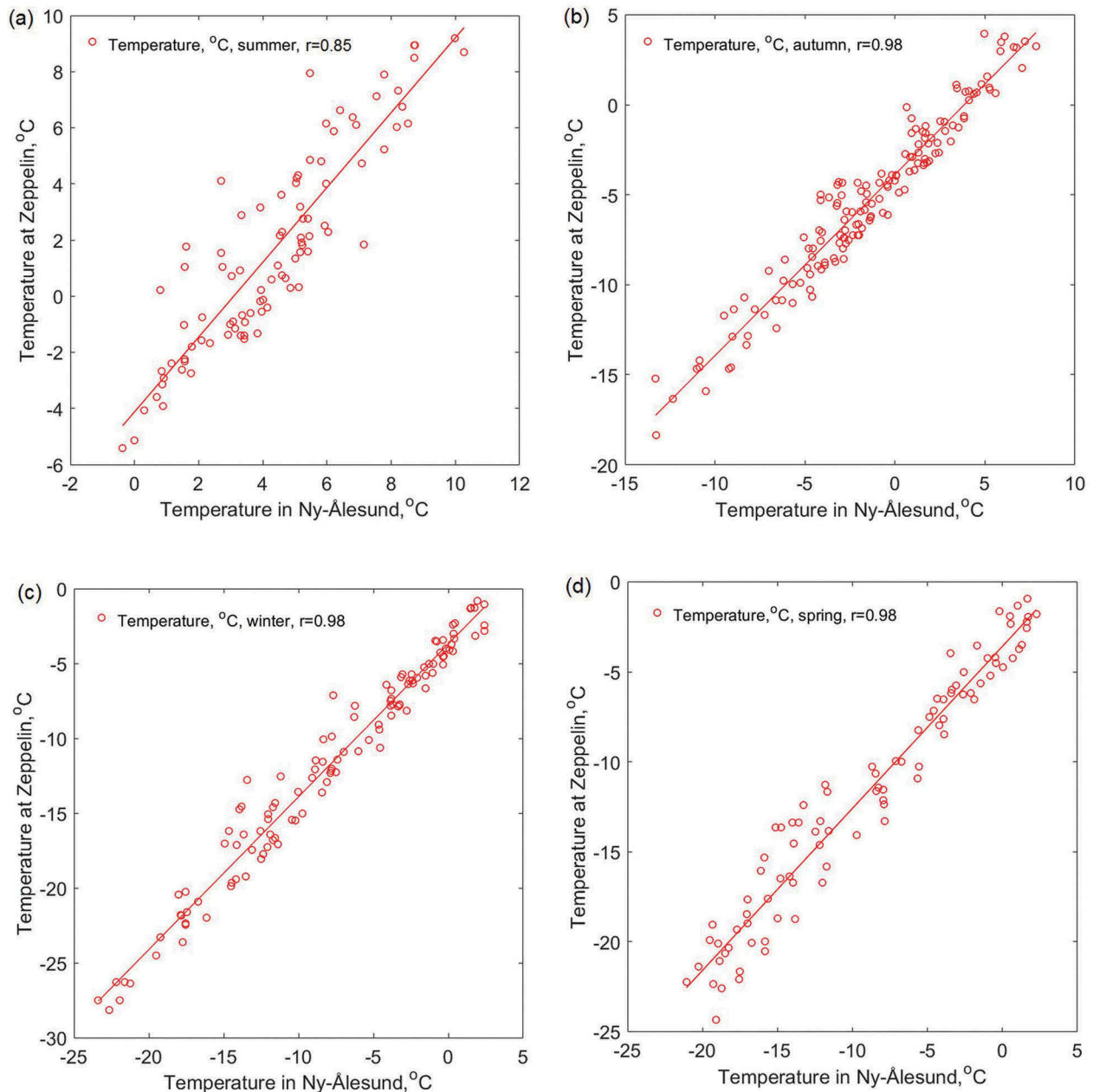
A main weakness in this study is the filter-sampling method, which affects the number of values below the detection limit, and consequently the correlation between the data sets. As Aas et al. (2007) stated, the reference European Monitoring and Evaluation

Programme method, based on the use of potassium hydroxide-impregnated filters for SO_2 detection, is not well suited to monitoring low background concentrations because of its high detection limit. The seasonal percentage of SO_2 values below the detection limit (L_d) in the data sets at both stations is very high irrespective of the season, while the percentage is lower in the XSO_4^{2-} data set (Table 4). The rate of missing data in the Ny-Ålesund station data set is higher than in the Zeppelin data set in all seasons.

Another uncertainty is related to the fact that only one radiosounding per filter measurement was utilized in the data analysis. This gives the information about the atmospheric stratification and vertical wind profile at the time of launching (generally at 12 UTC), but does not describe the profile evolution during the day. However, as one can see in Fig. 6 the lowest correlation between daily averaged temperature measurements at the Ny-Ålesund and Zeppelin stations were observed during summer. This points to a higher rate of non-linearity in interrelation between temperatures at the Ny-Ålesund and Zeppelin stations and, consequently, reflects complexity of the processes in the ABL. In general, the atmospheric lapse rate is formed under the combination of convection and radiation processes (Wallace & Hobbs 2006); however, we have seen from the high variation of specific humidity and frequently observed directional wind shear and clouds in

Table 4. Characteristics of the filter data sets.

Station	Characteristic	Compound	Season			
			summer (n = 154)	autumn (n = 182)	winter (n = 121)	spring (n = 92)
Ny-Ålesund	Rate of values below L_d (%)	SO ₂	45	42	45	43
		XSO ₄ ²⁻	31	41	35	10
Zeppelin	Rate of values below L_d (%)	SO ₂	45	54	40	49
		XSO ₄ ²⁻	21	32	17	14
Ny-Ålesund	Rate of missing data (%)	SO ₂ and XSO ₄ ²⁻	21	32	17	14
Zeppelin	Rate of missing data (%)	SO ₂ and XSO ₄ ²⁻	1	14	6	3

**Figure 6.** Seasonal plots of daily averaged air temperature measured at the Ny-Ålesund and Zeppelin stations: (a) summer; (b) autumn; (c) winter; (d) spring.

summer profiles that there have been air flows with quite different characteristics in the lowest 500 m. Interaction of these flows and radiation processes within the clouds may influence the correlation of daily temperature measured at the two stations, so the characteristics of the profiles are not only

instantaneous features of the ABL, but are important for the lapse rate formation throughout the day in summer.

The findings presented in this paper may be relevant for planning future fieldwork campaigns and comparing modelling results with measurements

done in a region with complex topography, such as the Ny-Ålesund area. Knowledge of the micrometeorological conditions of the study area is crucial if one wants to eliminate local effects by choosing the right location for the station or to contrast results from already existing stations situated close to each other. For comparison of historical data with modelling results, one needs to investigate local meteorological factors that may affect measurement results and choose the model resolution that correctly represents these factors. A study by Mölders et al. (2011) has shown that the combined chemical and meteorological model WRF-Chem with a resolution of 4 km tends to underestimate the inversion strengths, presents biases of temperature and wind speed and determines incorrect wind direction at low wind speeds. Furthermore, it has been stated that errors in modelled temperatures may lead to erroneous modelled concentrations of aerosols (Mölders et al. 2011). As there is a trade-off between the resolution and the computational time in the model, it is useful to know if the measurement results from the station are subject to a significant impact of local pollution and/or micrometeorological factors. This can be checked using the statistical methods applied in this article.

Conclusion

The correlation of daily sulphur dioxide (SO_2) and non-sea salt sulphate (XSO_4^{2-}) data sets from the Ny-Ålesund station and the Zeppelin mountain station has a large seasonal variation. No significant correlation between the SO_2 data sets has been observed in the summer data, while a very strong correlation is present in the winter data, with autumn and spring showing intermediate to moderate values of Pearson correlation coefficient. Although the correlation between the XSO_4^{2-} data sets is significant for all times of year, it is much lower for the summer data compared to other seasons.

The first hypothesis, stating the significance of the effect of temperature and humidity inversions on the correspondence between the data sets from the Ny-Ålesund and Zeppelin stations, is supported. In winter, concentration of XSO_4^{2-} at the Ny-Ålesund station is significantly higher in the days with temperature inversions, while in spring this effect is seen in data sets from both stations. Local meteorological conditions on the days with strong humidity inversions reduce and increase the sulphate concentration at the Ny-Ålesund station in spring and summer, respectively.

The second hypothesis has been rejected, since the directional shear appeared to be an insignificant factor, while the third hypotheses about the influence of

wind speed shear on the correspondence of measurements is relevant only for the summer season. In the absence of the wind speed shear, local pollution affects Ny-Ålesund sulphur dioxide and sulphate data set more strongly.

The fourth hypothesis, stating the effect of local summertime emissions from ship traffic on the correspondence between the data sets from the two stations, is partially supported. Local summertime ship traffic has a strong impact on the SO_2 Ny-Ålesund data set, while there is no statistically significant effect on the Zeppelin data set. The XSO_4^{2-} data sets at both stations are impacted by pollution from ships, but the influence on the Ny-Ålesund data set is more pronounced on days with strong humidity inversions.

The findings presented here are highly important for planning joint monitoring campaigns and the exchange and comparison of measurement results in Ny-Ålesund. Both anthropogenic factors, such as local pollution in summer, and natural ones, namely local circulation patterns and variation of temperature and humidity in the ABL, affect the correspondence between the data sets collected at the locations within the range of 2 km. Furthermore, the nature of the sulphur species studied here determines which factors affected the concentration of the measured compounds at the two stations.

The environmental phenomena described here still represent a challenge for modellers and need to be taken into account when comparing modelling results with in situ measurements taken at different heights in an area with complex topography.

Acknowledgements

The Norwegian Polar Institute is acknowledged for the detailed map of Svalbard available at <http://svalbardkartet.npolar.no>. Special thanks are given to the Norwegian Polar Institute for the support and coordination of research activities in Ny-Ålesund, which become a basis for this paper. The European Centre for Medium-Range Weather Forecasts is acknowledged for data from the ERA-Interim global atmospheric reanalysis data set used in the present work. Dr Kåre Edvardsen is thanked for reviewing this manuscript. The authors would like to thank Dr John J. Cassano and two anonymous reviewers for thorough reading of the manuscript, constructive comments and suggestions, which helped to improve the quality of the paper.

Disclosure statement

No potential conflict of interest was reported by the authors.

Funding

The filter sample measurements were done within the framework of the project Monitoring of Local Air Quality in Ny-Ålesund 2008-2010, supported by the Norwegian

Institute for Air Research, the Norwegian Polar Institute and the Svalbard Environmental Protection Fund. The authors also gratefully acknowledge support for the Ny-Ålesund radiosonde data from the Transregional Collaborative Research Center (TR 172), specifically the project Arctic Amplification: Climate Relevant Atmospheric and Surface Processes, and Feedback Mechanisms (AC)3, which is funded by the German Research Foundation (Deutsche Forschungsgemeinschaft).

ORCID

Alena Dekhtyareva  <http://orcid.org/0000-0003-4162-7427>

Marion Maturilli  <http://orcid.org/0000-0001-6818-7383>

References

- Aas W., Schaug J. & Hanssen J.E. 2007. Field intercomparison of main components in air in EMEP. *Water Air & Soil Pollution: Focus* 7, 25–31.
- AMAP 2006. *AMAP assessment 2006: acidifying pollutants, Arctic haze, and acidification in the Arctic*. Oslo: Arctic Monitoring and Assessment Programme.
- Anfossi D., Oetli D. & Degrazia G.A. 2004. Some aspects of turbulence and dispersion in low wind speed conditions. In C. Borrego & S. Incecik (eds.): *Air pollution modeling and its application XVI*. Pp. 331–338. Boston: Springer.
- Beine H.J., Engardt M., Jaffe D.A., Hov Ø., Holmén K. & Stordal F. 1996. Measurements of NO_x and aerosol particles at the Ny-Ålesund Zeppelin mountain station on Svalbard: influence of regional and local pollution sources. *Atmospheric Environment* 30, 1067–1079.
- Bolton D. 1980. The computation of equivalent potential temperature. *Monthly Weather Review* 108, 1046–1053.
- Braathen G.O., Hov Ø. & Stordal F. 1990. *Arctic atmospheric research station on the Zeppelin mountain (474 m a.s.l.) near Ny-Ålesund on Svalbard (78°54'29" N, 11°52'53"E)*. Lillestrøm: Norwegian Institute for Air Research.
- Chan Y.C., Simpson R.W., Mctainsh G.H., Vowles P.D., Cohen D.D. & Bailey G.M. 1997. Characterisation of chemical species in PM_{2.5} and PM₁₀ aerosols in Brisbane, Australia. *Atmospheric Environment* 31, 3773–3785.
- Chernokulsky A.V., Esau I., Bulygina O.N., Davy R., Mokhov I.I., Outten S. & Semenov V.A. 2017. Climatology and interannual variability of cloudiness in the Atlantic Arctic from surface observations since the late nineteenth century. *Journal of Climate* 30, 2103–2120.
- Dee D.P., Uppala S.M., Simmons A.J., Berrisford P., Poli P., Kobayashi S., Andrae U., Balmaseda M.A., Balsamo G., Bauer P., Bechtold P., Beljaars A.C.M., van de Berg L., Bidlot J., Bormann N., Delsol C., Dragani R., Fuentes M., Geer A.J., Haimberger L., Healy S.B., Hersbach H., Hólm E.V., Isaksen L., Kållberg P., Köhler M., Matricardi M., McNally A.P., Monge-Sanz B.M., Morcrette J.-J., Park B.-K., Peubey C., de Rosnay P., Tavolato C., Thépaut J.-N. & Vitart F. 2011. The ERA-Interim reanalysis: configuration and performance of the data assimilation system. *Quarterly Journal of the Royal Meteorological Society* 137, 553–597.
- Dekhtyareva A., Edvardsen K., Holmén K., Hermansen O. & Hansson H.-C. 2016. Influence of local and regional air pollution on atmospheric measurements in Ny-Ålesund. *International Journal of Sustainable Development and Planning* 11, 578–587.
- Eatough D.J., Caka F.M. & Farber R.J. 1994. The conversion of SO₂ to sulfate in the atmosphere. *Israel Journal of Chemistry* 34, 301–314.
- Eckhardt S., Hermansen O., Grythe H., Fiebig M., Stebel K., Cassiani M., Baecklund A. & Stohl A. 2013. The influence of cruise ship emissions on air pollution in Svalbard—a harbinger of a more polluted Arctic? *Atmospheric Chemistry and Physics* 13, 8401–8409.
- Elperin T., Kleerorin N., Liberman M.A., L'vov V.S. & Rogachevskii I. 2007. Clustering of aerosols in atmospheric turbulent flow. *Environmental Fluid Mechanics* 7, 173–193.
- EPA 2000. *Meteorological monitoring guidance for regulatory modeling applications*. EPA-454/R-99-005. Research Triangle Park, NC: US Environmental Protection Agency.
- Esau I. & Repina I. 2012. Wind climate in Kongsfjorden, Svalbard, and attribution of leading wind driving mechanisms through turbulence-resolving simulations. *Advances in Meteorology* 2012, article no. 568454, doi: 10.1155/2012/568454.
- Ferrero L., Cappelletti D., Busetto M., Mazzola M., Lupi A., Lanconelli C., Becagli S., Traversi R., Caiazzo L., Giardi F., Moroni B., Crocchianti S., Fierz M., Močnik G., Sangiorgi G., Perrone M.G., Maturilli M. & Vitale V. 2016. Vertical profiles of aerosol and black carbon in the Arctic: a seasonal phenomenology along 2 years (2011–2012) of field campaigns. *Atmospheric Chemistry and Physics* 16, 12601–12629.
- Fisher B. 2002. Meteorological factors influencing the occurrence of air pollution episodes involving chimney plumes. *Meteorological Applications* 9, 199–210.
- Hermansen O., Wasseng J., Bäcklund A., Noon B., Hennig T., Schulze D. & Barth V.L. 2011. *Air quality Ny-Ålesund. Monitoring of local air quality 2008–2010. Measurement results*. Kjeller: Norwegian Institute for Air Research.
- Hodal H., Falk-Petersen S., Haakon H., Kristiansen S. & Reigstad M. 2012. Spring bloom dynamics in Kongsfjorden, Svalbard: nutrients, phytoplankton, protozoans and primary production. *Polar Biology* 35, 191–203.
- Keller M.D., Bellows W.K. & Guillard R.R.L. 1989. Dimethyl sulfide production in marine phytoplankton. In E.S. Saltzman & W.J. Cooper (eds.): *Biogenic sulfur in the environment*. Pp. 167–182. Washington D.C.: American Chemical Society.
- Krzywinski M. & Altman N. 2014. Points of significance: nonparametric tests. *Nature Methods* 11, 467–469.
- Kupiszewski P., Leck C., Tjernström M., Sjogren S., Sedlar J., Graus M., Müller M., Brooks B., Swietlicki E., Norris S. & Hansel A. 2013. Vertical profiling of aerosol particles and trace gases over the central Arctic Ocean during summer. *Atmospheric Chemistry and Physics* 13, 12405–12431.
- Levasseur M. 2013. Impact of Arctic meltdown on the microbial cycling of sulphur. *Nature Geoscience* 6, 691–700.
- Liang J. & Jacobson M.Z. 1999. A study of sulfur dioxide oxidation pathways over a range of liquid water contents, pH values, and temperatures. *Journal of Geophysical Research—Atmospheres* 104, 13749–13769.
- Markowski P. & Richardson Y. 2006. On the classification of vertical wind shear as directional shear versus speed shear. *Weather and Forecasting* 21, 242–247.
- Matsumura S., Zhang X. & Yamazaki K. 2014. Summer Arctic atmospheric circulation response to spring

- Eurasian snow cover and its possible linkage to accelerated sea ice decrease. *Journal of Climate* 27, 6551–6558.
- Maturilli M., Herber A. & König-Langlo G. 2013. Climatology and time series of surface meteorology in Ny-Ålesund, Svalbard. *Earth System Science Data* 5, 155–163.
- Maturilli M. & Kayser M. 2016. Arctic warming, moisture increase and circulation changes observed in the Ny-Ålesund homogenized radiosonde record. *Theoretical and Applied Climatology* 130, 1–17.
- Meagher J.F. & Bailey E.M. 1983. The seasonal variation of the atmospheric SO₂ to SO₄²⁻ conversion rate. *Journal of Geophysical Research—Oceans* 88, 1525–1527.
- Mölders N., Tran H.N.Q., Quinn P., Sassen K., Shaw G. E. & Kramm G. 2011. Assessment of WRF/Chem to simulate sub-Arctic boundary layer characteristics during low solar irradiation using radiosonde, SODAR, and surface data. *Atmospheric Pollution Research* 2, 283–299.
- Moroni B., Becagli S., Bolzacchini E., Busetto M., Cappelletti D., Crocchianti S., Ferrero L., Frosini D., Lanconelli C., Lupi A., Maturilli M., Mazzola M., Perrone M.G., Sangiorgi G., Traversi R., Udisti R., Viola A. & Vitale V. 2015. Vertical profiles and chemical properties of aerosol particles upon Ny-Ålesund (Svalbard islands). *Advances in Meteorology*, article no. 292081, doi: [10.1155/2015/292081](https://doi.org/10.1155/2015/292081).
- NILU 1996. *EMEP manual for sampling and chemical analysis*. EMEP/CCC-report 1/95. Kjeller: Norwegian Institute for Air Research.
- Norwegian Polar Institute. 2016. *Report from the Ny-Ålesund Seminar. Tromsø, Norway, 23-25 September 2015*. Tromsø: Norwegian Polar Institute.
- Nygård T., Valkonen T. & Vihma T. 2014. Characteristics of Arctic low-tropospheric humidity inversions based on radio soundings. *Atmospheric Chemistry and Physics* 14, 1959–1971.
- Orr C., Hurd F.K. & Corbett W.J. 1958. Aerosol size and relative humidity. *Journal of Colloid Science* 13, 472–482.
- Quinn P.K., Shaw G., Andrews E., Dutton E.G., Ruoho-Airola T. & Gong S.L. 2007. Arctic haze: current trends and knowledge gaps. *Tellus B* 59, 99–114.
- Seinfeld J.H. & Pandis S.N. 2006. *Atmospheric chemistry and physics: from air pollution to climate change*. 2nd edn. New York: John Wiley & Sons
- Seuthe L., Iversen K.R. & Narcy F. 2011. Microbial processes in a high-latitude fjord (Kongsfjorden, Svalbard): II. Ciliates and dinoflagellates. *Polar Biology* 34, 751–766.
- Shikai C., Jianfeng H., Peimin H., Fang Z., Ling L. & Yuxin M. 2012. The adaptation of Arctic phytoplankton to low light and salinity in Kongsfjorden (Spitsbergen). *Advances in Polar Science* 23, 19–24.
- Sofiev M., Sofieva V., Elperin T., Kleeorin N., Rogachevskii I. & Zilitinkevich S.S. 2009. Turbulent diffusion and turbulent thermal diffusion of aerosols in stratified atmospheric flows. *Journal of Geophysical Research Atmospheres—Atmospheres* 114, D18209, doi: [10.1029/2009JD011765](https://doi.org/10.1029/2009JD011765).
- Stull R.B. 1988. *An introduction to boundary layer meteorology*. Dordrecht, The Netherlands: Kluwer Academic Publishers.
- Viana M., Hammingh P., Colette A., Querol X., Degraeuwe B., de Vlieger I. & van Aardenne J. 2014. Impact of maritime transport emissions on coastal air quality in Europe. *Atmospheric Environment* 90, 96–105.
- Vihma T., Kilpeläinen T., Manninen M., Sjöblom A., Jakobson E., Palo T., Jaagus J. & Maturilli M. 2011. Characteristics of temperature and humidity inversions and low-level jets over Svalbard fjords in spring. *Advances in Meteorology*, article no. 486807, doi: [10.1155/2011/486807](https://doi.org/10.1155/2011/486807).
- Walcek C.J. 2002. Effects of wind shear on pollution dispersion. *Atmospheric Environment* 36, 511–517.
- Wallace J.M. & Hobbs P.V. 2006. *Atmospheric science: an introductory survey*. 2nd edn. New York: Academic Press.
- Wang X.Y. & Wang K.C. 2014. Estimation of atmospheric mixing layer height from radiosonde data. *Atmospheric Measurement Techniques* 7, 1701–1709.
- Yin F., Grosjean D. & Seinfeld J.H. 1990. Photooxidation of dimethyl sulfide and dimethyl disulfide. I: mechanism development. *Journal of Atmospheric Chemistry* 11, 309–364.
- Yoch D.C. 2002. Dimethylsulfoniopropionate: its sources, role in the marine food web, and biological degradation to dimethylsulfide. *Applied and Environmental Microbiology* 68, 5804–5815.



Springtime nitrogen oxides and tropospheric ozone in Svalbard: results from the measurement station network

Alena Dekhtyareva^{a*}, M. Hermanson^b, A. Nikulina^c, O. Hermansen^d, T. Svendby^e, K. Holmén^f and R. Graversen^g

^aDepartment of Engineering and Safety, Faculty of Engineering and Technology, UiT The Arctic University of Norway, Tromsø, Norway, ORCID iD (<http://orcid.org/0000-0003-4162-7427>); ^bHermanson and Associates LLC, Minneapolis, USA; ^cDepartment of Research Coordination and Planning, Arctic and Antarctic Research Institute, Saint Peterburg, Russia; ^dDepartment of Monitoring and Information Technology, NILU - Norwegian Institute for Air Research, Kjeller, Norway; ^eDepartment of Atmosphere and Climate, NILU - Norwegian Institute for Air Research, Kjeller, Norway; ^fInternational director, Norwegian Polar Institute, Longyearbyen, Norway; ^gDepartment of Physics and Technology, Faculty of Science and Technology, UiT The Arctic University of Norway, Tromsø, Norway

Corresponding author: Alena Dekhtyareva, UiT The Arctic University of Norway, Postbox 6050 Langnes, 9037 Tromsø, alena.dekhtyareva@uit.no

Springtime nitrogen oxides and tropospheric ozone in Svalbard: results from the measurement station network

Measurement results from three independent research projects have been combined to identify the effect of emissions from various local sources on the background concentration of nitrogen oxides and tropospheric ozone in Svalbard. The hourly meteorological, NO_x and O₃ data from the ground-based stations in Adventdalen, Ny-Ålesund and Barentsburg were analysed along with daily radiosonde soundings and weekly data from O₃ sondes. The data from the ERA5 reanalysis have been used to evaluate the prevailing synoptic conditions during the fieldwork. Although the correlation between the NO_x concentrations in the three settlements was low due to dominant influence of the local atmospheric circulation, cases with common large-scale meteorological conditions increasing the local pollutant concentration at all sites were identified. In colder and calmer days and days with temperature inversions, the concentrations of NO_x were higher. In contrast to NO_x values, O₃ concentrations in Barentsburg and at the Zeppelin station in Ny-Ålesund correlated strongly, and hence were controlled by the prevailing synoptic situation and long-range transport of air masses. A special study with one of the NO_x sensors in Longyearbyen revealed elevated concentrations when ships were near the harbour. Further investigation of the effect of ship emissions on the air quality in Longyearbyen is recommended.

Keywords: atmospheric chemistry; air pollution; Arctic; meteorology, reactive nitrogen

Introduction

Fossil fuel combustion and biomass burning create high-temperature conditions leading to the reaction between atmospheric oxygen and nitrogen present in the fuel and in the air and formation of nitrogen oxides (NO_x=NO+NO₂) (Seinfeld and Pandis 2006). NO_x emitted locally in the Arctic or transported from mid-latitudes may increase the deposition of nitrates (NO₃⁻), which act as nutrients, and combined with climate change may cause changes in the relative abundances of species in nutrient-deficient

environments such as lakes in Svalbard (AMAP 2006). Aerosols, containing particulate nitrate, are formed from the gaseous nitric acid (HNO_3) produced through the oxidation of nitrogen dioxide (NO_2) by OH-radicals in the presence of sunlight or by the nighttime reaction with tropospheric ozone (O_3) (AMAP 2006).

However, high concentrations of NO_x may lead to regional soil and water acidification and have negative effects on human health (AMAP 2006). In addition to this, NO_x are vital for the formation of tropospheric ozone O_3 , which is a harmful air pollutant and greenhouse gas (IPCC 2013). The O_3 production and loss depends on RH/ NO_x (hydrocarbons and nitrogen oxides) and CO/ NO_x (carbon monoxide and nitrogen oxides) ratios and the presence or absence of sunlight. In the absence of sunlight during polar night, O_3 that have been produced within the long-range transported polluted air masses may accumulate in the Arctic. Hereby, the atmospheric lifetime of O_3 may be increased from days in summer to months in winter (AMAP/Quinn et al. 2008).

In spring, heterogeneous photochemical reactions with bromine compounds may occur over the sea-ice and snow-covered surfaces and result in tropospheric O_3 depletion in the region (Fan and Jacob 1992, Monks 2005, Simpson et al. 2015). According to the study performed by Beine et al. (1997b), the background NO_x values were lower than normal during the O_3 depletion events observed at the Zeppelin station in Svalbard. The reactions with Br-species, which result in oxidation of NO to NO_2 and removal of NO_2 by the reaction with BrO or OH-radical and formation of HNO_3 , were proposed as possible explanation to this phenomenon. However, it may also be explained by the fact that lower NO_x values are characteristic of the pristine air masses from the remote regions in the high Arctic. In contrast, elevated NO_x values are observed during the pollution episodes near the local emission sources or when NO_x are long-range

transported to the Arctic from mid-latitudes directly or in the form of peroxyacetyl nitrate (PAN), which is further thermally decomposed in-situ in the Arctic when the air temperature increases in spring (Beine et al. 1997a).

A diurnal variation in the background NO/NO₂ ratio has been observed in Svalbard in spring, and the increase in the ratio around noon becomes more pronounced from March to May (Beine et al. 1997a). The efficiency of NO₂ photolysis and formation of NO and O₃ enhances as insolation increases, despite concurrent rapid oxidation of NO by O₃ leading to formation of NO₂, a second part of the so-called daytime NO_x null-cycle (Wallace and Hobbs 2006). The latter reaction also explains the titration of O₃, which may be observed in the vicinity of large sources of NO such as cruise ships (Eckhardt et al. 2013). However, if the NO concentration is higher than 10 pptv and CO or hydrocarbons are present in sufficient quantities, excess of O₃ may be produced in the presence of sunlight (Wallace and Hobbs 2006).

Although Svalbard is a near pristine Arctic environment, where long-range transport is the dominant air pollution source, there are also local anthropogenic emissions on the archipelago. Coal power plants in Barentsburg and Longyearbyen and diesel-fuelled generator in Ny-Ålesund supply energy for heating and electricity (Vestreng et al. 2009, Dekhtyareva et al. 2016) (Fig. 1). The energy demand for heating in Longyearbyen is two times higher in winter than in summer due to lower temperatures in wintertime. In winter days, the production of energy for heating increases from 06:00 to 09:00 in the morning and then decreases steadily until it reaches its minimum at 03:00 in the night, while in summer the production varies little throughout the day (Tennbakk et al. 2018). In contrast to the energy needed for heating, the energy demand for electricity production is stable and mostly independent on the air temperature. The three biggest consumers of electricity are the coal power plant itself,

the mine Gruve 7 and the Svalbard Satellite Station SvalSat. There is a diurnal variation in the power demand with higher daytime values in winter. In summer, the power demand and its diurnal variations are lower, since the mine has reduced operation in July (Tennbakk et al. 2018). The power demand for heating in Ny-Ålesund and Barentsburg varies similarly to Longyearbyen, but the absolute values are different for all three settlements.

Svalbard residents use cars for transportation within the settlements and snowmobiles for springtime off-road traffic (Vestreng et al. 2009). There were around 2500 snowmobiles registered at Svalbard in 2007 (MOSJ 2018), and, according to the report issued by the Norwegian Climate and Pollution Agency (Vestreng et al. 2009), local NO_x emissions from these were three times higher than emissions from the gasoline cars. Current number of snowmobiles is around 2100, and it has been stable since 2011 (MOSJ 2018).

In order to minimize environmental impact from the usage of motorized vehicles in the terrain on snow covered and frozen ground, specific zones, where the snowmobile traffic is allowed, are established (Klima- og miljødepartementet 2001). Furthermore, because of complex terrain, most of the snowmobile routes are in valleys. Tourists and residents usually travel in groups consisting of up to 20 snowmobiles due to safety reasons. Consequently, the amount of pollutants emitted instantaneously by one motorcade may be significant. Previous studies have shown highly elevated levels of volatile organic compounds along snowmobile tracks (Reimann et al. 2009), however, no measurements of nitrogen oxides have previously been done.

NO_x concentrations in all three settlements may also be influenced by emissions from the ship traffic (Shears et al. 1998, Vestreng et al. 2009). However, it is the most

intensive in summer (Eckhardt et al. 2013, Dekhtyareva et al. 2016), while snowmobiles and power plants are dominant sources of NO_x in winter and spring seasons.

A two-month-long measurement campaign was organized in spring 2017 to assess the effect of emissions from various sources on the NO_x concentration in Longyearbyen. The data from Barentsburg and Ny-Ålesund have been analysed simultaneously to assess effect of local and mesoscale meteorological conditions on concentrations of pollutants.

Synoptic-scale north-easterly wind is prevailing in the Svalbard region (Hanssen-Bauer et al. 2019), but the large-scale flow is affected locally by topographical channelling and air density gradient from the inland glaciers to the warmer sea. The expected wind direction is along the axis of valleys or fjords towards the coast (Førland et al. 1997): from south-east in Longyearbyen and Ny-Ålesund and from south-south-east in Barentsburg. Nevertheless, despite the difference in local wind direction at the stations, there may be common mesoscale meteorological conditions promoting accumulation of pollutants in the atmospheric boundary layer (ABL) at all three sites such as absence of vertical wind speed shear and atmospheric temperature inversion (Dekhtyareva et al. 2018).

Meteorological conditions, namely wind speed, air temperature and humidity, affect the formation of aerosols and efficiency of pollution dispersion and deposition, while ultraviolet (UV) solar irradiance has an influence on photochemical reactions in the troposphere (Seinfeld and Pandis 2006). The photolysis of O_3 at the wavelengths below 320 nm may lead to production of OH-radical in presence of water vapour, which may further yield net O_3 production if CO, NO_x and hydrocarbons are present in sufficient quantities. NO_2 dissociates to NO and O in the range of wavelengths from 300 nm to 370nm. The photodissociation efficiency reduces gradually at higher

wavelengths and stops at 420nm (Seinfeld and Pandis 2006). The photolysis of dihalogens, an initial step needed for the reactions promoting springtime tropospheric O₃ depletion in the Arctic, is efficient even under low solar elevation and higher column ozone concentration (Simpson et al. 2015). Thus both UV-B and UV-A solar irradiance fractions with wavelengths from about 300 to 315 nm and from 315 to 400 nm (Seinfeld and Pandis 2006), respectively, may have influence on the springtime concentrations of NO_x and O₃ in Svalbard.

The main aim of the current article is to combine NO_x and O₃ data from three different research projects in Svalbard in order to identify specific factors affecting the concentration of measured compounds in Barentsburg, Longyearbyen and Ny-Ålesund and define conditions that promote accumulation of local and long-range transported pollution in all three settlements.

The meteorological in-situ and reanalysis data, UV, O₃ and NO_x observations have been used to test the following hypotheses:

- There is a diurnal pattern in concentration of NO_x at all three stations due to variable emission rate from the local sources of NO_x.
- Complex topography determines local circulation, and therefore variation of NO_x concentration measured at the stations will be dominated by micro- and mesoscale phenomena.
- Local emissions of NO_x in Ny-Ålesund and Barentsburg affect O₃ concentrations in the settlements.
- Despite the topographically induced features, there are common synoptic meteorological conditions, which have an influence on concentrations of NO_x and O₃ in the settlements.

Materials and methods

Measurements in Adventdalen (Longyearbyen)

In spring season, the main snowmobile route from Longyearbyen to the east coast of Spitzbergen goes along the road through the Adventdalen valley, and therefore there is daily snowmobile traffic nearby the CO₂ laboratory belonging to the University centre in Svalbard (UNIS CO₂ lab). The chemiluminescence NO/NO₂/NO_x analyser (model T200) was installed at the laboratory for the period from 23.03.2017 to 15.05.2017. The inlet of the sampling hose was secured outside from the window, while the temperature inside the laboratory was kept constant with the help of thermostat to maintain stable conditions needed for correct functioning of the analyser. The sensor was calibrated weekly using zero-air generator and certified NO gas with known concentration (800 ppb), and the NO_x data were scaled linearly to eliminate zero drift. The automatic weather station (UNIS AWS) is located nearby the UNIS CO₂ lab, and the data from the station have been used to assess local meteorological conditions.

In addition to the meteorological parameters from the Adventdalen station, data from UV monitors installed at the UNIS roof in Longyearbyen have been used. The sensors SKU 420 UV-A (315-380 nm) and SKU 430 UV-B (280-315 nm), produced by the SKYE Instruments, were calibrated 24th of August 2016.

Measurements in Barentsburg

The Russian Arctic and Antarctic Research Institute (AARI) performed the measurements in Barentsburg independently in frames of the air quality monitoring programme. The equipment installed in the settlement includes Chemiluminescence NO_x and UV Photometric Ozone Analysers produced by Environment S.A. and portable Vaisala weather station. The analysers continuously gather the data and

transmit them to the desktops in the laboratory facility of the Russian Scientific Centre in Barentsburg. The data with 20-minutes time resolution have been averaged to obtain hourly data. In contrast to equipment in Ny-Ålesund and Longyearbyen, the NO_x and O₃ analysers have not been calibrated during the field campaign. Therefore, the data from this station may be prone to drift. It is especially important to consider when one studies NO_x concentrations, since the NO_x values are usually very low in the remote Arctic environment (Dekhtyareva et al. 2016). On the other hand, the UV O₃ monitor is more stable and does not demand as frequent calibration as chemiluminescence instruments (Williams et al. 2006), and thus data from this instrument are more reliable.

Measurements in Ny-Ålesund

Continuous NO_x measurements are performed by the Norwegian institute for Air Research (NILU) in framework of the air quality monitoring programme in Ny-Ålesund (Johnsrud et al. 2018) . The analyser is installed in the middle of the settlement, 100m to the north-west from the meteorological station operated by the Norwegian meteorological institute. The hourly O₃ gas monitor data from the Zeppelin observatory located nearby the mountaintop (474m a.s.l.) two km to the southwest from Ny-Ålesund (for the exact location of the Zeppelin station see, for example, Figure 1b) in Dekhtyareva et al., 2018) have been used for comparison with the O₃ measurements in Barentsburg. The UV data obtained using multifilter radiometer GUV 541 at the Sverdrup station in Ny-Ålesund (Gröbner et al. 2010, Schmalwieser et al. 2017) and local meteorological observations from the Zeppelin station have been provided by NILU as well. The GUV radiometer is checked and corrected against a travelling reference instrument every year.

In addition to this, daily radiosonde and weekly ozone sonde data from the French–German AWIPEV research station in Ny-Ålesund have been used. Since temperature inversion and vertical wind shear may be important factors promoting accumulation of local pollution in the atmospheric boundary layer, the method for their detection in the radiosonde vertical profiles described by Dekhtyareva et al., 2018, has been applied. The days, when the temperature and wind speed were increasing with height on more than 0.3°C and 1.25ms^{-1} , respectively, in the lowest 500m, were defined as days with temperature inversions and vertical wind speed shear. In order to compare the O_3 sonde measurements with ground-level observations, the O_3 mixing ratio and ozone concentration have been calculated from the O_3 partial pressure using ideal gas law and molar volume of ozone at the temperature and pressure measured by the radiosonde (Seinfeld and Pandis 2006).

Daily radiosonde launches are operated at the AWIPEV station, using Vaisala RS92 radiosondes until April 2017 (Maturilli and Kayser 2016) and Vaisala RS41 radiosondes afterwards. In this study, we apply radiosonde data for March 2017, post-processed according to the principles of Reference Upper-Air Network GRUAN (Immler et al. 2010) and available via the GRUAN homepage www.gruan.org. As the RS41 is currently not processed by GRUAN, we applied the manufacturer's processed radiosonde data for April-May 2017 that are available in the database www.pangaea.de (Maturilli 2017a, 2017b). The analysed O_3 sonde data are stored in the Network for the Detection of Atmospheric Composition Change (NDACC) archive <ftp://ftp.cpc.ncep.noaa.gov/ndacc/station/nyalsund/ames/o3sonde/>.

Methods to study the effect of meteorological conditions on the concentration of measured compounds

The partial correlations are used in air pollution research to investigate the strength and

direction of relationship between concentration of atmospheric compounds and each of meteorological parameters whilst controlling for the effect of others (Liu et al. 2016, Su et al. 2016). The histograms of the chemical and meteorological data from all three stations have been plotted and Kolmogorov-Smirnov test for normality with 5% significance level (Lilliefors 1967) has been applied to observations in order to check if they are normally distributed. If the hypothesis about normality has been accepted, the Pearson's partial correlation has been applied to measure the strength of a linear association between the concentrations of measured compounds and one of meteorological variables controlling for the effect of others. In case of lack of normal distribution, the Spearman's rank partial correlation has been calculated to test if there is a statistically significant monotonic relationship between the chemical observations and meteorological parameters (Chalmer 1986). As stations in Ny-Ålesund and at the Zeppelin mountain are located at different altitudes in an area with complex topography and previous studies have shown significant difference in meteorological values at these sites (Dekhtyareva et al. 2016, 2018), separate meteorological data have been used for the correlation calculation. The UV data from the Sverdrup station in Ny-Ålesund have been used for the calculation of partial correlation with NO_x in Ny-Ålesund and O₃ at the Zeppelin station, while the UV data from UNIS in Longyearbyen have been used for the calculation of correlation with NO_x from Adventdalen. Since there was no UV data from Barentsburg available for the period of fieldwork, the partial correlations for this station have been calculated using meteorological data only.

The effect of the prevailing synoptic meteorological situation on the NO_x and O₃ concentration has been studied using hourly meteorological data from the global ERA5 reanalysis dataset with 31 km spatial resolution (Hersbach and Dee 2016).

To study long-range transport of O₃-depleted or enriched air masses, the following procedure has been implemented to detect joint O₃ decrease and increase events in the data from Barentsburg and the Zeppelin station:

- (1) Since the distance between the Zeppelin observatory and Barentsburg is more than 100 km, some time lag in correlation between the data from the two stations is expected. The allowable time lag has been defined based on the lagged linear correlation between the datasets. Maximum time lag, for which the correlation coefficient is higher or equal to the coefficient calculated for zero-hour lag, is defined as maximum allowable time lag.
- (2) Applying the air-quality extreme definition stated in Porter et al. (2015), O₃ levels below the 5th quantile and above the 95th quantile have been found separately for the Barentsburg and Zeppelin to define severe depletion and increase events, respectively.
- (3) Continuous episodes have been defined for the periods where the time difference between consecutive event points is less than 3 hours.
- (4) Minimum (maximum) O₃ concentrations within each event have been defined.
- (5) The time of minimum (maximum) within the events in Barentsburg and at the Zeppelin station have been compared and if the difference between them is less than maximum allowable time lag, the events at both stations have been classified as joint.

Then backward air mass trajectories have been simulated using the Hybrid Single Particle Lagrangian Integrated Trajectory (HYSPLIT) model for these joint events for 240 hours back in time to identify the source regions for the air masses (Stein et al. 2015). The 10-days simulation time has been chosen as a compromise between the

average lifetime of tropospheric O₃, which may be three to four weeks (Christiansen et al. 2017), and the uncertainty of modelled air mass trajectories that increases with travelled distance (Freud et al. 2017).

Methods to study the effect of local pollution in Ny-Ålesund and in Barentsburg on measured O₃ concentrations

As there were no O₃ data from Ny-Ålesund available, the O₃ and CO data from the Zeppelin station were used to study the influence of local NO_x emissions Ny-Ålesund on the O₃ concentration. CO indicates presence of other pollutants emitted simultaneously in the process of fossil fuel burning, and although the correlation between NO_x and CO concentration in the plumes depends on the engine and fuel type, age of the plume and environmental conditions (Li et al. 2015), we expect higher CO concentrations in the fresh plumes arriving to the Zeppelin station. Therefore, local pollution effect has been defined for O₃ measurements at the Zeppelin station when all three conditions were fulfilled:

- (1) wind direction measured both in Ny-Ålesund and at the Zeppelin station was northerly (above 270° or below 90°) since the diesel power plant is located in 300 m to the north-north-west from the NO_x monitor in Ny-Ålesund and 2 km to the north-north-east from the Zeppelin station;
- (2) NO_x concentrations were above mean value in Ny-Ålesund;
- (3) CO concentrations observed at the Zeppelin station were above mean value indicating the possible impact of local pollution.

To assess how the NO_x emissions in Barentsburg affect the local O₃ concentration there, the NO_x and O₃ data from the Barentsburg station have been compared. Positive anomalies in O₃ concentration were found for the same wind

directions where increased NO_x concentrations were observed, but this may be due to higher concentrations of O_3 in air masses, which were transported to Svalbard from the south and south-west. Since there are multiple sources of local pollution in Barentsburg, another method has been implemented:

- (1) the hours when NO_x concentrations were above average in Barentsburg have been defined;
- (2) O_3 values for these hours in the original and in the smoothed data series from Barentsburg have been compared.

Results and discussion

Comparison of NO_x and O_3 observations from Adventdalen, Barentsburg and Ny-Ålesund

There is a weak statistically significant positive correlation between NO , NO_2 and NO_x values measured in Adventdalen and in Ny-Ålesund (the Pearson correlation coefficients are $r_{\text{NO}}=0.13$, $r_{\text{NO}_2}=0.15$ and $r_{\text{NO}_x}=0.13$, $p<0.0001$ for all compounds). However, the data from all stations have shown significant autocorrelation, which may influence the inter-correlation of the three datasets. Therefore, in order to test the significance of the Pearson correlation coefficients stated above, a Monte Carlo approach has been applied (Graversen 2006). The artificial data series have been constructed keeping the power spectrums obtained from NO , NO_2 and NO_x data from Ny-Ålesund, but randomly changing the phase in the frequency domain. Then the artificial data sets were compared with the original NO , NO_2 and NO_x time series from Adventdalen, and the Pearson correlation coefficients have been calculated. The procedure have been repeated 5000 times for each variable to obtain reliable number of correlation coefficients. Statistical significance was obtained when the correlation

coefficients calculated for the artificial data time series were equal or higher to the one, calculated based on original data from Ny-Ålesund and Adventdalen in less than 5% of cases. In that case the correlation between the original NO, NO₂ and NO_x data from the Ny-Ålesund and Adventdalen is significant at a 95% level. On the contrary, no correlation is present with NO_x data from Barentsburg, where the measurement and calibration routine was different from the two stations stated above. Low correlation between the NO_x values at the three stations may indicate the importance of local emission sources and micrometeorology rather than the long-range sources of NO_x and synoptic conditions.

The comparison of the O₃ data series from the Zeppelin station (purple line in the Fig. 2) and Barentsburg (light green line in the Fig. 2) shows that the Barentsburg data contains much more high frequency variations. Indeed, the Barentsburg station is located inside the settlement, and the O₃ data from there is more prone to be influenced by the local NO_x pollution, while the Zeppelin station is situated far from the local emission sources. A 6-hours moving average filter has been applied to the O₃ Barentsburg data, and the results are shown as a dark green line in Fig. 2. The smoothed and original O₃ data from Barentsburg have been compared statistically: both two-sided Wilcoxon rank sum (WRS) test and the t-test show that the application of the low-pass filter on the O₃ from Barentsburg does not result in significant change in the concentration distribution. The correlation between O₃ concentrations at the Zeppelin station and in Barentsburg is strong (Pearson correlation coefficient $r=0.69$ both for smoothed and unsmoothed data, $p<0.001$). This indicates that O₃ concentrations at both stations are highly influenced by the meteorological conditions on the synoptic scale and local impacts are of minor importance.

We have applied methods described earlier, to define the effect of local NO_x emissions in Ny-Ålesund and Barentsburg on the O₃ concentrations in the settlements. As a result, 5% of O₃ data from the Zeppelin station may be influenced by the local pollution from Ny-Ålesund, and the statistically significant ($p < 0.0001$) decrease in O₃ mean (63.1 vs 72.0 µg/m³) and median (68.6 vs 75.8 µg/m³) concentrations has been revealed for this group. However, northerly wind that may transport local pollution from Ny-Ålesund also brings air masses, which have lower O₃ background value (Fig. 7 and 9a). Therefore, when one compares locally polluted air masses with the background air masses coming from the north, the difference in mean and median O₃ concentrations becomes statistically insignificant, 63.1 vs 66.5 µg/m³ and 71.0 vs 68.6 µg/m³, respectively. Consequently, the titration of O₃ by locally emitted NO_x occurs very rarely and may reduce the mean O₃ concentration from the background value by a few percent only.

Difference between the original and smoothed O₃ data from Barentsburg varies from -19% to 11% of the smoothed value, and there is a strong negative correlation between the magnitude of NO_x peak and the O₃ titration efficiency ($r = -0.65$, $p < 0.0001$). However, elevated NO_x concentrations in Barentsburg contribute to local O₃ titration and lead to average reduction of its concentration by 1% in comparison to the smoothed values. This effect is not statistically significant, and therefore other factors, such as variation in concentrations within long-range transported air masses, may be more important for explanation of difference between the O₃ Zeppelin and Barentsburg datasets.

Mean and median daytime (from 6:00 UTC to 17:00 UTC) and nighttime (from 18:00 UTC to 5:00 UTC) concentrations are shown in Table 1 (here the daytime and nighttime are defined based on snowmobile traffic pattern in the Adventdalen valley).

$\text{NO}_2/(\text{NO}+\text{NO}_2)$ -ratio is quite high in Adventdalen and in Barentsburg and exhibits diurnal variation, while it is much lower in Ny-Ålesund and there is no statistically significant difference between its day and night values. This may be explained by the fact that the measurement station in Ny-Ålesund was located much closer to the diesel power plant, a constant source of fresh NO_x emissions, where the NO_2/NO_x ratio is much lower irrespective to the time of the day (Kimbrough et al. 2017). However, the lowest hourly NO_2/NO_x ratio of 0.29 and the highest peak of NO_x were observed in Ny-Ålesund at 17:00 UTC 28th of April (Fig.2). The concentration of NO and NO_2 were $109.7 \mu\text{gm}^{-3}$ and $31.3 \mu\text{gm}^{-3}$, respectively, that indicates the presence of a strong emission source, for example snowmobiles, in the immediate vicinity from the station. Since it was a single NO_x peak in the data, NO_2/NO_x ratio was unusually low and the meteorological conditions were untypical for pollution accumulation in Ny-Ålesund (south-easterly wind with moderate speed of 5.3 ms^{-1}), this value has been excluded from further statistical analysis.

Average concentrations of measured compounds have been calculated for each hour of the day. The diurnal variation in NO, NO_2 and O_3 concentrations at the stations is shown in Fig. 3.

NO is a primary product of fossil fuel combustion (Arya 1999, Seinfeld and Pandis 2006), and higher NO/NO_x ratio is expected close to the emission source. The station in Adventdalen is located at a distance of five kilometres from the coal power plant (Fig. 4), and snowmobile traffic there is a temporarily emission source present during daytime mostly. In contrast, measurement stations in Barentsburg and Ny-Ålesund are located in the vicinity of the power plants releasing combustion products constantly at a variable rate (Fig. 5a and 5b). Thus, it is noticeable in Adventdalen that the NO concentration is close to zero during the night (dark blue bar in Fig. 3) in

absence of fresh traffic emissions and photochemical conversion of NO_2 to NO . As the traffic intensity increases during the day, NO concentration rises, however, so does the NO_2 concentration (red bar in Fig. 3) since there is rapid conversion of NO to NO_2 by reaction with O_3 .

One can see that the increase in the NO_x concentration is followed by the rising O_3 values in Barentsburg (black line in Fig. 3). In contrast, slight decrease in daytime O_3 concentration is observed at the Zeppelin station. However, according to the t-test and the WRS-test, there is no statistically significant difference between nighttime and daytime O_3 concentrations measured at the stations (Table 1).

The average NO and NO_2 concentrations measured at the stations are distributed unevenly over the wind directions. In Adventdalen, the southeasterly wind with wind speed of 4.1 ms^{-1} was dominating during the field campaign, and there was no significant difference between the daytime and nighttime observations. The highest average daytime NO and NO_2 concentrations were observed when the wind was from NE and SE in Adventdalen (Fig. 4). In contrast, the highest average nighttime NO_2 concentrations were detected when the wind was from NW, which reveals possible influence of the coal power plant. The average nighttime concentrations of NO were very low regardless of wind direction.

Figures 5a) and 5b) illustrate distribution of NO and NO_2 concentrations over wind directions in Ny-Ålesund and Barentsburg, respectively. South-easterly wind with average speed of 3.6 ms^{-1} and 3.9 ms^{-1} in daytime and nighttime, accordingly, was dominating in Ny-Ålesund. However, the highest average NO_x concentrations in Ny-Ålesund were measured when the wind was coming from the north (Fig. 5a)). It points clearly to the local diesel power plant as an emission source. Similar results regarding the influence of the local power plant in Ny-Ålesund on NO_x concentrations were

presented in Dekhtyareva et al., 2016 and Johnsrud et al. 2018. During the field campaign, the prevailing wind in Barentsburg was from south and south-east with average speed of 2.5 ms^{-1} and from south-east and east with mean speed of 2.3 ms^{-1} in daytime and nighttime, respectively. The NO_x concentrations measured there were much lower than in Ny-Ålesund and the location of the emission sources was much more difficult to define (Fig. 5b). Daytime concentrations were probably influenced by the pollution from the port area and from the coal power plant located to the west and south-west from the measurement station, respectively.

Since the data are not normally distributed, the Spearman partial correlations have been calculated in order to evaluate relationship between the NO_x and O_3 , local meteorological parameters and UV (Table 2).

The partial correlation of measured compounds with local wind speed is negative, varies from very weak for NO data from Ny-Ålesund and Barentsburg to moderate for NO_2 data from Ny-Ålesund and Adventdalen and is significant for all the sites ($p < 0.05$), except the Zeppelin station where the correlation with O_3 was negligible. This may be explained by the fact that the local NO_x emissions rarely reach the station, and thus the dispersion efficiency, which affects the possibility of local O_3 production and is dependent on the wind speed, is not crucial factor influencing the O_3 concentration measured there. In contrast, there is weak negative correlation between O_3 values and wind speed measured in Barentsburg. Indeed, light wind conditions may promote accumulation of O_3 precursors and local O_3 formation. Despite the fact that the local ground-level wind speed correlates significantly with all compounds measured in Ny-Ålesund, Barentsburg and Adventdalen, according to the Wilcoxon rank sum test (WRS-test), the vertical wind speed shear, detected in 55% of the radiosonde data, is not an important factor of influence. The radiosonde soundings are done only once a day

from Ny-Ålesund and the wind data from these measurements may not be representative for all the sites due to different mechanical and thermal processes controlling local circulations such as formation of katabatic winds and various mechanisms of wind channelling specific for each location (Esau and Repina 2012, Maturilli et al. 2013).

Temperature inversions were detected in 28% of all the days in the measurement campaign period. This frequency of inversion occurrence is quite low in comparison with the results from previous studies of Dekhtyareva et al., 2018, where it was observed in 60% of the springtime profiles in 2009. Despite low frequency of occurrence, temperature inversions have significant influence on dispersion efficiency, and, according to the WRS-test, the median daytime (from 06UTC to 18UTC) concentrations of NO_x at all three stations were higher ($p < 0.05$) for the days when the phenomenon was observed in the radiosonde data.

The correlation with atmospheric temperature is negative for NO and NO_2 in Ny-Ålesund and Adventdalen. This may be explained by enhanced accumulation of locally emitted NO_x in the ABL due to suppressed vertical mixing in cold days. In contrast, the correlation between NO_x concentration and air temperature and relative humidity is positive in Barentsburg. The major emission sources there are located on the seashore, and warmer marine air from west and south-west may bring local pollution to the station situated on the hill above them (Fig. 5b). There is moderate positive correlation between air temperature and O_3 both in Barentsburg and at the Zeppelin observatory. This indicates that the excess of O_3 might have been formed remotely and was transported to Svalbard with warmer air masses from mid-latitudes. Another explanation is that local colder air masses may have lower O_3 concentration due to halogen driven O_3 destruction.

The O₃ correlates negatively with relative humidity. Previous studies in Arctic and Antarctica have shown that the air masses transported across the sea-ice covered areas exposed to sunlight had high relative humidity values and low O₃ concentrations (Wessel et al. 1998).

There is a very weak positive correlation between the UV-A measured in Longyearbyen and NO and NO₂ concentrations in Adventdalen probably because the recreational snowmobile traffic increased with rising number of light hours per day. Other partial correlations between UV data and measured compounds are negligible and insignificant (absolute value of r is less than 0.1 and p>0.05).

Since the meteorological conditions affect the concentrations of measured compounds differently, one needs to study the weather regimes affecting NO_x (NO+NO₂) and O₃ concentrations separately.

According to the t-test, the average meteorological conditions were statistically different (p<0.001) when the sum of NO and NO₂ concentrations were above median vs hours with concentrations below or equal to median at all stations. Temperature was more than 1°C lower (-9.7 °C vs -8.6 °C), wind speed was more than 1 ms⁻¹ lower (3.0 ms⁻¹ vs 4.5 ms⁻¹) and the difference in pressure was 4 hPa (1012 hPa vs 1016 hPa) for the first group of values vs the second one. The difference between prevailing synoptic meteorological situation for both groups and mean for the whole period is shown in Figure 6. Hours when NO_x concentrations were elevated are characterized by lower wind speed, more frequently observed westerly air flow and lower mean sea level pressure, while in hours when NO_x values were below median, air masses were arriving from the north-east more frequently, wind speed and mean sea level pressure were higher than on average during the measurement campaign. However, the situations described above, when concentrations at all stations exhibited similar changes

simultaneously, occurs rarely, in 30% of all measurements distributed equally between the first and second groups. Indeed, NO_x concentrations depend strongly on local wind direction and location of the station relative to the main source of emissions as has been presented in Figures 4 and 5.

In accordance with the t-test, the average temperature, relative humidity and atmospheric pressure were statistically different ($p < 0.001$) for hours when the O₃ concentrations were above median vs hours with concentrations below or equal to median in Barentsburg and at the Zeppelin station. Temperature was more than 3°C higher (-7.2 °C vs -11.0 °C), relative humidity was 3% lower (72% vs 75%) and atmospheric pressure was more than 5 hPa lower (980 hPa vs 985 hPa) for the first group of values vs the second one. Note, that the average pressure has been calculated for Barentsburg (70m a.s.l.) and Zeppelin stations (474m a.s.l.). One can see, that there is a difference in prevailing synoptic meteorological situation for both groups and the mean for the whole period (Figure 7). Southerly air flow was more frequent and mean sea level pressure was lower for hours when O₃ concentrations were above median, while in hours when O₃ concentrations were below median, air masses were more often transported from the north and mean sea level pressure was higher than on average during the measurement campaign. O₃ concentrations in Barentsburg and at the Zeppelin station showed similar pattern of change in 63% of all measurements (the first and second group account for 30% and 33% of all data, respectively). This means that O₃ concentrations at both stations were influenced by the meteorological conditions on the synoptic scale to a much higher degree than NO_x concentrations.

The comparison of the vertical O₃ data from the ozone sondes from Ny-Ålesund (Fig. 8) and the ground-based measurements at the Zeppelin station and in Barentsburg (Fig. 2) reveals that the discrepancy in the data between the two stations may be

explained by the fact that the stations are located at different heights and measure air masses with uneven distribution of O₃ in the lowest 500m. If one contrasts the closest point to the sounding time in the observations made in Barentsburg and in Ny-Ålesund, similar tendencies as in the O₃ sonde data may be observed. For example, there is a significant difference between the data from Barentsburg and Ny-Ålesund (76.3 µg/m³ vs 59.0 µg/m³) for the measurement closest to the time of sounding on 26th of April, and the reduction of O₃ concentration with height between 50 and 500m is noticeable in the sounding data as well.

The lagged linear correlation between the original O₃ data from the Zeppelin station and the data from Barentsburg, which have been shifted forward in time, increases from $r=0.69$ (0-hour lag) to $r=0.74$ (4-hour lag) and reduces gradually to $r<0.69$ for 10-hour lag. Thus, the maximum allowable time lag for detection of joint extreme O₃ depletion and increase events in the data from Barentsburg and Zeppelin station is set to 9 hours. The limiting 5th and 95th quantiles for Barentsburg and Zeppelin stations are shown by dotted light green and purple lines in Fig. 2, accordingly.

Two joint O₃ depletion events (31.03.2017 and 06.05.2017) and three increase events (13.04.2017, 28.04.2017 and 03.05.2017) have been detected. The HYSPLIT trajectory analysis shows that these O₃ depletion events occurred when the cold air masses from the central Arctic reached Svalbard. The trajectory for the strongest depletion event is shown in Fig. 9a. The concentration of O₃ in the Arctic air masses may be lower because of lack of ozone precursors such as NO_x, hydrocarbons and CO needed for O₃ formation. Further depletion may have occurred due to photochemical reactions with bromine species over the sea-ice in the period from 27.03.2017 12:00 to 29.03.2017 12:00 when the simulated height of the lowest air masses arriving to the Zeppelin station and in Barentsburg was below 500m (red line in Fig. 9a). The

simulated sun flux was quite low, but probably sufficient enough to support the halogen induced O₃ destruction which may occur even under low light conditions (Simpson et al. 2015). The trajectories for the increase events revealed southerly origin of the air masses, but source regions were different for all three cases. In the first case, it was arriving from Northern part of Russia, in the second one from North America and Iceland, but the highest O₃ concentrations at both stations were observed 03.05.2017 when the air masses were transported from Europe (Fig. 9b). The conditions were favourable for O₃ production, since the solar flux was much higher than for the depletion event described above and the air above the source region most probably contained O₃ precursors. The simulated height over European sources for the lowest trajectory arriving to Barentsburg was around 1000m, while for the Zeppelin station it was around 3000m. This may explain why higher O₃ concentrations were observed in Barentsburg during this event.

Case study: short-term NO_x measurements in Longyearbyen to investigate influence of other pollution sources on local air quality

A case study to look at the influence of other pollution sources inside Longyearbyen on the local air quality was performed in the end of the measurement campaign. The NO_x sensor was placed at the third floor at UNIS, approximately 1 km to the south-east from the harbour (Fig. 4). The sensor was recalibrated with zero air and span NO concentration before and after relocation from Adventdalen, and the air inlet hose was secured outside the window. In addition to NO_x monitor, portable meteorological station Kestrel has been installed at the UNIS roof at 24 m height. One can see that first NO_x concentrations had been below 10µg·m⁻³, and then the peak in the values was been observed from 15:00 to 17:00 local time (Fig. 10). Elevated concentrations might be caused by the presence of ships in the harbour of Longyearbyen simultaneously. The

two-headed shape of the peak might be explained by the fact that, according to the local observations and data from the www.marinetraffic.com, the cargo ship Norbjørn departed and the offshore supply ship Polarsysssel arrived shortly after that.

The wind with mean speed of 2.4 ms^{-1} and south-westerly (SW) direction, along the river from the local valley Longyeardalen, was prevailing according to the Kestrel data (upper left corner in Fig. 10) when the elevated NO_x concentrations were observed in Longyearbyen. The local wind from SW might bring pollution from the reserve diesel generator located nearby UNIS. The generator works in cases of emergency, to warm up water used in central heating system in town and during maintenance of the coal power plant. It is unclear if the generator was working during the case study; therefore, its contribution to the pollution emitted by the ships is unknown.

However, one can see from the meteorological data from the automated weather station in Adventdalen (lower left corner in Fig. 10) that the Kestrel data from UNIS roof represent a local wind, while westerly and north-westerly wind were prevailing on a regional scale. The same is supported by the data from the Svalbard airport where north-westerly wind with average wind speed of 2.6 ms^{-1} was observed. On the synoptic scale, anticyclone was located to the north-west of Svalbard, and therefore clockwise wind direction around anticyclone was prevailing.

Unfortunately, it was not possible to continue observations in Longyearbyen due to technical error, which occurred with the NO_x monitor in the evening 16.05.2017. However, results from the current case study illustrate that local NO_x concentrations in the Longyearbyen town may be much higher than in the Adventdalen valley where maximum hourly NO_2 concentration of $21.8 \mu\text{g}\cdot\text{m}^{-3}$ was measured on Easter holiday, 13.04.2017. In that day, the combination of increased recreational traffic and mild weather conditions (wind speed below 1 ms^{-1} and air temperature -8°C) led to

accumulation of concentration 13 times higher than daytime hourly average measured during the field campaign. Such low wind speed is untypical for the wind regime in Adventdalen, where normally ventilation is sufficient to remove NO_x emitted by the current amount of motorized traffic. In contrast, influence of complex circulation patterns in Longyearbyen, formed by combination of the local wind from a narrow valley Longyeardalen and the synoptic scale wind steered along the axis of broader valley Adventdalen, and multiple stationary and mobile emission sources on the local air quality in the town deserve further investigation. Furthermore, the case study results reveal that ships emissions may have dramatic effect on NO_x concentration. Therefore, a summer field campaign, when the ship traffic in Svalbard is the most intensive, is necessary.

Conclusion

The NO_x measurement results from the three stations-network, Ny-Ålesund, Barentsburg and Longyearbyen, and O_3 data from two sites in Svalbard, Ny-Ålesund and Barentsburg, have been compared for the first time.

The diurnal pattern in concentration of NO_x at all three stations has been observed due to variable emissions from the local sources of NO_x . However, only data from Barentsburg and Adventdalen station show significant change in NO_2/NO_x ratio during the day, since the station in Ny-Ålesund is located close to a diesel power plant, a stationary source of fresh NO_x emissions contributing to higher NO concentration. Local emissions of NO_x in Ny-Ålesund and in Barentsburg may reduce O_3 concentrations in the settlements by a few percent from the background value due to ozone titration, but this does not occur very often, and there is no significant difference

in daytime and nighttime O₃ values measured in Barentsburg and at the Zeppelin station.

As expected, the large-scale wind is channelled by the local topographical features and this determines the wind direction and speed in all three settlements, and therefore the concentrations of NO_x measured at the stations correlate weakly. In Ny-Ålesund and Barentsburg, the stations are located in the way that downwind concentrations from the local sources are observed rarely, because the prevailing wind direction is different. The measurements in Adventdalen have been made downwind from the source, since both the snowmobile route and prevailing wind direction are along the valley. However, traffic is a temporary source of emissions and the mean wind speed in Adventdalen valley is high, and therefore mean NO_x concentrations there are low. Despite low correlation between the NO_x values from the three stations, there are common synoptic conditions that promote accumulation of local pollution in the settlements, namely, lower wind speed and air temperature and presence of temperature inversions. In contrast to NO_x, the concentrations of O₃ in Barentsburg and at the Zeppelin observatory are strongly correlated and depend on synoptic conditions that promote transport of air masses enriched or depleted in O₃. In other words, both these stations are regionally representative for O₃ measurements.

The measurements in Adventdalen reveal that the concentration of NO_x is highly dependent on the intensity of snowmobile traffic in the valley and prevailing meteorological conditions. Nevertheless, the highest concentrations of NO_x in Longyearbyen were measured during the case study at UNIS when a likely influence of the emissions from ships was revealed. The intensity of ships traffic in Svalbard region is highest in summer, thus, to investigate the magnitude of impact from ships emissions

on the local air quality, a new field campaign in Longyearbyen needs to be performed in that season.

Acknowledgements

Special thanks are given to Norwegian Polar Institute (NPI) and the University centre in Svalbard for the invaluable logistical assistance. Norwegian Institute for Air Research is acknowledged for the leasing of the equipment and technical support during the operation of the monitor. We would like to acknowledge Norwegian meteorological institute for the meteorological data from Ny-Ålesund available in the eklima.no database. NPI and the European Centre for Medium-Range Weather Forecasts are acknowledged for the map of Svalbard available at <http://svalbardkartet.npolar.no> and for data from the ERA5 global atmospheric reanalysis data set, accordingly. We would like to thank Dr. Marion Maturilli and Dr. Peter von der Gathen from the Alfred Wegener Institute Helmholtz Centre for Polar and Marine Research for processing and quality assurance of the radiosonde and ozone sonde data from Ny-Ålesund, respectively, and for the reviewing of current paper.

Funding

The measurements of NO_x in Adventdalen have been performed in frame the project 269953/E10 «Monitoring of nitrogen oxides from mobile and stationary sources at Svalbard» financed by the Arctic Field Grant funding established by Norwegian Research Council. The measurements of NO_x are performed by the NPI and NILU with a logistical support from Kings Bay AS in connection with the project «Limits of Acceptable Change» in Ny-Ålesund. Continuous O₃ measurements at the Zeppelin station are performed in the frame of the long-term programme for greenhouse gases monitoring and financed by NILU and Norwegian Environmental Agency. The measurements in Barentsburg have been done by AARI in the scope of the project «Air quality monitoring by automatic analysing stations in Barentsburg». The support from the Transregional Collaborative Research Center (TR 172) “Arctic Amplification: Climate Relevant Atmospheric and Surface Processes, and Feedback Mechanisms

(AC)3,” funded by the German Research Foundation (DFG, Deutsche Forschungsgemeinschaft) is acknowledged for the radiosonde data from Ny-Ålesund.

References

- AMAP/Quinn, P.K., Bates, T.S., Baum, E., Bond, T., Burkhardt, J.F. and co-authors. 2008. *The Impact of Short-Lived Pollutants on Arctic Climate*. AMAP Technical Report No.1. Arctic Monitoring and Assessment Programme (AMAP), Oslo, Norway.
- AMAP. 2006. *AMAP Assessment 2006: Acidifying Pollutants, Arctic Haze, and Acidification in the Arctic*. Arctic Monitoring and Assessment Programme (AMAP), Oslo, Norway.
- Arya S.P. 1999. *Air pollution meteorology and dispersion*. Oxford University press, New York, USA.
- Beine, H.J., Jaffe, D.A., Herring, J.A., Kelley, J.A., Krognes, T. and co-authors. 1997. High-Latitude Springtime Photochemistry. Part I: NO_x, PAN and Ozone Relationships. *J. Atmos. Chem.*, **27**, 127–153.
- Beine H.J., Jaffe, D.A., Stordal, F., Engardt, M., Solberg, S. and co-authors. 1997. NO_x during ozone depletion events in the arctic troposphere at Ny-Ålesund, Svalbard. *Tellus B*, **49** (5), 556–565. DOI: 10.1034/j.1600-0889.49.issue5.10.x
- Chalmer B.J. 1986. *Understanding Statistics*. Marcel Dekker Inc., New York, USA.
- Christiansen, B., Jepsen, N., Kivi, R., Hansen, G., Larsen, N. and co-authors 2017. Trends and annual cycles in soundings of Arctic tropospheric ozone. *Atmos. Chem. Phys.*, **17**, 9347–9364. DOI: 10.5194/acp-17-9347-2017.
- Dekhtyareva, A., Edvardsen, K., Holmén, K., Hermansen, O., and Hansson, H.-C. 2016. Influence of local and regional air pollution on atmospheric measurements in Ny-Ålesund. *Int. J. Sus. Dev. Plann.*, **11** (4), 578–587. DOI: 10.2495/SDP-V11-N4-578-587.
- Dekhtyareva, A., Holmén, K., Maturilli, M., Hermansen, O., and Graversen, R. 2018. Effect of seasonal mesoscale and microscale meteorological conditions in Ny-Ålesund on results of monitoring of long-range transported pollution. *Polar Res.*, **37** (1), 1508196. DOI: 10.1080/17518369.2018.1508196.
- Eckhardt, S., Hermansen, O., Grythe, H., Fiebig, M., Stebel, K. and co-authors. 2013. The influence of cruise ship emissions on air pollution in Svalbard – a harbinger

- of a more polluted Arctic? *Atmos. Chem. Phys.*, **13** (16), 8401–8409. DOI: 10.5194/acp-13-8401-2013.
- Esau, I. and Repina, I. 2012. Wind climate in Kongsfjorden, Svalbard, and attribution of leading wind driving mechanisms through turbulence-resolving simulations. *Adv. Meteorol.* Article ID 568454. DOI: 10.1155/2012/568454.
- Fan, S.-M. and Jacob, D.J. 1992. Surface ozone depletion in Arctic spring sustained by bromine reactions on aerosols. *Nature*, **359**, 522–524.
- Fischer, E. V., Jacob, D.J., Yantosca, R.M., Sulprizio, M.P., Millet, D.B. and co-authors. 2014. Atmospheric peroxyacetyl nitrate (PAN): a global budget and source attribution. *Atmos. Chem. Phys.*, **14**, 2679–2698. DOI: 10.5194/acp-14-2679-2014.
- Førland, E.J., Hanssen-Bauer, I., and Nordli, P.Ø. 1997. *Climate statistics and longterm series of temperature and precipitation at Svalbard and Jan Mayen*. Report No. 21/97 Klima, Norwegian Meteorological Institute, Oslo, Norway.
- Freud, E., Krejci, R., Tunved, P., Leaitch, R., Nguyen, Q.T. and co-authors. 2017. Pan-Arctic aerosol number size distributions: seasonality and transport patterns. *Atmos. Chem. Phys.*, **17**, 8101–8128. DOI: 10.5194/acp-17-8101-2017.
- Graversen, R.G. 2006. Do Changes in the Midlatitude Circulation Have Any Impact on the Arctic Surface Air Temperature Trend? *J. Climate*, **19**, 5422–5438. DOI: 10.1175/JCLI3906.1.
- Gröbner, J., Hülsen, G., Wuttke, S., Schrems, O., De Simone, S. and co-authors. 2010. Quality assurance of solar UV irradiance in the Arctic. *Photochem. Photobiol. Sci.*, **9** (3), 384–391. DOI: 10.1039/b9pp00170k.
- Hanssen-Bauer, I., Førland, E.J., Hisdal, H., Mayer, S., Sandø, A.B. and co-authors. 2019. *Climate in Svalbard 2100 – a knowledge base for climate adaptation*. NCCS report no. 1/2019. The Norwegian Centre for Climate Services, Norway.
- Hersbach, H. and Dee, D. 2016. ERA5 reanalysis is in production. *ECMWF newsletter*, (number 147), 7. Online at: <https://www.ecmwf.int/sites/default/files/elibrary/2016/16299-newsletter-no147-spring-2016.pdf>
- Immler, F.J., Dykema, J., Gardiner, T., Whiteman, D.N., Thorne, P.W. and co-authors. 2010. Reference quality upper-air measurements: Guidance for developing

- GRUAN data products. *Atmos. Meas. Tech.*, **3** (5), 1217–1231. DOI: 10.5194/amt-3-1217-2010.
- IPCC. 2013. *IPCC, 2013: Climate Change 2013: The Physical Science Basis. Contribution of Working Group I to the Fifth Assessment Report of the Intergovernmental Panel on Climate Change*. Cambridge University Press. Cambridge, United Kingdom and New York, NY, USA.
- Johnsrud, M., Hermansen, O., and Tørnkvist, K. 2018. *Air Quality in Ny-Ålesund. Monitoring of Local Air Quality 2016-2017*. NILU report 30/2018. NILU – Norwegian Institute for Air Research, Kjeller, Norway.
- Kimbrough, S., Chris, R. O., Snyder, M., and Richmond-Bryant, J. 2017. NO to NO₂ conversion rate analysis and implications for dispersion model chemistry methods using Las Vegas, Nevada near-road field measurements. *Atmos. Environ.*, **165** (2), 23–34. DOI: 10.1016/j.atmosenv.2017.06.027.
- Klima- og miljødepartementet. 2001. Lov om miljøvern på Svalbard (svalbardmiljøloven) [Law about environmental protection in Svalbard (Svalbard environmental law)]. Online at: <https://lovdata.no/dokument/NL/lov/2001-06-15-79>
- Li, J., Reiffs, A., Parchatka, U., and Fischer, H. 2015. In situ measurements of atmospheric CO and its correlation with NO_x and O₃ at a rural mountain site. *Metrol. Meas. Syst.*, **XXII** (1), 25–38. DOI: 10.1515/mms-2015-0001.
- Lilliefors, H.W. 1967. On the Kolmogorov-Smirnov Test for Normality with Mean and Variance Unknown. *J. Am. Stat. Assoc.*, **62** (318), 399–402. DOI: 10.2307/2283970.
- Liu, X., Sun, H., Feike, T., Zhang, X., Shao, L. and co-authors. 2016. Assessing the impact of air pollution on grain yield of winter wheat - A case study in the North China Plain. *PLoS ONE*, **11** (9), e0162655. DOI: 10.1371/journal.pone.0162655
- Maturilli, M. 2017a. High resolution radiosonde measurements from station Ny-Ålesund (2017-04). *Alfred Wegener Institute - Research Unit Potsdam, PANGAEA*. Online at: <https://doi.pangaea.de/10.1594/PANGAEA.879767>
- Maturilli, M. 2017b. High resolution radiosonde measurements from station Ny-Ålesund (2017-05). *Alfred Wegener Institute - Research Unit Potsdam, PANGAEA*. Online at: <https://doi.org/10.1594/PANGAEA.879820>

- Maturilli, M., Herber, A., and König-Langlo, G. 2013. Climatology and time series of surface meteorology in Ny-Ålesund, Svalbard. *Earth Syst. Sci. Data*, **5** (1), 155–163. DOI: 10.5194/essd-5-155-2013.
- Maturilli, M. and Kayser, M. 2016. Arctic warming, moisture increase and circulation changes observed in the Ny-Ålesund homogenized radiosonde record. *Theor. Appl. Climatol.*, **130**, 1–17. DOI: 10.1007/s00704-016-1864-0.
- Monks, P.S. 2005. Gas-phase radical chemistry in the troposphere. *Chem. Soc. Rev.*, **34**, 376–395. DOI: 10.1039/b307982c.
- MOSJ. 2018. Antall registrerte snøskutere [Number of registered snowmobiles]. *MOSJ (Miljøovervåking Svalbard og Jan Mayen)*. Online at: <http://www.mosj.no/no/pavirkning/ferdsel/snoskuter.html>.
- Porter, W.C., Heald, C.L., Cooley, D., and Russell, B. 2015. Investigating the observed sensitivities of air-quality extremes to meteorological drivers via quantile regression. *Atmos. Chem. Phys.*, **15**, 10349–10366. DOI: 10.5194/acp-15-10349-2015.
- Reimann, S., Kallenborn, R., and Schmidbauer, N. 2009. Severe aromatic hydrocarbon pollution in the Arctic town of Longyearbyen (Svalbard) caused by snowmobile emissions. *Environ. Sci. Technol.*, **43** (13), 4791–4795. DOI: 10.1021/es900449x.
- Roberts–Semple, D., Song, F., and Gao, Y. 2012. Seasonal characteristics of ambient nitrogen oxides and ground–level ozone in metropolitan northeastern New Jersey. *Atmos. Pollut. Res.*, **3** (2), 247–257. DOI: 10.5094/APR.2012.027.
- Schmalwieser, A.W., Gröbner, J., Blumthaler, M., Klotz, B., De Backer, H. and co-authors. 2017. UV Index monitoring in Europe. *Photochem. Photobiol. Sci.*, **16**, 1349–1370. DOI: 10.1039/c7pp00178a.
- Seinfeld, J.H. and Pandis, S.N. 2006. *Atmospheric Chemistry and Physics: From Air Pollution to Climate Change*. 2nd ed. John Wiley and Sons, Inc., New York, USA.
- Shears, J., Theisen, F., Bjørndal, A., and Norris, S. 1998. *Environmental impact assessment. Ny-Ålesund international scientific research and monitoring station, Svalbard*. Norwegian Polar Institute, Tromsø, Norway.

- Simpson, W.R., Brown, S.S., Saiz-Lopez, A., Thornton, J.A., and Von Glasow R. 2015. Tropospheric Halogen Chemistry: Sources, Cycling, and Impacts. *Chem. Rev.*, **115** (10), 4035–4062. DOI: 10.1021/cr5006638.
- Stein, A.F., Draxler, R.R., Rolph, G.D., Stunder, B.J.B., Cohen, M.D. and co-authors. 2015. NOAA's HYSPLIT atmospheric transport and dispersion modeling system. *BAMS*, (February), 2059–2077. DOI: 10.1175/BAMS-D-14-00110.1.
- Su, X., Gough, W., and Shen, Q. 2016. Correlation of PM 2.5 and meteorological variables in Ontario cities: statistical downscaling method coupled with artificial neural network. *WIT Trans. Ecol. Envir.*, **207**, 215–226. DOI: 10.2495/AIR160201.
- Tennbakk, B., Fiksen, K., Borsche, T., Grøndahl, R., Jarstein, S. and co-authors. 2018. *Alternativer for framtidig energiforsyning på Svalbard*. [Alternatives for future energy supply in Svalbard]. THEMA-Rapport 2018-09, THEMA Consulting Group, Oslo, Norway.
- Vestreng, V., Kallenborn, R., and Økstad, E. 2009. *Climate influencing emissions, scenarios and mitigation options at Svalbard*. Klima- og forurensningsdirektoratet, Oslo, Norway.
- Wallace, J.M. and Hobbs, P. V. 2006. *Atmospheric science: an introductory survey*. 2nd ed. Academic Press, New York, USA.
- Wessel, S., Aoki, S., Winkler, P., Weller, R., Herber, A. and co-authors. 1998. Tropospheric ozone depletion in polar regions A comparison of observations in the Arctic and Antarctic. *Tellus B*, **50** (1), 34–50. DOI: 10.3402/tellusb.v50i1.16020.
- Williams, E.J., Fehsenfeld, F.C., Jobson, B.T., Kuster, W.C., Goldan, P.D. and co-authors. 2006. Comparison of Ultraviolet Absorbance, Chemiluminescence, and DOAS Instruments for Ambient Ozone Monitoring. *Environ. Sci. Technol.*, **40** (18), 5755–5762. DOI: 10.1021/es0523542.

Table 1. Measurement results from Adventdalen, Barentsburg and Ny-Ålesund. Pairs with significant ($p < 0.05$) t- and WRS-test results are shown with bold font.

Compound and station	Daytime mean value, $\mu\text{g}\cdot\text{m}^{-3}$	Nighttime mean value, $\mu\text{g}\cdot\text{m}^{-3}$	p-value, t-test*	Daytime median value, $\mu\text{g}\cdot\text{m}^{-3}$	Nighttime median value, $\mu\text{g}\cdot\text{m}^{-3}$	p-value, WRS-test**
NO, Adventdalen	0,40	-0,02	0,000	0,15	-0,02	0,000
NO ₂ , Adventdalen	1,79	0,78	0,000	0,94	0,53	0,000
NO ₂ /(NO+NO ₂), Adventdalen	0,80	0,83	0,009	0,82	0,85	0,000
NO, Barentsburg	0,19	0,10	0,000	0,04	0,01	0,000
NO ₂ , Barentsburg	0,74	1,03	0,068	0,00	0,00	0,099
NO ₂ /(NO+NO ₂), Barentsburg	0,72	0,80	0,000	0,78	0,89	0,000
O ₃ , Barentsburg	71,12	69,47	0,139	74,50	71,33	0,051
NO, Ny-Ålesund	1,61	0,65	0,001	0,18	0,03	0,000
NO ₂ , Ny-Ålesund	1,56	0,63	0,000	0,29	0,05	0,000
NO ₂ /(NO+NO ₂), Ny-Ålesund	0,61	0,63	0,369	0,64	0,63	0,335
O ₃ , Zeppelin	70,95	72,12	0,203	74,20	76,40	0,057

*two-sided t-test compares daytime and nighttime concentrations at each station and checks if there is a significant difference in mean values for these two groups

**two-sided WRS-test compares daytime and nighttime concentrations at each station and checks if there is a significant difference in median values for these two groups

Table 2. Spearman partial correlations of NO, NO₂, O₃ and local meteorological parameters from Adventdalen, Barentsburg and Ny-Ålesund.

The significant correlations with $p < 0.05$ and absolute r-value ≥ 0.10 are shown with bold font.

Compound and station	Wind speed		Atm. temperature		Relative humidity		UV-A		UV-B	
	r-value	p-value	r-value	p-value	r-value	p-value	r-value	p-value	r-value	p-value
NO, Adventdalen	-0,22	<0.001	-0,11	<0.001	-0,01	0,791	0,11	<0.001	-0,07	0,017
NO ₂ , Adventdalen	-0,33	<0.001	-0,06	0,021	0,05	0,067	0,10	0,001	-0,09	0,001
NO, Barentsburg	-0,05	0,064	0,23	<0.001	0,10	0,001	-	-	-	-
NO ₂ , Barentsburg	-0,26	<0.001	0,26	<0.001	0,19	<0.001	-	-	-	-
O ₃ , Barentsburg	-0,09	0,002	0,47	<0.001	-0,19	<0.001	-	-	-	-
NO, Ny-Ålesund	-0,11	<0.001	-0,26	<0.001	-0,05	0,099	<0.01	0,907	0,03	0,309
NO ₂ , Ny-Ålesund	-0,33	<0.001	-0,31	<0.001	-0,05	0,068	0,04	0,181	-0,03	0,293
O ₃ , Zeppelin	0,07	0,018	0,46	<0.001	-0,30	<0.001	0,03	0,295	-0,08	0,005



Figure 1. Map of Svalbard with three settlements where the NO_x have been measured in spring 2017.

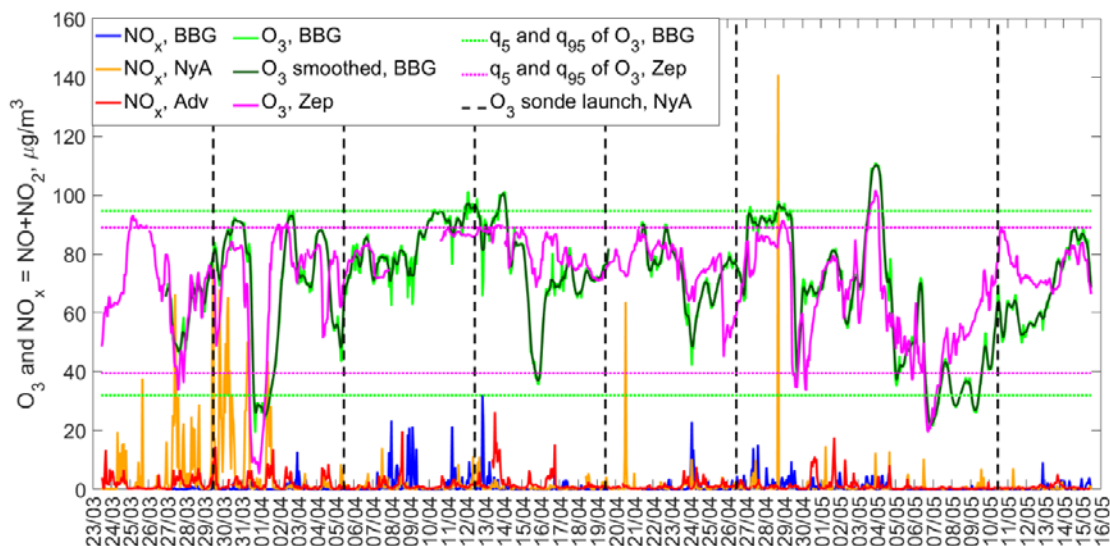


Figure 2. Time series of NO_x and O_3 concentrations from the measurement campaign. NO_x concentrations in Barentsburg, Ny-Ålesund and Adventdalen are shown with solid blue, orange and red lines, respectively. Original and smoothed O_3 concentration in Barentsburg are illustrated with light green and dark green solid lines, while O_3 concentration at the Zeppelin station is represented by solid purple line. Dotted light green and purple lines show the 5th and 95th quantiles limits of O_3 concentrations in Barentsburg and at the Zeppelin station, respectively. The dashed black line represents timing of the O_3 sounding in Ny-Ålesund.

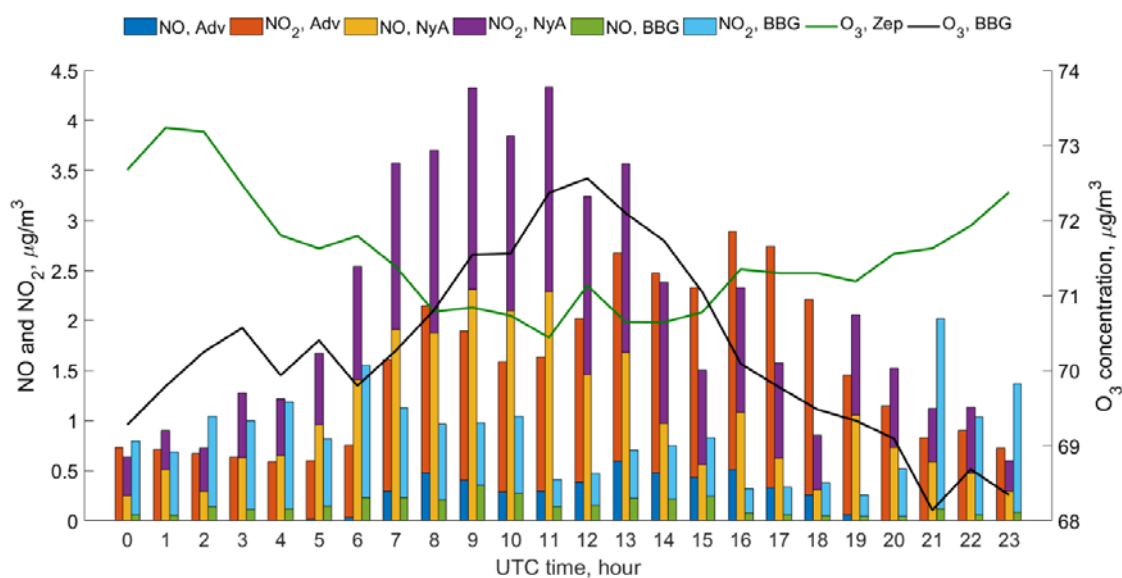


Figure 3. Variation of measured NO , NO_2 and O_3 concentrations depending on the time of the day (in UTC) in Adventdalen (Adv), Ny-Ålesund (NyA) and Barentsburg stations (BBG).

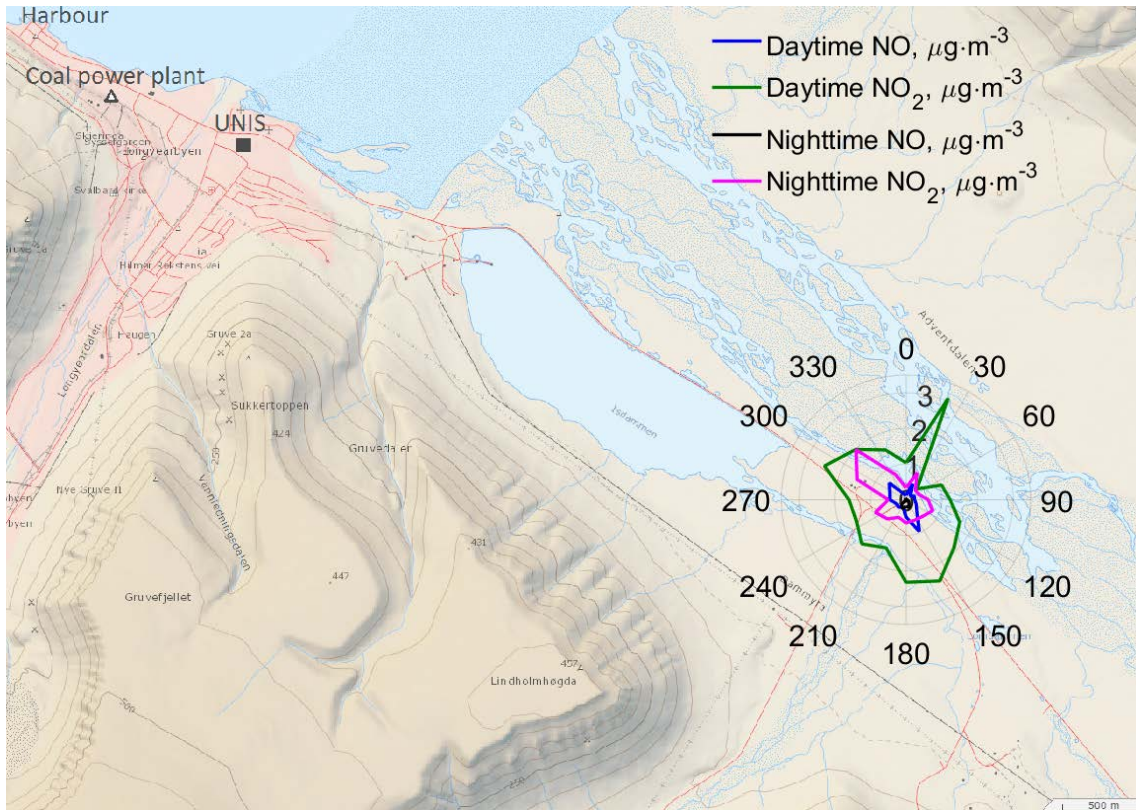


Figure 4. Distribution of average NO and NO₂ concentrations over wind directions in daytime and nighttime at the station in Adventdalen.

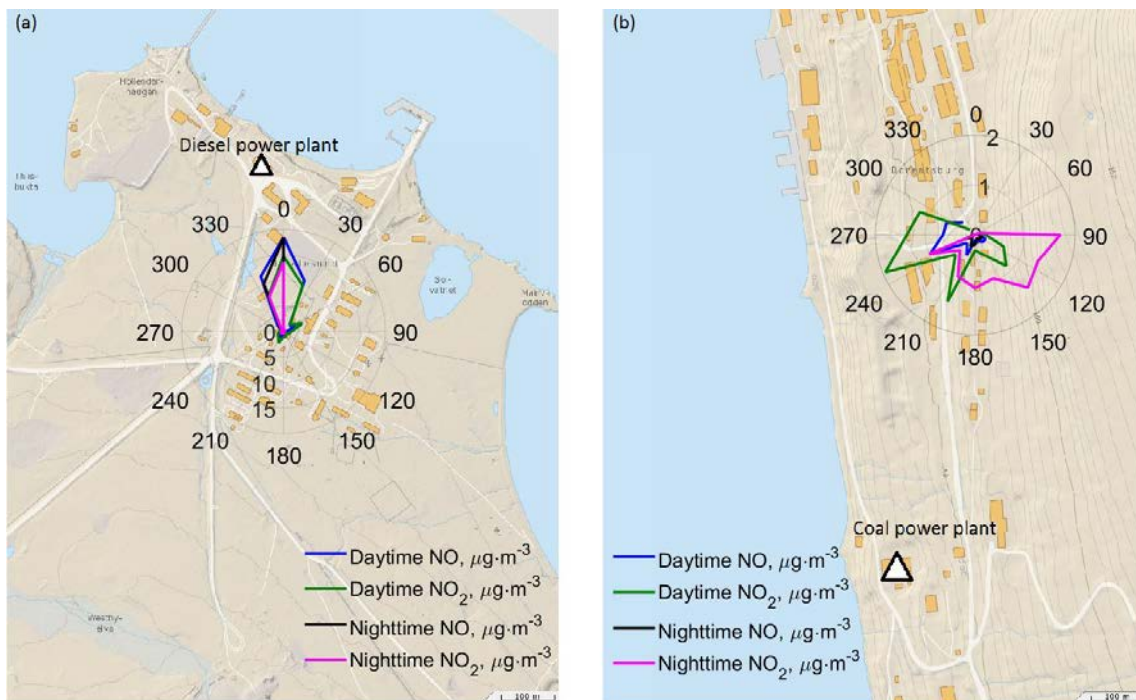


Figure 5. Distribution of average NO and NO₂ concentrations over wind directions in daytime and nighttime at the stations in Ny-Ålesund (a) and Barentsburg (b).

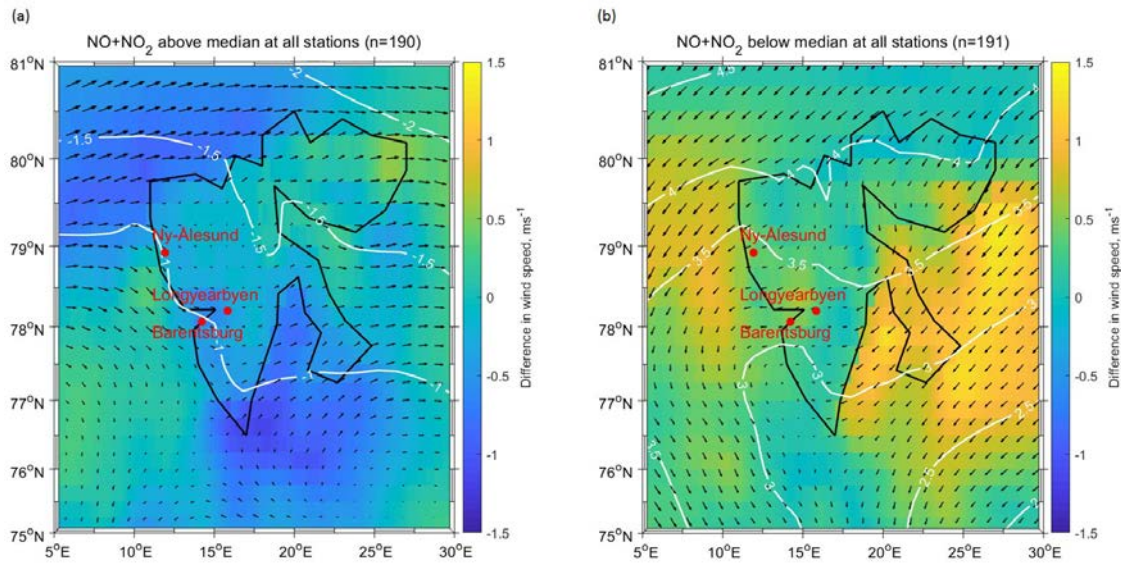


Figure 6. Mean deviation of the meteorological parameters from the mean for the whole field campaign based on the surface ERA5 data: a) for hours when the sum of NO and NO₂ concentrations were above median at all stations; b) hours when the sum of NO and NO₂ concentrations were below or equal to median at all stations. The colour scale show mean deviation of wind speed for each grid cell, the mean deviation of sea level pressure in hPa is shown by white contour lines. The black arrows represent mean deviation of wind direction and have the length relative to the difference in wind speed. They are plotted with resolution of 1° of longitude and 0.5° of latitude.

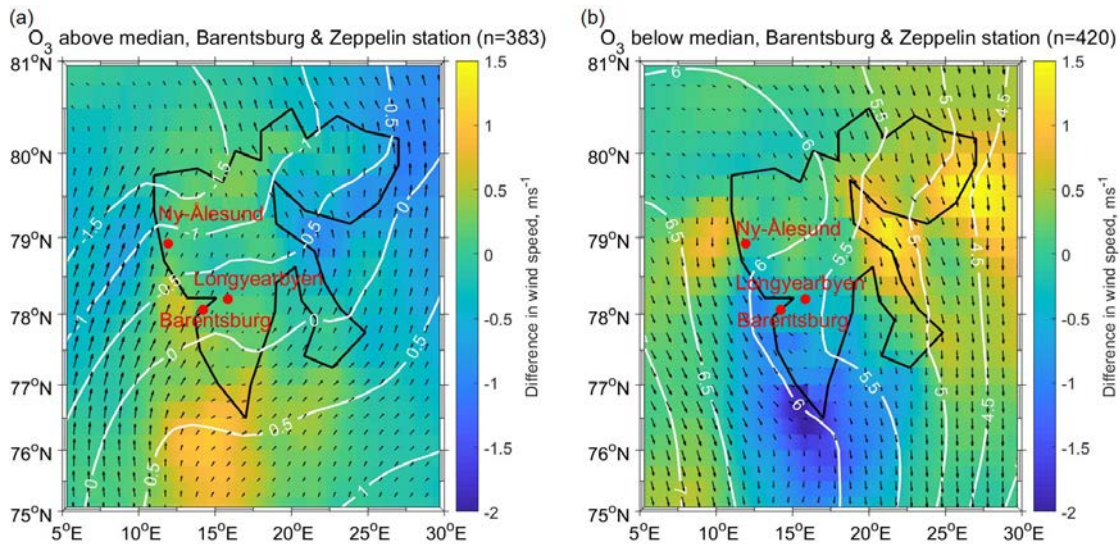


Figure 7. Mean deviation meteorological parameters from the mean for the whole field campaign based on the surface ERA5 data: a) for hours when O₃ concentrations were above median in Barentsburg and at the Zeppelin station; b) hours when O₃ concentrations were below or equal to median in Barentsburg and at the Zeppelin station. For detailed description of lines in the figure, see Fig. 6.

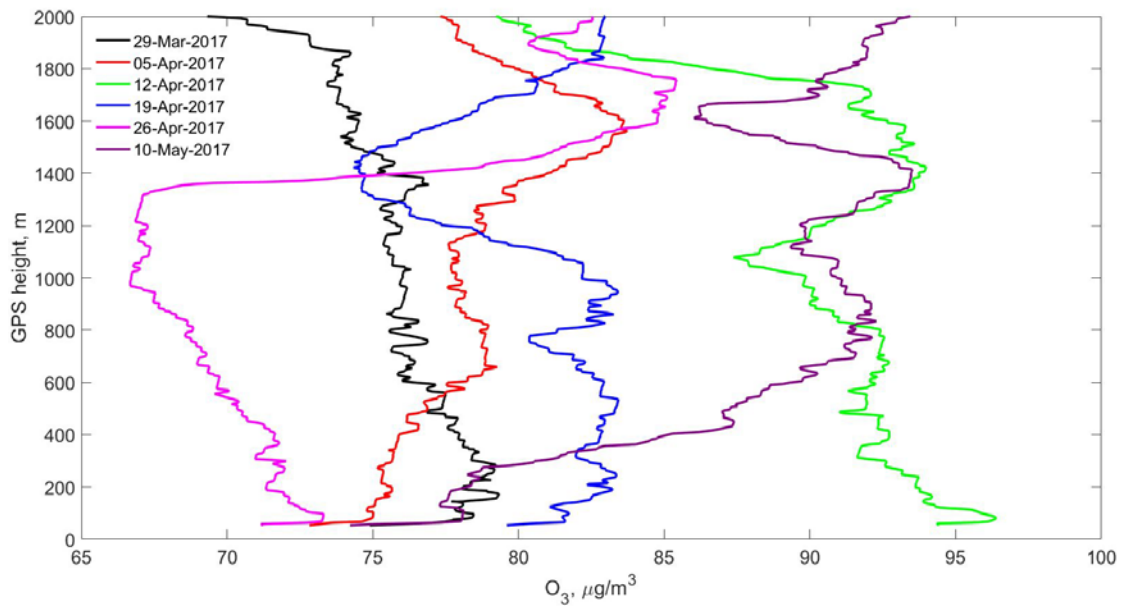


Figure 8. Ozone sonde data from Ny-Ålesund.

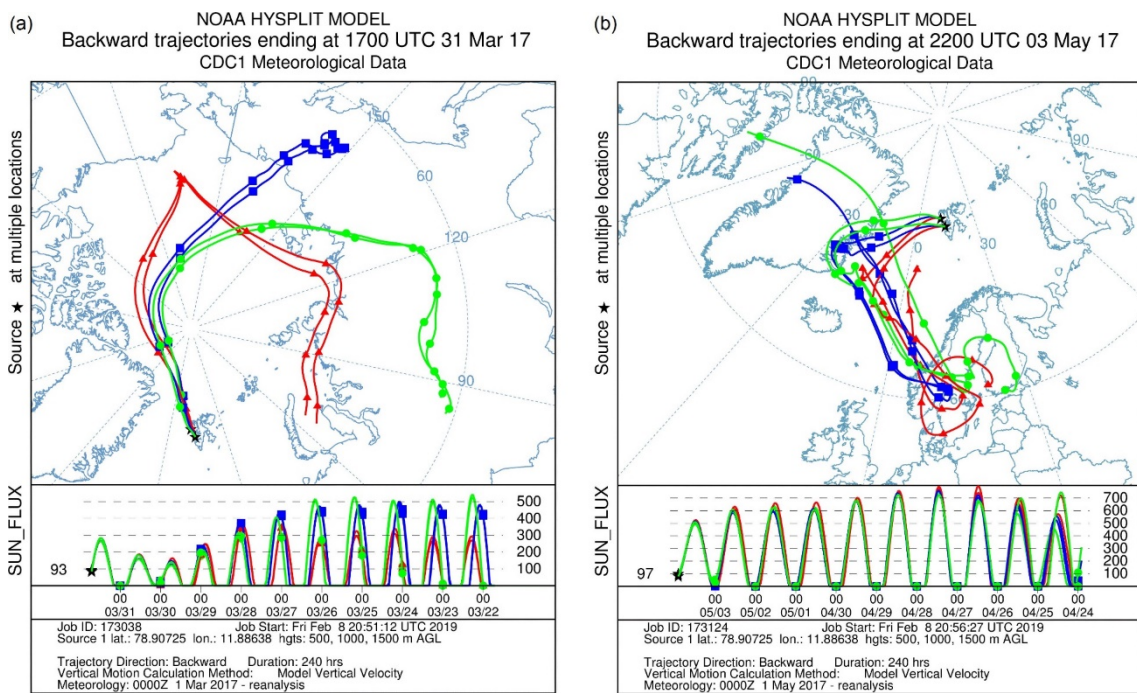


Figure 9. Air mass backward trajectories for the strongest O_3 depletion (a) and O_3 increase (b) events detected both in Barentsburg and at the Zeppelin station.

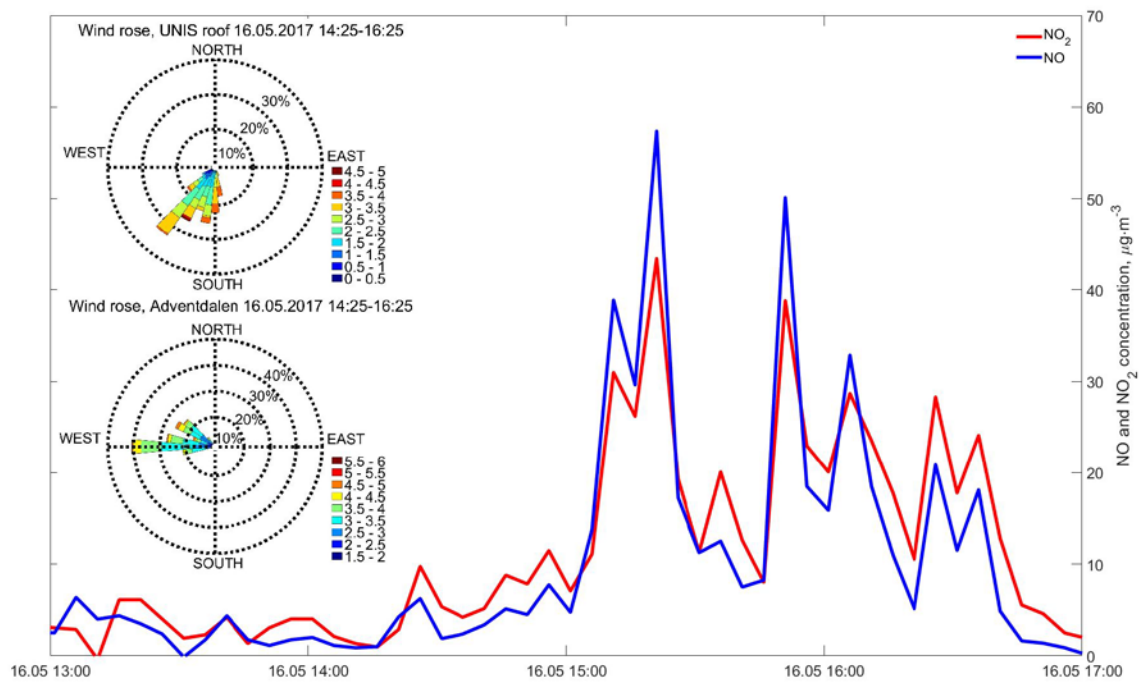


Figure 10. NO_x measurements at UNIS in Longyearbyen (wind roses for the measurements at UNIS roof and in Adventdalen are shown in the upper left and lower left corners of the figure, respectively).

Paper IV



Summer air pollution in Svalbard: emission sources, meteorology and air quality

Alena Dekhtyareva^{a*}, T.Drotikova^b, A. Nikulina^c, O. Hermansen^d, D. G. Chernov^e, D.Mateos^f, M. Herreras^f, C. Petroselli^g, L. Ferrero^h, A. Gregoričⁱ

^aDepartment of Engineering and Safety, Faculty of Engineering and Technology, UiT The Arctic University of Norway, Tromsø, Norway, ORCID iD (<http://orcid.org/0000-0003-4162-7427>); ^bDepartment of Arctic Technology, The University Centre in Svalbard, Norway; ^cDepartment of Research Coordination and Planning, Arctic and Antarctic Research Institute, Saint Peterburg, Russia; ^dDepartment of Monitoring and Information Technology, NILU - Norwegian Institute for Air Research, Kjeller, Norway; ^eLaboratory of Aerosol Optics, Division of the Radiation Components of the Climate, V.E. Zuev Institute of Atmospheric Optics of Siberian Branch of the Russian Academy of Science, Tomsk, Russia; ^fDepartment of Theoretical Physics, Atomic and Optics, Atmospheric Optics group, University of Valladolid, Valladolid, Spain; ^gDepartment of Chemistry, Biology and Biotechnology, University of Perugia, Perugia, Italy; ^hDepartment of Environment and Earth Sciences, The University of Milano-Bicocca, Milan, Italy; ⁱDepartment of Research & Development, Aerosol d.o.o., Ljubljana, Slovenia

Abstract

Air quality observations have been performed in three major settlements in Svalbard in summer 2018. The hourly concentrations of BC, SO₂, NO_x and O₃ and meteorological parameters has been measured at the ground-based stations in all sites and daily filter samples for PAH analysis have been collected in Longyearbyen. In addition to this, airborne meteorological measurements using radiosonde and tethered balloon have been performed in Ny-Ålesund and Longyearbyen. Increase of the local SO₂ and NO_x concentrations and titration of tropospheric O₃ due to ship emissions was observed in Longyearbyen and Ny-Ålesund. Extremely high concentrations of SO₂ and BC were observed in Barentsburg due to specific meteorological conditions leading to transport of the polluted air from the local coal power plant to the town. The combined influence of local and long-range transported air pollution was observed in Longyearbyen during the episodes of warm air advection over Svalbard, during which the air enriched in CO and O₃ was brought from mid-latitudes, and the conditions favourable for accumulation of local pollution near the ground were created simultaneously.

Introduction

Long-range transport of air pollution is a phenomenon often prevailing during winter and spring seasons in Svalbard [1], [2]. Although exceptional transport events may take place in summer as well [3], the background concentrations of air pollutants are typically low during that season [4]. However, local pollution sources such as ships become increasingly important in summer months [5], [6].

The two biggest settlements in Svalbard, Longyearbyen and Barentsburg, are located in Adventfjorden and Grønfjorden, the eastern and southern branches, respectively, of the wide fjord Isfjorden (Fig. 1a). The third biggest settlement, Ny-Ålesund, is situated in the north-western part of Svalbard in the narrow fjord Kongsfjorden. Although stricter regulations to the quality of the ships' fuel used in Svalbard have been applied, so that it is currently restricted to use heavy fuel oil in Kongsfjorden, Isfjorden remains the area where it is still allowed to use oil with maximum sulphur content 3.5% [7].

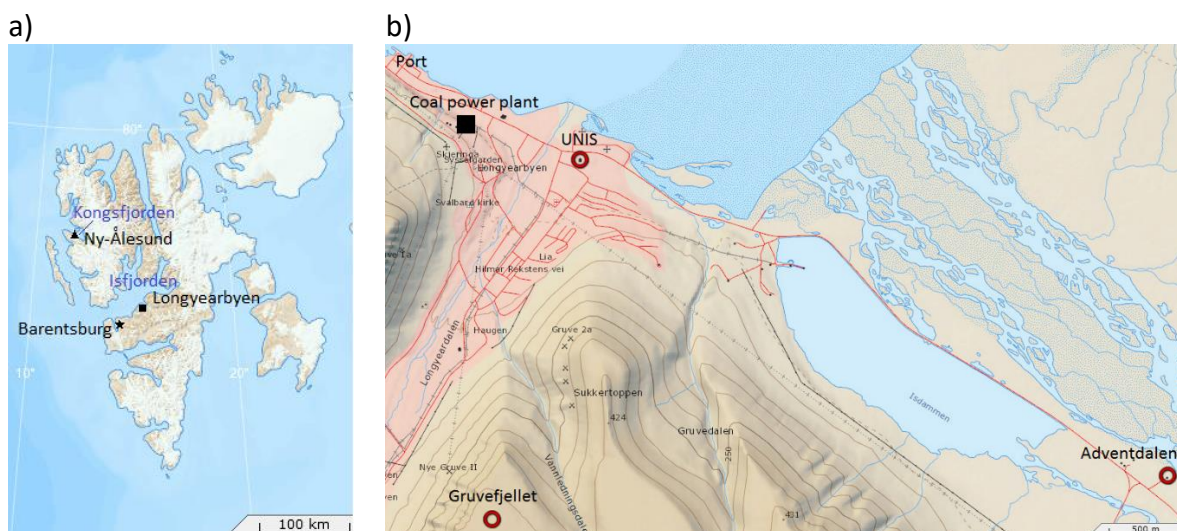


Figure 1 a) Map of Svalbard; b) local map of Longyearbyen

Number of cruise and expedition ships' passengers visiting the port of Longyearbyen (Fig. 1b) has increased by almost 60% (from 37085 to 59150) for the period from 2006 to 2017 and shows positive trend for these years ($R^2=0.76$) [8]. The traffic intensifies in summer because the cruise ships and transport vessels arrive to Longyearbyen more often than in other seasons. Furthermore, westerly winds with low wind speed are more often observed in summer, which may lead to accumulation of the pollution in the settlement [5]. Observations of nitrogen oxides performed in spring 2017 [9], indicate that ships currently may be the most significant point sources of nitrogen oxides ($\text{NO}_x = \text{NO} + \text{NO}_2$) in Longyearbyen. Previous studies have shown that the ship traffic is a substantial source of NO_x , sulphur dioxide (SO_2), black carbon (BC), particulate matter (PM) and polycyclic aromatic hydrocarbons (PAHs) in

Svalbard [5], [6], [10], [11], however, previously no measurements have been done in Longyearbyen to assess the influence of this emission source on the air quality in town. An overview of emissions from stationary sources, coal and diesel power plants [12]–[14] in Svalbard settlements, is given in Table 1. The data for Longyearbyen and Barentsburg are taken from the Norwegian emission database for 2017 [15], [16], while emissions in Ny-Ålesund are calculated based on the environmental impact assessment report published in 1998 [12]. Since no emission treatment system has been installed on the power plant in Ny-Ålesund, and the average diesel fuel consumption from 2001 to 2013 [17] was almost the same as reported in 1998, around 1000m³ per year, we assume that emission quantities have not changed dramatically. The PM for Ny-Ålesund in the Table 1 stands for soot, and we assume that PM emissions from the diesel power plant mainly consist of soot agglomerates. Indeed, previous studies of plume samples from diesel aggregates installed in two other Svalbard settlements, Pyramiden and Svea, revealed that soot is the dominating component in PM there. In contrast, PM from power plants in Longyearbyen and Barentsburg consists of fly ashes, soot and secondary aerosol [18]. The coal power plant in Barentsburg is currently the biggest stationary source of PM and NO_x in Svalbard and is the largest point source of SO₂ in Norway [15]. Emissions from the coal power plant in Longyearbyen decreased dramatically after installation of new emission treatment system in 2015 [16]. However, there are also several reserve generators in Longyearbyen, and total diesel consumption there was 419 tons in 2018 [16].

Table 1 NO_x, SO₂ and PM emissions from the stationary sources in three major settlements in Svalbard

Settlement	Compound, tons/year		
	NO _x	SO ₂	PM
Longyearbyen coal power plant	85.61	0.035	1.49
Barentsburg coal power plant	153.8	2233.06	177.92
Ny-Ålesund diesel generators	35.04	6.14	2.98

NO_x emissions have complex climate effect. The lifetime of CH₄ and other greenhouse gases is shortened by OH-radicals formed in the reaction between NO and hydroperoxyl radical HO₂, but NO_x also are precursors for the formation of tropospheric ozone (O₃), a short-lived greenhouse gas and strong oxidant [19]. Arctic vegetation is especially vulnerable to negative effects from air pollution, since, in addition to stresses, which local ecosystems exhibit due to climate change, long photoperiods characteristic for high-latitudes summers intensify foliar

injury caused by elevated levels of O₃ [20], [21].

The primary and secondary anthropogenic aerosols may have different climate effect. Primary aerosols containing BC are light absorbing and have positive radiative forcing. Moreover, BC deposited on snow covered surfaces such as glaciers reduces surface albedo dramatically and intensify melting [19]. In contrast, NO_x and SO₂ are oxidized to sulphate and nitrate, respectively, in the atmosphere, leading to an increase in number of secondary aerosol particles, which have direct effect on the amount of solar radiation reaching the surface and an indirect climatic effect as they are important for the formation of clouds and affect clouds' physical properties [22]. In addition to climate influence, high ground-level concentration of BC containing aerosol has strong negative impact on human health, partly due to carcinogenic effect of the PAHs and other chemical compounds of varying toxicity absorbed onto the fine particles emitted in the process of fossil fuel burning [23], [24].

Meteorological conditions affect air quality in the settlements. Temperature inversions and low wind speed reduce the efficiency of pollutant dispersion and may lead to accumulation of air pollutants close to the ground. The frequency of inversion occurrence is lowest in summer, however, this season is characterized by lowest median wind speed, therefore adverse weather conditions for dispersion of pollutants may occur as well [4], [9].

The main aim of this study is to assess summer levels of air pollutants in the three major Svalbard settlements, identify influence of dominant emission sources on local air quality and define the atmospheric conditions promoting accumulation of air pollutants in cases when elevated concentrations have been observed.

Following research questions have been stated:

1. How do major local stationary emission sources affect air quality in Svalbard settlements in summer?
2. What is the current influence of ship traffic on air quality in Longyearbyen and Ny-Ålesund?
3. What is the influence of synoptic-scale meteorology on accumulation of local pollution in the settlements and what conditions prevail during the long-range transport of air pollutants to Svalbard in summer? Is it possible to separate these weather regimes?
4. What affects the vertical structure of summer atmospheric boundary layer (ABL) in Adventdalen (Longyearbyen) and Ny-Ålesund? How is the vertical local ABL structure related to the distribution of air pollutants in Adventdalen?

Methods

Ground-based measurements in Longyearbyen, Barentsburg and Ny-Ålesund

The seven channels aethalometer, NO_x, SO₂ and O₃ analysers (UNIS in Fig. 1b), instrument numbers 1-4 in Table 2) were placed in the office at the third floor at the University Centre in Svalbard (UNIS), where the inlet of the sampling hose was fixed outside from the window.

Table 2 Measurements in Longyearbyen

N	Instrument, Model	Measurement	Period	Data owner
1	Aethalometer, AE33	Equivalent aerosol concentration at 7 wavelength	26.06.18-16.08.18	Aerosol d.o.o.
2	NO _x Chemiluminescence analyser, T200	NO, NO ₂ , NO _x concentration	26.06.18-16.08.18	UiT The Arctic University of Norway (UiT)
3	UV Fluorescence SO ₂ , T100	SO ₂ concentration	26.06.18-16.08.18	UiT
4	Photometric O ₃ analyser, T400	O ₃ concentration	26.06.18-16.08.18	UiT
5	TE-PUF Poly-Urethane Foam High Volume Air Sampler	16 PAH concentrations from 12 discrete samples	14.07.18-24.09.18	The University Centre in Svalbard (UNIS)
6	Automatic Sun Tracking Photometer CE 318	Aerosol optical depth, angstrom exponent, precipitable water	17.07.18-13.08.18	The University of Valladolid (UVa)
7	The Kestrel 5500 Weather Meter	Temperature, relative humidity, pressure, wind speed, wind direction	26.06.18-16.08.18	UiT
8	Automatic weather stations	Temperature, relative humidity, pressure, wind speed, wind direction	26.06.18-16.08.18	UNIS
9	Vaisala, TTS111, tethered balloon	Temperature, relative humidity, pressure, wind speed, altitude	03.07.18-15.08.18	UiT
10	Microaethalometer, AE51, tethered balloon	Equivalent aerosol concentration at 880 nm	03.07.18-15.08.18	The University of Perugia
11	Miniature Diffusion Size Classifier, MiniDISC, tethered balloon	Particle number concentration	06.07.18-11.08.18	The University of Milan-Bicocca

The SO₂ and NO_x monitors have been calibrated *in-situ* with use of zero-air generator and standard SO₂ and NO gases with concentration of 361 ppb and 777ppb, respectively. The clean air test and the size selective inlet inspection and cleaning were performed on the aethalometer once a month. The O₃ monitor was weekly calibrated online by the technical personnel from the Norwegian Institute for Air Research.

Since the nearest automatic weather stations were located few kilometres away, at the Svalbard airport and nearby the UNIS CO₂ lab in Adventdalen, the portable environmental meter Kestrel 5500 Pocket Weather Tracker was installed at the UNIS roof to obtain local meteorological data (UNIS in Fig. 1b); number 7 in Table 2). The meteorological data from the two automatic weather stations operated routinely by UNIS (Adventdalen and Gruvefjellet in Fig. 1b); number 8 in Table 2) have been used for comparison with tethered balloon measurements and ERA5 data.

In addition to BC, SO₂ and NO_x, fossil fuel burning elevates the concentrations of PAHs [25], and therefore 15 daily filter samples were collected for PAH analysis during the days when big ships were present in Longyearbyen, and 5 samples after the measurement campaign in autumn 2018. Before the sampling, the GE Whatman (101.6 mm) quartz microfiber filters were heated for 6 h at 450 °C to remove any potential organic contamination, wrapped in aluminium foil, sealed in polyethylene bags, and stored in desiccator until deployed in the air sampler. Air samples were collected on the filters by use of a high-volume sampler (TISCH-1000 by Tisch Environmental, Inc., USA; about 14 m³·h⁻¹) on a roof of UNIS at 24 m height in 0.9 and 1.2 km distances from a coal-fired power plant and a cruise ship port, respectively, in July-September 2018. Sampling duration was approximate 24 hours. Total volume of each sample was about 330 m³. After collection, filters were wrapped in aluminium foil, sealed in polyethylene bags, and stored at -20 °C until the analysis was done. One field blank was performed every five samples.

BC is emitted by the same pollution sources as PAH. Moreover, the surface of BC particles is porous and has high surface to volume ratio, and thus works as an effective adsorbent for non-polar substances such as PAHs [26]. The available laboratory resources are limited, and therefore, two-step procedure has been implemented to choose seven filter samples with potentially high concentration of PAH out of 15, which had been collected during summer 2018:

- 1) Average concentrations of BC have been calculated for the periods when the filter samples have been installed at the UNIS roof.
- 2) Days when BC concentrations were higher than the average daily value for the campaign period have been chosen.

The difference in PAHs composition is expected between the samples taken from 14th July 2018 to 26th July 2018, since the reserve diesel generator was a source of energy in Longyearbyen, while during other days the energy in Longyearbyen was produced only by the coal power plant. In addition to meteorological measurements and PAH sampling, sun

photometer has been installed at the UNIS roof.

SO₂, NO_x, O₃ and meteorological measurements (AARI in Fig. 2a; instruments number 1,2, 3 and 4 in Table 3) were performed in Barentsburg at the same station as during the spring measurement campaign in 2017 [9].

Table 3 Measurements in Barentsburg

N	Instrument, Model	Measurement	Period	Data owner
1	NO _x Chemiluminescence analyser, AC32M Environnement S.A.	NO concentration	01.06.18-31.08.18	Arctic and Antarctic Research Institute (AARI)
2	UV Fluorescence SO ₂ , AF22M Environnement S.A.	SO ₂ concentration	01.06.18-31.08.18	AARI
3	UV Photometric O ₃ analyser, O342 Environnement S.A.	O ₃ concentration	01.06.18-31.08.18	AARI
4	Portable Vaisala weather station, WXT20 Vaisala	Temperature, relative humidity, pressure, wind speed, wind direction	01.06.18-31.08.18	AARI
5	Aethalometer, MDA-02 IAO SB RAS	Equivalent aerosol concentration at the wavelengths of 460, 530, 590, and 630 nm	01.06.18-31.08.18	V.E. Zuev Institute of Atmospheric Optics of Siberian Branch of the Russian Academy of Science (IAO SB RAS)
6	Automatic Sun Tracking Photometer SP-9 IAO SB RAS	Aerosol optical depth, angstrom exponent, precipitable water	01.06.18-31.08.18	IAO SB RAS

AARI personell calibrated SO₂ and NO_x monitors 29.06.2018 and 04.08.2018 using standard SO₂ and NO gases with concentrations of 100ppb and the monitors' internal zero-air generator. In addition to this, on the 8th of August 2018, the UiT personnel calibrated the Barentsburg instruments using the same standard SO₂ and NO gases as in Longyearbyen. The calibration revealed that the NO and SO₂ data were correct, however, the conversion of NO to NO₂ was not functioning properly. Therefore, only NO and SO₂ data from Barentsburg have been used for further analysis.

The aethalometer MDA-02 and sun photometer SP-9 IAO SB RAS are installed in another building located 300m to the south from the first station, closer to the coal power plant (IAO SB RAS in Fig. 2a; instruments number 5 and 6). The measurement principle of the aethalometer developed by IAO SB RAS is described in [27] and [28]. The black carbon

concentrations were obtained from the 530nm channel data of the MDA-02 aethalometer, thus they were compared with AE33 data from Longyearbyen measured at closest wavelength of 520nm. The influence of local pollution on sun photometer data in Barentsburg has been eliminated by the data screening and removal of the values obtained during the episodes when prevailing wind was from coal power plant, while data from aethalometer are utilized unchanged in order to investigate the effect of local emission sources on air quality.

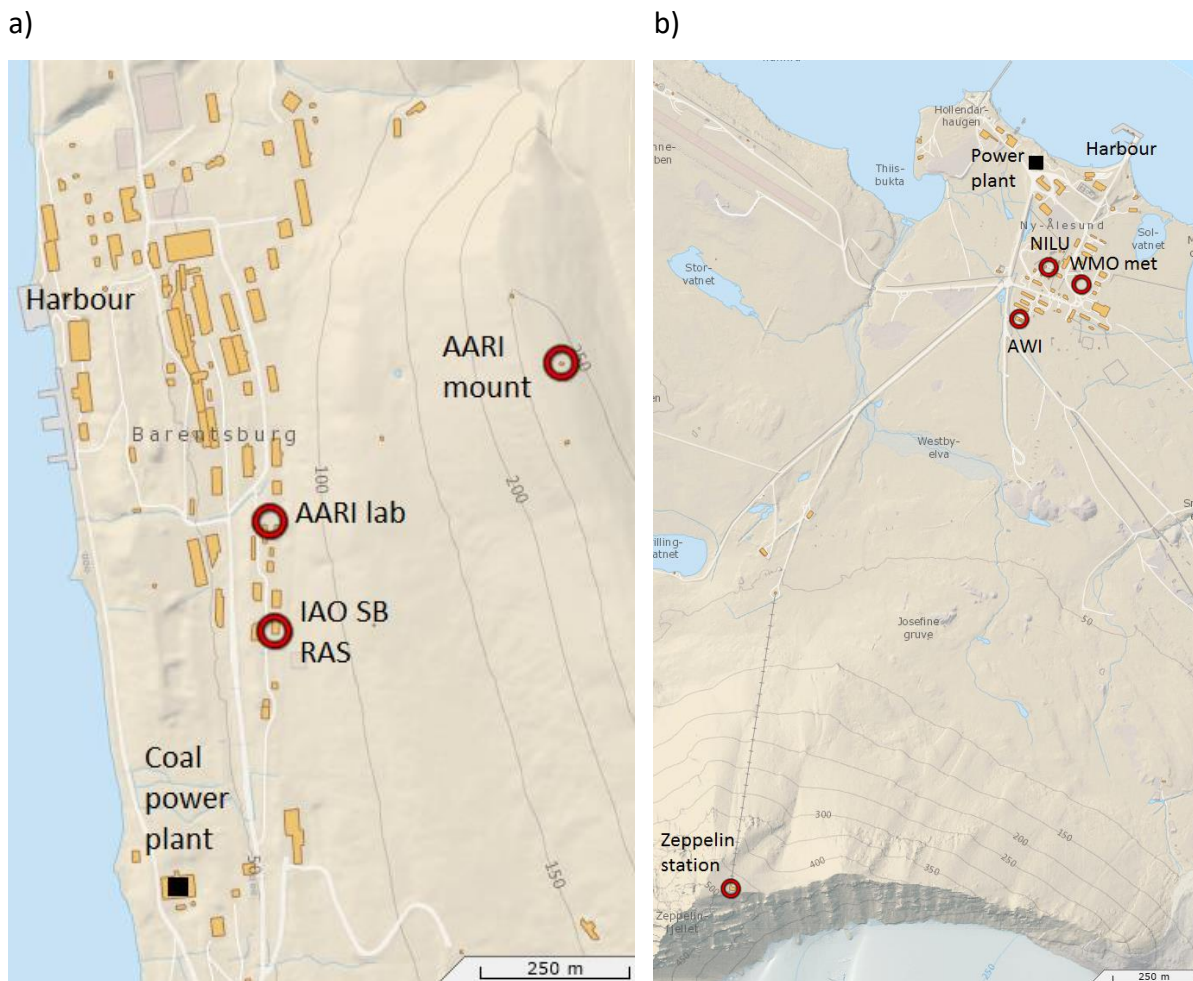


Figure 2 Local maps of Barentsburg (a) and Ny-Ålesund (b)

SO₂ and NO_x monitors in Ny-Ålesund are installed in the middle of the settlement (NILU station in Fig. 2b; instruments number 1 and 2 in Table 4). Detailed description of the instruments installed there is given in [4], [5], [9]. The automatic WMO weather station (Fig. 2b; instrument number 3 in Table 4) is operated by the Norwegian meteorological institute and provides continuous meteorological data of high quality. These data were used for analysis together with the chemical measurements from the NILU station. CO and O₃ measurements are performed at the Zeppelin station (Fig. 2b; instruments number 4 and 5 in Table 4), located at the mountain top (474 m a.s.l.) 2km to the south-east from Ny-Ålesund. Previous studies have shown that due to complex topography and elevation, separate

meteorological data from Zeppelin station (instrument number 6 in Table 4) should be used for analysis of chemical data obtained there [5]. In addition to the gaseous ground-based measurements, columnar aerosol measurements were performed in Ny-Ålesund from the roof of AWI station using sun photometer of the same type as was used in Longyearbyen (Fig. 2b; instrument number 7 in Table 4).

Table 4 Measurements in Ny-Ålesund

N	Instrument, Model	Measurement	Period	Data owner
1	NO _x Monitor, T200	NO, NO ₂ , NO _x concentration	26.06.18-16.08.18	Norwegian Institute for Air Research (NILU)
2	UV Fluorescence SO ₂ , T100	SO ₂ concentration	26.06.18-16.08.18	NILU
3	WMO weather station	Temperature, relative humidity, pressure, wind speed, wind direction	01.06.18-31.08.18	Norwegian Meteorological Institute
4	Photometric O ₃ , T400	O ₃ concentration	26.06.18-16.08.18	NILU
5	Picarro G2401 temp 2017-NRT CO gas analyser	CO concentration	26.06.18-16.08.18	NILU
6	Automatic weather station (HMP-155 Vaisala and WMT-700 Vaisala)	Temperature, relative humidity, pressure, wind speed, wind direction	26.06.18-16.08.18	NILU
7	Automatic Sun Tracking Photometer Ce 318	Aerosol optical depth, Angström exponent, precipitable water	01.07.18-31.08.18	UVa
8	Balloon-borne Sonde, Vaisala RS41	Temperature, relative humidity, pressure, wind speed, wind direction, altitude	01.07.18-31.08.18, 4 times per day	Alfred Wegener Institute Helmholtz Centre for Polar and Marine Research
9	Ozone sonde	O ₃ concentration	28.06.2018-09.08.18, weekly	Alfred Wegener Institute Helmholtz Centre for Polar and Marine Research

The data obtained from the sun photometer measurements in Longyearbyen (Fig. 1b) and Ny-Ålesund (Fig. 1b) were included in the AEROSOL ROBOTIC NETWORK (AERONET), a global network originally intended to satellite products validation. However, through the years and thanks to the high reliability, stability and the wide spreading of its measurements, AERONET has become one of the main references to the remote sensing monitoring of the atmosphere.

The CIMEL Sun/Sky photometer CE318 is the main instrument of the network counting with two measurement routines, the direct sun measurement and an irradiance sky spectral measurement known as almucantar. Both of them present at several wavelengths (340, 380, 440, 500, 675, 870 and 1020 nm).

The data selected for this study corresponds to the Version 3, and is the level 2 of quality assurance. AERONET data present a high traceability and a standard calibration protocol between all the stations. Furthermore, Level 2 data are cloud screened which implies that punctual failures or instrument errors are filtered out.

Airborne measurements in Longyearbyen and Ny-Ålesund

Besides the ground-based measurements, tethered balloon launches with “Vaisala” meteorological sensors, microaethalometer AE51 [29] and MiniDISC portable particle counter [30] were performed from the UNIS CO₂ laboratory located in the valley Adventdalen approximately 5 km to the south-east from Longyearbyen (Fig. 1b, instrument number 9, 10 and 11 in Table 2). Although local pollution from ships and the power plant may reach the station only if the wind from north-west is prevailing, and therefore the launching location is not ideal for the air quality studies; it has been chosen in order not to disturb the aircraft traffic in the area. All the measurements have been performed in cooperation with the Svalbard airport in the hours when no planes or helicopters were arriving or departing from Longyearbyen. The tethered balloon with less than 3.25 m³ of helium was used in the hours when ground-based wind speed was below 10m/s since stronger wind could potentially damage the equipment. In the days when the launch was cancelled due to high wind speed, the wind was in direction from the Adventdalen valley, therefore, there was no influence of local air pollution from the town on concentrations near the UNIS CO₂ lab. Due to air-traffic and meteorological restrictions, only 78 (39 up and 39 down) vertical meteorological profiles were obtained for 52 days of ground-based measurements. 95% of the launches were performed between 12:00 and 18:00 UTC, and only 5% were made from 18:00 to 00:00. The MiniDISC and AE51 could not be used when the air humidity was too high (relative humidity above 90% was used as a threshold), thus only 37 BC and 26 particle number concentration profiles were obtained.

The following procedure has been implemented for tethered balloon profiles processing:

- 1) The rate of pressure and temperature change with time dp/dt and dT/dt have been calculated for ascending and descending profiles separately.
- 2) The calculated rates have been checked for normality of distribution using Kolmogorov-

Smirnov test in the Matlab software.

3) Since the data are not normally distributed, a robust measure to detect outliers has been chosen. The outliers in the dp/dt and dT/dt data have been defined as all points more than three scaled median absolute deviation (MAD) from the median values [31].

4) Pressure values for these outlier points are changed to the linearly interpolated value between closest non-outlier pressure points. As the sampling rate is irregular, the interpolation is done taking into account local time interval between two nearest non-outlier points.

5) This method removes only extreme outliers; it does not smooth the data and the processing result is still close to the original values.

6) The height has been calculated from pressure using hypsometric equation [32], which is common to use for radiosonde profiles.

7) To compare BC profiles with the meteorological values, the height, temperature and wind speed have been averaged for 30 sec periods according to the timing at AE51 sensor.

8) Since from time to time there was an up-and-down drift of the balloon, and since the removal of rough outliers and 30 sec averaging does not always compensate for this drift, the BC and MiniDISC concentration plots have been made for 50 m average in height.

9) When non-averaged data were plotted, additional smoothing has been performed using 1-2-1 smoothing filter as suggested by [33].

Meteorological and O₃ soundings have been performed by the Alfred Wegener Institute Helmholtz Centre for Polar and Marine Research from the French–German AWIPEV research station in Ny-Ålesund (AWI in Fig. 2b); instrument number 8 and 9 in Table 4). The manufacturer's processed radiosonde data for July 2018 are available in the database www.pangaea.de [34], while the data for August 2018 are available on request. The ozone is measured by electrochemical concentration cell [35]. The analysed data are stored in the Network for the Detection of Atmospheric Composition Change (NDACC) archive <ftp://ftp.cpc.ncep.noaa.gov/ndacc/station/nyalsund/ames/o3sonde/>.

Laboratory analysis of PAH filter samples from Longyearbyen

Following chemicals and solvents were used for PAH analysis: 16 Priority PAHs defined by the United States Environmental Protection Agency (EPA) and 16 deuterated EPA Priority PAHs mixtures, 99.3-99.9% purity, obtained from Chiron AS, Norway. 1,2,3,4-Tetrachloronaphthalene was from Cambridge Isotope Laboratories, Inc. and dichloromethane and n-hexane, GC-capillary grade, were purchased from VWR.

Prior to extraction, samples were spiked with known amounts of deuterated 16 PAHs surrogate

standard mixture. QFFs were placed in centrifuge glass tubes with 12 ml of DCM and vortexed for 1.5 min. Samples were then centrifuged for 5 min at 4,500 rpm. Supernatant was collected, concentrated to near dryness under a gentle nitrogen (99.999%) stream and dissolved in a small volume of n-hexane (500 μ L).

Sample extracts were purified on natural silica SPE cartridges (500 mg, 3 mL; Macherey Nagel). Alkanes were removed with 1 mL n-hexane. PAHs were then eluted with 9 mL 35:65 (v/v) DCM–n-hexane. After concentration under a gentle nitrogen stream almost to dryness, residues were re-dissolved with n-hexane. Recovery standard 1,2,3,4-Tetrachloronaphthalene was added prior to mass spectrometer (MS) analysis to evaluate recoveries of labelled PAHs surrogates. One lab blank was performed every five samples.

Samples were analysed using Thermo TRACE gas chromatograph equipped with Thermo TriPlus-100LS autosampler and coupled with Thermo Polaris Q ion trap mass spectrometer. Compounds were separated on DB5-MS+DG column (30+10 m Duragard \times 0.25 mm \times 0.25 μ m film thickness; Agilent J&W, USA) under electron ionization (EI) mode. Detector temperature was 200 $^{\circ}$ C. A volume of 1 μ L was injected at 300 $^{\circ}$ C in splitless mode (splitless time 3.0 min) for analysis. The GC oven temperature started at 70 $^{\circ}$ C for 3.0 min, was increased at 40 $^{\circ}$ C min^{-1} to 170 $^{\circ}$ C, next at 10 $^{\circ}$ C min^{-1} to 240 $^{\circ}$ C, and then increased at 5 $^{\circ}$ C min^{-1} to 310 $^{\circ}$ C. Ultra-pure Helium (99.9999 %) was used as carrier gas, at a constant flow rate of 1.0 mL min^{-1} . Transfer line temperature was 325 $^{\circ}$ C. The MS was run in selected ion monitoring (SIM) mode.

Target compounds were identified by matching of retention times and fragmentation profiles against corresponding standards, and were quantified using corresponding internal standard and the 8-point calibration curves.

Ship traffic analysis and air quality assessment

During the campaign, the ship traffic in Longyearbyen has been logged based on the arrival and departure data reported at the marinetraffic.com. Although the cruise ships have not visited Longyearbyen every day, there have been plenty of smaller ships in the harbour or anchored in the fjord. Therefore, a parameter indicating the ship size and emissions has been chosen for the data analysis. Gross tonnage (GT) have been previously used for this purpose in other air pollution studies [36], [37]. Ships spend some time in Adventfjorden before arrival and after departure, therefore analogously with previous studies the time interval two hours before arrival and two hours after departure has been used to study the effect of ships emissions on the air quality in Longyearbyen [5], [6]. The ship traffic data from Ny-Ålesund

reported at the marinetraffic.com have been studied similarly.

In order to assess the air quality in the towns, Norwegian air quality standards have been applied to check if the pollutant concentrations exceeded these limits in Ny-Ålesund and Longyearbyen [38]. Although located on Norwegian territory, Barentsburg is a Russian coal mining settlement and Russian Federal service for hydrometeorology and environmental monitoring provides environmental information about the town in the yearly “Overview of the environmental pollution” reports [39], therefore Russian air quality limit values may be applied there as well [40].

Influence of synoptic scale meteorological conditions on concentrations of air pollutants

To check the influence of meteorological conditions on the ground level concentrations, the measurement results have been divided into two groups with concentrations of compounds below or equal to their median and above the median. Statistical significant difference in meteorological conditions for the two groups has been defined using Wilcoxon rank sum (WRS) test [4]. In addition to this, daily concentrations of all measurement compounds have been calculated. For the days with extreme pollution accumulation above 95 quantile of the daily value for each compound [41] and days when long-range transport of aerosol has been identified based on the CO and sun photometer data from Ny-Ålesund, the effect of the prevailing synoptic meteorological situation on the concentrations has been studied using hourly meteorological data from the global ERA5 reanalysis dataset [42]. Finally, backward air mass trajectories have been simulated using the Hybrid Single Particle Lagrangian Integrated Trajectory (HYSPLIT) model for the events when long-range transport of aerosols has been identified for 240 hours back in time to indicate the source regions of the air masses [43].

Results

The prevailing wind directions in Longyearbyen was north-westerly-westerly and southerly in approximately 70% and 30% of measurements, respectively. Easterly and south-easterly direction was detected in 49% of the wind data from Ny-Ålesund, while in approximately 1/3 of the measurement hours the wind was coming from the north-west and north. These results are consistent with previous studies [5]. The wind from south-south-west was present in Barentsburg 57% of all measurement time. Wind directions along the fjords are characteristic for Svalbard, where the large-scale flows are topographically channelled and local thermally driven flows from colder to warmer areas are present [9]. However, this has an implication on

the frequency for which the concentrations of air pollutants are measured downwind from the major sources in each of the settlements. One may expect more frequent inflow of locally polluted air from the coal power plants in Longyearbyen and Barentsburg to the measurement sites (Fig. 1a and Fig. 2a), while the site in Ny-Ålesund is rarely influenced by the air masses impacted by local emissions (Fig. 2b). Indeed, there is a frequent inflow of air with higher BC and NO concentrations to the Longyearbyen station (Fig. 3a), and the smallest difference between the mean and median concentrations of air pollutants is observed there (Table 5).

Table 5 Mean and median concentrations of measured compounds at the stations

Station	O ₃ , µg·m ⁻³		SO ₂ , µg·m ⁻³		NO, µg·m ⁻³		NO ₂ , µg·m ⁻³		BC, ng·m ⁻³	
	mean	median	mean	median	mean	median	mean	median	mean	median
Longyearbyen	44,5	44,9	0,3	0,3	2,3	1,2	5,4	3,5	197	147
Barentsburg	53,4	53	16,1	2,2	4,9	3,2	-	-	263	37
Ny-Ålesund	52	50,8	0,1	0	2,9	0,2	2,1	0,4	-	-

The mean and median concentrations of tropospheric O₃ with NO_x are lowest in Longyearbyen mainly due to titration of tropospheric O₃ with NO_x since there are moderate negative correlations between NO and O₃ ($r=-0.52$, $p<0.0001$) and NO₂ and O₃ ($r=-0.56$, $p<0.0001$), while correlation between O₃ and SO₂ is very weak ($r=-0.16$, $p<0.0001$). Strong positive correlation between NO and BC values ($r=0.73$, $p<0.0001$) indicates that most of NO_x and BC come from the same emission sources, while correlation of NO with SO₂ ($r=0.29$, $p<0.0001$) is weak. There is a clear diurnal pattern for all weekdays in NO and BC data from Longyearbyen with absolute values of autocorrelation coefficients increasing to $r>0.15$ every 24 hours. This pattern most probably occurs due to local car traffic near the station and is independent on wind direction. In contrast, the autocorrelation in SO₂ data and O₃ data is not so pronounced with $r>0.2$ only for the first 24 hours interval. According to the WRS-test, median daytime (06 UTC-17 UTC) concentrations of SO₂, NO and BC were significantly higher than the nighttime (17 UTC-05 UTC) values, while O₃ concentrations were significantly lower ($p<0.01$).

In accordance with the power plant SO₂ and PM emission data (Table 1), one may expect stronger influence of the power plant in Barentsburg on the local air quality than in other settlements. Certainly, the highest mean SO₂ and BC concentrations were measured in this town (Table 5). However, since the station is not always downwind from the major sources (coal power plant and harbour area), the autocorrelation coefficients support the hypothesis that the concentration at the station depends on the persistency of wind direction with $r>0.2$

only at 24 and 48 intervals when similar wind direction is present. However, according to the WRS-test a significant difference in median daytime and nighttime values is present only in BC data. The pattern of NO concentrations in Barentsburg is unique having a smooth shape of the peaks rather than sharp increase of hourly concentrations as in Longyearbyen and Ny-Ålesund (Fig.3b). Indeed, the autocorrelation coefficient remains above 0.2 for the first 42 hours interval. In addition to this, there is a significant negative correlation between NO and wind speed ($r=-0.37$, $p<0.001$). This may indicate that in presence of some pollution source, such as, for example, emissions from a ship in Barentsburg harbour and calm wind conditions which persist for a longer time than several hours, there is insufficient ventilation of the local ABL. Unfortunately, no ship data from Barentsburg are available.

Despite the fact that previous short-term sampling campaigns performed there have not revealed the concentrations exceeding the Russian air quality limits [39], [44], the station in Barentsburg is influenced by acute pollution when certain meteorological conditions are present. Such situation occurred 9th, 10th and 11th of July 2018 when the wind bringing pollution from the power plant to town dominated during a period of three days. Daily SO₂ concentrations exceeded the Russian allowable limit of 50 $\mu\text{g}\cdot\text{m}^{-3}$ three times in this period (Fig. 3b) and the Norwegian limit of 125 $\mu\text{g}\cdot\text{m}^{-3}$ once, on 10th of July. In that day, the SO₂ concentration reached its peak values and was above Russian 20-minutes limit of 500 $\mu\text{g}\cdot\text{m}^{-3}$ three times, while the Norwegian hourly limit of 350 $\mu\text{g}\cdot\text{m}^{-3}$ was exceeded two times. NO concentrations were correlated with SO₂ values very strongly ($r=0.98$ and $p<0.0001$), however, daily NO values were not higher than 3.3 $\mu\text{g}\cdot\text{m}^{-3}$. There is a strong correlation between SO₂ and BC concentrations ($r=0.75$ and $p<0.0001$), despite the fact that the aethalometer was installed at the IAO SB RAS station, it was closer to the power plant, and the polluted air was detected there prior to the AARI station. The daily average BC concentrations of 2241 $\text{ng}\cdot\text{m}^{-3}$ were more than 8 times higher than average for the campaign. There was south-south-westerly wind direction and the wind speed was high, 5.6 $\text{m}\cdot\text{s}^{-1}$, in that day. Strong positive correlations between the wind speed and SO₂ concentration ($r=0.62$, $p=0.001$) and wind speed and air temperature ($r=0.78$, $p<0.001$) were present.

In order to investigate the meteorological conditions, which caused the semi-persistently high pollution levels lasted over three days in Barentsburg, we need to assess the behaviour of the plume from the coal power plant depending on the local atmospheric stability. The persistency of pollution for such a long period might indicate that the observed episode may be a coastal fumigation event when a plume from a stack located on the sea shore undergoes

little diffusion due to stable stratification above and is rapidly transported with the onshore wind into the internal ABL forming above the land [45]. In this case, downward turbulent mixing below the stable layer brings warmer polluted air to the ground level. In order to confirm this hypothesis, the gradient Richardson number Ri_m [45] has been calculated using the meteorological data from two Barentsburg stations located at different heights, 70m and 255m (AARI lab and AARI mount, respectively, in the Figure 2a). Ri_m varied from -0.08 to 0.01 in the three days, from 9th to 11th of July, which indicates quasi-stationary, near-neutral stability due to mechanical mixing which is often present during strong winds and overcast skies. Indeed, the median wind speed at the AARI mount station was much higher than at the AARI lab station, $13.1\text{ m}\cdot\text{s}^{-1}$ vs $4.6\text{ m}\cdot\text{s}^{-1}$, and the calculated median lapse rate based on the data from the two stations was superadiabatic, $-11.7^\circ\text{C}/1000\text{m}$, an indicator of unstable to neutral conditions. Similarly, no inversion was present in the radiosonde profiles from Ny-Ålesund for this period. Thus the hypothesis about coastal fumigation is inconsistent and, most probably, the coning behaviour of the plume was present. According to the classical air pollution meteorology [45], normally these conditions do not lead to high concentrations at the ground level. However, due to local topography, the town and the AARI lab station are located on the hill above the coal power plant, and in conditions when there is no lifting of the plume, but direct transport of it to the town by strong wind from south-south-west, high concentrations may be observed even in absence of the atmospheric inversion. Thus, long-term observations of atmospheric stability, wind and SO_2 concentrations are needed to define the frequency of the occurrence of adverse meteorological conditions affecting air quality in Barentsburg.

As expected from the amount of emissions (Table 1) and from prevailing wind direction, the median concentrations of measured compounds were the lowest in Ny-Ålesund (Table 5); however, one can see that there were several discrete high peaks of NO concentration (Fig.3c). Despite very low concentrations there is a clear diurnal pattern for all weekdays in SO_2 data from Ny-Ålesund with $r > 0.45$ for the first 24 hours and absolute values of autocorrelation coefficients increasing to $r > 0.15$ every succeeding 24 hours. The station is located at the distance of 50m from one of the major roads in Ny-Ålesund and may be influenced by local car emissions. However, the marine biogenic emissions of SO_2 from Kongsfjorden may cause this diurnal pattern as well [4]. In contrast, the diurnal pattern in the autocorrelation in NO data is not so pronounced with $r = 0.14$ for the first 24 hours interval only. According to the WRS-test, there was a significant difference in median daytime and

nighttime values of NO and SO₂ data in Ny-Ålesund. In contrast to the O₃ data from Longyearbyen, which showed diurnal pattern, the autocorrelation coefficient for O₃ concentrations measured at the Zeppelin station was steadily declining to $r < 0.2$ for the first 32 hours and exhibited a pronounced maximum at 113 and pronounced minimum at 136 hours of lag. Since similar pattern was observed in O₃ data from Barentsburg, this may indicate influence of large-scale circulation. The pattern of CO concentration measured at the Zeppelin station follows the variation in O₃ data there closely (Fig.3c).

One can see that irrespectively of wind direction, the lowest O₃ values are observed in Longyearbyen (Fig.4 a), while concentrations in Ny-Ålesund and Barentsburg are quite similar. The number of local NO_x sources is much higher in Longyearbyen where both ship and road traffic are more intensive than in other settlements, while NO_x emissions from the coal power plant there are similar to those in Barentsburg. The NO/NO_x ratio is higher in fresh emissions [9], therefore the distribution of NO over wind directions points towards the nearest local sources of NO_x: power plant situated 300m to the north from the measurement station in Ny-Ålesund (Fig. 4b) and port areas and roads located to the south-west and to the north from the NO_x monitors in Barentsburg and Longyearbyen, respectively. In Barentsburg, the biggest source of SO₂ and BC is coal power plant, and there is strong positive correlation between the SO₂ and BC ($r=0.77$, $p < 0.0001$) and the values of these compounds measured downwind from the power plant are extremely high and (Fig4c, d). In Ny-Ålesund and Longyearbyen, the port area is the source of SO₂.

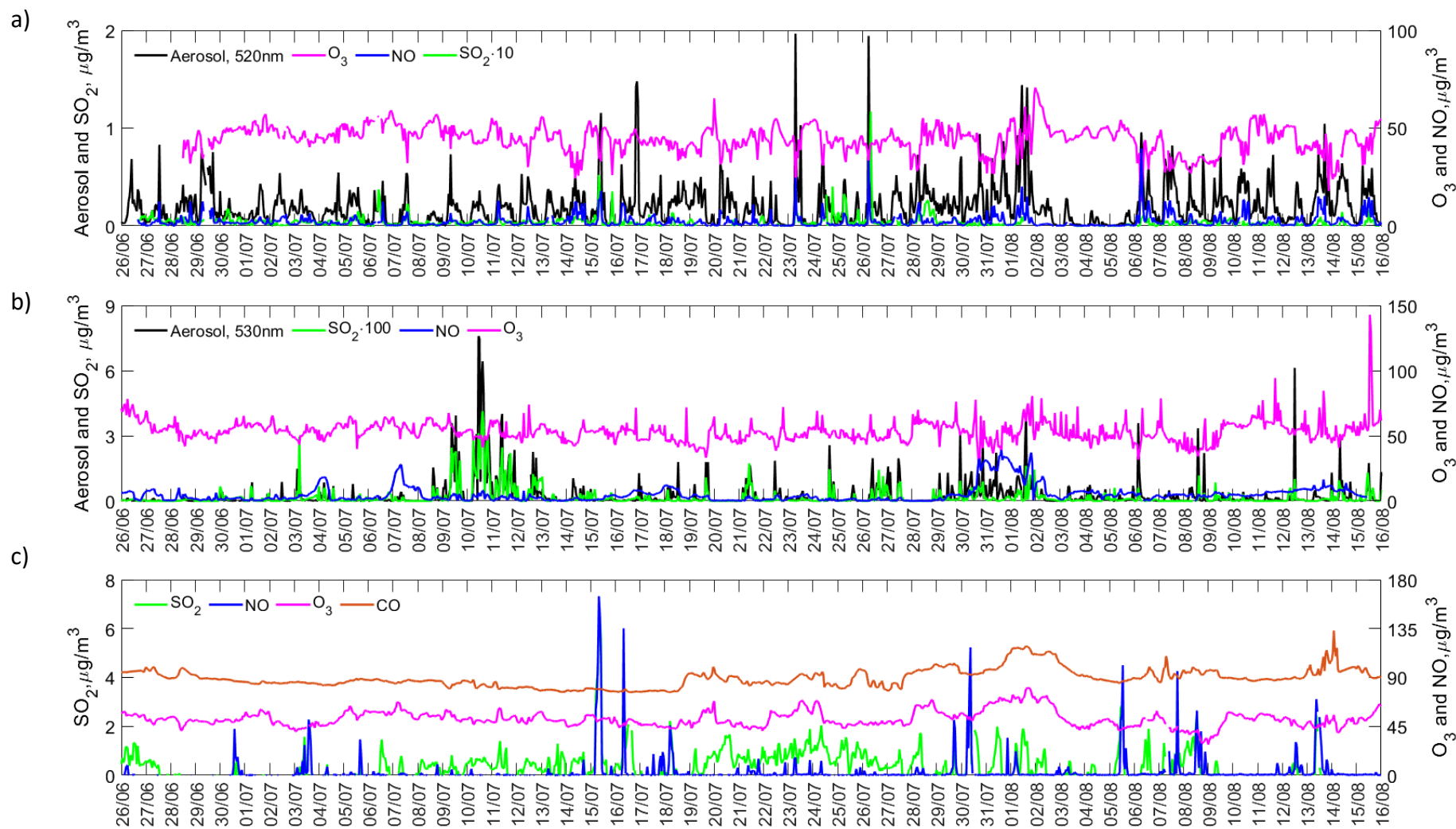


Figure 3 Concentrations of measured compounds in: a) Longyearbyen; b) Barentsburg; c) Ny-Ålesund

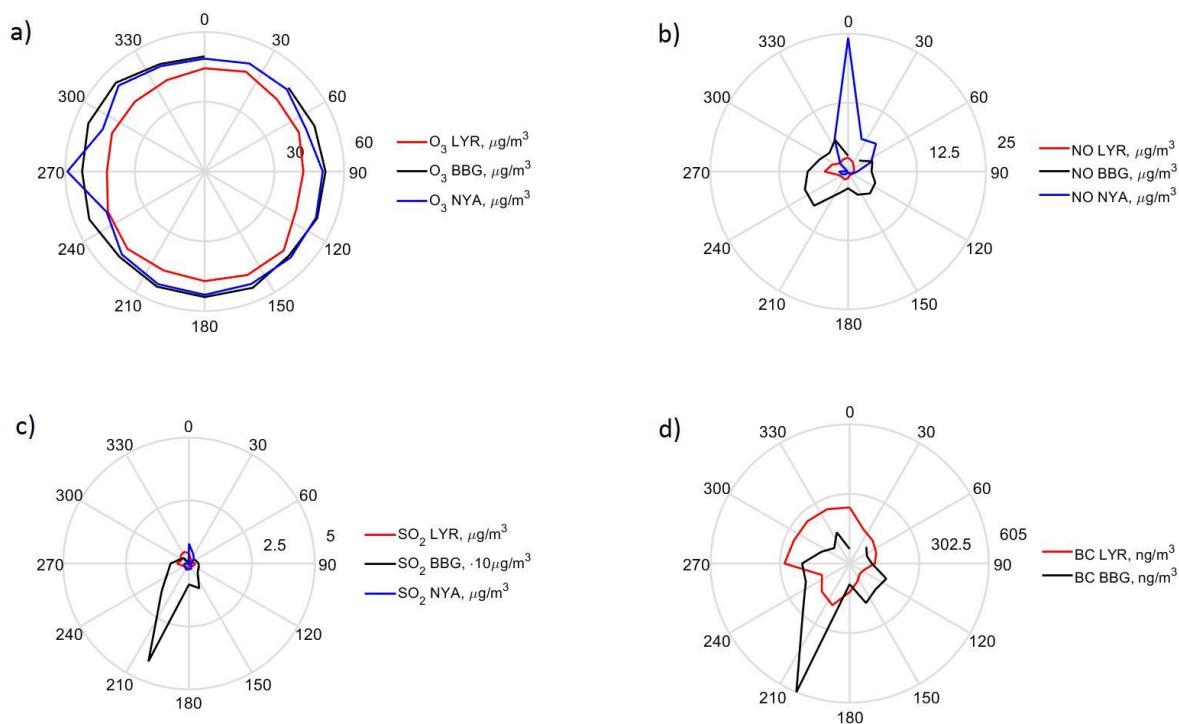


Figure 4 Distribution of concentrations over wind directions: a) O₃; b) NO; c) SO₂; d) BC

Influence of ships emissions and local power plants on air quality in Longyearbyen, Ny-Ålesund and Barentsburg

According to the statistics from Longyearbyen anchorage and port reported in marinetraffic.com, ships with total GT>100 may have influenced the air quality in town in 44% of the time. Number of individual ships with GT>100 is 21. According to the statistics from Ny-Ålesund port, ships with total GT>100 may have influenced the air quality in town in 45% of the time, and the number of individual ships with GT>100 is 27. However, the median GT and 95-quantile of GT for ships visiting Longyearbyen were much higher than in Ny-Ålesund: 6344 tonnes vs 2183 tonnes and 131954 tonnes vs 39618 tonnes, respectively. This means that although the number of ships with GT>100 was higher in Ny-Ålesund, the size of ships and, consequently, amount of emissions were higher in Longyearbyen. Based on the location of major emission sources, port area and power plant, hours when the air in Longyearbyen may be mostly influenced by the long-range transported pollution and car traffic have been defined as hours, when the wind speed was above 2 m/s and wind direction could be reliably measured as between 90 and 180 degrees (Fig. 4). Only 17% of the hourly data fits to this criteria. Average concentrations of NO, NO₂, SO₂ and BC were very low (0.6, 1.7, 0.04 and 76 μg/m³, respectively) while O₃ values were 11% higher than when the wind was from other directions.

The WRS test has been performed to check if the influence of ship traffic on air quality was significant. The test results with p-value <0.05 are shown with bold font in Table 6.

Table 6 Median concentrations of compounds in Longyearbyen and Ny-Ålesund based on wind direction and absence or presence of ships with GT>100. The WRS test results with p-value <0.05 are shown with bold font.

Settlement	Wind direction	Median concentrations, $\mu\text{g}/\text{m}^3$				
		NO	NO ₂	SO ₂	BC	O ₃
Longyearbyen	E (91°-179°), ships absent	0.3	0.7	0.03	0.065	48.3
Longyearbyen	E (91°-179°), ships present	0.4	0.8	0.04	0.088	46.7
Longyearbyen	Other directions (0°-90° and 180°-360°), ships absent	1.1	3.6	0.3	0.136	44.5
Longyearbyen	Other directions (0°-90° and 180°-360°), ships present	2.1	5.2	0.3	0.213	43.9
Ny-Ålesund	91°-269°, ships absent	0.10	0.33	-0.05	-	51.1
Ny-Ålesund	91°-269°, ships present	0.09	0.37	0.29	-	50.8
Ny-Ålesund	0°-90° and 270°-360°, ships absent	0.20	0.4	-0.06	-	51.3
Ny-Ålesund	0°-90° and 270°-360°, ships present	0.52	0.8	0.13	-	49.8

Statistically significant influence of ship traffic on local BC, SO₂, NO and NO₂ concentrations have been observed throughout campaign in Longyearbyen. Generally, the average hourly BC, SO₂, NO and NO₂ concentrations were on 52%, 38%, 73% and 37% higher in the time period two hours before arrival and two hours after departure of the ships with total GT above 100. However, influence of ships emissions on O₃ concentration was insignificant reducing the O₃ values on only 1% in comparison with hours without ships.

According to WRS-test, there was statistically significant difference in median concentration of SO₂, NO, NO₂ and O₃ between the two groups: with ships and without ships with GT>100 in Ny-Ålesund. Average hourly SO₂, NO and NO₂ concentrations in the settlement were on 3.6 times, 23%, 34% higher, while O₃ concentration at the Zeppelin station was 2% lower in the time period of two hours before arrival and two hours after departure of the ships with total GT above 100. Effect of ships emissions on average SO₂ concentration is stronger in Ny-Ålesund, because the absolute background concentration is very low due to absence of other

significant sources of SO₂. In contrast, in Longyearbyen only background concentrations (when wind is from the east) are comparable with background concentration in Ny-Ålesund (0.04 µg/m³), however, average background concentration for all other wind directions was 5 times higher than in Ny-Ålesund.

As the coal power plant and harbour are co-located in respect to the measurement station in Longyearbyen, the concentration of PAH on filter samples is influenced by these two major sources and may be impacted by traffic emissions from the nearby road to some extent.

However, since the sampler was placed at the UNIS roof, the effect of road emissions is likely to be small. Total concentration of 16 PAH compounds in seven samples collected in summer (14.07-14.08) and 5 samples collected in autumn (17.09-24.09) varied from 108 to 2040 pg/m³ and from 70 to 881 pg/m³, respectively. Average and median total PAH concentrations were almost three times higher for the summer samples than for the autumn samples. This is due to the fact that prevailing wind direction during summer sampling was north-westerly, downwind from the major sources mentioned above, while during autumn measurements it was south-easterly, from the Adventdalen valley.

The percentage of PAH in summer and autumn samples is shown in Figure 5a) and Figure 5b), respectively. Five summer samples and one autumn sample dominated by naphthalene were collected in days when north-westerly and westerly was observed. The coal combustion may be the source of this compound [46], however, Agrawal et al., 2010 found it to be dominant in PAH compounds in emissions from ship main engine [47], and similar results, which show prevalence of naphthalene family compounds in ship exhaust, are presented by Cooper, 2003 [48]. The lifetime of naphthalene is in the order of one day, and the compound is further transformed to nitro-naphthalene through the reaction with hydroxyl-radical and nitrates [49]. The reaction rate depends on environmental parameters, such as air temperature, amount of sunlight and air composition. Thus, studies of nitro-metabolites of PAHs from local emission sources in Svalbard may give further insight into environmental fate of naphthalene. The highest total PAH concentration for the whole campaign was measured when the biggest ship was visiting Longyearbyen.

There is a strong linear correlation between total PAH concentrations and total GT of ships in the sampling days in summer ($r=0.995$, $p=0.005$). Seven from 16 PAHs show tendency to increase with rising total daily GT: naphthalene, acenaphthylene, fluoranthene, pyren, chrysene, benzo(k)fluoranthene and benzo(ghi)perylene. There was an outlier from this rule, 1st of August. In that day the lowest mean wind speed of 0.9 m·s⁻¹ and the highest mean air temperature of 11°C were observed, and the total PAH concentration showed

disproportionally high increase with respect to the total GT.

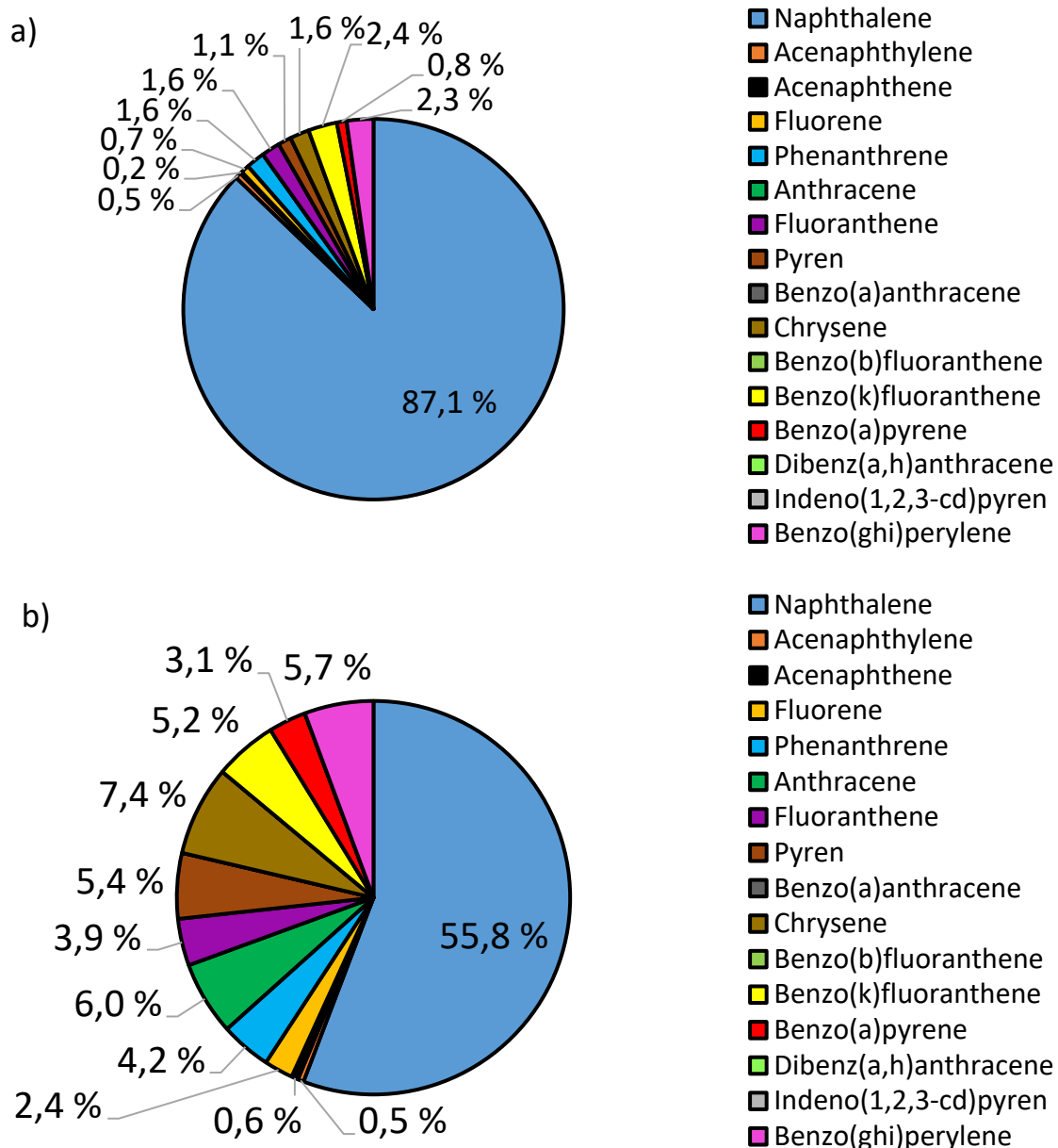


Figure 5 Total percentage of PAHs in summer (a) and autumn (b) samples.

There were two days in summer, when the coal power plant was closed on maintenance, and Longyearbyen was supplied by energy from the reserve diesel power plant located 70m to south-west from the measurement station. For these days, the southerly wind was prevailing and the total PAH concentration was much lower: 108.3 pg/m^3 and 141.6 pg/m^3 . The percentage of PAH compounds was more evenly distributed within the samples: phenanthrene, naphthalene, benzo(k)fluoranthene and benzo(ghi)perylene contributed with 22%, 16%, 15% and 14% of total PAH concentration in this group, respectively, while the contribution of each of the remaining PAHs was less than 10%.

PAHs commonly present on soot particles [50], such as chrysene, benzo(b)fluoranthene,

benzo(k)fluoranthene, benzo(a)pyrene, benzo(ghi)perylene, have been detected in both groups of samples. Taking into account prevailing wind direction during autumn measurements and increased percentage of benzo(a)pyrene, benzo(k)fluoranthene, fluoranthene and pyrene, indicators of diesel emissions [51], and benzo(ghi)perylene, a marker for gasoline combustion [52], in the filter samples, one may conclude that the influence of road traffic pollution on PAH distribution was more pronounced in autumn. However, the sum of naphthalene, acenaphthylene, acenaphthene, fluorene and phenanthrene, highly abundant compounds in vehicle emissions [52], was higher for the summer samples and t-test with $p\text{-value} < 0.1$ showed that average concentrations of acenaphthylene were higher in this group. Anthracene absorbed on particles reacts with ozone more readily when sunlight is present [53] and in distilled water its photodegradation rate by sunlight is high [54]. This may explain why this compound has only been found in the autumn group of samples collected when insolation and air humidity decreased.

Vertical black carbon and particulate profiles and meteorological soundings in Adventdalen and Ny-Ålesund

During the fieldwork period from 26 June to 16 August 2018, 188 radiosonde soundings were made from Ny-Ålesund. Temperature inversions were detected in around 40% from them (76 profiles). In the Ny-Ålesund soundings, 80% of all inversions were observed from 00:00 to 12:00 and from 18:00 to 00:00, while only 20% of all inversions were observed in the soundings performed from 12:00 to 18:00, a typical time of tethered balloon launch in Adventdalen.

37 radiosonde soundings from Ny-Ålesund, performed closest to the time of tethered balloon launch in Adventdalen, have been chosen for comparison. Temperature inversions with inversion strength above 0.3C and inversion depth more than 10m were detected in 24 profiles (65% from total). The overview of profile properties in Ny-Ålesund and Longyearbyen are given in Table 7. In six profiles from Ny-Ålesund, the altitude of the inversion bottom, where the temperature started rising, was higher than the maximum height reached by the tethered balloon in Adventdalen in the same day. There was a technical issue with launching of tethered balloon. In the days when wind speed aloft was lower than near the ground, the rope to which the meteorological and chemical sensors were attached was not straight, and when it occasionally went down too much and could touch nearby buildings in Adventdalen, the upward measurements were stopped and the instruments were taken down to the ground despite the fact that the balloon did not reach the maximum permitted height of observations,

1000m. Indeed, maximum height of 33% of Adventdalen profiles were less than 500m. For this group, according to WRS-test, median ground-level wind speed was significantly higher than for the rest of profiles (5.4 m/s vs 4.3 m/s). Therefore, direct comparison of temperature inversion statistics from the two stations would be ambiguous due to difference in maximum height of observations at the two stations. However, there were some common features in the profiles from the two measurement sites. According to the WRS-test, median profile wind speed and air temperature below 1000m in Ny-Ålesund and Adventdalen were significantly higher for the measurements with temperature inversions starting below 500m, than for these with inversion starting above 500m (shown in bold in the Table 7). The opposite relationship is observed for relative humidity in the two groups. Profiles without temperature inversions at the both measurement sites had highest median wind speed and lowest median profile temperature.

Synoptic scale meteorological situation for the three groups (without temperature inversions in Adventdalen, with temperature inversions detected below 500m height and with inversions starting above 500m) are shown in Figures 6 a), 6b) and 6c), respectively. Both first and second group of days were characterized by high-pressure system located to the south-east from Svalbard. However, the south-westerly wind with higher wind speed was prevailing during the first group of measurements, while in the second group the wind speed was lower and air masses transported from the south were warmer, since higher air temperatures were over Scandinavia. In the last group of days, the north-westerly wind with low wind speed was bringing humid air from North Atlantic to Svalbard. Results of wind measurements for the same three groups from Longyearbyen (24 m a.s.l.), Adventdalen (15 m a.s.l.) and Gruvefjellet (464 m a.s.l.) are shown in Figure 6 d), e) and f). The mean wind speed observed in Adventdalen was almost the same for the three groups, however, according to the data from the Gruvefjellet station the wind speed aloft was lower for the days with temperature inversions. The wind direction in Adventdalen was always north-westerly, along the valley axis, while in the days without temperature inversion the wind direction observed at Gruvefjellet (Fig. 6d) was similar to the large scale flow (Fig. 6a). In most cases, north-westerly and westerly wind direction in Longyearbyen was favourable for transport of local pollutants towards Adventdalen valley, where BC soundings were performed, except few days when south-westerly flow was observed in the town similarly to the measurements made at the Gruvefjellet station.

Table 7 Comparison of meteorological profiles Ny-Ålesund and Adventdalen: median values of temperature t, relative humidity RH, wind speed v, temperature inversion strength TIS and bottom height of lowest inversion zTb. The significant results of the WRS-test are shown with bold font.

Sounding place	Profiles without temperature inversion				Profiles with zTb<500m						Profiles with zTb>=500m					
	%	t, °C	RH, %	v, m/s	%	t, °C	RH, %	v, m/s	TIS, °C	zTb, m	%	t, °C	RH, %	v, m/s	TIS, °C	zTb, m
Ny-Ålesund	35	2.2	90	3.7	40	5.8	80	3.2	0.6	54	24	2.5	93	2.1	0.9	781
Adventdalen	58	4.9	74.2	4.6	32	7.0	72.9	3.3	0.5	153	10	5.1	86.8	1.9	0.5	716

Table 8 Characteristics of 50m averages BC and particle profiles

Groups of Adventdalen profiles	Number of profiles		Group median concentration		Group median of maximum concentration in profiles		Median height in m of maximum concentration in profiles		Median BC concentration in Longyearbyen*, ng·m ⁻³
	BC	Particles	BC, ng·m ⁻³	particles, cm ⁻³	BC, ng·m ⁻³	particles, cm ⁻³	BC	particles	
Profiles without temperature inversion	43	32	94	483	147	644	350	100	158
Profiles with zTb<500m	25	16	94	1745	210	3080	100	0	181
Profiles with zTb>=500m	6	0	110	-	194	-	550	-	199

*BC concentration in Longyearbyen is calculated for the period of two hours before the sounding to the time of tethered balloon launch with BC sensor in Adventdalen.

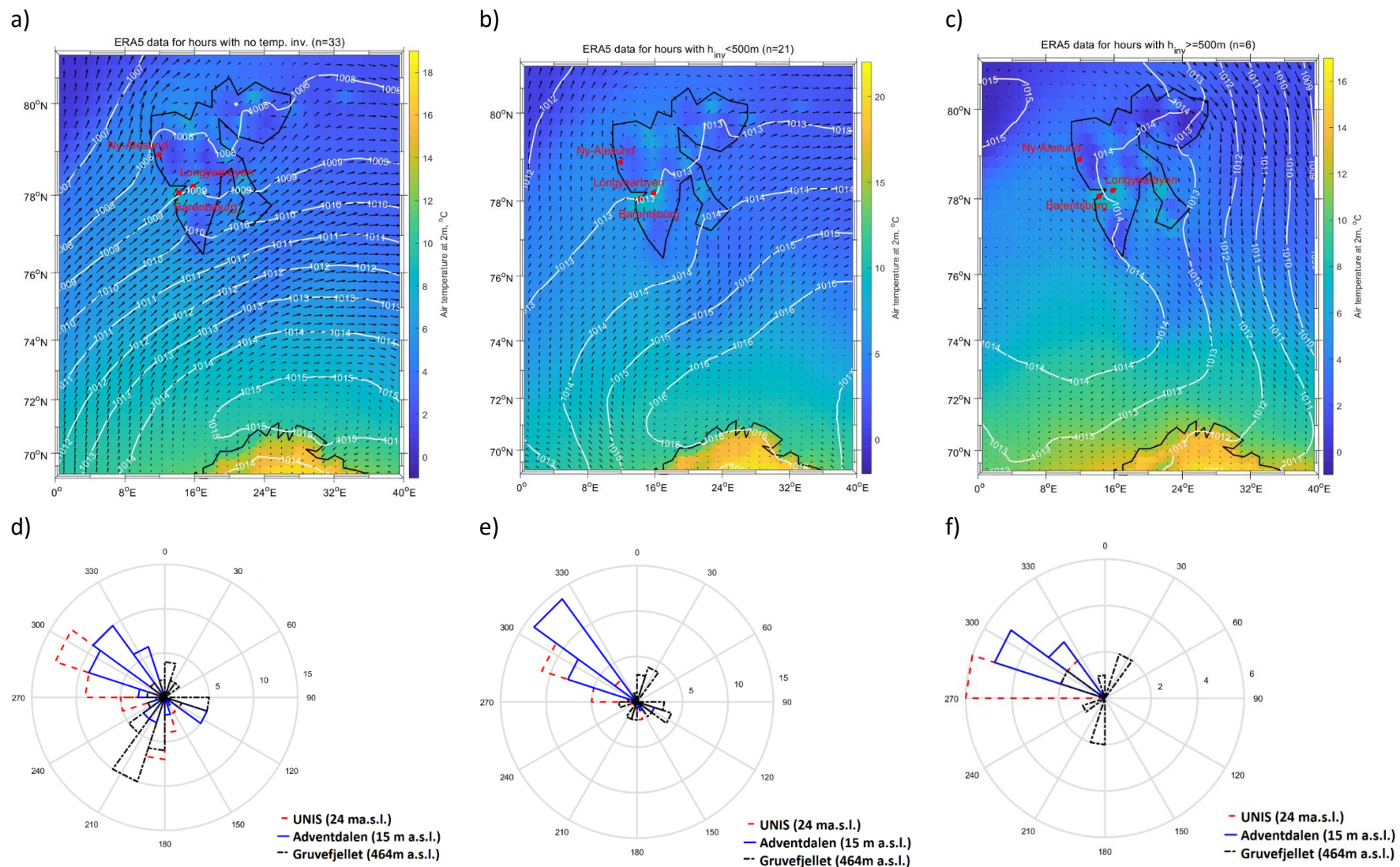


Figure 6 a), b), c) Meteorological conditions for the three groups of Adventdalen profile data described in Table 7: mean air temperature in °C (colour scale), wind direction (black arrows with the length relative to the wind speed) and mean sea-level pressure in hPa (white lines) in the

Svalbard area (black outline) and Ny-Ålesund, Longyearbyen and Barentsburg (red dots) based on ERA5 data; d), e), f) wind rose from the observations in Longyearbyen (UNIS), Adventdalen and Gruvefjellet for the same three groups

The Aethalometer Optimized Noise-Reduction Averaging (ONA) post-processing algorithm for BC data suggested by [55], have been tried since the median concentrations of BC measured in Adventdalen were quite low ($88\text{ng}\cdot\text{m}^{-3}$). The ONA-algorithm uses a predefined difference in the light attenuation ATN for averaging between the measurement points. It finds first point when the ATN difference is equal to a set ATN difference (the lowest value of 0.0 was used as suggested by [56] to remove only negative values). If the programme does not find the predefined ΔATN , it checks next points until it finds it, and then gives the average value for all the points, which were skipped. The algorithm works well when there are few negative values in the data, but since the values from the profiles in Adventdalen have too many negative values in some of the profiles, it has not perform well.

Therefore, the results of black carbon profile measurements have been averaged for 50m layers to reduce the level of negative noise in the data. However, there were still some values below zero in the 50m-averaged data. The statistics of vertical BC and particulate concentration measurements for the three groups, defined in Table 7, is shown in Table 8.

There is positive statistically significant correlation between the height of maximum BC concentrations and height of minimum wind speed in the profiles ($r=0.44$, $p<0.001$). Indeed, in 92% of all profiles the height of maximum BC concentration is less or equal to the height of minimum wind speed. On average, maximum BC concentrations could be found 230m below the height of minimum wind speed. The correlation between height of maximum concentration and height of the maximum temperature is insignificant.

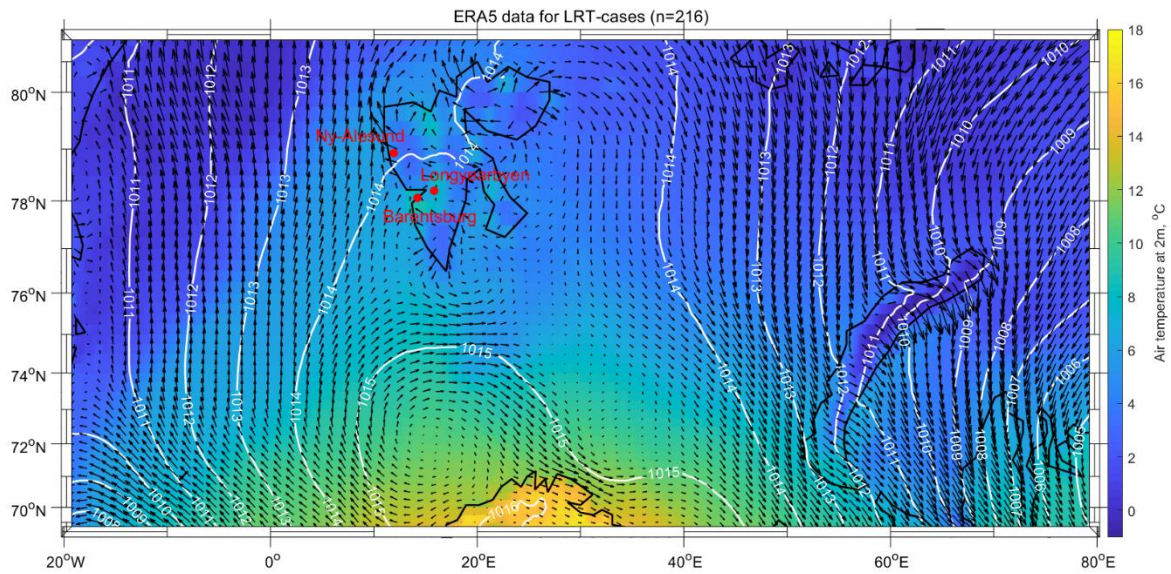
Since the number of profiles with $z_{\text{Tb}} \geq 500\text{m}$ is very small, the groups with $z_{\text{Tb}} < 500\text{m}$ and $z_{\text{Tb}} \geq 500\text{m}$ have been combined into one group with 31 BC profiles ($n_{\text{BC}}=31$) and 16 particulate profiles ($n_{\text{part}}=16$) and compared with a group when no temperature inversions were observed ($n_{\text{BC}}=43$, $n_{\text{part}}=32$). According to the WRS-test, there is no statistically significant difference between median BC concentrations for the two groups, while the median concentration of particles in the profiles with temperature inversion was significantly higher than in profiles where no inversions were observed ($p<0.001$). Group medians of maximum BC and particle concentrations in profiles with temperature inversions were significantly higher. Similarly, median BC concentration measured in Longyearbyen for the period of two hours before the sounding to the time of tethered balloon launch with BC sensor in Adventdalen was higher when temperature inversion was observed.

Events of long-range transport of air pollution based on AOD and CO data from Ny-Ålesund

CO is correlated with the aerosol at the source region since it is emitted from biomass and fossil fuel burning. However, during the transport the particles may be removed from the air masses through dry and wet deposition [57]. CO measurements performed at the Zeppelin station may at times be influenced by local pollution brought up to the mountain from Ny-Ålesund, but, according to the previous studies, these cases are rare and may occur only a few percent of the total measurement time. Moreover, the titration of tropospheric O₃ has been observed nearby the NO_x sources such as diesel fuelled power plant or ships [6], [9]. Hours, when the CO and O₃ data at the Zeppelin station may be impacted by the local pollution, have been excluded from the calculation of daily values based on the wind direction data in Ny-Ålesund and at the Zeppelin station as it has been done in previous studies [9]. Then the quantiles of the daily CO and O₃ values have been calculated. When daily CO concentrations were above median values plus one median absolute deviation (MAD) for the whole campaign, there was a possible long-range transport of polluted air masses. Nine days with CO concentration above the set limit have been identified. In six of nine days defined above as days with possible long-range transport of air pollution, the mean air temperature was 8.5°C, there was prevailing NW-wind with mean wind speed of 1.1 ms⁻¹ and daily concentrations of BC exceeded median plus MAD in Longyearbyen. In the remaining three days, when there was possible long-range transport of pollutants to Svalbard, but no local increase of concentrations in Longyearbyen, according to the WRS-test, the mean wind speed and air temperature there were significantly higher, 5.3 ms⁻¹ and 9.6°C, respectively, and the prevailing wind direction was southerly. There were 16 days when no long-range transported pollution was detected at the Zeppelin, while elevated BC were observed in Longyearbyen due to local pollution. During these days, the mean air temperature was much lower, 7.5°C, and NW wind with mean speed of 2.2 ms⁻¹ prevailed. Synoptic scale meteorological situation for the days when both local and long-range transported pollution may have influenced air quality in Longyearbyen and when only local pollution may have affected BC concentration there are shown in Figure 7 a) and Figure 7 b).

Mean BC concentrations measured in Longyearbyen were on average 32% higher in days when both local and long-range transported pollution influenced the air quality in Longyearbyen vs days when only local pollution was dominating, 337ng·m⁻³ vs 256 ng·m⁻³.

a)



b)

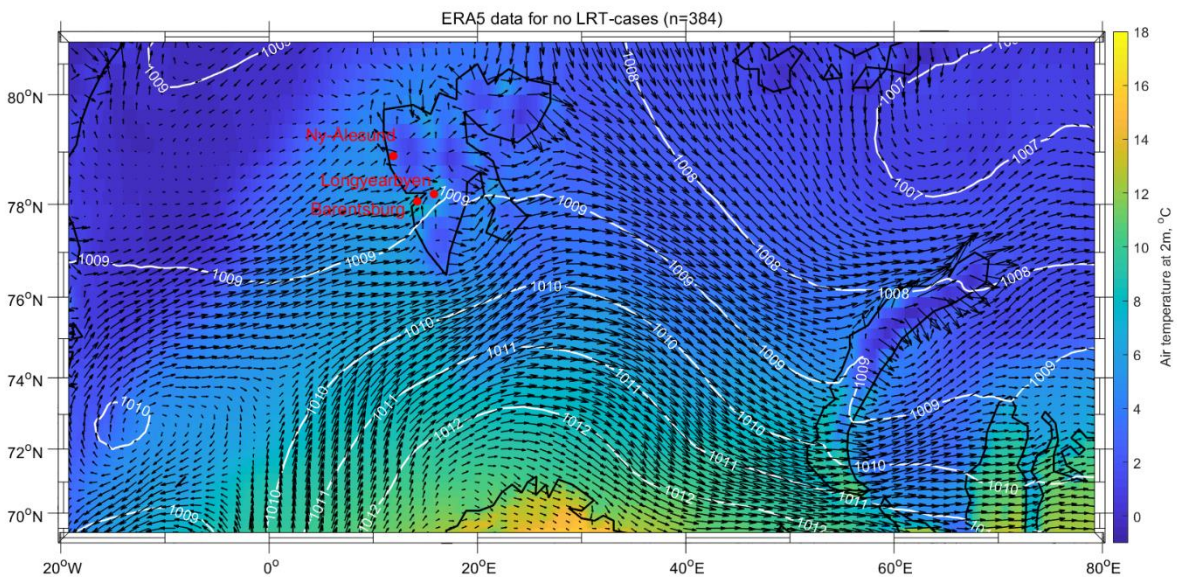


Figure 7 Synoptic-scale meteorological conditions (mean air temperature in °C (colour scale), wind direction (black arrows with the length relative to the wind speed) and mean sea-level pressure in hPa (white lines) in the Svalbard area (black outline) and Ny-Ålesund, Longyearbyen and Barentsburg (red dots)) based on ERA5 data for the hours: a) when both long-range transported and local pollution may have affected BC concentration in Longyearbyen; b) when only local pollution was present

The CO concentration has been measured at the Zeppelin station at a height of 474m a.s.l., but no data about vertical distribution of CO values are available. Thus, if the polluted air masses were above the level of the Zeppelin station, they would be undetected by the monitor there. Therefore, another quantity, which is often used for studies of long-range transported

pollution, aerosol optical depth (AOD), can be applied to study events of elevated transport of polluted air masses. Unfortunately, clear sky conditions are needed for the sun photometer to correctly retrieve total column properties of aerosol and water vapour content from the sun and sky radiance measurements. Therefore, this instrument is not perfectly suitable for the Arctic summer campaigns, when the cloudy conditions are most common [4]. Thus, these data may give us information about the long-range transport events only in cloud-free hours. In Figure 8 the evolution of the aerosol optical depth (AOD) measured by the photometers can be found at two wavelengths (340 and 870 nm) shown by blue and black colours respectively. The x-axis represents the UTC time corresponding to the different days of 2018. The three different stations, the two from AERONET, Ny-Ålesund and Longyearbyen, and the Barentsburg station, are marked with the different dot shapes: cross, triangle and square, respectively. The three stations present a high consistency, with similar values for both wavelengths; especially in the days, where near to low typical values can be found. The ground-based site with the higher AOD values is Longyearbyen, because the data from this site was not scrutinized to eliminate local influence.

On the other hand, two major aerosol outbreak events may be identified in the AOD data from Ny-Ålesund and Longyearbyen: 05th of August and 13th of August. AOD values over 0.8 in Ny-Ålesund and Longyearbyen were detected at 340 nm and values over 0.2 (especially in Longyearbyen) at 870 nm.

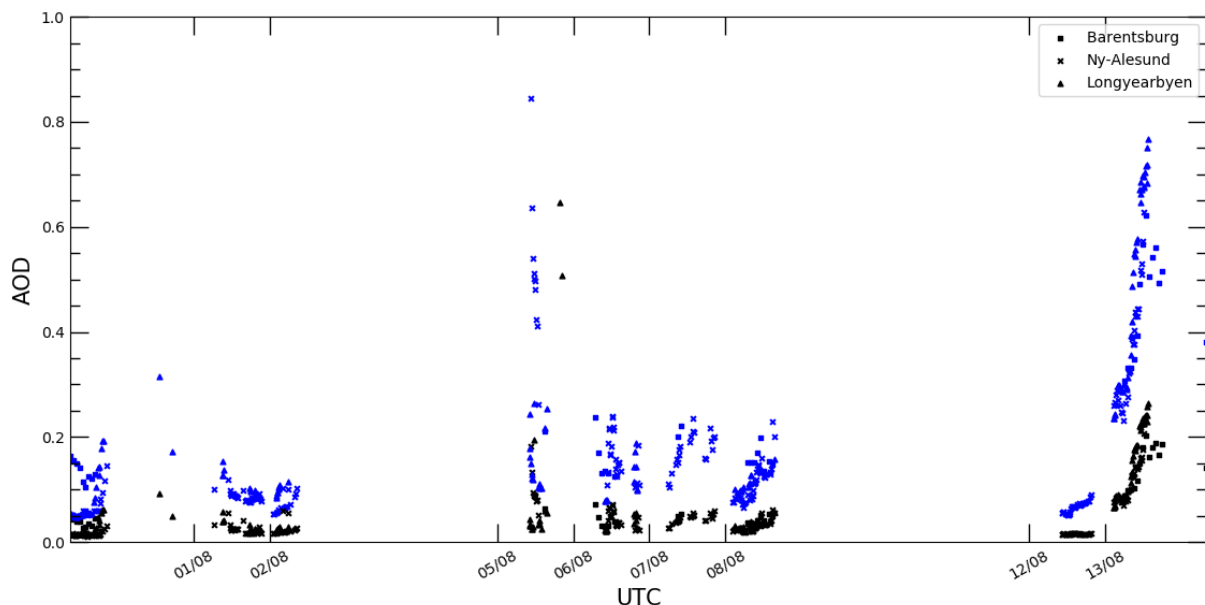


Figure 8 Aerosol optical depth at two wavelengths: 340nm (blue) and 870nm (black)

The Ångström exponent indicates the prevailing aerosol size due to dependence of the spectral shape of the extinction from the particle size [58]. The evolution of the Ångström exponent

between the two channels 440 and 870 nm is shown in Figure 9, where also a high consistency among the three stations (marked by three different dots and colours) can be found in all the temporal selected period. In this case, no significant variation of this parameter can be detected between the expected climatological behaviour and the two events of August. Nevertheless, there is a remarkable presence of large size particles at the Longyearbyen station during the 5th of August. Probably local particles of bigger size could be brought aloft from the ground there since the average wind speed was two times higher ($3.5 \text{ m}\cdot\text{s}^{-1}$) than at two other stations. The southerly wind direction and low BC concentration measured in Longyearbyen by ground-based instruments indicate that the particles were not coming from the major local pollution sources.

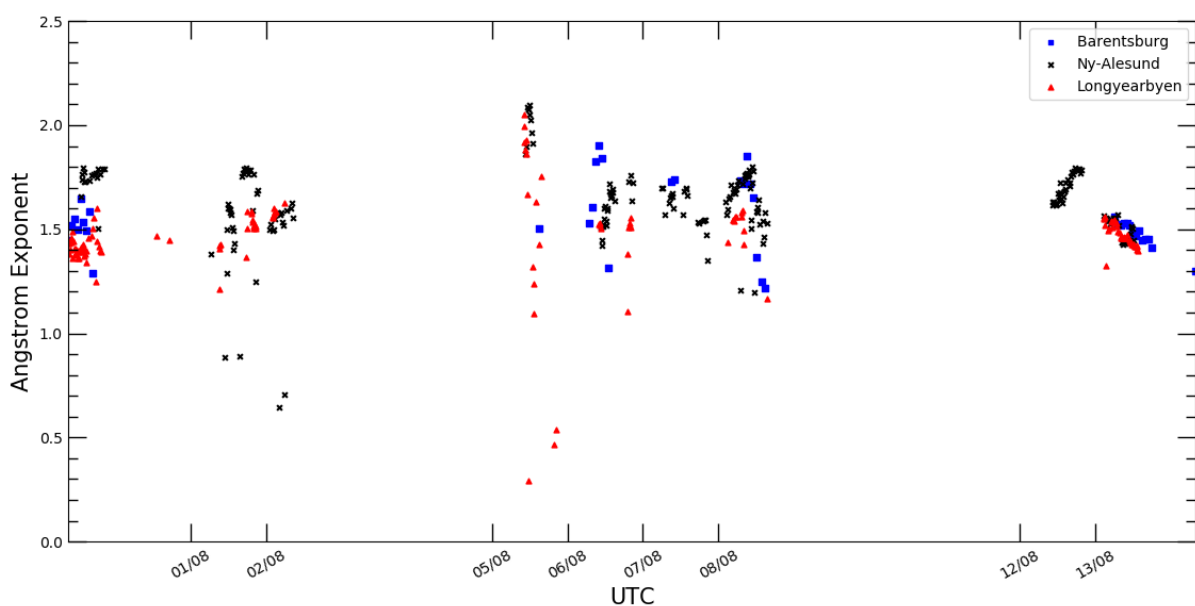


Figure 9 Ångström exponent 440/870 nm at the three stations

According to the data from HYSPLIT-model for the 5th of August, the air masses arriving below 2000m height were from Greenland (Fig. 10a), while trajectories arriving above this height to Ny-Ålesund and Longyearbyen could bring some air pollution from Eurasia (Fig. 10b). This is probably the reason why no elevated concentrations of BC were detected by ground-level instruments and CO observations in Longyearbyen and at the Zeppelin station, respectively, in that day.

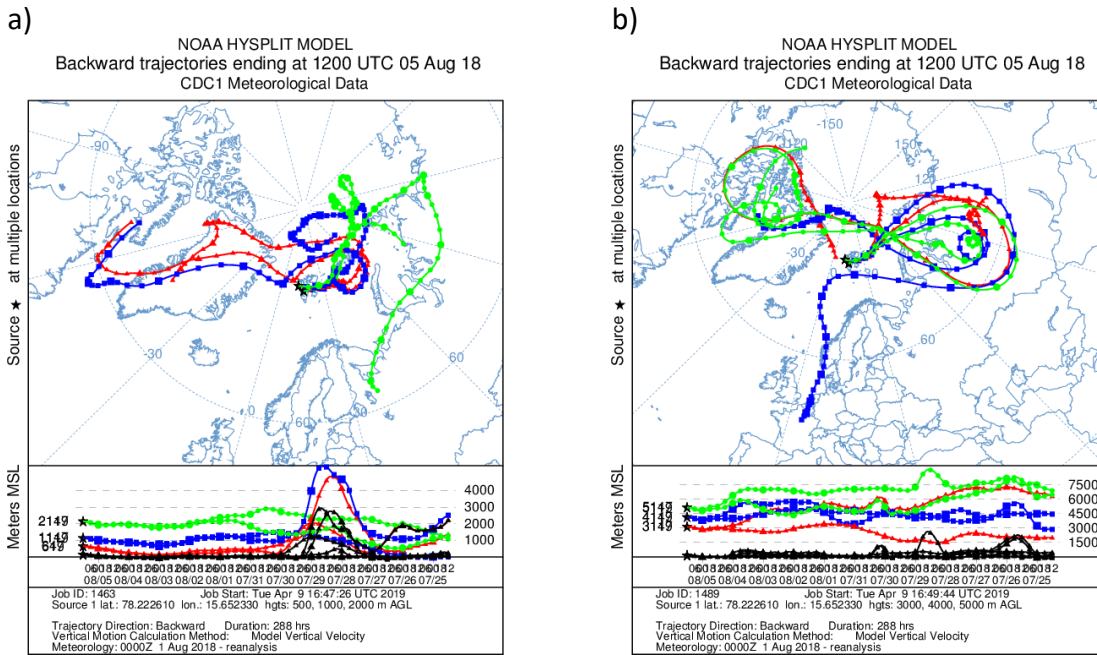


Figure 10 HYSPLIT air mass trajectories for 5th of August: a) below 2000m; b) above 2000m

Figure 11a) shows the Ångström Exponent 440/870 nm as a function of the AOD at 500 nm at the three stations marked by three different dots and colours. As it can be observed, in the event of the August 13th there is no special variation of the Angstrom Exponent in any of the three stations, and their values are around 1.5. This is an indicator of the presence of small particles in the atmospheric column. The Angstrom Exponent results are in line with the size distributions obtained with AERONET inversion algorithm.

Figure 11b) shows the size distribution inversions for August 13th for Longyearbyen and Ny-Ålesund (AERONET sites). There is a large concentration of particles with radius below 0.4 μm , so that event is dominated by the fine mode particles.

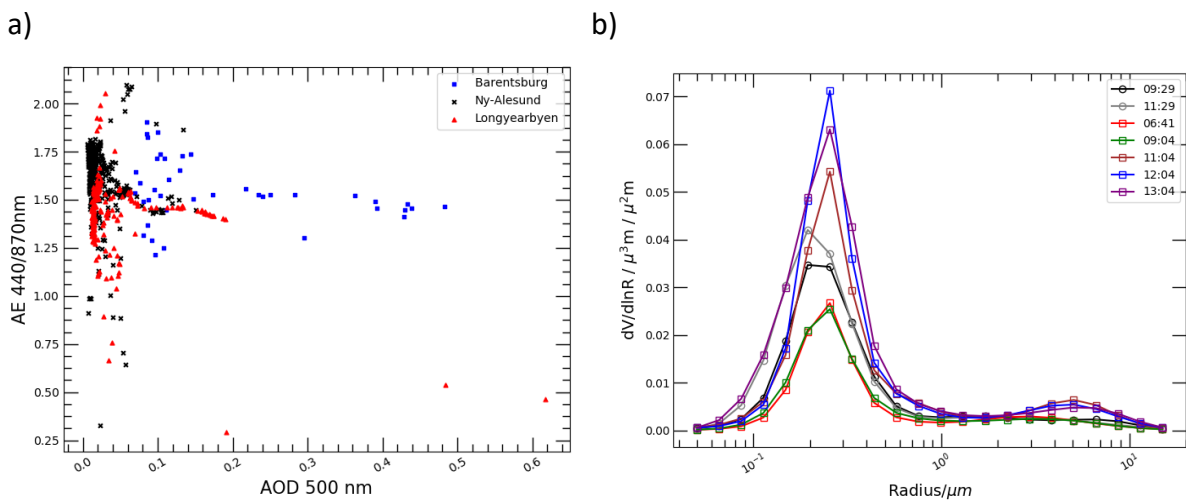


Figure 11 a) Angstrom Exponent 440/870 nm as a function of the AOD at 500 nm; b) size

distribution inversions for August 13th for Longyearbyen and Ny-Ålesund

The ground-level concentrations of BC in Longyearbyen and CO at the Zeppelin station were much higher on 13th of August. This may be explained by the fact that trajectories arriving at 500m height above Ny-Ålesund and Longyearbyen in that day indicated transport of air masses from Eurasia (Fig. 12a). The median BC concentrations measured in profile from soundings in Adventdalen in that day were higher than normal ($294 \text{ ng}\cdot\text{m}^{-3}$). BC concentrations and meteorological parameters smoothed using 1-2-1 filter are shown in Figure 12b). There were two layers with elevated concentrations: the first one was located below 100m with maximum value of $420 \text{ ng}\cdot\text{m}^{-3}$ at 68m and the second once between 800 and 900m with maximum value of $635 \text{ ng}\cdot\text{m}^{-3}$ at 890m. The first layer coincides with local maximum of relative humidity, while the air was less humid in the second one. There was no pronounced temperature inversion most probably due to mixing of the ABL due to high wind speed. The two maxima of wind speed in the profile were located above the maxima of BC concentration: $5.8 \text{ m}\cdot\text{s}^{-1}$ and $4.6 \text{ m}\cdot\text{s}^{-1}$ at the heights of 154m and 960m, respectively.

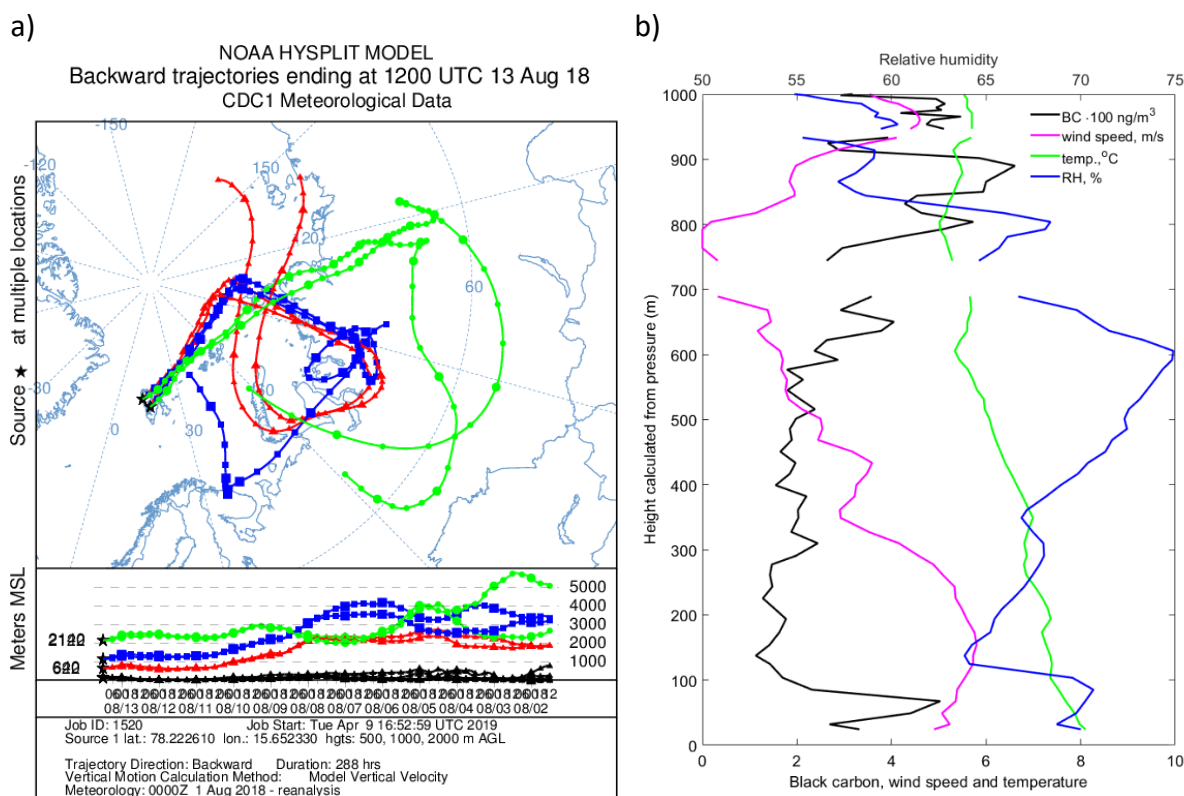


Figure 12 a) HYSPLIT air mass trajectories for 13th of August; b) BC vertical distribution and meteorological parameters measured in Adventdalen

Case study 1st August: the day with highest BC and NO_x concentration in Longyearbyen

An extreme example of days when both local pollution and long-range transported pollution

may have affected local air quality in Longyearbyen is 1st of August 2018. The highest daily values of NO₂ and BC values in Longyearbyen and CO concentration at the Zeppelin station were observed in that day, 15.1 μg·m⁻³, 538 ng·m⁻³ and 116.3 μg·m⁻³, respectively.

This event may be caused by combination of increased local emissions from ships and accumulation of pollutants within the ABL due to adverse weather conditions and by long-range transport of pollution from mid-latitudes. According to the analysis performed by the World Weather Attribution organization, a persistent high-pressure anomaly over Scandinavia caused long periods with extremely hot weather and reduced precipitation, which lasted from May to July 2018 [59]. The reanalysis data from ERA5 confirms that there was a period of anomalously hot weather over Northern Scandinavia from 29th of July to 1st of August 2018 (Figure 13a). At the grid point near the latitude of Tromsø (69.75°N 19°E), for example, daily average air temperatures in this period exceeded 22°C, while four-day maximum temperature average was 26.7°C there. It is extremely hot weather for Tromsø, a town located beyond the Arctic Circle, where, according to statistics presented by the Norwegian Meteorological Institute available on yr.no, daily average temperatures in the time of the year are normally 10°C lower. Warm air masses were transported from Scandinavia to Svalbard, and air temperatures in Longyearbyen and in Ny-Ålesund increased up to 14.5°C and up to 13.7°C, respectively. Average wind speed was very low: 1.4 m/s in Longyearbyen, 1.7 m/s in Ny-Ålesund. Elevated concentrations of CO and O₃ were observed at the Zeppelin station from 28th of July to the 3rd of August (Fig. 1), and 240-hours backward air mass trajectories modelled in HYSPLIT indicated possible long-range source of air pollution on the 1st of August (Fig. 13b).

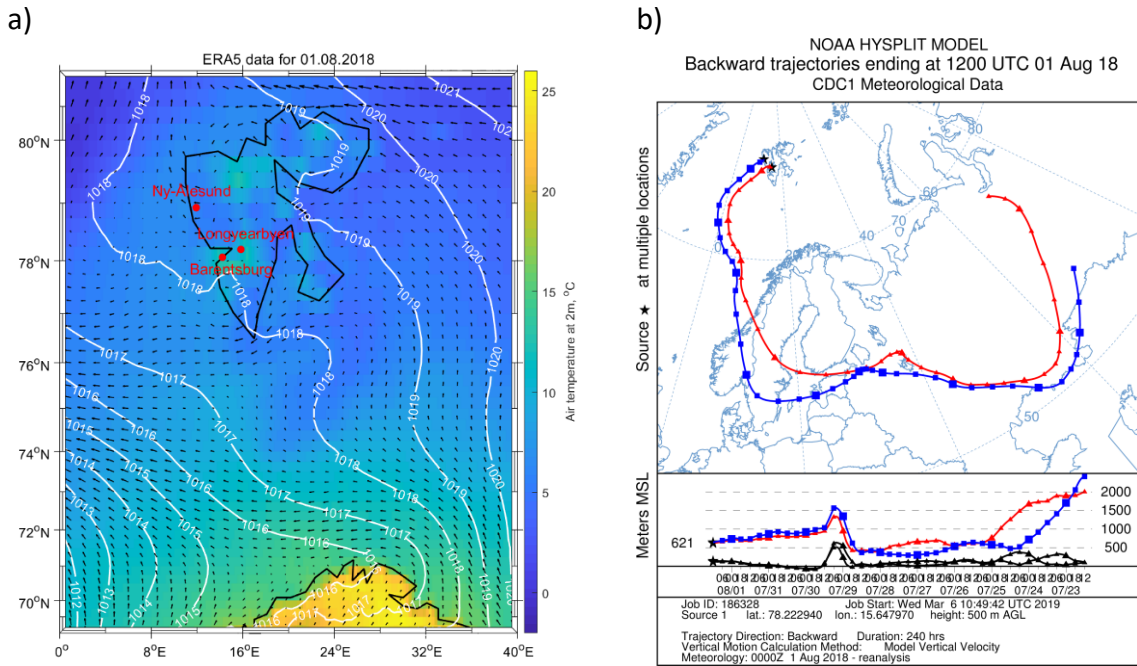


Figure 13 Average meteorological conditions over Svalbard on 1st of August based on ERA5 data (a) and 240-hours backward air mass trajectories modelled in HYSPLIT (b)

However, temperature inversions were observed in the radiosonde and tethered balloon soundings at the both stations in the same day (Fig. 14), and thus combined with low wind speed, created conditions favourable for accumulation of local pollution close to the ground. In this day, light wind conditions and saturation below the inversion layer promoted formation of thick haze in Longyearbyen. The smoke from the power plant and ships was trapped beneath the inversion and visibility was noticeably reduced.

The temperature measured at the level of lowest measurement was 10.3°C, while maximum temperature of 13.1°C was detected at the height of 256m (Fig. 14a). The median wind speed below this level was very low, 1.8m/s. Maximum BC concentration (603ng/m³) was observed at height of 156m where the minimum wind speed of 0.1m/s was observed. The ozone vertical profile in Ny-Ålesund was characterized by three maxima within the lowest 1000m (Fig. 14b): 82.2 µg/m³ at 200m and 83.5 µg/m³ at 601m and 703m. The first O₃ maxima was observed below the level where the minimum wind speed was detected. However, the ozone concentration at 1663m was even higher, 106 µg/m³.

On the 2nd of August, the wind direction changed and wind speed increased, the temperature inversion was destroyed by mechanical mixing and warm air from aloft was brought down to the surface. This led to dramatic reduction of the pollutant concentrations in Longyearbyen.

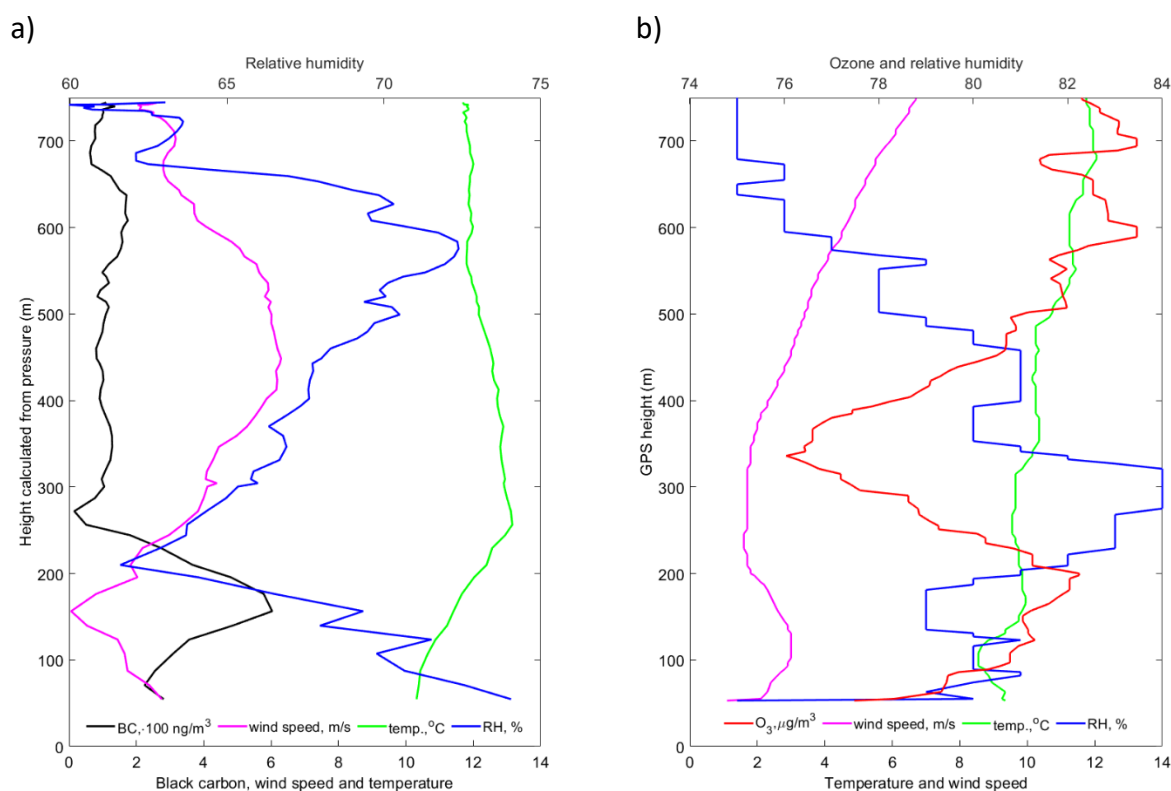


Figure 14 Tethered balloon profile from launch performed at 15:19 01.08.2019 in Adventdalen (a) and ozone sonde profile from launch performed at 17:05 01.08.2019 in Ny-Ålesund (b).

Discussion

In order to compare the ground-based BC data from Longyearbyen and the profile data from Adventdalen, AE51 sensor was in-situ calibrated with the stationary monitor AE33 at UNIS eight times throughout the campaign with average calibration period of two hours each time. The temperature, humidity and wind speed range during the calibrations were 4.4°C-14.4°C, 60%-100%, 0 m·s⁻¹-7.6m·s⁻¹, respectively. AE33 data had 1-minute resolution and were compared with 1-minute averaged data from AE51. The worst and the best correlation between the two instruments were obtained 21.07 and 01.08, accordingly, when the mean concentration of BC measured by AE33 was the lowest (191 ng·m⁻³) and the highest (1051 ng·m⁻³), respectively. However, relationship between the BC concentrations and correlation coefficient is not linear. We have divided all the calibration AE33 and AE51 data into 4 groups of almost equal size (~300 values in each) according to calculated AE33 BC concentration quartiles: BC values below 143 ng·m⁻³, from 143 ng·m⁻³ to 297 ng·m⁻³, from 297 ng·m⁻³ to 610 ng·m⁻³ and above > 610 ng·m⁻³. As high time resolution BC data is often

noisy, especially at lower concentrations [56], [60], post-processing ONA-algorithm for noise reduction suggested by [55] was implemented on 30-seconds AE51 data before 1-minute averaging. The noise for AE51 1-minute averaged original data and data processed using ONA-algorithm was calculated for each group using the formula suggested by [55] and relative deviation of AE51 data from AE33 data was calculated using equation [56]. One can see that the correlation between AE51 and AE33 data increases rapidly for the BC concentrations exceeding a 4th quartiles' limit, while relative deviation is the lowest for the same group (Table 9). The same procedure has been done for quartiles of air temperature, relative humidity and wind speed to check if these values influence the correlation, but no significant difference in correlation coefficients has been found for different groups within the range of meteorological parameters during calibration.

Table 9 Calibration results between AE51 and AE33

Concentration group	Noise AE51, ng/m ³	Noise AE51-ONA, ng/m ³	Relative deviation (A51 and AE33)	Relative deviation (AE51-ONA and AE33)	Pearson r (A51 and AE33)	Pearson r (A51-ONA and AE33)
BC<q25	90	45	0.9±3.5	1.25±4.34	0,29	0,27
q25<=BC<q50	132	96	0.27±0.74	0.3±0.69	0,38	0,36
q50<=BC<q75	174	169	0.1±0.49	0.06±0.49	0,33	0,33
BC>q75	401	375	-0.04±0.33	-0.05±0.33	0,78	0,77
Total	220	166	0.31±1.83	0.39±2.26	0,87	0,87

The concentrations of BC measured during soundings in Adventdalen were very low, often within 1st quartile of AE33 data, therefore, there is high uncertainty in absolute values of BC data measured by AE51. However, since 50m-average values were applied to study profiles' statistics, this averaging eliminated some of the noise, and thus, the BC change throughout individual profile should still be possible to study.

In addition to the uncertainty in the BC data from the portable sensor, the ship traffic data may be imprecise. Although MarineTraffic utilizes the AIS data from the worldwide receiving station network, the data coverage may vary from region to region and depends on the data sharing agreements with third-parties. There is also inherent deficiencies in the data quality since the VHF radio signal coverage is limited to terrestrial range of 30 miles, and the

received data may be incomplete, corrupted or formatted differently from the AIS standard. These factors affect the completeness of the data available for the internal post-processing within MarineTraffic system [61]. Further studies using the data from the Norwegian Coastal Administration (kystverket.no) may be needed to assess the difference in ship traffic data and to study the influence of ship traffic on the air quality in Barentsburg. Unfortunately, at the time of publication, these data were not available.

Previous studies have shown that the volatile PAHs such as naphthalene and fluorene are dominating compounds measured in the Svalbard zone [62]. Therefore, measurement results from the Zeppelin station are needed to identify the contribution from the local sources in Longyearbyen to the background PAHs concentrations. Similarly, BC values from the Zeppelin station would give the information about the increase of BC concentrations due to long-range transport events and allow to compare the BC concentrations in Longyearbyen and Barentsburg with the background level.

Conclusion

This article is the first comprehensive study comparing a broad range of air quality parameters measured in three Svalbard settlements. The summer levels of air pollutants in two Norwegian towns, Longyearbyen and Ny-Ålesund, did not exceed the Norwegian air quality standards, while concentrations of BC and SO₂ were at times extremely high in Barentsburg in 2018. The 20-minutes, hourly and daily air quality limits for SO₂ were exceeded there when the wind was coming from the local coal power plant.

There was no ship traffic data from Barentsburg, but according to the data Longyearbyen, the concentrations of BC, SO₂, NO_x and PAHs increased significantly due to ships' emissions. Similar results are obtained for Ny-Ålesund, but the relative influence of ship traffic on SO₂ concentration was higher there, while the absolute influence was lower due to lower background concentrations.

Temperature inversions, created because of the warm air advection from Scandinavia to Svalbard, promote the conditions favourable for accumulation of local pollutants in the ABL. However, elevated concentrations may be observed in Longyearbyen even in absence of the long-range transported pollution. In these days, colder air masses were brought by the large-scale westerly wind. The wind direction changed to north-westerly due to channelling along the Adventdalen valley, and locally polluted air was efficiently transported from the major local emission sources, the coal power plant and ships, to the town.

The vertical structure of summer ABL in Adventdalen (Longyearbyen) and Ny-Ålesund was

similar with higher median wind speed and lower air temperatures in the profiles without temperature inversions and higher air temperature and lower wind speed in the profiles with inversions at both sites. In the days with inversions, higher maximum BC concentrations and particle concentrations were observed in Adventdalen profiles and by ground-based measurements in Longyearbyen.

The work gives insight into the parameters important for the air quality in the changing Arctic. Increased pollution from the ship traffic accompanied by the higher air temperatures and lower wind speed create conditions favourable for accumulation of local pollution near the settlements, while similar meteorological conditions may prevail during long-range transport events. The impact of these factors on local ecosystems and health of the Arctic populations deserves further investigation.

Acknowledgements

The authors would like to thank Norwegian Polar Institute and the University Centre in Svalbard for the logistical support during the field work in Longyearbyen. Professor Rune Graversen is acknowledged for thorough review of the article. Dr. Kim Holmén is gratefully thanked for the invaluable advice on local pollution sources in Ny-Ålesund and Longyearbyen. Research technician Vitaly Dekhtyarev is acknowledged for support with electronic equipment and data processing during the field work in Longyearbyen in 2018. The authors would also like to thank field assistant Michael Lonardi for the help with tethered balloon launching.

Funding

The Research Council of Norway financed the pilot study in Longyearbyen. The field work was a part of the project “Strengthening cooperation on air pollution research in Svalbard” received the support via Svalbard Strategic Grant.

References

- [1] J. Heintzenberg, H.-C. Hansson, and H. Lannefors, “The chemical composition of arctic haze at Ny-Ålesund, Spitsbergen,” *Tellus*, vol. 33, no. 2, pp. 162–171, 1981.
- [2] P. K. Quinn, G. Shaw, E. Andrews, E. G. Dutton, T. Ruoho-Airola, and S. L. Gong, “Arctic haze: current trends and knowledge gaps,” *Tellus B*, vol. 59, no. 1, pp. 99–114, Feb. 2007.
- [3] J. Lisok *et al.*, “Radiative impact of an extreme Arctic biomass-burning event,” *Atmos. Chem. Phys.*, vol. 18, pp. 8829–8848, 2018.

- [4] A. Dekhtyareva, K. Holmén, M. Maturilli, O. Hermansen, and R. Graversen, “Effect of seasonal mesoscale and microscale meteorological conditions in Ny-Ålesund on results of monitoring of long-range transported pollution,” *Polar Res.*, vol. 37, no. 1, p. 1508196, 2018.
- [5] A. Dekhtyareva, K. Edvardsen, K. Holmén, O. Hermansen, and H.-C. Hansson, “Influence of local and regional air pollution on atmospheric measurements in Ny-Ålesund,” *Int. J. Sustain. Dev. Plan.*, vol. 11, no. 4, pp. 578–587, 2016.
- [6] S. Eckhardt *et al.*, “The influence of cruise ship emissions on air pollution in Svalbard – a harbinger of a more polluted Arctic?,” *Atmos. Chem. Phys.*, vol. 13, no. 16, pp. 8401–8409, Aug. 2013.
- [7] “Utvidet tungoljeforbud,” *Sysselmannen på Svalbard*, 2015. [Online]. Available: <https://www.sysselmannen.no/Nyheter/2015/02/Utvidet-tungoljeforbud/>.
- [8] “Statistics Port of Longyearbyen 2006-2017,” *Port of Longyearbyen*. [Online]. Available: http://portlongyear.no/wp-content/uploads/2017/02/Statistics_2006-2017.pdf. [Accessed: 11-May-2018].
- [9] A. Dekhtyareva *et al.*, “Springtime nitrogen oxides and tropospheric ozone in Svalbard: results from the measurement station network,” *Atmosphere (Basel)*, 2019.
- [10] V. Vestreng, R. Kallenborn, and E. Økstad, “Climate influencing emissions, scenarios and mitigation options at Svalbard,” Klima- og forurensningsdirektoratet, Oslo, Norway, 2009.
- [11] A. Evenset and G. N. Christensen, “Environmental impacts of expedition cruise traffic around Svalbard,” Tromsø, 2011.
- [12] J. Shears, F. Theisen, A. Bjørndal, and S. Norris, “Environmental impact assessment. Ny-Ålesund international scientific research and monitoring station, Svalbard,” Tromsø, 1998.
- [13] A. Abramova, S. Chernianskii, N. Marchenko, and E. Terskaya, “Distribution of polycyclic aromatic hydrocarbons in snow particulates around Longyearbyen and Barentsburg settlements, Spitsbergen,” *Polar Rec. (Gr. Brit.)*, vol. 52, no. 267, pp. 645–659, 2016.
- [14] M. Marquès, J. Sierra, T. Drotikova, M. Mari, M. Nadal, and J. L. Domingo, “Concentrations of polycyclic aromatic hydrocarbons and trace elements in Arctic soils : A case-study in Svalbard,” *Environ. Res.*, vol. 159, no. July, pp. 202–211, 2017.
- [15] Miljødirektoratet, “Trust Arcticugol Barentsburg, kraftverk og gruvevirksomhet,” 2018. [Online]. Available:

- <https://www.norskeutslipp.no/no/Diverse/Virksomhet/?CompanyID=23694>. [Accessed: 03-Apr-2019].
- [16] Miljødirektoratet, “Longyearbyen lokalstyre, Longyear Energiverk,” 2019. [Online]. Available: <https://www.norskeutslipp.no/no/Diverse/Virksomhet/?CompanyID=5115#>. [Accessed: 03-Apr-2019].
- [17] G. Sander, “Limits of acceptable change caused by local activities in Ny-Ålesund. Report from a pre-project , containing a proposal for a main project,” Tromsø, 2014.
- [18] S. Weinbruch, T. Drotikova, N. Benker, and R. Kallenborn, “Particulate and gaseous emissions of power generation at Svalbard (AtmoPart),” 2015.
- [19] IPCC, “IPCC, 2013: Climate Change 2013: The Physical Science Basis. Contribution of Working Group I to the Fifth Assessment Report of the Intergovernmental Panel on Climate Change,” Cambridge University Press, Cambridge, United Kingdom and New York, NY, USA, 2013.
- [20] C. M. Futsaether, A. V. Vollsnes, O. M. Kruse, U. G. Indahl, K. Kvaal, and A. B. Eriksen, “Daylength influences the response of three clover species (*Trifolium* spp.) to short-term ozone stress,” *Boreal Environ. Res.*, vol. 20, no. 1, pp. 90–104, 2015.
- [21] A. B. Eriksen, A. V. Vollsnes, C. M. Futsaether, and O. M. O. Kruse, “Reversible phytochrome regulation influenced the severity of ozone-induced visible foliar injuries in *Trifolium subterraneum* L.,” *Plant Growth Regul.*, vol. 68, no. 3, pp. 517–523, 2012.
- [22] A. Possner, A. M. L. Ekman, and U. Lohmann, “Cloud response and feedback processes in stratiform mixed-phase clouds perturbed by ship exhaust,” *Geophys. Res. Lett.*, vol. 44, pp. 1964–1972, 2017.
- [23] N. A. Janssen *et al.*, “Health effects of black carbon,” Copenhagen, Denmark, 2012.
- [24] I. Kloog, B. Ridgway, P. Koutrakis, B. A. Coull, and J. D. Schwartz, “Long- and Short-Term Exposure to PM_{2.5} and Mortality,” *Epidemiology*, vol. 24, no. 4, pp. 555–561, 2013.
- [25] D. Lack, “The Impacts of an Arctic Shipping HFO Ban on Emissions of Black Carbon.,” Queensland, Australia, 2016.
- [26] G. Shrestha, S. J. Traina, and C. W. Swanston, “Black carbon’s properties and role in the environment: A comprehensive review,” *Sustainability*, vol. 2, no. 1, pp. 294–320, 2010.
- [27] V. S. Kozlov, E. P. Yausheva, S. A. Terpugova, M. V. Panchenko, D. G. Chernov, and V. P. Shmargunov, “Optical – microphysical properties of smoke haze from Siberian forest fires in summer 2012,” *Int. J. Remote Sens.*, vol. 35, no. 15, pp. 5722–5741,

- 2014.
- [28] В. С. Козлов, В. П. Шмаргунов, and В. В. Полькин, “СПЕКТРОФОТОМЕТРЫ ДЛЯ ИССЛЕДОВАНИЯ ХАРАКТЕРИСТИК ПОГЛОЩЕНИЯ СВЕТА АЭРОЗОЛЬНЫМИ ЧАСТИЦАМИ,” *ПРИБОРЫ И ТЕХНИКА ЭКСПЕРИМЕНТА*, vol. 5, pp. 1–3, 2008.
- [29] L. Ferrero, G. Mocnik, B. S. Ferrini, M. G. Perrone, G. Sangiorgi, and E. Bolzacchini, “Vertical profiles of aerosol absorption coefficient from micro-Aethalometer data and Mie calculation over Milan,” *Sci. Total Environ.*, vol. 409, no. 14, pp. 2824–2837, 2011.
- [30] L. Ferrero *et al.*, “Vertical profiles of aerosol and black carbon in the Arctic : a seasonal phenomenology along 2 years (2011 – 2012) of field campaigns,” *Atmos. Chem. Phys.*, vol. 16, pp. 12601–12629, 2016.
- [31] P. J. Rousseeuw and M. Hubert, “Robust statistics for outlier detection,” *WIREs Data Min. Knowl. Discov.*, vol. 1, pp. 73–79, 2011.
- [32] J. M. Wallace and P. V. Hobbs, *Atmospheric science: an introductory survey*, 2nd ed. New York: Academic Press, 2006.
- [33] X. Y. Wang and K. C. Wang, “Estimation of atmospheric mixing layer height from radiosonde data,” *Atmos. Meas. Tech.*, vol. 7, pp. 1701–1709, 2014.
- [34] M. Maturilli, “High resolution radiosonde measurements from station Ny-Alesund (2018-07),” *Alfred Wegener Institute - Research Unit Potsdam, PANGAEA*, 2018. [Online]. Available: <https://doi.org/10.1594/PANGAEA.894698>.
- [35] W. Steinbrecht *et al.*, “Results of the 1998 Ny-Ålesund Ozone Monitoring Intercomparison,” *J. Geophys. Res.*, vol. 104, no. D23, pp. 30,515-30,523, 1999.
- [36] D. Contini *et al.*, “The direct influence of ship traffic on atmospheric PM 2.5 , PM 10 and PAH in Venice,” *J. Environ. Manage.*, vol. 92, p. 2119e2129 Contents, 2011.
- [37] D. Stenersen, “Operational data from shipping in the Geirangerfjord, Nærøyfjord og Aurlandsfjord,” Trondheim, Norway, 2017.
- [38] Nasjonalt folkehelseinstitutt, “Luftkvalitetskriterier. Virkninger av luftforurensning på helse,” Oslo, 2013.
- [39] Федеральная служба по гидрометеорологии и мониторингу окружающей среды, “Обзор состояния и загрязнения окружающей среды в Российской Федерации за 2017 год,” МОСКВА, 2018.
- [40] Главный государственный санитарный врач Российской Федерации, “Об утверждении гигиенических нормативов ГН 2.1.6.3492-17 ‘Предельно

- допустимые концентрации (ПДК) загрязняющих веществ в атмосферном воздухе городских и сельских поселений’ (с изменениями на 31 мая 2018 года),” *ПОСТАНОВЛЕНИЕ*, 2017. [Online]. Available: <http://docs.cntd.ru/document/556185926>. [Accessed: 04-Apr-2019].
- [41] W. C. Porter, C. L. Heald, D. Cooley, and B. Russell, “Investigating the observed sensitivities of air-quality extremes to meteorological drivers via quantile regression,” *Atmos. Chem. Phys.*, vol. 15, pp. 10349–10366, 2015.
- [42] H. Hersbach and D. Dee, “ERA5 reanalysis is in production,” *ECMWF Newsl.*, no. number 147, p. 7, 2016.
- [43] A. F. Stein, R. R. Draxler, G. D. Rolph, B. J. B. Stunder, M. D. Cohen, and F. Ngan, “NOAA’s HYSPLIT atmospheric transport and dispersion modeling system,” *Bull. Am. Meteorol. Soc.*, no. February, pp. 2059–2077, 2015.
- [44] Федеральная служба по гидрометеорологии и мониторингу окружающей среды, “Обзор состояния и загрязнения окружающей среды в Российской Федерации за 2015 год,” МОСКВА, 2016.
- [45] S. P. Arya, *Air pollution meteorology and dispersion*. New York: Oxford University press, 1999.
- [46] European Commission, “European Union Risk Assessment Report. Naphtalene,” Luxembourg: Office for Official Publications of the European Communities, 2003.
- [47] H. Agrawal, W. A. Welch, S. Henningsen, J. W. Miller, and D. R. C. Iii, “Emissions from main propulsion engine on container ship at sea,” *J. Geophys. Res.*, vol. 115, p. D23205, 2010.
- [48] D. Cooper, “Exhaust emissions from ships at berth,” *Atmos. Environ.*, vol. 37, no. 27, pp. 3817–3830, Sep. 2003.
- [49] C. Jia and S. Batterman, “A Critical Review of Naphthalene Sources and Exposures Relevant to Indoor and Outdoor Air,” *Int. J. Environ. Res. Public Health*, vol. 7, pp. 2903–2939, 2010.
- [50] C. K. Li and R. M. Kamens, “The use of polycyclic aromatic hydrocarbons as source signatures in receptor modeling,” *Atmos. Environ.*, vol. 27, no. 4, pp. 523–532, 1993.
- [51] W. J. Shields, S. Ahn, J. Pietari, K. Robrock, and L. Royer, “Atmospheric Fate and Behavior of POPs,” in *Environmental Forensics for Persistent Organic Pollutants*, G. O’Sullivan and C. Sandau, Eds. Elsevier B.V., 2014, pp. 199–290.
- [52] K. F. Ho *et al.*, “Emissions of gas- and particle-phase polycyclic aromatic hydrocarbons (PAHs) in the Shing Mun Tunnel , Hong Kong,” *Atmos. Environ.*, vol.

- 43, pp. 6343–6351, 2009.
- [53] J. Ma, Y. Liu, Q. Ma, C. Liu, and H. He, “Heterogeneous photochemical reaction of ozone with anthracene adsorbed on mineral dust,” *Atmos. Environ.*, vol. 72, pp. 165–170, 2013.
- [54] M. A. Callahan *et al.*, “Water-related environmental fate of 129 priority pollutants Volume II. Halogenated aliphatic hydrocarbons, halogenated ethers, monocyclic aromatics, phthalates esters, polycyclic aromatic hydrocarbons, nitrosamines, miscellaneous compounds,” Washington, DC., 1979.
- [55] G. S. W. Hagler, T. L. B. Yelverton, R. Vedantham, A. D. A. Hansen, and J. R. Turner, “Post-processing method to reduce noise while preserving high time resolution in aethalometer real-time black carbon data,” *Aerosol Air Qual. Res.*, vol. 11, no. 5, pp. 539–546, 2011.
- [56] Y.-H. Cheng and M.-H. Lin, “Real-Time Performance of the microAeth® AE51 and the Effects of Aerosol Loading on Its Measurement Results at a Traffic Site,” *Aerosol Air Qual. Res.*, vol. 13, pp. 1853–1863, 2013.
- [57] Q. Coopman, T. J. Garrett, D. P. Finch, and J. Riedi, “High Sensitivity of Arctic Liquid Clouds to Long-Range,” *Geophys. Res. Lett.*, vol. 45, pp. 372–381, 2018.
- [58] C. Toledano *et al.*, “Aerosol optical depth and Ångström exponent climatology at El Arenosillo AERONET site (Huelva, Spain),” *Q. J. R. Meteorol. Soc.*, vol. 133, pp. 795–807, 2007.
- [59] World Weather Attribution, “Heatwave in northern Europe, summer 2018,” *Heatwave in northern Europe, summer 2018*, 2018. [Online]. Available: <https://www.worldweatherattribution.org/attribution-of-the-2018-heat-in-northern-europe/>. [Accessed: 02-May-2019].
- [60] J. Backman *et al.*, “On Aethalometer measurement uncertainties and an instrument correction factor for the Arctic,” *Atmos. Meas. Tech.*, vol. 10, no. 12, pp. 5039–5062, 2017.
- [61] A. King, “Four ways MarineTraffic ensures AIS data accuracy,” *MarineTraffic Blog*, 2018. [Online]. Available: <https://www.marinetraffic.com/blog/four-ways-marinetraffic-ensures-ais-data-accuracy/>. [Accessed: 20-May-2019].
- [62] L. Ferrero *et al.*, “Chemical Composition of Aerosol over the Arctic Ocean from Summer ARctic EXpedition (AREX) 2011 – 2012 Cruises : Ions , Amines , Elemental Carbon , Organic Matter , Polycyclic Aromatic Hydrocarbons , n-Alkanes , Metals , and Rare Earth Elements,” *Atmosphere (Basel)*, vol. 10, no. 54, pp. 1–32, 2019.